13 July 2007 | S10

Science

AAAS

One just right for you.

Find the cycler that best reflects your needs among the full line of Bio-Rad amplification products.

Bio-Rad is committed to providing you with the best tools for your PCR needs. This dedication is proven by our history of innovation, quality, and regard for researchers' needs.

- Flexible, space-saving dual blocks and multi-bay instruments
- The only modular real-time cycler upgrade with a thermal gradient; choose from 1 to 5 colors
- Innovative enzymes that work where others fail
- PCR tubes, plates, and sealers for any application
- Dedicated technical support by experienced scientists

Bio-Rad offers the most complete line of thermal cyclers anywhere.

For more information, visit us on the Web at **www.bio-rad.com/amplification/**

Purchase of this instrument conveys a limited non-transferable immunity from suit for the purchaser's own internal research and development and for use in applied fields other than Human In Vitro Diagnostics under one or more of U.S. Patents Nos. 5,656,493, 5,333,675, 5,475,610 (claims 1, 44, 158, 160–163 and 167 only), and 6,703,236 (claims 1–7 only), or corresponding claims in their non-U.S. counterparts, owned by Applera Corporation. No right is conveyed expressly, by implication or by estoppel under any other patent claim, such as claims to apparatus, reagents, kits, or methods such as 5' nuclease methods. Further information on purchasing licenses may be obtained by contacting the Director of Licensing, Applied Biosystems, 850 Lincoln Centre Drive, Foster City, California 94404, USA.

Bio-Rad's real-time thermal cyclers are licensed real-time thermal cyclers under Applera's United States Patent No. 6,814,934 B1 for use in research and for all other fields except the fields of human diagnostics and veterinary diagnostics.

TaKaRa

Real Time PCR

qRT-PCR Kits with SYBR® Green

PrimeScript™

For Fast and Accurate Quantification

One Step SYBR® PrimeScript™ RT-PCR Kit (Perfect Real Time) provides simple, accurate and quick performance for real time PCR. It contains PrimeScript™ RTase for efficient cDNA synthesis of any RNA template, having excellent elongation through higher-order structures. A two step reaction can be performed using PrimeScript™ RT reagent kit with SYBR® *Premix Ex Taq*™ (Perfect Real Time).

Features:

- **High Sensitivity:** Target quantification from Picogram of total RNA.
- **Accurate Quantification:** Over 5-6 orders of magnitude using total RNA as a template.

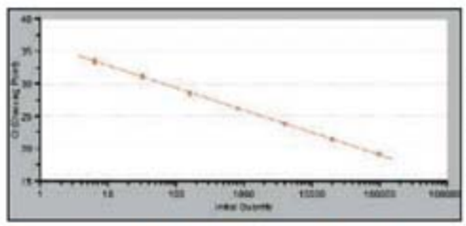

An Excellent Linear Standard Curve using the One Step SYBR® PrimeScript™ RT-PCR Kit (Perfect Real Time).

- **Simple and Quick Reaction Assembly:** Premix formulations save time and minimize possibility of contamination.
- **Versatile:** Use on any real time PCR instrument. Supplied with ROX reference dyes.
- **High specificity:** Optimized buffer and *Ex Taq*™ HS minimize non-specific amplification and primer-dimer formation.

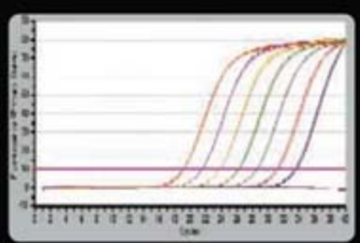

The One Step SYBR® PrimeScript™ RT-PCR Kit (Perfect Real Time) was used to detect rat Rplp2 transcript from 6.4 pg to 100 ng total RNA. An excellent amplification curve and a single peak on the melting curve show superior efficiency, specific amplification and accurate quantification.

One step or Two Step RT-PCR kits for TaqMan® Probe Detection are also available.

PrimeScript™ and *Ex Taq*™ are trademarks of Takara Bio Inc. TaqMan® is a registered trademark of Roche Molecular Systems. Purchase of this product includes an immunity from suit under patents specified in the product insert to use only the amount purchased for the purchaser's own internal research. No other patent rights (such as 5' Nuclease Process patent rights) are conveyed expressly, by implication, or by estoppel. Further information on purchasing licenses may be obtained by contacting the Director of Licensing, Applied Biosystems, 850 Lincoln Centre Drive, Foster City, California 94404, USA.

TaKaRa

www.takara-bio.eu

Japan:
Takara Bio Inc.
+81 77 543 7247
www.takara-bio.com

USA: Not available in US
Takara Bio USA
888-251-6618
www.takarabiousa.com

Europe:
Takara Bio Europe S.A.S.
+33 1 3904 6880 •
www.takara-bio.eu

China:
Takara Biotechnology (Dalian) Co., Ltd.
+86 411 8764 1681
www.takara.com.cn

Korea:
Takara Korea Biomedical Inc.
+82 2 2081 2525
www.takara.co.kr

Pure protein is the challenge.
PURE Expertise is the solution.

Imagine having the combined knowledge of hundreds of chromatography experts at your disposal. You'd be able to purify even the most challenging protein and gain the edge in your research. Well now you have it. PURE Expertise is the distillation of 50 years' chromatography experience – available online. Simply put, it's everything you need to gain the best results in protein purification.

Download our purification handbook at **www.gelifesciences.com/pure**

imagination at work

GE Healthcare Bio-Sciences AB, a General Electric Company.
Björkgatan 30, 751 84 Uppsala, Sweden
© 2007 General Electric Company – All rights reserved.
GE12-07. First printed 07/2007

Volume 317, Issue 5835

COVER

Changes in the intensity and distribution of future rainfall may have a substantial effect on human activities. As Earth warms, climate models predict that global rainfall will increase, but by a small amount. In contrast, satellite observations during the past two decades suggest that the increase in future rain may be much larger than previously expected. See page 233.

Photo: Morey Milbradt/Brand X/Corbis

DEPARTMENTS

EDITORIAL

NEWS OF THE WEEK

NEWS FOCUS

LETTERS

BOOKS *ET AL.*

POLICY FORUMS

PERSPECTIVES

CONTENTS continued >>

The most wonderful discovery made by scientists is science itself.

Jacob Bronowski
Mathematician (1908-1974)

Shimadzu transcends modern assumptions and limits to shine a beam of light on yet undiscovered scientific truths. Shimadzu believes in the value of science to transform society for the better. For more than a century, we have led the way in the development of cutting-edge technology to help measure, analyze, diagnose and solve problems. The solutions we develop find applications in areas ranging from life sciences and medicine to flat-panel displays. We have learned much in the past hundred years. Expect a lot more.

www.shimadzu.com

SHIMADZU

Science

SCIENCE EXPRESS

www.sciencexpress.org

APPLIED PHYSICS

Radiationless Electromagnetic Interference: Evanescent-Field Lenses and Perfect Focusing

R. Merlin

A new method is proposed for subwavelength imaging in which interference produced from planar subwavelength structures in a plate focuses light on the plate's surface.

10.1126/science.1143884

ASTRONOMY

Detection of Circumstellar Material in a Normal Type Ia Supernova

F. Patat et al.

Detection of gas around a Type Ia supernova, a standard distance reference, implies that the progenitor white dwarf exploded after cannibalizing a red giant companion star.

10.1126/science.1143005

NEUROSCIENCE

Spatial Regulation of an E3 Ubiquitin Ligase Directs Selective Synapse Elimination

M. Ding, D. Chao, G. Wang, K. Shen

In developing worms, the pruning of excess synapses requires proteosome-mediated protein degradation and is selectively prevented by a neural adhesion molecule.

10.1126/science.1145727

TECHNICAL COMMENT ABSTRACTS

NEUROSCIENCE

BREVIA

EVOLUTION

The sex ratio in a butterfly population shifted very rapidly from close to zero males to a 1-to-1 male-female ratio in only a few generations.

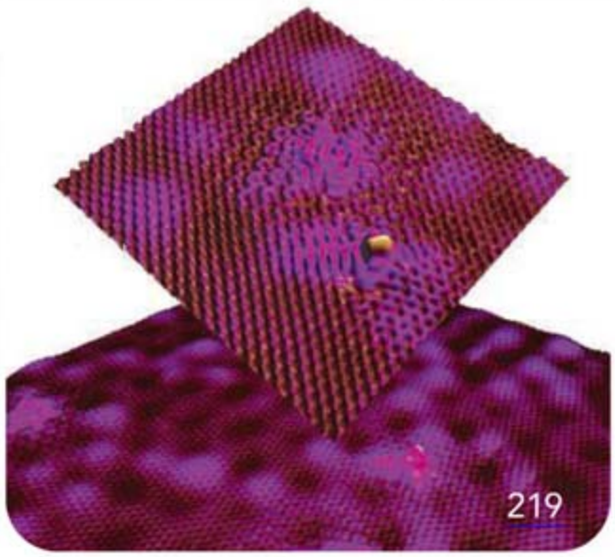

CREDIT (BOTTOM): G. M. RUTTER, GEORGIA TECH/N. P. GUISINGER, NIST

RESEARCH ARTICLE

NEUROSCIENCE

During normal suppression of emotional memories, the prefrontal cortex inhibits memory-related brain regions, a process that may go awry in certain psychiatric conditions.

REPORTS

APPLIED PHYSICS

Scanning tunneling spectroscopy shows that electronically active defects in graphene sheets scatter electrons, leading to constructive interference.

MATERIALS SCIENCE

A tandem solar cell, in which two cells are connected by a transparent conductor in order to use more of the solar spectrum, can be synthesized entirely from solution.

CHEMISTRY

A ligand with three coordinating sulfur groups mimics a bacterial enzyme and cleaves toxic mercury compounds. >> *Perspective p. 205*

GEOCHEMISTRY

Magmatic gas compositions show that a type of volcanic explosion is driven by gas rising up from several kilometers, deeper than suggested by the accompanying earthquakes.

CONTENTS continued >>

Solved!

INNOVATION @ WORK

Innovative Solutions for Ion Channel Research

Puzzled over who will meet your ion channel research needs? Look no further. We have the most extensive line of innovative products for ion channel research.

- Subunit selective antibodies
- Toxins
- Inhibitors and activators
- RNAi libraries
- PCR/Amplification Reagents, Quantitative PCR, Real-time PCR
- Cloning Systems, kTransfection Reagents, Competent Cells, Expression Vectors
- Cell Culture Media, Supplements, Growth Factors

Sigma is the Solution.

Visit sigma.com/ionchannelsolutions for more information.

Sigma also offers these convenient online tools for your research:

Search Your Favorite Gene
sigma.com/yfg

Sigma-RBI Handbook of Receptor Classification and Signal Transduction
sigma.com/ehandbook

Pathfinder Interactive Pathways
sigma.com/pathfinder

sigma.com

Accelerating Customers' Success through Leadership in **Life Science**, **High Technology** and **Service**

SIGMA-ALDRICH CORPORATION • BOX 14508 • ST. LOUIS • MISSOURI 63178 • USA

SIGMA®

REPORTS *CONTINUED...*

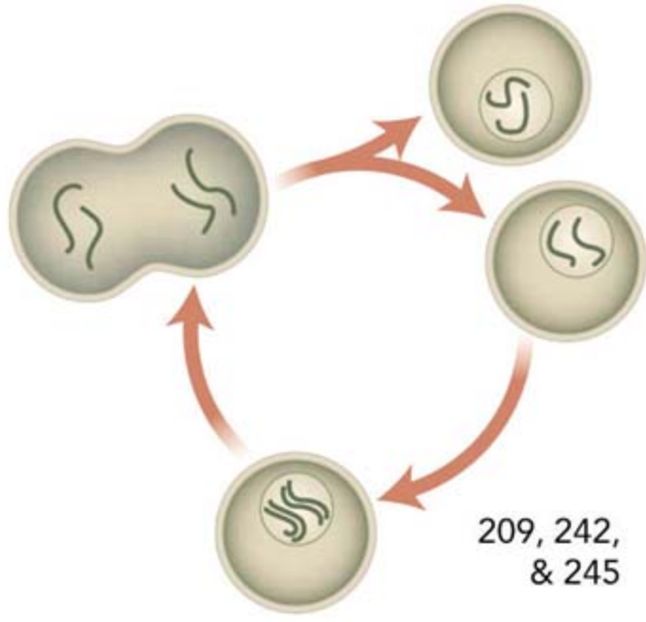

AAAS
ADVANCING SCIENCE, SERVING SOCIETY

SCIENCE (ISSN 0036-8075) is published weekly on Friday, except the last week in December, by the American Association for the Advancement of Science, 1200 New York Avenue, NW, Washington, DC 20005. Periodicals Mail postage (publication No. 484460) paid at Washington, DC, and additional mailing offices. Copyright © 2007 by the American Association for the Advancement of Science. The title SCIENCE is a registered trademark of the AAAS. Domestic individual membership and subscription (51 issues): $142 ($74 allocated to subscription). Domestic institutional subscription (51 issues): $710; Foreign postage extra: Mexico, Caribbean (surface mail) $55; other countries (air assist delivery) $85. First class, airmail, student, and emeritus rates on request. Canadian rates with GST available upon request, GST #1254 88122. Publications Mail Agreement Number 1069624. **Printed in the U.S.A.**

Change of address: Allow 4 weeks, giving old and new addresses and 8-digit account number. **Postmaster:** Send change of address to AAAS, P.O. Box 96178, Washington, DC 20090–6178. **Single-copy sales:** $10.00 current issue, $15.00 back issue prepaid includes surface postage; bulk rates on request. **Authorization to photocopy** material for internal or personal use under circumstances not falling within the fair use provisions of the Copyright Act is granted by AAAS to libraries and other users registered with the Copyright Clearance Center (CCC) Transactional Reporting Service, provided that $18.00 per article is paid directly to CCC, 222 Rosewood Drive, Danvers, MA 01923. The identification code for *Science* is 0036-8075. *Science* is indexed in the *Reader's Guide to Periodical Literature* and in several specialized indexes.

CONTENTS continued >>

AAAS & NPA

Here's your link to career advancement

AAAS is at the forefront of advancing early-career researchers —offering job search, grants and fellowships, skill-building workshops, and strategic advice through ScienceCareers.org and our Center for Careers in Science & Technology.

NPA, the National Postdoctoral Association, is providing a national voice and seeking positive change for postdocs—partnering with AAAS in career fairs, seminars, and other events. In fact, AAAS was instrumental in helping the NPA get started and develop into a growing organization and a vital link to postdoc success.

If you're a postdoc or grad student, go to the AAAS-NPA link to find out how to spell career success.

AAAS.org/NPA

NATIONAL POSTDOCTORAL ASSOCIATION

Science
AAAS

SCIENCENOW

www.sciencenow.org DAILY NEWS COVERAGE

Hot Jupiters Wet Too
Water confirmed in atmospheres of giant extrasolar planets.

Digging for DNA That Drives Colon Cancer
Three independent teams hit on same genetic variant.

Earth First for Astrobiologists
Panel recommends the study of strange beings on Earth before searching in space.

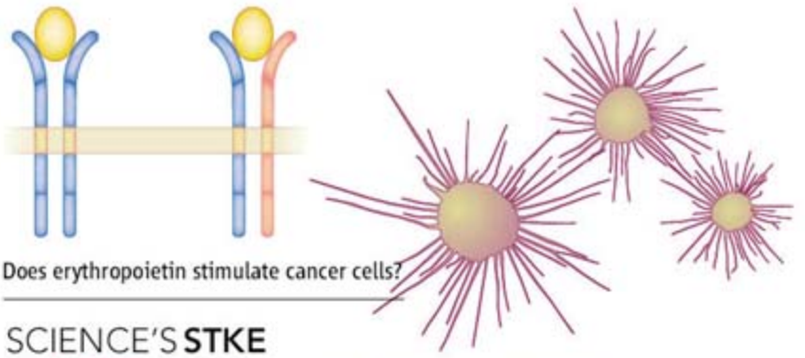

Does erythropoietin stimulate cancer cells?

SCIENCE'S STKE

www.stke.org SIGNAL TRANSDUCTION KNOWLEDGE ENVIRONMENT

PERSPECTIVE: Does Erythropoietin Have a Dark Side? Epo Signaling and Cancer Cells
A. J. Sytkowski
Clinical studies have raised the possibility of a growth-promoting action of Epo on cancer cells.

ST NETWATCH: NetWorKIN
Use an algorithm that combines localization and sequence information to study protein phosphorylation; in Bioinformatics Resources.

ST NETWATCH: Cytoscape
The site provides tools for visualizing and analyzing molecular interaction networks; in Modeling Tools.

Combining painting and biology.

SCIENCECAREERS

www.sciencecareers.org CAREER RESOURCES FOR SCIENTISTS

US: Be Careful What You Wish For
B. Benderly
Will the planned doubling of physical science research funding leave some scientists worse off than before?

US: Opportunities—Consulting on the Side
P. Fiske
There are lots of reasons for postdocs and graduate students to seek out consulting work.

EUROPE: Illustrating Nature
E. Pain
Diana Marques combines her passions for painting and biology in scientific illustration work.

UK: From the Archives—The Scientific Conference Guide (Or, How to Make the Most of Your Free Holiday)
K. Arney
Don't sit through an uninteresting talk when you could be checking out the posters or shopping.

SCIENCEPODCAST

Listen to the 13 July *Science* Podcast to hear about suppressing emotional memories, biomagnification of chemicals in the food chain, genetic insights into autism, and more.
www.sciencemag.org/about/podcast.dtl

Separate individual or institutional subscriptions to these products may be required for full-text access.

Imagine...

ZYMO RESEARCH

The Beauty of Science is to Make Things Simple

Plasmid DNA Purification *Directly* From Culture

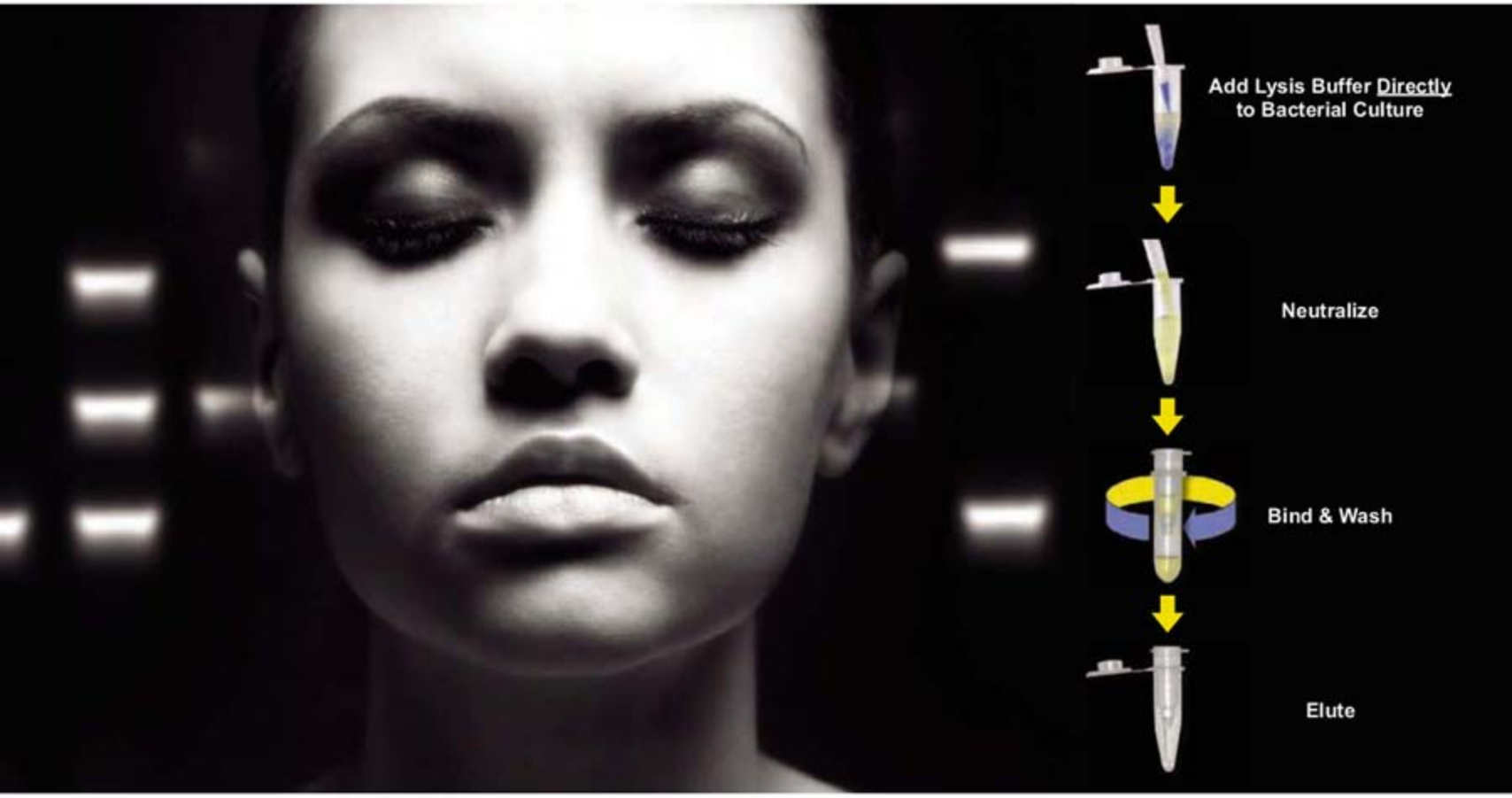

The ***Pellet-Free*** procedure of the Zyppy™ Plasmid Miniprep Kit bypasses conventional cell-pelleting and resuspension steps.

- Fastest (~8 minutes for 1-5 preps.), simplest procedure for purifying the highest quality plasmid DNA.
- Innovative colored buffers* permit error-free visual identification of complete bacterial cell lysis and neutralization.

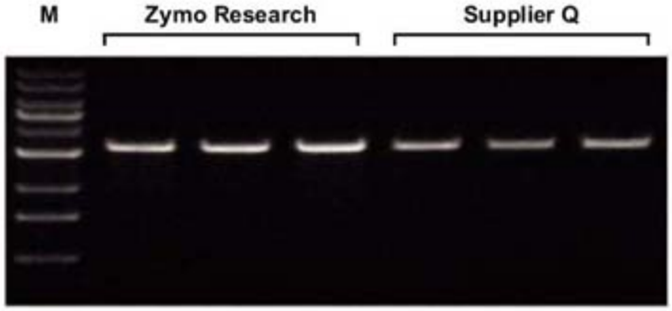

***Eco*R I digestion of a 3 kb plasmid DNA isolated from a 600 µl *E. coli* culture using the Zyppy™ Plasmid Miniprep Kit or a kit from Supplier Q. The amount of DNA loaded was standardized based on culture volume input. Performed in triplicate. M, ZR 1 kb DNA Marker.**

Free samples and 50% discounts are available**

*Technologies are patent pending. **For a limited time for U.S. customers only.

1-888-882-9682 USA
+1-714-288-9682 INTL
www.zymoresearch.com

Deep Gas, Destructive Eruptions

The explosive activity of Italian volcano Stromboli makes it a dangerous neighbor for local populations, tourists, and volcanologists. The explosions are thought to be caused by gas slugs that rise faster than the surrounding magma and generate seismic activity near the surface of the volcano. However, the source of the gas is unclear. During quiescent and explosive periods, **Burton *et al.*** (p. 227) have measured spectroscopic variations in the gas composition emanating from Stromboli that indicates the gas has a deep origin. Using a gas-solubility model, they show that gas slugs form 3 kilometers beneath the summit craters, at the base of the volcanic pile and away from seismological processes at the surface.

Graphene Transport Up Close

Defects may play a critical role in the transport properties of graphene (single sheets of graphite supported on a substrate), especially in possible applications in electronic devices. **Rutter *et al.*** (p. 219) used scanning tunneling spectroscopy to probe the local electronic properties of graphene bilayers grown epitaxially on a silicon carbide substrate. They show that the transport properties are critically influenced by the microscopic properties of the sample, particularly electronically active defects in graphene that can scatter the electrons and cause interference and localization.

Cleaving Alkyl Mercury

Bacteria have evolved a group of enzymes that can deactivate highly toxic alkyl mercury contaminants, but many of the molecular details underlying their mode of action remain unclear. The organomercurial lyase *MerB* specifically accomplishes scission of Hg–C bonds. **Melnick and Parkin** (p. 225; see the Perspective by **Omichinski**) report that a ligand bearing three coordinating sulfur groups, analogous to active-site cysteines in the enzyme, efficiently induces reaction of a mercury methyl, ethyl, or cyanomethyl center with a thiol to liberate the alkane or nitrile. Characterization of the Hg methyl and ethyl complexes in the solid state and in solution reveals that although an overall two-coordinate geometry is favored, the metal interacts rapidly with the additional sulfur groups in the ligand, which appear to promote reactivity lacking in other molecular Hg compounds.

CREDITS (TOP TO BOTTOM): NICOLE MÉTRICH/CNRS, FRANCE; SAKAMOTO *ET AL.*

Oxygen Reservoir

Oxygen isotopic anomalies have been found for planets, asteroids, and comets, but their origin remains an outstanding problem in cosmochemistry. In the early solar system, two isotopically distinct nebular reservoirs, one rich in ^{16}O and the other rich in ^{17}O and ^{18}O, appear to have been mixed together. However, measuring their original ratios in secondary minerals is difficult because aqueous environments allow isotope exchange between water and rocks. **Sakamoto *et al.*** (p. 231, published online 14 June; see the Perspective by **Young**) have found a distinctive material in the matrix of a primitive carbonaceous chondrite meteorite (Acfer 094) that is highly enriched in ^{17}O and ^{18}O relative to the Earth. It formed by oxidation of iron-nickel metal and sulfides by water in the protoplanetary disk. This meteorite is the most extreme ^{16}O-depleted material that is not demonstrably a presolar grain, and may be sampling a $^{17,18}O$-rich reservoir in the early solar system.

More Rain Likely

Climate models and observations both suggest that global precipitation and the amount of water in the atmosphere will rise with temperature, but models predict that rainfall will increase only half as fast as humidity. **Wentz *et al.*** (p. 233, published online 31 May; see the cover) analyzed satellite data on precipitation and found that precipitation and total atmospheric water content have actually increased at approximately the same rate during the past 20 years. The reason why models predict a difference between the rise of atmospheric water content and rainfall is unclear, but these results suggest that the potential for global warming to cause drought may be less than was feared.

Suppressing Emotional Memories

Can people suppress emotional memories and, if so, how do they do it? By examining activity in brain regions that support memory processing, **Depue *et al.*** (p. 215) provide evidence that an active memory suppression mechanism really exists. First, one portion of prefrontal

Continued on page 167

Perfecting qPCR

Quanta BIO SCIENCES

cDNA Synthesis for qPCR

Exceptional representation from less starting material every time.

Introducing qScript™, from Quanta BioSciences, the new standard for reproducibility, specificity, speed, and sensitivity in cDNA synthesis for qPCR. No other product delivers better sample representation, faster, and easier. qScript™ is available in several formats:

- **qScript™ cDNA Supermix**: The first and only optimized one-tube 1st strand cDNA synthesis for 2-step RT-PCR.
- **qScript™ cDNA Synthesis Kit**: Broad reproducibility for 2-step RT-PCR.

qRT-PCR of 5' end of TRRAP gene. 100 ng and 100 pg input levels corresponding to 1 pg and 1 ng of RNA in the first-strand reaction.

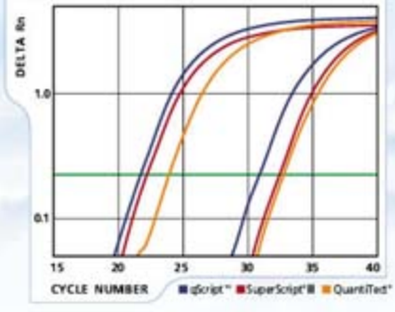

- **qScript™ Flex cDNA Kit**: Priming flexibility and sensitivity for 1st strand cDNA synthesis.
- **qScript™ One-Step qRT-PCR Kit**: Maximum RT-PCR efficiency, sensitivity, and specificity.

The founders of Quanta Biosciences have a legacy of leading the development of pioneering reagents including SuperScript® 1-Step RT-PCR kits, Platinum® *Taq*, iScript™, and iQ™ Supermix. qScript™ is their latest industry-defining product.
To learn more about qScript™ visit **quantabio.com**

qScript™ is a trademark of Quanta BioSciences, Inc. SuperScript® and Platinum® *Taq* are registered trademarks of Invitrogen Corporation. QuantiTect® is a registered trademark of Qiagen N.V. iScript™ and iQ™ are trademarks of Bio-Rad Laboratories, Inc. Quanta BioSciences is licensed for qPCR. See quantabio.com for details.

Order in North America through: VWR vwr.com 1.800.932.5000

Continued from page 165

cortex suppresses regions involved in the sensory aspects of memory. Second, a different part of prefrontal cortex suppresses brain regions that support memory processes as well as those brain areas that support emotional associations with memory. The results may help to explain the lack of control exhibited in a variety of psychiatric disorders, over emotional memories and thoughts, and extend our understanding of brain mechanisms that control their formation.

Chemical Consequences

Global regulators of commercial chemicals apply a scientific paradigm that relates the biomagnification potential of the chemical in food webs to the chemical's hydrophobicity. However, **Kelly *et al.*** (p. 236; see the news story by **Kaiser**) show that current methods fail to recognize the food web biomagnification potential of certain chemicals. Certain chemicals do not biomagnify in most aquatic food chains, but biomagnify to a high degree in air-breathing animals, including humans, because of low respiratory elimination. Thus, additional criteria for evaluating biomagnification and toxicity in chemicals that biomagnify are required.

Crystallized Kinase Regulation

Many human cancers involve gain-of-function mutations in the phosphoinositide 3-kinase PI3Kα. The kinase is a heterodimer of a catalytic subunit (p110α) and a regulatory subunit (p85α), with both subunits comprising multiple domains. **Miled *et al.*** (p. 239; see the Perspective by **Lee *et al.***) have determined the crystal structure of the adaptor-binding domain of p110α bound to the inter-SH2 domain of p85α at 2.4 angstrom resolution, and have performed functional studies to investigate the effect of oncogenic mutations in the helical domain of p110α on its interaction with the N-terminal SH2 domain of p85α. The studies suggest how these two classes of mutations cause the up-regulation of PI3Kα that can lead to cancer.

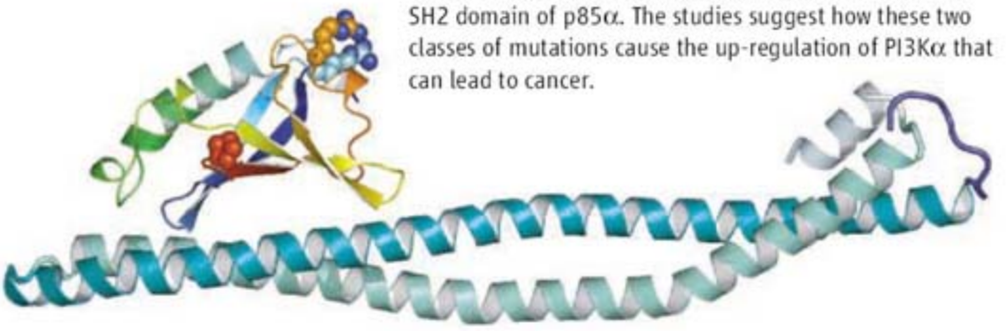

Cohesin Does the Business

To ensure the sorting of a complete complement of chromosomes to both daughter cells in cell division, sister chromatids are bound together by a ring-shaped molecular complex called cohesin. The accurate repair of double-stranded lesions in DNA also relies on cohesion between homologous regions of sister chromatids. Both these processes are often misregulated in cancer. Cohesion has been thought to require ongoing DNA replication (see the Perspective by **Watrin and Peters**). **Ünal *et al.*** (p. 245) and **Ström *et al.*** (p. 242) now show in yeast that double-stranded breaks can induce cohesion in the absence of replication, and that the deposition of cohesin is not limited to the region of the break but extends across the entire genome, and thus may play a role in maintaining genome stability.

Growth Hormone and Development

During development, genes are often transcribed in a temporally and spatially regulated manner. The murine growth hormone gene is differentially expressed in the developing pituitary gland. **Lunyak *et al.*** (p. 248) now examine the region surrounding the growth hormone gene and show that a repeated DNA sequence (short interspersed nuclear element B2) in the growth hormone locus functions as an insulator to produce a boundary for chromatin domains and limit the action of regulatory factors such as enhancers and silencers.

CREDITS (TOP TO BOTTOM): DEPUE *ET AL.*; MILED *ET AL.*

Antimicrobial Peptides

www.cellsciences.com

Antimicrobial peptides are important members of the host defense system. They have functions in inflammation, wound repair and regulation of the adaptive immune system.

Cell Sciences offers the following peptides, antibodies and ELISA kits. Check our website for newly added products. Secure commerce & daily shipping worldwide.

Alpha-Defensin 1-3
Apidaecin
Bactericide (Gram-negative)
Bactericide (Gram-negative/ Gram-positive)
BLP-1
BPI
Calprotectin
Cecropin A
CHIPS
CRISP-3
Elafin/SKALP
Elastase
Fungicide
Galectin-3
Histatin-5
Histatin-8
Indolicidin
Lactoferrin
LBP
LL-37
Lysozyme
Magainin I
Mannose Receptor
Melittin
MPO
MRP-8/MRP-14
Neutroph Defensin 1-3
Neutroph Defensin 5
Ovispirin (OV-1)
Ovispirin (OV-2)
Polymyxin B
Proteinase 3 (PR3)
S100A8/A9
SAAP
SLPI
SMAP29
TfR1
TfR2

cell sciences®
480 Neponset St., Bldg. 12A
Canton, MA 02021
TEL (781) 828-0610
EMAIL info@cellsciences.com
Toll free (888) 769-1246
www.cellsciences.com

Make sure to mention
key code L35AD when registering!

Cambridge Healthtech Institute's Fifth Annual

Discovery on Target 2007

October 15-18, 2007
World Trade Center • Boston, Massachusetts

Developing Inhibitors for Promising Drug Targets

www.DiscoveryOnTarget.com

RNAi for Drug Discovery and Therapeutics
Best Practices from the Bench to the Clinic

Kinase Inhibitors
Moving Forward into Clinical Studies

HDAC Inhibitors
Meeting the Challenge of Chemical Development of HDAC Inhibitors

Ion Channels
An Emerging Target for Therapeutic Development

Nuclear Hormone Receptor Modulators
Targets for Drug Discovery

Oligonucleotide-Based Therapeutics
Lessons Learned

Cambridge Healthtech Institute
250 First Ave, Suite 300, Needham, MA 02494
T: 781-972-5400 or toll-free in the U.S. 888-999-6288
F: 781-972-5425 • www.healthtech.com

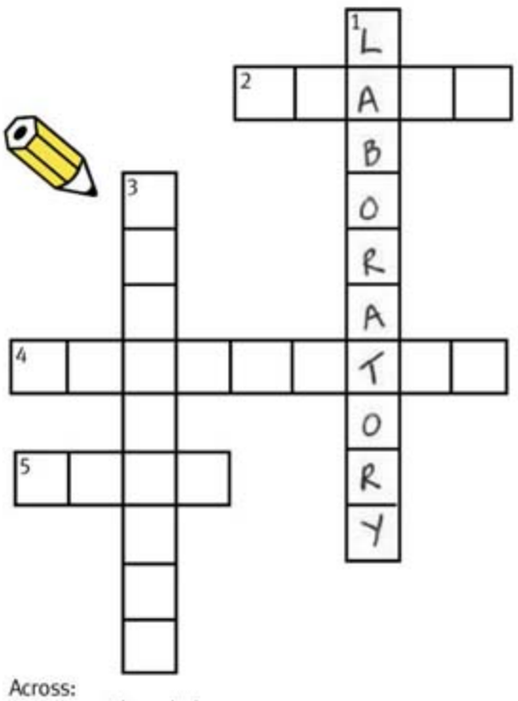

Across:
2. To impart knowledge
4. The science of matter
5. A method for trying or assessing

Down:
1. Place equipped to conduct scientific experiments
3. Variety; multiformity

1. laboratory, 2. teach, 3. diversity, 4. chemistry, 5. test

Searching for some fresh ideas about science education?

Find answers in *Science*'s Education Forum.

The *Science* Education Forum is a dynamic source of information and new ideas on every aspect of science education, as well as the science and policy of education. The forum is published in the last issue of every month and online, in collaboration with the Howard Hughes Medical Institute.

Keep up-to-date with the latest developments at:
www.sciencemag.org/education

What's your perspective?

Do you have ideas or research you'd like to share in the *Science* Education Forum? We're now looking for thoughtful, concise submissions (around 2,000 words) for 2007.

To submit your paper, go to:
www.submit2science.org

Science
AAAS

Donald Kennedy is Editor-in-Chief of *Science*.

Mixed Messages About Climate

EVERY ONCE IN A WHILE, SOMETHING SO UNEXPECTED EMERGES FROM THE Administration in Washington, DC, that it just boggles the mind. On 1 June, I opened the front page of the *New York Times* to see two pictures of President Bush. Under the photo dated 2000, he says this about global warming: "I don't think we know the solution to global warming yet, and I don't think we've got all the facts . . . " But under the 2007 picture, he is calling for a multinational framework for reducing greenhouse gases. Although my environmental friends will hold their applause, this is sounding like progress.

I turn on National Public Radio—same day, same breakfast—and Steve Inskeep is interviewing Michael Griffin, director of the National Aeronautics and Space Administration (NASA). Now, Griffin has been challenged before about morale problems at NASA resulting from the scrapping of various robotic space missions and the fate of Earth-observation programs. So I am astonished to hear Griffin say, in answer to a question about whether NASA has cut anything to make room for the Moon-Mars project, "we have not cut any major priorities." That may have also stunned Inskeep, who turned quickly to a question about global warming.

Here is Griffin's verbatim answer: "I am aware that global warming—I am aware that global warming exists. I understand that the bulk of scientific evidence accumulated supports the claim that we've had about a 1° centigrade rise in temperature over the last century to within an accuracy of about 20%." He added: "I have no doubt that global—that a trend of global warming exists. I am not sure that it is fair to say that it is a problem we must wrestle with."

So the president is telling us that we must lead the G8 nations to set long-term goals for cutting greenhouse gas emissions and is calling on other high-polluting nations to join in the negotiations. Meanwhile, the head of Bush's science agency responsible for Earth observation from space doubts that it's a problem we must wrestle with. Recall that for years, this Administration has been trying to muzzle NASA's Jim Hansen for speaking out on global warming. How strange! Hansen is on message, and his NASA boss is off message!

Soon we are back to climate change, and here is Griffin again: "First of all, I don't think it's within the power of human beings to assure that the climate does not change, as millions of years of history have shown. And second of all, I guess I would ask which human beings, where and when, are to be accorded the privilege of deciding that this particular climate we have right here today, right now, is the best climate for all other human beings. I'm—I think that's a rather arrogant position for people to take." In the first sentence, I guess he's saying that because climates have changed in the deep past, we may not have the power to prevent such change. Of course, we don't know how to engineer a new glacial age or convert one into the Holocene. But it's plain that by mitigating greenhouse gas emissions we might conserve the comparatively balmy climate that our species has lived in for 10,000 years. The second part asks whether particular groups or individuals would have the right to say that the present climate is best or whether some other one is. Well, we have what we have; letting it heat up by doing business as usual sounds pretty arrogant, too. The answer to "who decides" would appear to be that we all do, presumably through a multilateral framework rather like the one the president is now suggesting.

At least, I hope that's right. Griffin has already gotten some press about his statements, but most of the coverage has lost the main point, which is about confusion in government. Do look at the transcript (www.npr.org/about/press/2007/053107.griffinaudio.html) in case you think I am confused or making all this up. I had gotten so used to consistency among the main players in this Administration that all this strikes me as beyond belief.

– Donald Kennedy

10.1126/science.1145963

CREDIT: BILL INGALLS/NASA

EDITED BY GILBERT CHIN AND JAKE YESTON

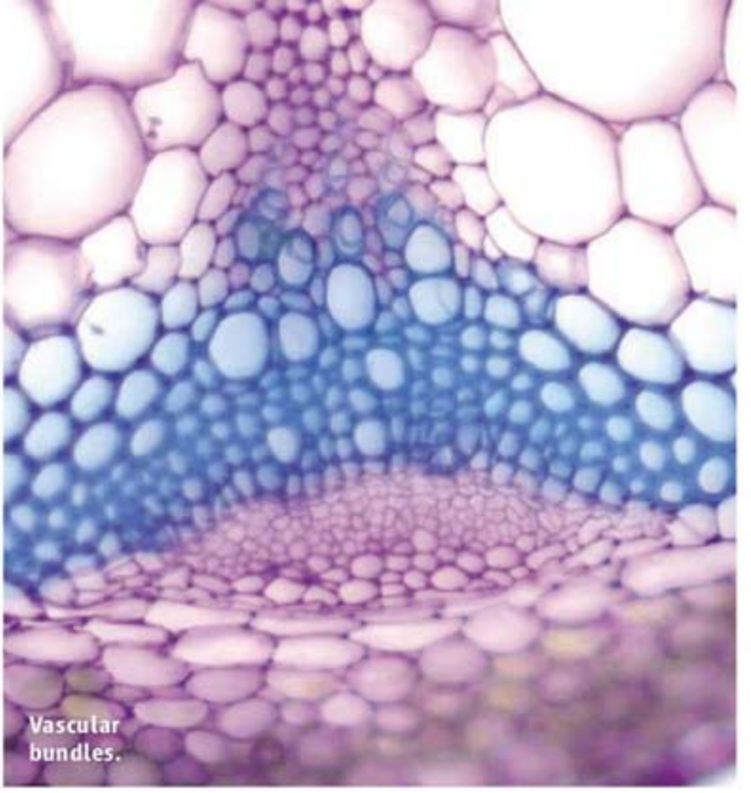
Vascular bundles.

PLANT SCIENCE

Standing Tall

Vascular meristems, though less well known than their flashier sister the apical meristem, have perhaps the bigger job; they produce most of the biomass that makes up plant stems and tree trunks. The vascular meristems also produce the phloem and xylem responsible for the transportation of nutrients throughout the plant. It is the seasonal changes in growth rates from these vascular meristems that give rise to the rings observed in cross-sections of woody trees. Fisher and Turner have identified a mutation in *Arabidopsis* Landsberg *erecta* that affects the organization of those tissues arising from the vascular meristem. In *phloem intercalated with xylem* (*pxy*) mutant plants, the phloem and xylem tissues are not as neatly separated as they are supposed to be, and the cell divisions are not as coordinated as usual. The vessels are irregular in shape and trajectory, and the mature plant is much shorter than the wild type. The protein encoded by *PXY* has sequence features that resemble those of receptor kinases, and *PXY* is expressed in leaves, roots, and stems. The authors speculate that *PXY* may be involved in determining the correct orientation of the cell division plane. — PJH

Curr. Biol. **17**, 1061 (2007).

CELL BIOLOGY

Break Up to Make Up

In animal cells, the endoplasmic reticulum (ER) forms a lacelike network throughout the cytoplasm; in addition, a distinct domain of the ER is used to surround the nuclear material to form the nuclear envelope. ER networks can be produced in cell-free systems, and their formation requires the activity of a pair of ER proteins, Rtn4a and DP1/NogoA. Audhya *et al.* further examined the process of ER network formation in vitro and studied ER dynamics within living cells. In embryos of the nematode *Caenorhabditis elegans*, depletion of the homologs of Rtn4a and DP1/NogoA—RET-1 and YOP-1—produced cellular defects in the peripheral ER network. Furthermore, a member of the small guanosine triphosphatase Rab family, RAB-5, was required for ER network formation in vitro, and in nematode embryos, reduction of RAB-5 also caused peripheral ER defects. RAB-5, RET-1, and YOP-1 were also important in the kinetic control of nuclear envelope disassembly at the beginning of mitosis, as depleting them resulted in the generation of daughter cells with atypical double nuclei. Previously, Rab5 has been shown to be important in the regulation of membrane trafficking during endocytosis. Its effects on ER morphology appear to be independent of these functions, because other perturbations that directly affect endocytosis did not lead to similar defects in ER morphology or to nuclear envelope breakdown during mitosis. — SMH

J. Cell Biol. **178**, 43 (2007).

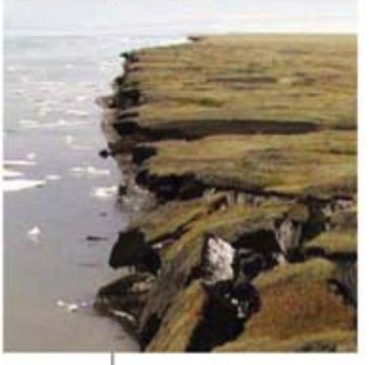

CLIMATE SCIENCE

Warming to Coastal Erosion

High northern latitudes are displaying, as predicted, exceptional sensitivity to recent climate warming, as temperatures there have soared more quickly than in any other part of the world. The effects of these rising temperatures are likely to be dramatic. For example, huge expanses of permafrost are in imminent danger of melting, which would have a tremendous impact on such areas as biogeochemical processes involving greenhouse gases, the physical stability of structures built on the previously frozen ground, and the geomorphology of the region. Mars and Houseknecht have combined data from topographic maps and satellite images to document how coastal land loss and thermokarst lake expansion and drainage have affected a segment of the Beaufort Sea coast of Alaska over the past 50 years. They find that coastal erosion rates more than doubled between the early and later parts of that period, and that the acceleration of coastal erosion rates is due to the longer warm seasons, as open water and wave action associated with earlier pack ice breakup affect the coast. — HJS

Geology **35**, 583 (2007).

CHEMISTRY

Actin Openers Gently Closed

The iejimalide natural products—each composed of a 24-membered ring bearing a peptide tail—pose a considerable synthetic challenge, because the seven C=C double bonds throughout the cycle labilize adjacent chiral centers. Moreover, as Fürstner *et al.* discovered in preliminary explorations, the most apparently selective site for closing the ring—an ester linkage—proves uncooperatively prone to side reactions. The authors instead relied on olefin metathesis for the cyclization, demonstrating remarkable selectivity for the desired reaction site in the presence of so many alternative double bonds. A further advantage of the metathesis protocol was the efficiency of the catalyst at ambient temperature, which protected the precarious molecular framework from thermal rearrangement or decomposition. Having prepared iejimalide B, the authors adapted their synthetic strategy to diversify the structure of the peptide tail. The key was the use of a trimethylsilylethylcarbonate protecting group on nitrogen, which could be easily removed after the cycliza-

CREDITS (TOP TO BOTTOM): FISHER AND TURNER, *CURR. BIOL.* **17**, 1061 (2007); GARY CLOW, USGS

tion step and replaced by a range of acyl or sulfonyl substituents. Like the natural product itself, these analogs proved surprisingly adept at actin depolymerization in cells, raising the prospect of multiple biochemical investigations with this compound class. — JSY

J. Am. Chem. Soc. **129**, 10.1021/ja072334v (2007).

PSYCHOLOGY

The Power of Suggestion

Although it is not uncommon to forget to swing by the grocer's after work only to realize not having done so after arriving at one's front door, it is a quite different experience to have recovered an apparently forgotten memory decades later, especially one pertaining to childhood sexual abuse. Geraerts *et al.* have attempted to assess whether these so-called discontinuous memories are as reliable as continuous (that is, never forgotten) memories of abuse, where reliability was defined operationally as the success with which independent interviewers were able to elicit corroborative evidence from another victim of the alleged perpetrator, from the actual abuser, or from a contemporaneous confidant. In a sample of 130 adults (recruited via advertisement) with either discontinuous or continuous memories of abuse, they find no difference in the percentages (roughly 40%) for which corroboration could be obtained, except in cases where the discontinuous memories were recovered during the course of therapy; for these 16 people, it was not possible to substantiate the recalled events. The authors propose that expectations or suggestions arising during therapy may contribute to the "recovery" of false memories. — GJC

Psychol. Sci. **18**, 564 (2007).

PHYSICS

OH Trapped by Magnets

Confining atoms with a combination of optical and magnetic fields has led to the formation of new states of matter and provided a tunable test bed to explore many-body atomic and electronic interactions; however, its extension to molecules has been slow. Ultracold molecules (milikelvin temperatures and below) are of interest for a number of additional applications, including studies of quantum phase transitions and precision spectroscopy. One approach to confining polar molecules has relied on inhomogeneous electric fields. Sawyer *et al.* present an alternative method that traps molecules magnetically. They demonstrate the technique on hydroxyl (OH) radicals, which have appreciable magnetic as well as electric dipole moments. Lifetimes in the magnetoelectrostatic trap ranged from 20 to 500 ms, depending on the background pressure. The technique allows the additional degree of freedom of an electrical field to be superimposed onto the trapped molecules and should facilitate further studies in the direction of controlled molecular collisions and chemical reactions. — ISO

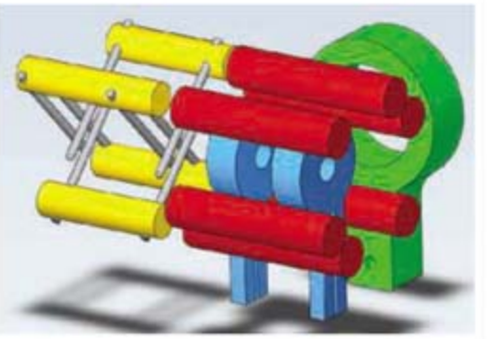

Phys. Rev. Lett. **98**, 253002 (2007).

CREDIT: SAWYER *ET AL.*, *PHYS. REV. LETT.* **98**, 253002 (2007)

Science stke AAAS

www.stke.org

<< Developmental Effects of Decapping

The balance between synthesis and degradation controls mRNA abundance. Goeres *et al.* have found that the 5′ to 3′ mRNA degradation pathway involves an mRNA decapping complex and is crucial for seedling development in *Arabidopsis*. The phenotypes of *varicose* (*vcs*) and *trident* (*tdt*) mutants were similar: defective leaf formation with vein defects, short roots with swollen root hairs, and swollen hypocotyls. Confocal microscopy revealed that the shoot apical meristem cells were disorganized in the *vcs* and *tdt* plants and that leaf primordia were absent in seedlings that were 3 days old, which is when the leaf primordia would normally appear. Further analysis suggested that the *tdt* vascular phenotype arose as a consequence of defective formation of the provascular cell specification, which is controlled by auxin signaling, in the hypocotyl-to-cotyledon transition zone. *TDT* encodes a protein homologous to DCP2, which in yeast and mammals is an mRNA decapping enzyme. VCS, which interacts with TDT, appears to be important for localizing TDT to cytoplasmic P bodies, which are sites of mRNA decapping and degradation. However, in *vcs* and *tdt* mutants, not all mRNAs exhibited decreased decay rates, suggesting that this particular mRNA decay pathway was specific to a subset of transcripts. — NRG

Plant Cell **19**, 1549 (2007).

Science AAAS

EDITOR-IN-CHIEF

The American Association for the Advancement of Science (AAAS), publisher of *Science*, is initiating a search for **Editor-in-Chief**. The journal is published weekly with worldwide circulation to members of the AAAS and institutional subscribers, including libraries. *Science* serves as a forum for the presentation and discussion of important issues relating to the advancement of science, with particular emphasis on the interactions among science, technology, government, and society. It includes reviews and reports of research having interdisciplinary impact.

In selecting an editor-in-chief, the Board of Directors will attach special weight to evidence of significant achievement in scientific research, editorial experience and creativity, awareness of leading trends in the scientific disciplines, and managerial abilities.

Applications or nominations should be accompanied by complete curriculum vitae, including refereed publications, and should be sent to:

Gretchen Seiler
Executive Secretary
Search Committee
1200 New York Avenue, NW
Washington, DC 20005

Salary is negotiable based on qualifications and experience. Application materials should be sent by **August 15, 2007**.

The AAAS is an Equal Opportunity Employer.

www.sciencemag.org

Science

1200 New York Avenue, NW
Washington, DC 20005
Editorial: 202-326-6550, FAX 202-289-7562
News: 202-326-6581, FAX 202-371-9227

Bateman House, 82-88 Hills Road
Cambridge, UK CB2 1LQ
+44 (0) 1223 326500, FAX +44 (0) 1223 326501

SUBSCRIPTION SERVICES For change of address, missing issues, new orders and renewals, and payment questions: 866-434-AAAS (2227) or 202-326-6417, FAX 202-842-1065. Mailing addresses: AAAS, P.O. Box 96178, Washington, DC 20090-6178 or AAAS Member Services, 1200 New York Avenue, NW, Washington, DC 20005

INSTITUTIONAL SITE LICENSES please call 202-326-6755 for any questions or information

REPRINTS: Author Inquiries 800-635-7181
Commercial Inquiries 803-359-4578

PERMISSIONS 202-326-7074, FAX 202-682-0816

MEMBER BENEFITS Bookstore: AAAS/BarnesandNoble.com bookstore www.aaas.org/bn; Car purchase discount: Subaru VIP Program 202-326-6417; Credit Card: MBNA 800-847-7378; Car Rentals: Hertz 800-654-2200 CDP#343457, Dollar 800-800-4000 #AA1115; AAAS Travels: Betchart Expeditions 800-252-4910; Life Insurance: Seabury & Smith 800-424-9883; Other Benefits: AAAS Member Services 202-326-6417 or www.aaasmember.org.

science_editors@aaas.org	(for general editorial queries)
science_letters@aaas.org	(for queries about letters)
science_reviews@aaas.org	(for returning manuscript reviews)
science_bookrevs@aaas.org	(for book review queries)

Published by the American Association for the Advancement of Science (AAAS), *Science* serves its readers as a forum for the presentation and discussion of important issues related to the advancement of science, including the presentation of minority or conflicting points of view, rather than by publishing only material on which a consensus has been reached. Accordingly, all articles published in *Science*—including editorials, news and comment, and book reviews—are signed and reflect the individual views of the authors and not official points of view adopted by the AAAS or the institutions with which the authors are affiliated.

AAAS was founded in 1848 and incorporated in 1874. Its mission is to advance science and innovation throughout the world for the benefit of all people. The goals of the association are to: foster communication among scientists, engineers and the public; enhance international cooperation in science and its applications; promote the responsible conduct and use of science and technology; foster education in science and technology for everyone; enhance the science and technology workforce and infrastructure; increase public understanding and appreciation of science and technology; and strengthen support for the science and technology enterprise.

INFORMATION FOR AUTHORS

See pages 120 and 121 of the 5 January 2007 issue or access www.sciencemag.org/feature/contribinfo/home.shtml

EDITOR-IN-CHIEF **Donald Kennedy**
EXECUTIVE EDITOR **Monica M. Bradford**
DEPUTY EDITORS **R. Brooks Hanson, Barbara R. Jasny, Katrina L. Kelner**
NEWS EDITOR **Colin Norman**

EDITORIAL SUPERVISORY SENIOR EDITOR Phillip D. Szuromi; **SENIOR EDITOR/PERSPECTIVES** Lisa D. Chong; **SENIOR EDITORS** Gilbert J. Chin, Pamela J. Hines, Paula A. Kiberstis (Boston), Marc S. Lavine (Toronto), Beverly A. Purnell, L. Bryan Ray, Guy Riddihough, H. Jesse Smith, Valda Vinson, David Voss; **ASSOCIATE EDITORS** Jake S. Yeston, Laura M. Zahn; **ONLINE EDITOR** Stewart Wills; **ASSOCIATE ONLINE EDITOR** Tara S. Marathe; **BOOK REVIEW EDITOR** Sherman J. Suter; **ASSOCIATE LETTERS EDITOR** Etta Kavanagh; **EDITORIAL MANAGER** Cara Tate; **SENIOR COPY EDITORS** Jeffrey E. Cook, Cynthia Howe, Harry Jach, Barbara P. Ordway, Jennifer Sills, Trista Wagoner; **COPY EDITORS** Lauren Kmec, Peter Mooreside; **EDITORIAL COORDINATORS** Carolyn Kyle, Beverly Shields; **PUBLICATIONS ASSISTANTS** Ramatoulaye Diop, Chris Filiatreau, Joi S. Granger, Jeffrey Hearn, Lisa Johnson, Scott Miller, Jerry Richardson, Brian White, Anita Wynn; **EDITORIAL ASSISTANTS** Maris M. Bish, Emily Guise, Patricia M. Moore, Jennifer A. Seibert; **EXECUTIVE ASSISTANT** Sylvia S. Kihara; **ADMINISTRATIVE SUPPORT** Maryrose Madrid

NEWS SENIOR CORRESPONDENT Jean Marx; **DEPUTY NEWS EDITORS** Robert Coontz, Eliot Marshall, Jeffrey Mervis, Leslie Roberts; **CONTRIBUTING EDITORS** Elizabeth Culotta, Polly Shulman; **NEWS WRITERS** Yudhijit Bhattacharjee, Adrian Cho, Jennifer Couzin, David Grimm, Constance Holden, Jocelyn Kaiser, Richard A. Kerr, Eli Kintisch, Andrew Lawler (New England), Greg Miller, Elizabeth Pennisi, Robert F. Service (Pacific NW), Erik Stokstad; **INTERNS** Benjamin Lester, Marissa Cevallos, Veronica Raymond; **CONTRIBUTING CORRESPONDENTS** Barry A. Cipra, Jon Cohen (San Diego, CA), Daniel Ferber, Ann Gibbons, Robert Irion, Mitch Leslie, Charles C. Mann, Evelyn Strauss, Gary Taubes; **COPY EDITORS** Rachel Curran, Linda B. Felaco, Melvin Gatling; **ADMINISTRATIVE SUPPORT** Scherraine Mack, Fannie Groom; **BUREAUS** Berkeley, CA: 510-652-0302, FAX 510-652-1867, New England: 207-549-7755, San Diego, CA: 760-942-3252, FAX 760-942-4979, Pacific Northwest: 503-963-1940

PRODUCTION DIRECTOR James Landry; **SENIOR MANAGER** Wendy K. Shank; **ASSISTANT MANAGER** Rebecca Doshi; **SENIOR SPECIALISTS** Jay Covert, Chris Redwood; **SPECIALIST** Steve Forrester; **PREFLIGHT DIRECTOR** David M. Tompkins; **MANAGER** Marcus Spiegler; **SPECIALIST** Jessie Mudjitaba

ART DIRECTOR Kelly Buckheit Krause; **ASSOCIATE ART DIRECTOR** Aaron Morales; **ILLUSTRATORS** Chris Bickel, Katharine Sutliff; **SENIOR ART ASSOCIATES** Holly Bishop, Laura Creveling, Preston Huey, Nayomi Kevitiyagala; **ASSOCIATE** Jessica Newfield; **PHOTO EDITOR** Leslie Blizard

***SCIENCE* INTERNATIONAL**

EUROPE (science@science-int.co.uk) **EDITORIAL: INTERNATIONAL MANAGING EDITOR** Andrew M. Sugden; **SENIOR EDITOR/PERSPECTIVES** Julia Fahrenkamp-Uppenbrink; **SENIOR EDITORS** Caroline Ash (Geneva: +41 (0) 222 346 3106), Stella M. Hurtley, Ian S. Osborne, Stephen J. Simpson, Peter Stern; **ASSOCIATE EDITOR** Joanne Baker; **EDITORIAL SUPPORT** Deborah Dennison, Rachel Roberts, Alice Whaley; **ADMINISTRATIVE SUPPORT** Janet Clements, Jill White; **NEWS: EUROPE NEWS EDITOR** John Travis; **DEPUTY NEWS EDITOR** Daniel Clery; **CORRESPONDENT** Gretchen Vogel (Berlin: +49 (0) 30 2809 3902, FAX +49 (0) 30 2809 8365); **CONTRIBUTING CORRESPONDENTS** Michael Balter (Paris), Martin Enserink (Amsterdam and Paris), John Bohannon (Vienna); **INTERN** Krista Zala

ASIA Japan Office: Asca Corporation, Eiko Ishioka, Fusako Tamura, 1-8-13, Hirano-cho, Chuo-ku, Osaka-shi, Osaka, 541-0046 Japan; +81 (0) 6 6202 6272, FAX +81 (0) 6 6202 6271; asca@os.gulf.or.jp; **ASIA NEWS EDITOR** Richard Stone +66 2 662 5818 (rstone@aaas.org); **CONTRIBUTING CORRESPONDENTS** Dennis Normile (Japan: +81 (0) 3 3391 0630, FAX 81 (0) 3 5936 3531; dnormile@gol.com); Hao Xin (China: + 86 (0) 10 6307 4439 or 6307 3676, FAX +86 (0) 10 6307 4358; cindyhao@gmail.com); Pallava Bagla (South Asia: +91 (0) 11 2271 2896; pbagla@vsnl.com)

AFRICA Robert Koenig (contributing correspondent, rob.koenig@gmail.com)

EXECUTIVE PUBLISHER **Alan I. Leshner**
PUBLISHER **Beth Rosner**

FULFILLMENT & MEMBERSHIP SERVICES (membership@aaas.org) **DIRECTOR** Marlene Zendell; **MANAGER** Waylon Butler; **SYSTEMS SPECIALIST** Andrew Vargo; **CUSTOMER SERVICE SUPERVISOR** Pat Butler; **SPECIALISTS** Tamara Alfson, Laurie Baker, Latoya Casteel, Vicki Linton; **DATA ENTRY SUPERVISOR** Cynthia Johnson; **SPECIALISTS** Tomeka Diggs, Tarrika Hill, Erin Layne

BUSINESS OPERATIONS AND ADMINISTRATION DIRECTOR Deborah Rivera-Wienhold; **BUSINESS MANAGER** Randy Yi; **SENIOR BUSINESS ANALYST** Lisa Donovan; **BUSINESS ANALYST** Jessica Tierney; **FINANCIAL ANALYSTS** Michael LoBue, Farida Yeasmin; **RIGHTS AND PERMISSIONS: ADMINISTRATOR** Emilie David; **ASSOCIATE** Elizabeth Sandler; **MARKETING DIRECTOR** John Meyers; **MARKETING MANAGERS** Darryl Walter, Allison Pritchard; **MARKETING ASSOCIATES** Julianne Wielga, Mary Ellen Crowley, Catherine Featherston, Alison Chandler, Lauren Lamoureux; **INTERNATIONAL MARKETING MANAGER** Wendy Sturley; **MARKETING EXECUTIVE** Jennifer Reeves; **MARKETING/MEMBER SERVICES EXECUTIVE** Linda Rusk; **JAPAN SALES** Jason Hannaford; **SITE LICENSE SALES DIRECTOR** Tom Ryan; **SALES AND CUSTOMER SERVICE** Mehan Dossani, Kiki Forsythe, Catherine Holland, Wendy Wise; **ELECTRONIC MEDIA: MANAGER** Lizabeth Harman; **PROJECT MANAGER** Trista Snyder; **ASSISTANT MANAGER** Lisa Stanford; **SENIOR PRODUCTION SPECIALIST** Walter Jones; **PRODUCTION SPECIALISTS** Nichele Johnston, Kimberly Oster

ADVERTISING DIRECTOR WORLDWIDE AD SALES Bill Moran

PRODUCT (science_advertising@aaas.org); **CONSUMER & SPONSORSHIP SALES MANAGER** Tina Morra: 202-326-6542 **MIDWEST** Rick Bongiovanni: 330-405-7080, FAX 330-405-7081 • **WEST COAST/W. CANADA** Teola Young: 650-964-2266 **EAST COAST/E. CANADA** Christopher Breslin: 443-512-0330, FAX 443-512-0331 • **UK/EUROPE/ASIA** Michelle Field: +44 (0) 1223-326-524, FAX +44 (0) 1223-325-532 **JAPAN** Mashy Yoshikawa: +81 (0) 33235 5961, FAX +81 (0) 33235 5852; **SENIOR TRAFFIC ASSOCIATE** Deiandra Simms

COMMERCIAL EDITOR Sean Sanders: 202-326-6430

CLASSIFIED (advertise@sciencecareers.org); **U.S.: RECRUITMENT SALES MANAGER** Ian King: 202-326-6528, FAX 202-289-6742; **INSIDE SALES MANAGER: MIDWEST/CANADA** Daryl Anderson: 202-326-6543; **NORTHEAST:** Allison Millar: 202-326-6572; **SOUTHEAST:** Tina Burks: 202-326-6577; **WEST:** Nicholas Hintibidze: 202-326-6533; **SALES COORDINATORS** Erika Bryant, Rohan Edmonson, Leonard Marshall, Shirley Young; **INTERNATIONAL: SALES MANAGER** Tracy Holmes: +44 (0) 1223 326525, FAX +44 (0) 1223 326532; **SALES** Christina Harrison, Alex Palmer; **SALES ASSISTANT** Louise Moore; **JAPAN:** Jason Hannaford: +81 (0) 52 757 5360, FAX +81 (0) 52 757 5361; **ADVERTISING PRODUCTION OPERATIONS MANAGER** Deborah Tompkins; **SENIOR PRODUCTION SPECIALISTS** Robert Buck, Amy Hardcastle; **SENIOR TRAFFIC ASSOCIATE** Christine Hall; **PUBLICATIONS ASSISTANT** Mary Lagnaoui

AAAS BOARD OF DIRECTORS RETIRING PRESIDENT, CHAIR John P. Holdren; **PRESIDENT** David Baltimore; **PRESIDENT-ELECT** James J. McCarthy; **TREASURER** David E. Shaw; **CHIEF EXECUTIVE OFFICER** Alan I. Leshner; **BOARD** John E. Dowling, Lynn W. Enquist, Susan M. Fitzpatrick, Alice Gast, Linda P. B. Katehi, Cherry A. Murray, Thomas D. Pollard, Kathryn D. Sullivan

AAAS
ADVANCING SCIENCE, SERVING SOCIETY

SENIOR EDITORIAL BOARD

John I. Brauman, *Chair, Stanford Univ.*
Richard Losick, *Harvard Univ.*
Robert May, *Univ. of Oxford*
Marcia McNutt, *Monterey Bay Aquarium Research Inst.*
Linda Partridge, *Univ. College London*
Vera C. Rubin, *Carnegie Institution*
Christopher R. Somerville, *Carnegie Institution*
George M. Whitesides, *Harvard Univ.*

BOARD OF REVIEWING EDITORS

Joanna Aizenberg, *Harvard Univ.*
R. McNeill Alexander, *Leeds Univ.*
David Altshuler, *Broad Institute*
Arturo Alvarez-Buylla, *Univ. of California, San Francisco*
Richard Amasino, *Univ. of Wisconsin, Madison*
Meinrat O. Andreae, *Max Planck Inst., Mainz*
Kristi S. Anseth, *Univ. of Colorado*
John A. Bargh, *Yale Univ.*
Cornelia I. Bargmann, *Rockefeller Univ.*
Marisa Bartolomei, *Univ. of Penn. School of Med.*
Brenda Bass, *Univ. of Utah*
Ray H. Baughman, *Univ. of Texas, Dallas*
Stephen J. Benkovic, *Pennsylvania St. Univ.*
Michael J. Bevan, *Univ. of Washington*
Ton Bisseling, *Wageningen Univ.*
Mina Bissell, *Lawrence Berkeley National Lab*
Peer Bork, *EMBL*
Dianna Bowles, *Univ. of York*
Robert W. Boyd, *Univ. of Rochester*
Paul M. Brakefield, *Leiden Univ.*
Dennis Bray, *Univ. of Cambridge*
Stephen Buratowski, *Harvard Medical School*
Jillian M. Buriak, *Univ. of Alberta*
Joseph A. Burns, *Cornell Univ.*
William P. Butz, *Population Reference Bureau*
Peter Carmeliet, *Univ. of Leuven, VIB*
Gerbrand Ceder, *MIT*
Mildred Cho, *Stanford Univ.*
David Clapham, *Children's Hospital, Boston*
David Clary, *Oxford University*
J. M. Claverie, *CNRS, Marseille*
Jonathan D. Cohen, *Princeton Univ.*
Stephen M. Cohen, *EMBL*
Robert H. Crabtree, *Yale Univ.*
F. Fleming Crim, *Univ. of Wisconsin*
William Cumberland, *UCLA*
George Q. Daley, *Children's Hospital, Boston*
Edward DeLong, *MIT*
Emmanouil T. Dermitzakis, *Wellcome Trust Sanger Inst.*
Robert Desimone, *MIT*
Dennis Discher, *Univ. of Pennsylvania*
Scott C. Doney, *Woods Hole Oceanographic Inst.*
W. Ford Doolittle, *Dalhousie Univ.*
Jennifer A. Doudna, *Univ. of California, Berkeley*
Julian Downward, *Cancer Research UK*
Denis Duboule, *Univ. of Geneva/EPFL Lausanne*
Christopher Dye, *WHO*
Richard Ellis, *Cal Tech*
Gerhard Ertl, *Fritz-Haber-Institut, Berlin*
Douglas H. Erwin, *Smithsonian Institution*
Barry Everitt, *Univ. of Cambridge*
Paul G. Falkowski, *Rutgers Univ.*
Ernst Fehr, *Univ. of Zurich*
Tom Fenchel, *Univ. of Copenhagen*
Alain Fischer, *INSERM*
Jeffrey S. Flier, *Harvard Medical School*
Chris D. Frith, *Univ. College London*
John Gearhart, *Johns Hopkins Univ.*
Wulfram Gerstner, *Swiss Fed. Inst. of Technology*
Charles Godfray, *Univ. of Oxford*
Christian Haass, *Ludwig Maximilians Univ.*
Dennis L. Hartmann, *Univ. of Washington*
Chris Hawkesworth, *Univ. of Bristol*
Martin Heimann, *Max Planck Inst., Jena*
James A. Hendler, *Rensselaer Polytechnic Inst.*
Ray Hilborn, *Univ. of Washington*
Ove Hoegh-Guldberg, *Univ. of Queensland*
Ary A. Hoffmann, *La Trobe Univ.*
Ronald R. Hoy, *Cornell Univ.*
Evelyn L. Hu, *Univ. of California, Santa Barbara*
Olli Ikkala, *Helsinki Univ. of Technology*
Meyer B. Jackson, *Univ. of Wisconsin Med. School*
Stephen Jackson, *Univ. of Cambridge*
Steven Jacobsen, *Univ. of California, Los Angeles*
Peter Jonas, *Universität Freiburg*
Daniel Kahne, *Harvard Univ.*
Bernhard Keimer, *Max Planck Inst., Stuttgart*
Elizabeth A. Kellog, *Univ. of Missouri, St. Louis*
Alan B. Krueger, *Princeton Univ.*
Lee Kump, *Penn State*
Mitchell A. Lazar, *Univ. of Pennsylvania*
Virginia Lee, *Univ. of Pennsylvania*
Anthony J. Leggett, *Univ. of Illinois, Urbana-Champaign*
Michael J. Lenardo, *NIAID, NIH*
Norman L. Letvin, *Beth Israel Deaconess Medical Center*
Olle Lindvall, *Univ. Hospital, Lund*
Richard Losick, *Harvard Univ.*
Ke Lu, *Chinese Acad. of Sciences*
Andrew P. MacKenzie, *Univ. of St. Andrews*
Raul Madariaga, *École Normale Supérieure, Paris*
Anne Magurran, *Univ. of St. Andrews*
Michael Malim, *King's College, London*
Virginia Miller, *Washington Univ.*
Yasushi Miyashita, *Univ. of Tokyo*
Richard Morris, *Univ. of Edinburgh*
Edvard Moser, *Norwegian Univ. of Science and Technology*
Andrew Murray, *Harvard Univ.*
Naoto Nagaosa, *Univ. of Tokyo*
James Nelson, *Stanford Univ. School of Med.*
Roeland Nolte, *Univ. of Nijmegen*
Helga Nowotny, *European Research Advisory Board*
Eric N. Olson, *Univ. of Texas, SW*
Erin O'Shea, *Harvard Univ.*
Elinor Ostrom, *Indiana Univ.*
Jonathan T. Overpeck, *Univ. of Arizona*
John Pendry, *Imperial College*
Philippe Poulin, *CNRS*
Mary Power, *Univ. of California, Berkeley*
Molly Przeworski, *Univ. of Chicago*
David J. Read, *Univ. of Sheffield*
Les Real, *Emory Univ.*
Colin Renfrew, *Univ. of Cambridge*
Trevor Robbins, *Univ. of Cambridge*
Barbara A. Romanowicz, *Univ. of California, Berkeley*
Nancy Ross, *Virginia Tech*
Edward M. Rubin, *Lawrence Berkeley National Lab*
J. Roy Sambles, *Univ. of Exeter*
Jürgen Sandkühler, *Medical Univ. of Vienna*
David S. Schimel, *National Center for Atmospheric Research*
Georg Schulz, *Albert-Ludwigs-Universität*
Paul Schulze-Lefert, *Max Planck Inst., Cologne*
Terrence J. Sejnowski, *The Salk Institute*
David Sibley, *Washington Univ.*
Montgomery Slatkin, *Univ. of California, Berkeley*
George Somero, *Stanford Univ.*
Joan Steitz, *Yale Univ.*
Elsbeth Stern, *ETH Zürich*
Thomas Stocker, *Univ. of Bern*
Jerome Strauss, *Virginia Commonwealth Univ.*
Marc Tatar, *Brown Univ.*
Glenn Telling, *Univ. of Kentucky*
Marc Tessier-Lavigne, *Genentech*
Michiel van der Klis, *Astronomical Inst. of Amsterdam*
Derek van der Kooy, *Univ. of Toronto*
Bert Vogelstein, *Johns Hopkins*
Christopher A. Walsh, *Harvard Medical School*
Graham Warren, *Yale Univ. School of Med.*
Colin Watts, *Univ. of Dundee*
Julia R. Weertman, *Northwestern Univ.*
Jonathan Weissman, *Univ. of California, San Francisco*
Ellen D. Williams, *Univ. of Maryland*
R. Sanders Williams, *Duke University*
Ian A. Wilson, *The Scripps Res. Inst.*
Jerry Workman, *Stowers Inst. for Medical Research*
John R. Yates III, *The Scripps Res. Inst.*
Martin Zatz, *NIMH, NIH*
Huda Zoghbi, *Baylor College of Medicine*
Maria Zuber, *MIT*

BOOK REVIEW BOARD

John Aldrich, *Duke Univ.*
David Bloom, *Harvard Univ.*
Angela Creager, *Princeton Univ.*
Richard Shweder, *Univ. of Chicago*
Ed Wasserman, *DuPont*
Lewis Wolpert, *Univ. College, London*

Applied Biosystems

Three-time Award Winning RNAi Products. Full-time RNAi Expertise.

The Life Science LSIA 2007 Industry Awards

Ambion, now an Applied Biosystems Business, has won the Life Science Industry Award for "Best in Class" RNAi Products for the third year in a row. Chosen this year from a field of 28 suppliers, this award represents the voice of more than 3,000 life scientists—you, our customers. *The Scientist* magazine sponsors this prestigious award with the support of The Life Science Executive Exchange and The Science Advisory Board. BioInformatics, LLC, a leading market research firm collects the votes and tallies the results.

www.ambion.com/rnai

- *Silencer*® Pre-designed siRNAs
- *Silencer*® Validated siRNAs
- Custom siRNAs
- *Silencer*® Control siRNAs
- siRNA Libraries
- *Silencer*® In Vivo Ready siRNAs
- Transfection/Electroporation of siRNAs
- Analysis of siRNAs and RNAi Effects
- In Vitro Transcription of siRNAs
- siRNA Expression Vectors
- In Vitro Transcription of Long dsRNAs
- GeneAssist™ Pathway Atlas

Tell us about your research and get a

free GeneAssist™ Pathway Atlas mug

Visit www.ambion.com/surveys/rnai *to take the short survey.*

For Research Use Only. Not for use in diagnostic procedures. Applied Biosystems and AB (Design) are registered trademarks of Applera Corporation or its subsidiaries in the US and/or certain other countries. Ambion and *Silencer* are registered trademarks and GeneAssist is a trademark of Ambion, Inc. in the US and/or certain other countries. The free mug is available while supplies last and the offer is only valid in the US, Canada, and Europe. This offer is void where prohibited. © Copyright 2007 Applied Biosystems. All rights reserved

U.S./Canada (English) 800-327-3002
U.S./Canada (French) 800-668-6913
Fax +1-512-651-0201

Europe
tel +44 (0)1480-373-020
fax +44 (0)1480-373-010

Japan
tel 81 (0) 3 5566 6230
fax 81 (0) 3 5566 6507

Direct free phone numbers, distributors:
www.appliedbiosystems.com

Ambion®

What's the quickest link to advances in the world of science?

AAAS

AAAS Advances—the free monthly e-newsletter exclusively for AAAS members.

Each month, AAAS members keep up with the speed of science via a quick click on the newsletter Advances.

Look for the next issue of Advances delivered to your inbox mid month. Look up archived issues at aaas.org/advances.

Features include:

- A special message to members from Alan Leshner, AAAS CEO
- Timely news on U.S. and international AAAS initiatives
- Just-released reports and publications
- Future workshops and meetings
- Career-advancing information
- AAAS members-only benefits

All for AAAS members only.

aaas.org/advances

Science
AAAS

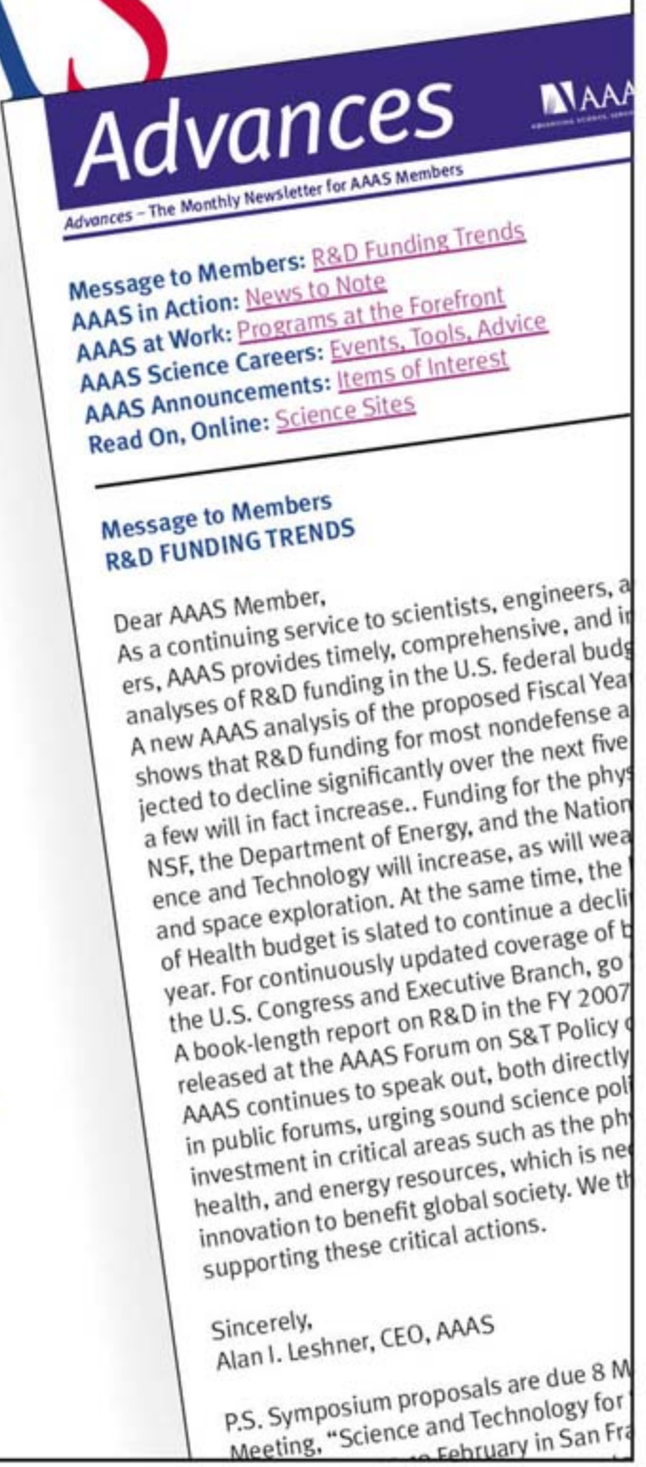
Advances

Advances – The Monthly Newsletter for AAAS Members

Message to Members: R&D Funding Trends
AAAS in Action: News to Note
AAAS at Work: Programs at the Forefront
AAAS Science Careers: Events, Tools, Advice
AAAS Announcements: Items of Interest
Read On, Online: Science Sites

Message to Members
R&D FUNDING TRENDS

Dear AAAS Member,
As a continuing service to scientists, engineers, a
ers, AAAS provides timely, comprehensive, and i
analyses of R&D funding in the U.S. federal budg
A new AAAS analysis of the proposed Fiscal Yea
shows that R&D funding for most nondefense a
jected to decline significantly over the next five
a few will in fact increase.. Funding for the phys
NSF, the Department of Energy, and the Nation
ence and Technology will increase, as will wea
and space exploration. At the same time, the
of Health budget is slated to continue a decli
year. For continuously updated coverage of b
the U.S. Congress and Executive Branch, go
A book-length report on R&D in the FY 2007
released at the AAAS Forum on S&T Policy
AAAS continues to speak out, both directly
in public forums, urging sound science poli
investment in critical areas such as the phy
health, and energy resources, which is ne
innovation to benefit global society. We th
supporting these critical actions.

Sincerely,
Alan I. Leshner, CEO, AAAS

P.S. Symposium proposals are due 8 M
Meeting, "Science and Technology for
February in San Fra

Migraine-inspired painting.

Art that Jars

Some images are literally eyesores. Scientists have long known that the wrong mix of shapes and colors can cause discomfort, headaches, or even seizures. Now, they're starting to figure out why.

Psychologist Arnold Wilkins of the University of Essex, U.K., and artist Debbie Ayles—who creates paintings inspired by her migraines—used a Sciart grant from the Wellcome Trust to tease out the keys to annoying art. Focus groups at an exhibition of Ayles's work last year helped identify narrow stripes and juxtaposed complementary colors as inducers of discomfort. Wilkins then compared the subjective ratings of a variety of paintings with each picture's energy intensity, measured by Fourier analysis of stripes' spatial frequency.

At a talk in Cambridge, U.K., last week, Wilkins said the pictures the focus groups found unpleasant featured vertical stripes at the width that we're visually most sensitive to—about 3 stripes per degree of the visual field (a finger held at arm's length corresponds to about 1 degree). The stripe factor applies to type fonts, too—letter length and thickness make Times New Roman a slower read than Verdana, says Wilkins. He says his results can be applied to design, from picking an optimal type size and font for children's books to choosing public murals.

What's Current In E-Chem

NET WATCH

What happens when you zap a chemical solution is the electrochemist's bailiwick. However, general readers can charge up their brains on the field's applications and history at the Electrochemistry Encyclopedia,* edited by retired chemist Zoltan Nagy of the Argonne National Laboratory in Illinois. The subjects of the 25 expert-written chapters range from electroplating to electric fish to pioneering electrochemists. Read about electrochemical machining, which uses a current to shape hard-to-work alloys, or explore the life of the Italian scientist Alessandro Volta, who sparked the nascent discipline more than 200 years ago by building the first battery.

If your memory short-circuits over unfamiliar terms, click over to the linked dictionary † that furnishes 800 definitions. >>

* electrochem.cwru.edu/ed/encycl

† electrochem.cwru.edu/ed/dict.htm

The Health Benefits Of Paleocuisine

Swedish men with diabetes showed a dramatic drop in their blood sugar after 3 months on a "Paleolithic" diet, according to researchers in Sweden, who found that a diet free of grains and dairy products worked better than the oft-recommended "Mediterranean" diet.

Of 29 men with heart disease and diabetic conditions, 14 showed blood sugar returning to normal after restricting themselves to lean meat, fish, fruits, root vegetables, eggs, and nuts. What's more, their glucose tolerance improved by 26%, as shown when glucose levels were tested after they ate sugars. But the 15 men on the Mediterranean diet, whose intake included grains and dairy products, showed only a 7% improvement in glucose tolerance, according to Lund University physician Staffan Lindeberg, whose study was published online this month in *Diabetologia*. Lindeberg says the study was inspired when he learned in the 1990s that Papua New Guinea's Trobriand islanders, who live on a "preagricultural" diet, had no heart disease or diabetes.

Lindeberg speculates that a Stone Age diet may owe its success with diabetics to the absence of "bioactive substances," such as the casein protein in milk and lectin in grains, which may impair glucose tolerance—as they do in studies of rats.

Evolutionary nutritionist Loren Cordain of Colorado State University in Fort Collins says the study is "significant" because "it represents one of the first well-controlled trials of a modern paleo-like diet to ever have been conducted."

BEAUTY WITH BRAWN

Lustrous mother-of-pearl may fetch millions, but the material's might, not its iridescence, is what has scientists swooning. Mother-of-pearl, or nacre, is 3000 times stronger than the brittle mineral aragonite of which it's composed. Now, physicists at the University of Wisconsin, Madison, have shined synchrotron radiation on thin layers of nacre to reveal its secret: irregular columns of crystals, like clumsily stacked bricks, resist breaking. Their report is in the 29 June *Physical Review Letters*.

CREDITS (TOP TO BOTTOM): D. AYLES; J. MILLER/UNIVERSITY OF WISCONSIN, MADISON

Institutional Site License Available

Q What can *Science* STKE give me?

A The definitive resource on cellular regulation

STKE – Signal Transduction Knowledge Environment offers:

- A weekly electronic journal
- Information management tools
- A lab manual to help you organize your research
- An interactive database of signaling pathways

STKE gives you essential tools to power your understanding of cell signaling. It is also a vibrant virtual community, where researchers from around the world come together to exchange information and ideas. For more information go to www.stke.org

To sign up today, visit promo.aaas.org/stkeas

Sitewide access is available for institutions.
To find out more e-mail stkelicense@aaas.org

Science stke AAAS

EDITED BY YUDHIJIT BHATTACHARJEE

Movers

WEARY. When Alan Bernstein (left) agreed to lead the newly minted Canadian Institutes of Health Research (CIHR) in 2000, he vowed to spend as much as 30% of the agency's budget—6 times erstwhile spending levels—on research targeting population, health services, and other national needs. Bernstein has since accomplished that goal, but he's so worn out from battling community opposition to the shift that he plans to resign 3 years before the end of his second term.

The new emphasis was fine in the early years, he says, when CIHR was receiving double-digit increases and there was enough money for other grant competitions. But in the last 3 years, the budget has grown much more slowly, causing the community to complain about how CIHR was divvying up its money. As a result, the agency recently created a committee—made up primarily of directors of CIHR's 13 research institutes—to decide how to split the pie.

Still, Bernstein, 60, says he'll be leaving in October on a high note. "Getting the CIHR going in the right direction, I think that's done," he says.

PIONEERS

SMOKELESS CITY. Civil engineer Russel Jones has been tapped to lead the latest effort aimed at bolstering Arab science. The Masdar project is a green city and alternative energy center to be built in Abu Dhabi, capital of the United Arab Emirates (UAE). The $5 billion, 6-square-kilometer, zero-emission township will include The Masdar Institute, to be focused on graduate education and research on alternative energy, such as solar power and biofuels. Last week, Jones, who will serve as the institute's president, made offers to 11 scientists from around the world. Until the institute is built—by 2009—the researchers will be housed at the Massachusetts Institute for Technology in Cambridge, under a 5-year, $35 million agreement with the school.

Jones, who helped create the undergraduate Hashemite University in Zarqa, Jordan, in 1996, says he was energized by oil-drenched Abu Dhabi's plans to diversify its energy investments. The institute expects to forge links with some of the 1500 energy firms the UAE hopes to attract to the new city.

POLITICS

NO STRANGER TO SCIENCE. Ian Pearson may be a businessman turned politician, but he's been given the job of shaping British research policy in Gordon Brown's new government. The new science honcho is one of five ministers in the newly created Department for Innovation, Universities and Skills (DIUS) (*Science*, 6 July, p. 28).

A Labour Party politician since 1994, he most recently served as minister for climate change and environment in Tony Blair's Cabinet, helping to introduce the Climate Change Bill that is currently working its way through Parliament. "Despite not being a natural environmentalist during his time at the environment ministry, the government began to take the issue of climate change much more seriously," says Martyn Williams, climate change campaigner for Friends of the Earth in London.

Members of Brown's Administration have said they're committed to continuing the healthy increases to the science budget that occurred during Blair's Administration. Pearson (below) faces the problems of poor science teaching in high schools and a declining number of science students at university (*Science*, 18 May, p. 965). "You don't have to be a scientist to be science minister, but he will need a broad knowledge of schools and business," says Peter Cotgreave of the U.K.'s Campaign for Science and Engineering.

AWARDS

GRUBER PRIZES. A Japanese neuroscientist and a U.S. genomicist each have won $500,000 from the Peter and Patricia Gruber Foundation. Shigetada Nakanishi, head of the Osaka Bioscience Institute, receives the neuroscience award for identifying new genes and proteins that play a role in brain function, as well as pinpointing neuronal receptors involved in the biochemical processes underlying learning, memory, and vision. Maynard Olson, a professor at the University of Washington in Seattle, wins the genetics prize for pioneering a technique for cloning and storing large chunks of DNA, which helped pave the way for the human genome project.

Three Q's >>

After 11 years as head of the National Science Teachers Association, **Gerry Wheeler** says, "it's time to let someone else have all the fun." Wheeler will retire from the 55,000-strong organization in August 2008.

Q: What are the keys to improving U.S. science education?

Science, scale, and standards. We need to help teachers improve their content knowledge. And with 2 million science teachers in the classroom, we need to work on a bigger scale. We also need to streamline the standards that specify what children should learn.

Q: Has the No Child Left Behind Act been a help or a hindrance to science teachers?

It's changed the landscape in a good way, I think, by putting the spotlight on accountability. But we need to make sure that science doesn't get lost in the emphasis on testing student achievement in reading and math.

Q: What's standing in the way of change?

Business leaders get it, and politicians get it. But parents don't get it. I was part of the Sputnik generation, when there was a huge push for kids to learn more science. That's no longer the case.

Got a tip for this page? E-mail people@aaas.org

CREDITS (TOP TO BOTTOM): CIHR; STEVE BARRETT PHOTOGRAPHY; B. MATHUR/REUTERS

The 2006 greenhouse 182

Bioaccumulating organics 182

ASTROPHYSICS

Enormous Detector Forces Rethink Of Highest Energy Cosmic Rays

MERIDA, MEXICO—When, a decade ago, physicists in Japan reported seeing far more ultrahigh-energy cosmic rays than expected, some theorists interpreted the excess as a hint of exotic new particles—perhaps supermassive relics from the big bang that could be part of the mysterious dark matter whose gravity holds the galaxies together. But the controversial excess of superenergetic particles from space has a simpler explanation, researchers with a far larger detector array now say: It doesn't exist.

That conclusion, reported here* last week, may be the most important early result from the Pierre Auger Observatory, which sprawls across the Pampa Amarilla in western Argentina. It's also a disappointment for researchers in the field of ultrahigh-energy cosmic rays. "It is less sexy than before, that's for sure," says Yoshiyuki Takahashi of the University of Alabama, Huntsville.

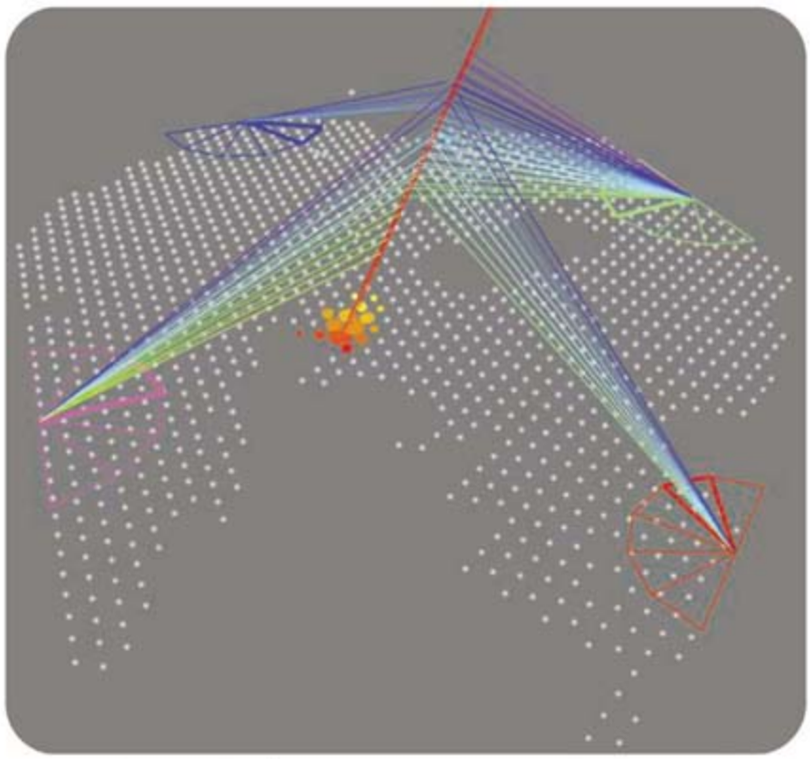

Four eyes. All four of Auger's fluorescence detectors spotted this high-energy cosmic ray. The gigantic array sees no excess of highest energy rays.

Still, plenty of mystery remains. Auger and other arrays do see some cosmic rays with the energy of a large hailstone, and physicists still can't say how or where in the heavens a single subatomic particle might gain such energy. But now that researchers see that the number of cosmic rays dives as expected at very high energies, explanations will likely turn from exotic particles to the astrophysics of stars and galaxies.

The purported excess sparked controversy years ago (*Science*, 21 June 2002, p. 2134). From 1990 to 2004, physicists with the Akeno Giant Air Shower Array (AGASA) west of Tokyo spotted roughly a dozen particles crashing to earth at energies of 100 exa-electron volts (EeV), about 100 million times higher than any particle accelerator has achieved. Physicists believe cosmic rays gain energy as they swirl in magnetic fields, and they couldn't think of any object in space both big enough and wielding a strong enough magnetic field to contain particles until they reach such staggering energies. So some speculated that the rays blast out of the decays of supermassive particles.

The excess also clashed with an energy limit predicted in the 1960s. If each ray is a proton, then at energies above about 40 EeV it should interact with the photons in the afterglow of the big bang, the cosmic microwave background, in a way that saps its energy to 40 EeV within a distance of 300 million light years. If AGASA was seeing rays with energies above this "GZK cutoff," then they had to originate in the cosmic neighborhood.

Moreover, another group saw no excess. Whereas AGASA researchers detected 11 rays with energies greater than 100 EeV, physicists with the High-Resolution Fly's Eye (Hi-Res) detector at the U.S. Army's Dugway Proving Ground in Utah saw only a couple. The two detectors are very different, however. When a high-energy cosmic ray strikes the atmosphere, it triggers a cascade of billions of particles called an extensive air shower. AGASA used 111 detectors spread over 100 square kilometers of ground to measure the showers. In contrast, Hi-Res used twin batteries of specialized telescopes to detect the light produced when the shower causes nitrogen molecules in the air to fluoresce.

The Auger array uses both techniques. Covering 3000 square kilometers and comprising more than 1300 surface detectors and 24 fluorescence telescopes in four batteries, the almost-completed array has already collected enough data to rule out the excess. "If AGASA had been correct, then we should have seen 30 events [at or above 100 EeV], and we see two," says Alan Watson of the University of Leeds, U.K., who is the spokesperson for the Auger collaboration. The Auger data also show that very few of the most energetic rays are photons. As supermassive particles ought to decay readily into photons, that finding undermines exotic-particle musings, says Glennys Farrar, a theorist at New York University who joined the 300-member Auger collaboration in September.

Meanwhile, researchers working with Hi-Res, which stopped taking data last year, say the shape of their final spectrum of cosmic ray energies definitely proves the rays are running up against the GZK cutoff. "It looks very much like what everyone has been predicting," says Pierre Sokolsky of the University of Utah in Salt Lake City. "It's the classic GZK signature." Others aren't so sure. Auger's data suggests the highest energy rays comprise protons and heavier nuclei, which don't feel the GZK drag, Watson says. Instead of being ▶

CREDIT: PIERRE AUGER OBSERVATORY

* 30th International Cosmic Ray Conference, 3–11 July

Capturing carbon 184

Autism and the synapse 190

slowed, the nuclei may never be accelerated to 40 EeV, he says.

Whatever its cause, the fall-off leads some to question the need to build a bigger array, as the Auger team hopes to do in the Northern Hemisphere. "Once you see the cutoff—even if you disagree about what it is—then building a bigger detector hardly gets you anything," because there are so few higher energy particles to capture, says Gordon Thomson, a Hi-Res member from Rutgers University in Piscataway, New Jersey. Members of the Hi-Res and AGASA teams are building a detector in Utah called the Telescope Array, which will be three-eighths the size of Auger. That may be just the right size, Thomson says.

Others say that only a bigger array can amass enough data to trace the fall-off in detail. "Now we understand that above the GZK cutoff there are ten times less cosmic rays than we thought 10 years ago, so we may need a detector ten times as big as Auger," says Masahiro Teshima of the Max Planck Institute for Physics in Munich, Germany, who worked on AGASA and is working on the Telescope Array.

The few highest energy, straightest flying particles will be crucial for determining whether high-energy cosmic rays emanate from particular points or patches in the sky, says James Cronin of the University of Chicago, Illinois, who, with Watson, dreamed up the Auger array in the early 1990s. Such "anisotropy" might reveal the rays' origins, and "if we can show an anisotropy, then that's a brilliant breakthrough," he says. Mapping the sky could take a decade—although Cronin and Watson hint they may have already seen something exciting that's not yet ready for release. **–ADRIAN CHO**

HIV/AIDS

India Slashes Estimate of HIV-Infected People

Contrary to previous estimates, India does not have more HIV-infected people than any country in the world, says a new analysis by government health officials. Improved and widened surveys of the country's massive population has led India's National AIDS Control Organization (NACO) to slash by more than half the estimated number of people infected, from 5.7 million to 2.5 million. NACO, which announced the new figures on 6 July, says HIV thus infects 0.36% of the country's adults, rather than 0.9%. "The figures are now much more realistic," says N. K. Ganguly, the head of the Indian Council of Medical Research in New Delhi who chaired a meeting that reviewed the new NACO numbers. Ganguly, who long worried that epidemiologists had exaggerated the scale of India's epidemic, adds that he was "very happy" that a look back analysis also found that HIV was not gaining ground in this huge country.

The Joint United Nations Programme on HIV/AIDS (UNAIDS), which advised NACO and earlier issued the higher estimate, supports the new figures. "We're much more confident that the estimates being put out are as accurate as they can be," says epidemiologist Peter Ghys, who heads the UNAIDS branch that produces the oft-cited estimates for most countries.

In the past, India's HIV estimates have relied heavily on a limited number of "sentinel" surveillance sites, like clinics for pregnant women. But such analyses capture more data from urban than rural areas and miss many high-risk groups such as injecting drug users or men who have sex with men. The new analysis includes data from 400 new sentinel sites added since 2006—there were just 764 in 2005—as well as voluntary blood samples taken from more than 100,000 people in a national household survey.

NACO's estimates of HIV-infected people still are far from exact, ranging from 2 million to 3.1 million. But that's more certainty than portrayed by UNAIDS in 2006, which estimated India's HIV-infected population at 3.4 million to 9.4 million. The range is "some indication that at the time we were not as confident as we are today about the estimates," says UNAIDS's Ghys.

The lowered estimates and the reanalysis of data back to 2002 indicate that the country has had a stable epidemic with a "marginal decline" last year, NACO says. This challenges the idea that India is on an "African trajectory"—with the virus moving from concentrated risk groups such as sex workers and truck drivers to ▶

Country	HIV/AIDS cases (millions)	Adult prevalence (%)	Population (millions)
South Africa	5.5	18.6	44
Nigeria	2.9	3.9	135
India	2.5	0.3	1,129
Mozambique	1.8	16.1	21
Swaziland	0.22	33.4	1.1
United States	1.2	0.6	301

No longer number one. Much wider sampling, including a national household survey that goes well beyond the "sentinel" surveillance sites, like the clinic above in Kolkata, has led to new, lower estimates of size of the AIDS epidemic in India.

CREDITS: MALCOLM LINTON (PHOTO); UNAIDS/CIA/NACO (DATA)

INSPIRED BY THE PAST

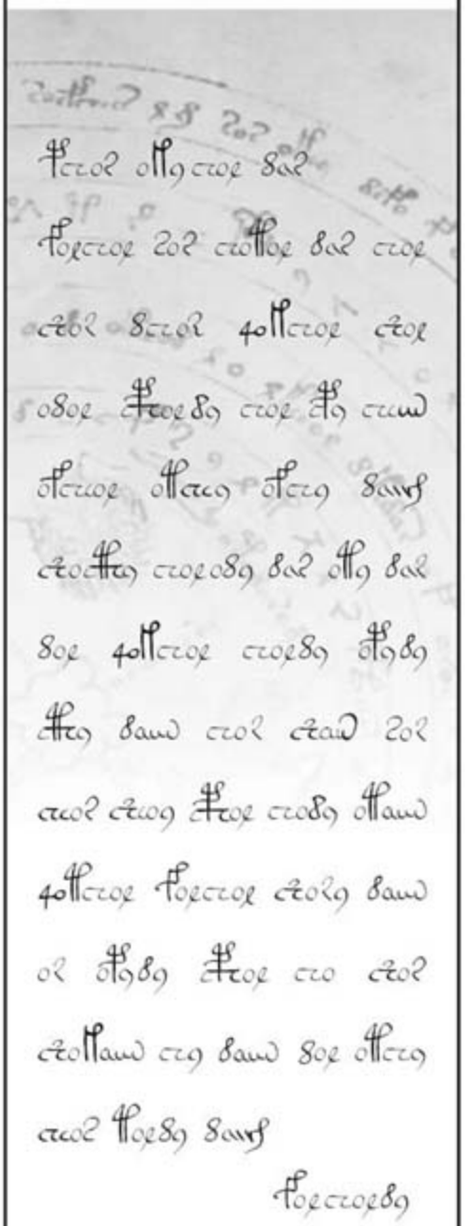

"Rome was not built in a day."

Dedicated foundations please contact:

R.D.S. HOTTMANN
Postfach 760428
22054 Hamburg
Germany

Digital image by courtesy of Yale University Beinecke Rare Book and Manuscript Library

© 2007. All rights reserved.

What makes a first-class news story?

Jennifer Couzin

- 2006 article selected for inclusion in *The Best American Science Writing 2007*
- 2004 article selected for inclusion in *The Best American Science Writing 2005*
- 2003 Evert Clark/Seth Payne Award for Young Science Journalists

A first-class writer.
Award-winning journalists write for *Science*—with 12 top awards in the last four years. That's why we have the most compelling stories, and the biggest readership of any general scientific publication. To see the complete list of awards go to: sciencemag.org/newsawards

Science
AAAS

Who's helping bring the gift of science to everyone?

"As a child I got very interested in space travel. When I was six my father gave me some books on rockets and stars. And my universe suddenly exploded in size because I realized those lights in the sky I was looking at were actually places.

I wanted to go there. And I discovered that science and technology was a gift that made this possible. The thrill of most Christmas presents can quickly wear off. But I've found that physics is a gift that is ALWAYS exciting.

I've been a member of AAAS for a number of years. I think it's important to join because AAAS represents scientists in government, to the corporate sector, and to the public. This is very vital because so much of today's science is not widely understood.

I also appreciate getting *Science* because of the breadth of topics it covers."

Jim Gates is a theoretical physicist and professor at the University of Maryland. He's also a member of AAAS.

See video clips of this story and others at www.aaas.org/stories

AAAS
ADVANCING SCIENCE, SERVING SOCIETY

the general population—a controversial assertion made by epidemiologist Richard Feachem, former head of the Global Fund to Fight AIDS, Tuberculosis and Malaria (*Science*, 23 April 2004, p. 504). India expert and epidemiologist Robert Bollinger of Johns Hopkins University in Baltimore, Maryland, co-authored a 9 October 2004 *Lancet* article with Indian colleagues that explicitly criticized Feachem's prediction. "Frankly, I wouldn't be surprised if there were 6.1 million or 5 million or 2.5 million infected people, but the point is the epidemic is different in India," says Bollinger. A key distinction, he says, is outside of commercial sex workers, Indian women rarely have more than one sexual partner at the same time, a major driver of epidemics.

Suniti Solomon, who runs a private clinic in Chennai, YRG Care, stresses that India still faces a formidable challenge. "Whatever the numbers, if we are complacent … the virus will spread faster," says Solomon. And she says many infected people still do not have access to anti-HIV drugs. The country is also seeing "worrying" rates of people who fail to respond to treatment and need more expensive second-line drugs, she says.

According to an April report issued by UNAIDS, the World Health Organization, and UNICEF, India had just over 55,000 people receiving anti-HIV drugs as of November 2006. The report, which relied on the old calculations of HIV prevalence, estimated that the number of people in need of immediate treatment ranged from 627,000 to 1.6 million. The new numbers mean "fewer people need treatment today and will need treatment in the future," says Ghys. Yet he, too, cautions that this doesn't suddenly make scaling up treatment simple.

UNAIDS's latest figures estimate that 39.5 million people worldwide are infected with HIV, which the revised Indian numbers would lower to 36.3 million. South Africa now has the unfortunate distinction of having more HIV-infected people—5.5 million as of 2005—than any country in the world.

–JON COHEN

AWARDS

Science Wins Communication Award

Science and *Nature* have jointly been named recipients of the prestigious 2007 Prince of Asturias Award for Communication and Humanities.

The award is made annually by Spain's Prince of Asturias Foundation, formed in 1980 under the presidency of His Royal Highness Prince Felipe de Borbón, heir to the throne of Spain. The foundation honors accomplishments by individuals, groups, or organizations in eight categories: communication and humanities, social sciences, arts, letters, scientific and technical research, international cooperation, concord, and sports.

In a statement, the foundation noted: "Some of the most important and innovative work of the last 150 years has appeared on the pages of *Science* and *Nature*, thus contributing to the birth and development of many disciplines, including Electromagnetism, Relativity, Quantum Theory, Genetics, Biochemistry and Astronomy. … In 2001, the international community learned of the description of the human genome from the pages of both publications."

This year's awardees in other categories are former Vice President Al Gore (international cooperation), Bob Dylan (arts), developmental geneticists Ginés Morata of the Spanish National Research Council and Peter Lawrence of Cambridge University in the United Kingdom (scientific and technical research), and Hebrew writer and professor Amos Oz of the Ben-Gurion University in Israel (letters). Awards for social sciences, sports, and concord have not yet been announced.

"We are delighted and deeply honored that our journal's contributions to public discourse on science and technology have been recognized by Spain's Crown Prince Foundation," said *Science*'s Editor-in-Chief Donald Kennedy.

The awards will be presented at a ceremony in Oviedo, Spain, in October.

CREDITS (TOP TO BOTTOM): NOAA; 2007 PRINCE OF ASTURIAS FOUNDATION

Winds of Change

The head of the U.S. National Hurricane Center in Miami, Florida, has been placed on leave after a rebellion by fellow forecasters and staff. William Proenza (left), a longtime National Weather Service official and forecaster, has publicly complained about the center's budget since becoming director 7 months ago. One gripe was that its parent agency, the National Oceanic and Atmospheric Administration (NOAA), hadn't prepared to replace the aging QuikSCAT, a NASA satellite. Proenza had warned that its loss could worsen 3-day hurricane track forecasts by 16%.

But prominent center staff questioned the satellite's importance. And, in an unusually public letter last week, 23 of 50 center staff called for Proenza's removal, lamenting the "unfortunate public debate" over the center's forecasting ability. In May, NOAA chief Conrad Lautenbacher called Proenza's bluntness "one reason why we love him," but in a letter this week to center staff, he said there was "anxiety and disruption" at the center and that Proenza was leaving. Officials, who aren't saying why the move was made, have put center deputy Edward Rappaport in charge.

–ELI KINTISCH

Space Probes Add Side Trips

NASA is sending two decorated veterans out to collect more scientific data. After already having traveled 3.2 billion kilometers to pick up 1 microgram of dust from comet Wild 2 and having dropped it back to Earth for analysis, NASA's Stardust spacecraft will be visiting comet Tempel 1 in 2011. NASA's Deep Impact spacecraft fired a massive copper projectile at the comet on 4 July 2005, and researchers want Stardust to image the resulting impact crater to learn about the structure and porosity of the comet's nucleus. "A revisit is always a good idea," says Gerhard Schwehm, head of solar system science at the European Space Agency, although he warns that "Stardust's hardware was designed for a different purpose."

Meanwhile, Deep Impact also has been given a new assignment. It plans to fly past comet Boethin on 5 December 2008 after looking for transiting planets around other stars. NASA science chief Alan Stern says the new missions get "more from our budget."

–GOVERT SCHILLING

Overheated. Too many voracious pine bark beetles are surviving milder western winters.

CLIMATE CHANGE

Record U.S. Warmth of 2006 Was Part Natural, Part Greenhouse

Climate scientists usually hesitate to point to a single climate extreme and say, "That's the greenhouse at work." Climate naturally swings to and fro so much that it can be tough to pick out the influence of the strengthening greenhouse on a hurricane season, say, or on one country's climate over the course of a year.

But four National Oceanic and Atmospheric Administration (NOAA) climate scientists report in a paper in press at *Geophysical Research Letters* that the greenhouse was behind more than half of last year's record-breaking warmth across the contiguous United States. By their reckoning, global warming in 2006 was aggravating all manner of U.S. extremes: severe droughts, the rising cost of air conditioning, the cold-sensitive pine bark beetle ravaging once-cool western forests, and maybe even some midwinter daffodils.

Last January, NOAA announced that 2006 was the warmest year for the lower 48 states since record-keeping began in 1895; temperatures even eclipsed the El Niño–fueled record of 1998. According to a NOAA press release, El Niño was contributing to 2006's unusual warmth, and the strengthening greenhouse was probably involved too. But NOAA couldn't say which climate phenomenon was more important in setting the new record.

So climate dynamicists Martin Hoerling, Jon Eischeid, Xiao-Wei Quan, and TaiYi Xu of NOAA's Earth System Research Laboratory in Boulder, Colorado, decided to find out what was behind the record. First, to gauge the influence of last year's El Niño, they checked on what 10 actual El Niño warmings of the tropical Pacific had done to U.S. temperatures. They found a slight overall cooling, not a warming, concentrated in the northern states. Then, in two climate models, they simulated the effect of a warmer tropical Pacific on U.S. temperatures. Again, they found a slight cooling. That "leads us to conclude that it was very unlikely that El Niño either caused or materially contributed to the record 2006 warmth," they write.

Next, the NOAA group checked on what greenhouse gases might have con- ▶

ECOTOXICOLOGY

Canadian Study Reveals New Class of Potential POPs

Dioxin, PCBs, the pesticide DDT—these pollutants are considered among the most dangerous on the planet because they don't break down easily, are highly toxic, and build up in the food chain. Because these chemicals stay put in our body fat, even tiny amounts in food can add up over time and contribute to health problems such as cancer. So worrisome are the risks that more than 140 countries have endorsed a 2001 international treaty that aims to banish a dozen of these substances from the environment.

Now on p. 236, a Canadian team reports that efforts to crack down on persistent organic pollutants, or POPs, may have missed an entire set of them. The problem is that risk assessment experts now finger potential POPs based on whether they build up in fish food webs. That assumption, the authors argue, based on modeling and field data, could be missing chemicals that fish remove from their bodies but that become concentrated in the tissues of mammals and birds, which have a different respiratory physiology.

One-third of the 12,000 or so organic chemicals on the market in Canada fit this new category, say the study's authors at Simon Fraser University in Burnaby, British Columbia. This study did not examine whether these chemicals are actually harming wildlife and people, they and others are quick to point out. Still, the work "is really raising a red flag and saying we've got to pay attention to this," says ecotoxicologist Lawrence Burkhard of the U.S. Environmental Protection Agency in Duluth, Minnesota.

Biomagnification means that the level of a toxin in animals' tissues rises as one moves up the food chain. For instance, as larvae eat algae, fish eat the larvae, and bigger fish eat smaller fish, the toxin present in the algae becomes increasingly concentrated; top predators like swordfish and polar bears end up with the highest doses in their tissues. This can happen with stable, fatsoluble chemicals that aren't easily excreted in urine or feces. Biomagnification was first studied in the late 1960s in aquatic food webs, explains Frank Gobas, professor at Simon Fraser University and leader of the study. To screen chemicals, scientists began

Toxic web. This wolf devouring a caribou carcass may be ingesting toxic organic chemicals that the caribou picked up from eating lichen.

CREDITS (TOP TO BOTTOM): DAVID MCNEW/GETTY IMAGES; RON NIEBRUGGE/WILDNATUREIMAGES.COM

tributed. Because they had no prior examples of the recent run-up in greenhouse gases, the researchers were limited to analyzing simulations. They looked at 18 models that included greenhouse gases rising since the late 19th century to the present. Averaged over the models, the simulated greenhouse warming spanned the entire contiguous United States—much like the 2006 warmth, when every one of the lower 48 states was warmer than normal. The model average in 2006 accounted for "more than half of the observed warmth," the researchers report. "The record 2006 warmth was primarily due to human influences."

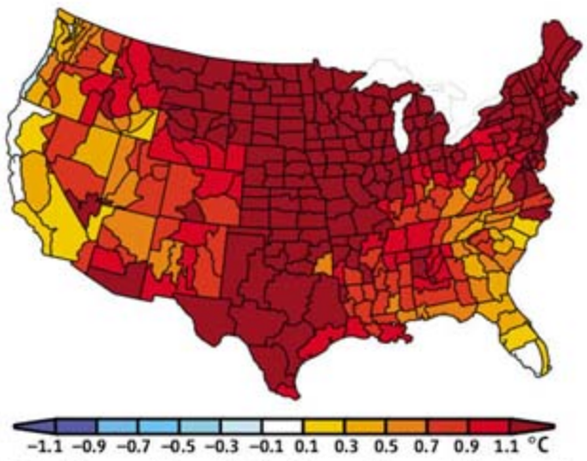

Warmth everywhere. All 48 of the contiguous states shared in the greenhouse-fueled warmth of 2006.

"I could come up with a slightly different conclusion," says meteorologist David Karoly of the University of Melbourne, Australia. Rather than blame half of the record warmth on the greenhouse, he would say that the new results show that added greenhouse gases have considerably upped the chances of a year like 2006. He agrees, however, that greenhouse gases made "a substantial contribution to the warmth of 2006."

Whatever the phrasing, the same greenhouse contribution is at work over the United States this year as last. But what are the chances that the natural jostling of the climate system will bring enough extra warmth to the year to set back-to-back records? It's possible, the NOAA group calculates, but not likely: The odds are only 16%. Still, the past spring was the fifth warmest on record for the contiguous United States. The heat is on again? **–RICHARD A. KERR**

using a property known as Kow, which indicates how readily a chemical dissolves in water compared with fat and thus predicts how easily it will move from a fish's blood lipids into water through its gills. Low-Kow, or more watersoluble, chemicals don't build up in the fish food chain and were assumed to be safe.

Environmental chemists realized, however, that this assumption might not hold in food chains involving mammals and birds because their lungs are in contact with air, not water. This means that many chemicals that are relatively soluble in water and therefore don't accumulate in fish might remain in the tissues of land animals if they aren't volatile enough to easily move from the lungs into the air (predicted by a property called Koa). Supporting this idea, some organic chemicals that don't biomagnify in fish appeared to be doing so in other wildlife and humans.

To explore this hypothesis, Gobas and graduate student Barry Kelly and colleagues collected plant and animal tissue samples—from lichens to beluga whales killed in Inuit hunts—in the Arctic, where, because of weather patterns and cold temperatures, organic pollutant levels are high. They tested the samples not only for known POPs but also for several chemicals with a low Kow but high Koa, which suggested they might biomagnify in air-breathing animals.

The measured levels of contaminants for various animals in aquatic and land food webs were similar to those predicted from a bioaccumulation model incorporating Koa and Kow, suggesting the model was correct. Chemicals with low Kow and high Koa stood out as potentially risky. Several of the contaminants studied, such as the insecticide lindane, have been proposed for the POPs treaty already. But many others with similar properties have not been scrutinized, Gobas says. The bottom line: "We're missing a lot of chemicals" that may be building up in the food web, Gobas says.

Canada and countries in Europe that are working through lists of industrial chemicals to identify new potential POPs will now need to revise their approach, says chemist Derek Muir of Environment Canada. He adds, however, that the model has limitations. For one thing, it assumes the chemicals aren't metabolized; many of them probably are, which may convert them to a form that is easily excreted. Procter & Gamble senior scientist Annie Weisbrod agrees: the Koa of chemicals "will matter in some cases," she says, "but the number of chemicals [that bioaccumulate] will not be a third of those in commerce." **–JOCELYN KAISER**

CREDIT: M. HOERLING *ET AL.*, *GEOPHYSICAL RESEARCH LETTERS* (2007)

Stem Cell Debate Reignites

The Stowers Institute for Medical Research in Kansas City, Missouri, has again delayed expansion plans because of opposition to research with human embryonic stem cells. Last fall, Missouri voters narrowly approved a measure to prevent the state legislature from prohibiting human ES cell work. But the thin margin of victory has prompted some opponents to try to overturn the measure in 2008. A proposed resolution in the legislature failed earlier this year, but Donn Rubin of the Missouri Coalition for Lifesaving Cures says he expects more attempts. "Missourians deserve the opportunity to vote to ban all human cloning," the Missourians Against Human Cloning said in a statement. Stowers says that the continuing controversy has scared off top recruits and put plans to double the institute's size on hold for now. **–GRETCHEN VOGEL**

Two Cheers for EIT

A key European Parliament committee gave its qualified blessing this week to the European Institute of Technology (EIT) proposed by the European Commission (EC). The EIT has met with little enthusiasm from scientists and industry (*Science*, 20 October 2006, p. 399), but some politicians are fans. Last month, relevant European ministers approved the idea, and now the parliament's Industry, Research and Energy panel has endorsed it, too. But the committee rejected the EC's plan to take the E.U.'s €308 million contribution to the EIT's €2.4 billion budget from existing innovation funds, calling also for an EIT pilot phase. The European Parliament will debate the plan in September. **–MARTIN ENSERINK**

Hot Times, Tough Sledding

A report released last week by the U.S. climate science program paints a murky but grim picture of the effort needed to cut greenhouse gas emissions. Three independently developed models of how that might be done came up with costs that varied by a factor of 8 and ranged to "substantial" levels, even with some optimistic assumptions. "Technically," stabilizing atmospheric greenhouse gases "is not impossible," concluded report author James Edmonds of the Pacific Northwest National Laboratory. Similar work summarized by the Intergovernmental Panel on Climate Change suggested that tackling the problem "is affordable," says economist William Pizer, of Washington, D.C.–based Resources for the Future, who said this report's "central tendencies" were "closer to the truth." **–RICHARD A. KERR**

Making Dirty Coal Plants Cleaner

A daunting task awaits the utility industry as it scrambles to catch the carbon spewing from today's generation of plants

PITTSBURGH, PENNSYLVANIA—American Electric Power (AEP), the biggest user of coal in the United States, has long supported research on ways to curb carbon emissions from its 26 generating plants. But this spring, Michael Morris, its CEO, surprised an audience of fossil fuel scientists, engineers, and business executives gathered here when he pronounced that techniques to extract carbon from flue gases could be developed soon—if consumers are willing to pay for them. "If we want cleaner air, it's going to cost something," he declared. The fact that a power industry executive is even talking in these terms is a new departure, says Sarah Forbes of Potomac-Hudson Engineering Inc., a Bethesda, Maryland–based consulting firm. She sees it as a "bold" signal that the Columbus, Ohio–based utility, at least, is getting serious about carbon capture.

Emissions from the world's 2100 coal-fired power plants are responsible for roughly a third of the CO_2 generated by human activity. In the United States, roughly 600 plants produce about 30% of the 7 billion metric tons of greenhouse gases emitted by all U.S. humanmade sources, easily surpassing the amount produced by cars and all other industries combined. Additionally, the share of electricity generated by coal in the United States is expected to climb from 48% today to 55% by 2030. And the United States is not alone. Last year, China, which derives about 80% of its electricity from coal and recently surpassed the United States as the world's biggest CO_2 emitter, brought online two major coal plants a week. "If we don't solve the climate problem for coal, we're not going to solve the climate problem," says Princeton physicist Robert Williams, a coal expert.

In practice, making coal plants cleaner means removing as much of the CO_2 generated from flue gases as possible before they are vented into the atmosphere. One approach popular with industry and the federal government is called the Integrated Gasification Combined Cycle (IGCC), which creates hydrogen to burn and CO_2 to be sequestered. (The U.S. Department of Energy [DOE] plans to spend $1 billion for a full-scale public-private plant called FutureGen that's scheduled to open in 2012.) Once extracted, the carbon dioxide would then be stored, most likely underground, at a cost and by an exact method that are still uncertain.

But only a handful of such plants are running commercially worldwide, and none currently stores the CO_2 underground. A second approach, applicable to most existing plants, would remove the CO_2 from the flue stream after combustion. The industry standard, in limited use today, employs a molecule called monoethanolamine (MEA), which has been used for decades as a solvent to bind with CO_2 and separate it from natural gas.

Planners have long figured that building new facilities optimized for reduced emissions would be cheaper than retrofitting existing plants, in part because of the large amount of energy needed to extract the CO_2. But the retrofit option is becoming more attractive. One reason is the growing support for near-term caps on carbon dioxide emissions (*Science*, 8 June, p. 1412). The recent U.N. Intergovernmental Panel on Climate Change report on mitigating greenhouse warming puts a premium on early action to curb carbon emissions. That means retrofitting existing plants may be more important than building cleaner ones that won't go on line for 20 years.

The cost of retrofitting also seems likely to decline as scientists develop new technologies; at the same time, the projected cost of new construction, including IGCC plants, is sharply rising in step with prices for

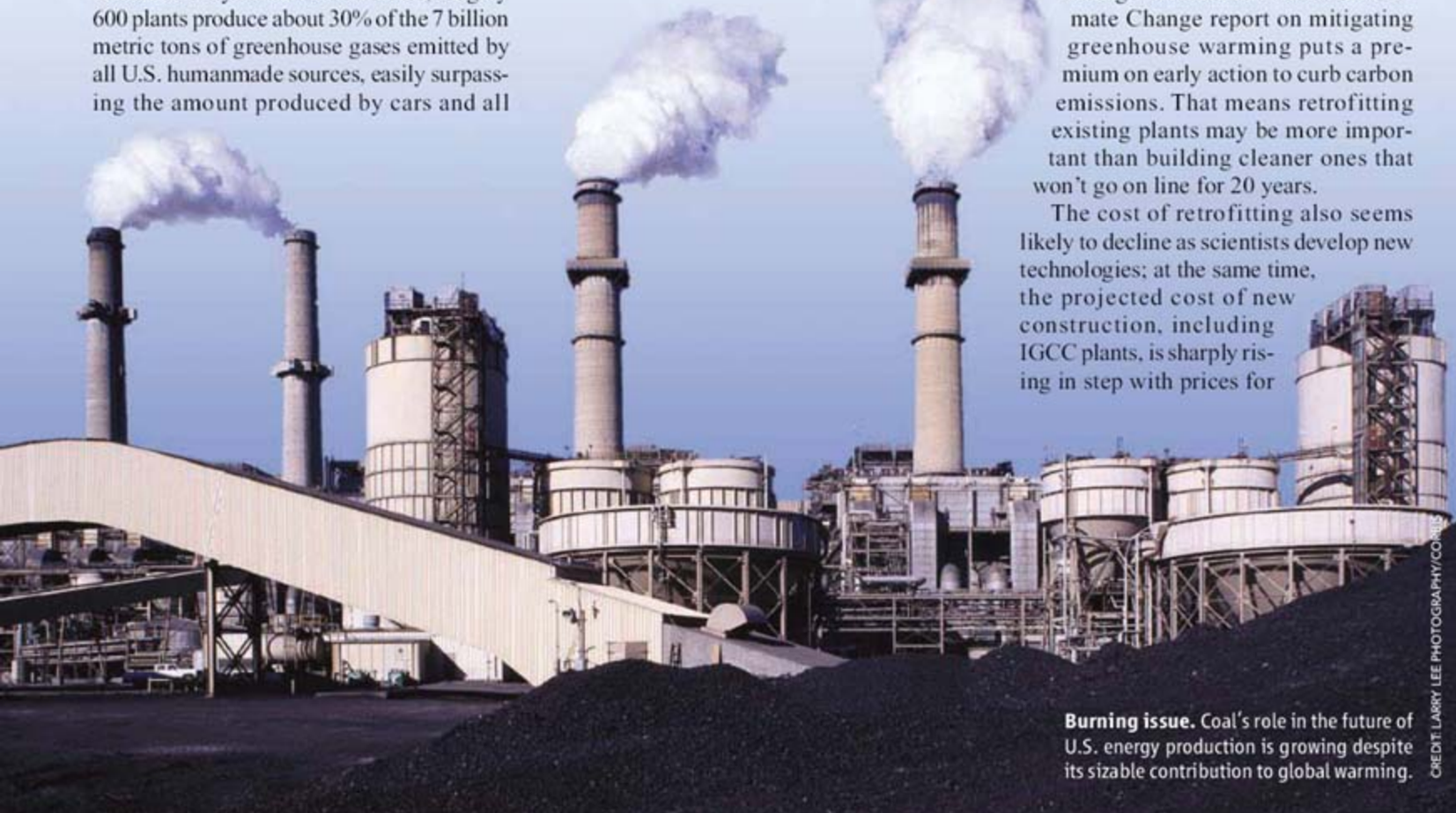

Burning issue. Coal's role in the future of U.S. energy production is growing despite its sizable contribution to global warming.

CREDIT: LARRY LEE PHOTOGRAPHY/CORBIS

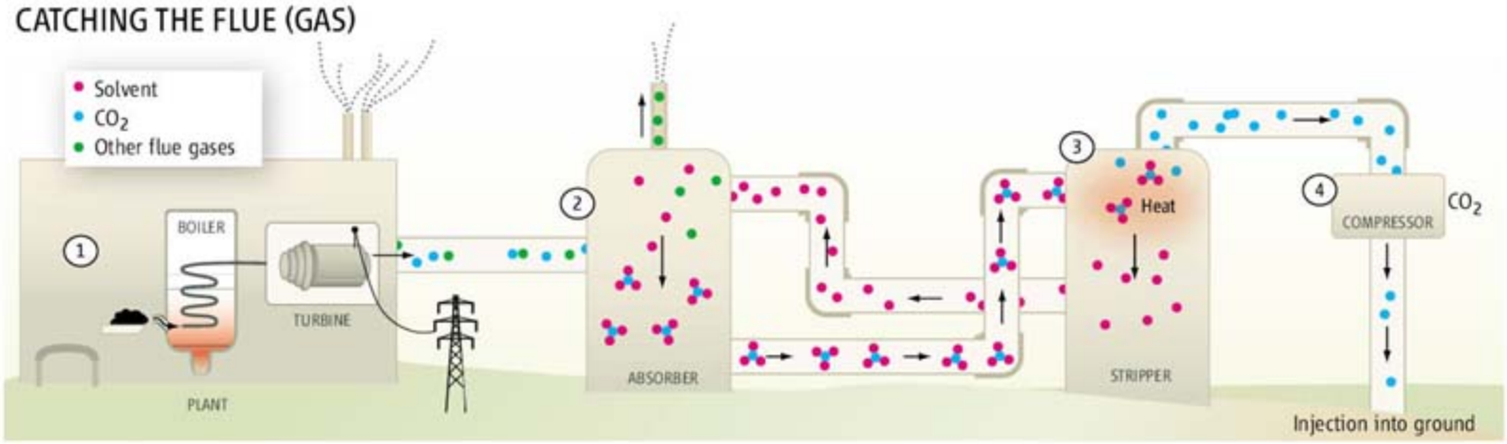

How a retrofit works. (1) Most coal plants burn coal to create steam, running a turbine that produces electricity. After treatment for pollutants, the flue gas, a mixture of CO_2 (blue) and other emissions (green), goes out a smokestack. To collect CO_2 for storage, however, the mixture of gases is directed to an absorber (2), where a solvent like MEA (pink) bonds with the CO_2 molecules. The bonded CO_2–solvent complexes are separated in the stripper (3), which requires heat. More energy is needed for the next step (4), which produces a purified CO_2 stream for ground storage as well as solvent molecules that can be reused. (Schematic not to scale.)

industrial materials like concrete and steel. "It's a big change," says engineer Jonathan Gibbins of Imperial College, London. "For a long time carbon capture meant [methods like] FutureGen, which was something wonderful that was 15 or 20 years ahead."

Taking a sip

Nestled among the green hills of coal country in Cumberland, Maryland, about 2 km from the Potomac River, the 7-year-old Warrior Run plant burns 652,000 metric tons of coal each year. That makes it one of the newest and smallest facilities operated by its owner, AES corporation. But what also sets it apart is its ability to collect some of the carbon dioxide from the emissions generated in its boiler and sell it commercially to beverage gas distributors. "If you've had a Coke today, you've probably ingested some of our product," says plant manager Larry Cantrell.

Cantrell's experience operating Warrior Run gives him some insight into the economics of capturing carbon, and the numbers aren't very encouraging. Warrior Run must generate 202 megawatts (MW) of power to meet its target of selling 180 MW. Roughly 4 MW of the gross total produced goes to provide the energy required for the MEA process to grab CO_2, which captures only 5% of the plant's CO_2 emissions. Grabbing more would divert much more energy; the cost of removing the carbon dioxide by pipeline, truck, or geological injection would drain profits even further.

Although current off-the-shelf technologies for carbon capture are improving, they still have a long way to go. A 2001 DOE study of a 433 MW plant in Conesville, Ohio, calculated that adding an MEA unit to capture 96% of its CO_2 emissions would cut the plant's net output by about 40%. And using the technology would raise electricity bills by 36% or more, according to a recent Massachusetts Institute of Technology study. Last year, DOE updated its Conesville study and found that the use of improved MEA technology, including more concentrated mixtures, more heat sharing, and larger and more tightly packed columns (see diagram), would allow the plant to capture 90% of CO_2 with only a 30% reduction in power output. That's better, but it's still a big hit.

Rearranging the inner workings of a plant's heat exchangers and turbines promises to make a bigger difference than simply siphoning steam off for a retrofit bolted onto the plant's edge, says engineer Wolfgang Arlt of Universität Erlangen-Nurnberg, Germany. His recent simulated retrofit with MEA produced a 9% loss in total plant efficiency instead of 11% without the reoptimizing tweaks. "That's a big difference" over years of operation and thousands of plants, says Arlt.

Some scientists think that alternatives chemically similar to MEA offer greater hope. One uses a cooled stream of ammonium carbonate as the solvent to pull carbon dioxide from flue gas, releasing the gas when boiled. Data from a year-long experiment with chilled ammonia at the bench scale, run by the French energy giant Alstom, suggests that the method needs only 15% as much steam from the plant to capture the same amount of CO_2 as an equivalent MEA effort. That's because the solvent grabs CO_2 less tightly, requiring less energy to release it.

Alstom is now building a 30-meter-tall unit to capture 15,000 metric tons of CO_2 per year from a Pleasant Prairie, Wisconsin, coal plant operated by We Energies. AEP plans to try the technique at plants in West Virginia and Oklahoma, where engineers hope to use the gas to help extract additional oil from nearby fields. The main goal of the work is to quantify the energy demands, says Alstom's Robert Hilton, but he's also hoping to power the process with heat now wasted instead of precious steam.

A grab bag of approaches

The reason solvents are needed at all is because CO_2 makes up only a small fraction of the flue gas created and emitted by coal plants. Another retrofitting technique

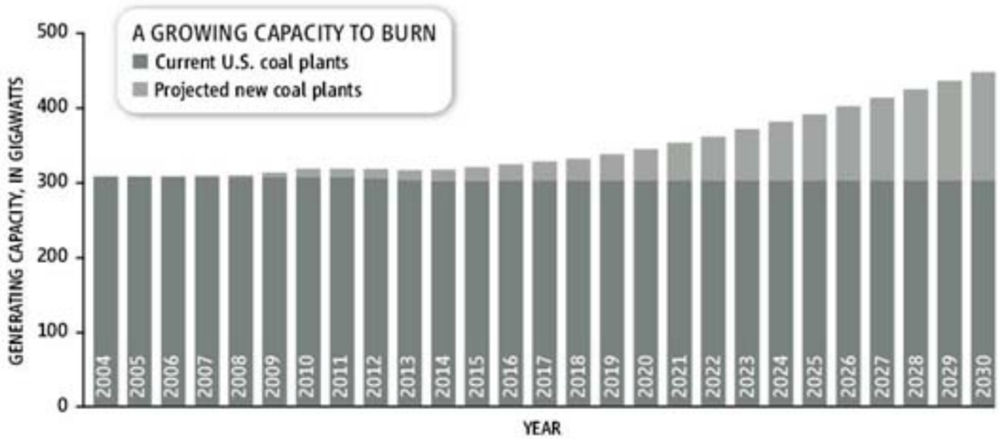

Mainstays. New plants are projected to be built in the U.S. soon, but the current fleet is going nowhere fast.

CREDIT: P. HUEY/SCIENCE; SOURCE: POTOMAC-HUDSON ENGINEERING INC.; SOURCE: U.S. DEPARTMENT OF ENERGY

A CAREER CO_2 HUNTER GOES AFTER BIG GAME

For 30 years, Michael Trachtenberg, a fast-talking, 66-year-old former neuroscientist, has been working on an enzyme that removes carbon dioxide from various environments. Now, with the coal industry and government finally focusing on reducing greenhouse gas emissions, Trachtenberg is hoping to parlay his expertise and moxie into a commercial success.

Improbably, Trachtenberg began his career as an epilepsy researcher, studying the connection between that disorder and the brain's ability to process carbon dioxide with an enzyme called carbonic anhydrase. While working at the University of Texas Medical Branch in Galveston, he learned that oil companies pump carbon dioxide into depleted wells to extract more crude. In 1991, Trachtenberg formed a company, Carbozyme, with the goal being to use the enzyme to grab carbon dioxide from coal plant emissions and sell it to oil firms. The venture flopped, but by then he was hooked on CO_2. Applying his knowledge in work funded by NASA, Trachtenberg next created a device to maintain CO_2 and moisture levels inside an astronaut's space suit that was smaller and cheaper than what the space agency was using at the time.

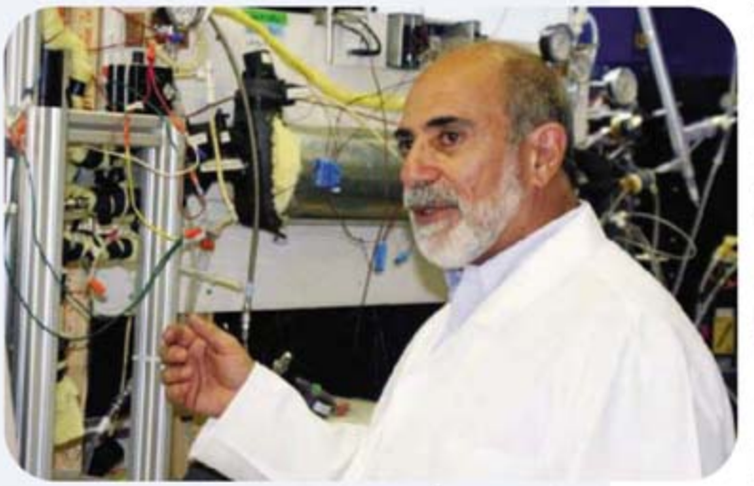

Using your noggin. Michael Trachtenberg's technique for carbon capture involves an enzyme found in the human brain.

Now that "everyone and their mother" are suddenly interested in capturing carbon, Trachtenberg predicts an industry consolidation in which "there won't be many of us little guys [left]." But he's hoping Carbozyme, reconstituted in 2003, can hold its own against the likes of Mitsubishi and General Electric. A $7.4 million grant this year from the Department of Energy (DOE)—the biggest award to one team from a $24 million pot—will allow the Monmouth Junction, New Jersey, company and its industry partners to carry out basic and applied research on post-combustion CO_2 capture. (Carbozyme's technology uses the enzyme in membranes to catalyze the conversion of CO_2 to bicarbonate ions, reversing the process with the same enzyme by altering the pressure.) He says that preliminary results show that his CO_2 absorber is dozens of times more cost efficient than the current state-of-the-art technology using a molecule called monoethanolamine.

Trachtenberg's schedule at a recent carbon capture conference in Pittsburgh, Pennsylvania, showed how far he's come since his days as an academic scientist: In addition to attending presentations, he juggled hushed sit-downs with some of the biggest names in the coal industry. A gregarious self-promoter, he's also learned how to protect his intellectual property. Scrutinizing slides before a public meeting with other DOE grantees, he explains: "I'm making damn sure that there's nothing proprietary in those presentations."

–E.K.

involves the seemingly paradoxical goal of producing flue gases that are richer in CO_2. The method, called oxy-firing, burns coal in a pure oxygen stream, producing CO_2 and little else. After only minor processing, the flue gas can be injected into the ground. Such equipment could be attached to existing boilers "more or less as is," says University of Utah chemical engineer Eric Eddings.

Last year, boilermaker Babcock and Wilcox ended a 7-year oxy-firing test in Alliance, Ohio, using a burner only 5% the size of those used in a typical coal plant. Preliminary results suggest that oxy-firing would raise a typical U.S. customer's electric bill by 44%—compared with more than 50% for MEA—without accounting for storage costs. Complicating the equation, says Babcock and Wilcox's Kip Alexander, is that "everyone is trying to get cost estimates on equipment that hasn't been built yet."

One drawback to oxy-firing, says University of Texas chemical engineer Gary Rochelle, is the need to make permanent changes to the boiler, the heart of a coal plant. By contrast, treating flue gas gives operators the option of changing the carbon-stripping technique by swapping equipment off the end of the plant. That flexibility could make emissions cuts easier for industry: The Conesville study, for example, suggested that capturing half the carbon emissions from the plant would cost half as much as capturing all of the CO_2.

Keeping options open for relatively new steam-powered plants is a big worry of coal experts, especially for those eyeing the Asian juggernaut. Gibbins hopes to spread the word about technical advances during a visit to China later this year. He plans to encourage Chinese utilities to include particular features—such as space for new equipment and certain steam fittings—on their prodigiously growing coal fleet so that they're ready if researchers, mostly in the West, succeed in making capture cheaper over the next decade.

Other methods to grab CO_2 from flue gas are still at the bench stage. They include giant molecules that can pluck out CO_2 with spindly arms called dendrimers, cagelike molecules that capture the CO_2, or biological catalysts (see sidebar). The initial barrier for each technology is the high cost of producing the molecules. But the methods also hint at some attractive benefits. One problem with MEA is its volatility, which requires a company to run a chiller plant on site to remove the evaporated solvent from the concentrated CO_2. But ionic liquids, a relatively new class of chemicals that are liquid at room temperature, have low volatility, and chemists are finding they might be useful for removing carbon dioxide.

The search for carbon-clutching tools is attracting researchers from a variety of fields previously unrelated to coal, like nanotechnology. Researchers at the University of Notre Dame, for example, were trying to use ionic liquids to make environmentally friendly solvents for the chemical industry when they discovered that the CO_2 involved kept dissolving in the ionic liquid. "We didn't expect the carbon dioxide to be so soluble," says Notre Dame chemical engineer Edward Maginn.

Now, DOE is funding basic work with the chemicals for carbon capture, and Maginn's team is examining how to make cheap-to-synthesize solvents that grab CO_2 just firmly enough. "It's a very small [but] growing field," he says. And every little bit helps a community that's trying to tackle a problem from a virtual standing start, says Babcock and Wilcox's Alexander. "We need to demonstrate a lot of things," he says.

–ELI KINTISCH

CREDIT: CARBOZYME INC.

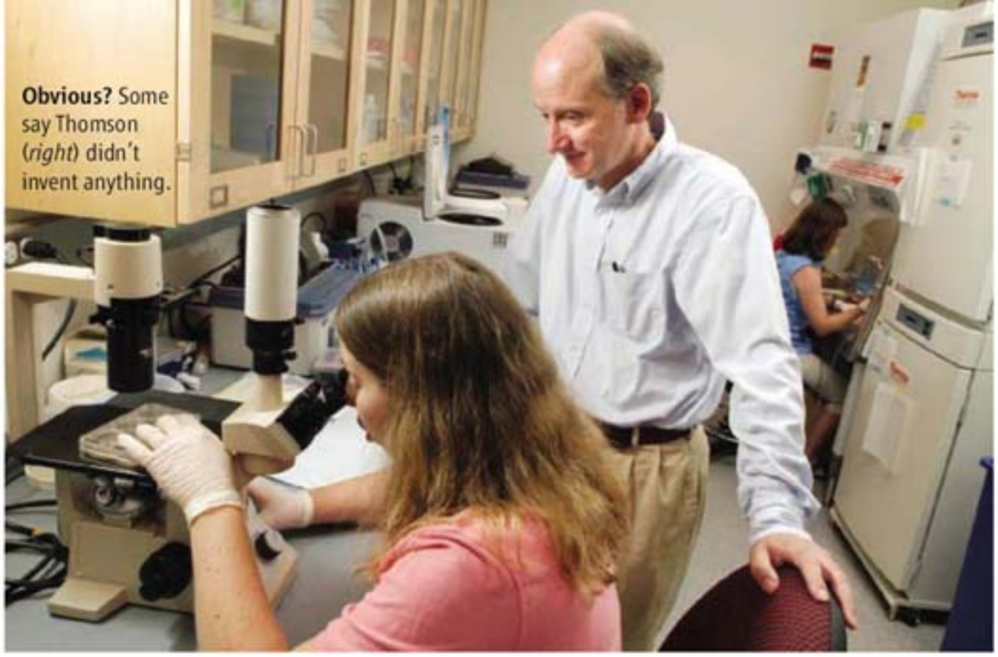

Obvious? Some say Thomson (*right*) didn't invent anything.

CREDIT: JEFF MILLER/UNIVERSITY OF WISCONSIN, MADISON

STEM CELLS

Prominent Researchers Join the Attack on Stem Cell Patents

James Thomson's work deserves praise but no patents for doing what others could have achieved with the proper resources, critics say

Four prominent stem cell scientists have filed "declarations" in support of a citizens' group that is trying to break the University of Wisconsin's hold on patents for human embryonic stem (ES) cells.

Joining the fray are Harvard researchers Chad Cowan and Douglas Melton, as well as Alan Trounson of Australia's Monash University. A new statement was also submitted by Jeanne Loring of the Burnham Institute for Medical Research in San Diego, California, who has been advising the Foundation for Taxpayer and Consumer Rights, which filed the initial complaint last July.

In April, the U.S. Patent and Trademark Office (PTO) issued a preliminary ruling upholding the taxpayer foundation's challenges to three existing patents (*Science*, 13 April, p. 182) covering primate and human ES cells, which are based on the work of University of Wisconsin, Madison, researcher James Thomson and held by the Wisconsin Alumni Research Foundation (WARF). WARF narrowed its claims in response to the ruling, excluding human ES cells from sources other than fertilized eggs, such as cloning. But WARF is standing pat in face of the latest onslaught. Spokesperson Andrew Cohn says it will have no response to the statements, which contain "nothing new."

The scientists' statements reiterate the taxpayer foundation's central arguments: that the feat by Thomson—who announced the first successful cultivation of human ES cells in 1998 (*Science*, 6 November 1998, p. 1145)—was "obvious" and therefore unpatentable since it was the outcome of using already-known technology.

The four scientists emphasize that Thomson deserves all the accolades he has received. But they argue that he was just lucky in having access to abundant funding (from Geron Corporation in Menlo Park, California) and fresh frozen human embryos (from Israel). "I believe that had any other stem cell scientist been given the same starting material and financial support, they could have made the same accomplishment," stated Melton.

WARF argues that for 2 decades after the discovery of mouse ES cells, people "repeatedly tried and failed" to cultivate sustainable lines from other mammals including sheep, pigs, hamsters, cows, and humans. But none of these efforts was successful until Thomson reported the first monkey ES cell line in 1995. WARF cites Ariff Bongso at the National University of Singapore as a researcher who tried and failed to cultivate human ES cells pre-Thomson. Bongso derived a human cell line in 1994 but was unable to maintain it. WARF also emphasizes that Thomson was the first to report that Leukemia Inhibitory Factor, or LIF, although necessary for cultivating mouse ES cells, is not needed with human cells.

The challengers counter that "not a single scientist in the field tried and failed to achieve Thomson's accomplishment"—not for lack of know-how but because they did not have the proper resources. They also cite Bongso's work, arguing that with a little more time he would have gotten it right. Trounson says he had "work in progress" cultivating human ES cells at the time Thomson reported his breakthrough (Trounson's work was published in 2000). Melton points out that his team in the past few years has successfully isolated human ES cells "by simply following … methods taught for deriving mouse, rat, pig, and sheep ES cells. We did so without recourse to Dr. Thomson's publications. … "

Colin Stewart, a stem cell researcher at the Institute of Medical Biology in Singapore, is the only outside expert who has offered a declaration to the PTO in support of WARF's position. Stewart, co-discoverer of the role of LIF in mouse ES cell culture, basically argues that existing methods for cultivating mouse cells did not provide adequate guidance for cultivating human ones. (Stewart was not available for comment.)

Some lawyers have gone to bat for WARF. In a blog posted on 4 July, Chicago, Illinois, biotech lawyer Kevin Noonan points out it is difficult to maintain that the invention was anticipated by "prior art" given the acknowledged "absence of appropriate starting materials"—human embryos. "The best the art could provide is a suggestion about how human stem cells *might* be produced," he writes. Madison, Wisconsin, patent attorney Grady Frenchick is confident the patents will hold up. "Everybody's going to use [Thomson's] method of isolation and cultivation. That's truly the breakthrough," he says.

But it is difficult to find a stem cell researcher other than Stewart or Thomson who thinks WARF's patents are justified. "I know of no one other then the folks … associated with WARF and these patents who is in favor of how they are handling this," says Fred Gage of the Salk Research Institute in San Diego, California.

Johns Hopkins University stem cell researcher John Gearhart agrees with the challengers. "The procedure James [Thomson] used to generate human ES cells was one that had been basically reported [back in the '80s] for generating mouse ES cells," says Gearhart. The LIF argument is a red herring, he adds. Even though Thomson found it was not necessary for growing human cells, its presence does not interfere with culturing them.

Gearhart says he doubts "whether the patent office really understood what was going on" when it issued WARF's patents. "They were not very rigorous." But with so many eyes now on it, the PTO is presumably giving the issue more than routine scrutiny.

–CONSTANCE HOLDEN

CREDIT: J. BOHANNON/SCIENCE

PROFILE: ALBERT AMMERMAN

Exploring the Prehistory of Europe, in a Few Bold Leaps

Archaeology's Renaissance man takes a new plunge—into the topic that made him leave a life of literature for a "$10-a-day" life

NISSI BAY, CYPRUS—For the operator of the bungee jump here at the Olympic Lagoon Resort, it is a strange request. The Cypriot Department of Antiquities wants him to give a ride to a visiting American academic. A tall man in khaki trousers, Albert Ammerman steps over the coiled bungee cord and joins the operator in the metal cage. The crane hoists them 60 meters over the bay—the point at which most passengers are bound at the ankles and dive screaming into the air—and then Ammerman has the crane pivot farther, dangling the cage above the bone-white escarpment flanking the resort. Here Ammerman pulls out a camera and snaps shots of the land below.

"People came here on boats 12,000 years ago. It's one of the most important archaeological sites on Cyprus," Ammerman says, surprising the tattooed bungee operator. Most people consider it a waste area, full of jagged rocks that hurt the feet—there have been plans to bulldoze it for a hotel. As the bungee operator swings the cage back over the water, he asks, "Are you sure you wouldn't like to have a go?" Ammerman chuckles, and cocks his head to consider the plunge.

Ammerman, 64, is no stranger to wild leaps into the unknown. Indeed, they have defined his career. But in spite of changing research areas—and even fields—about once a decade, Ammerman has made important advances again and again. "He is truly a Renaissance man of archaeology," says Nicola Terrenato, an archaeologist at the University of North Carolina at Chapel Hill. A decade ago, Ammerman all but abandoned the topic that launched his career, the origins of agriculture. But after a chance discovery on Cyprus's shore a few years ago, he has come back with a radical hypothesis—that sea-going people dominated the coasts and islands of the Mediterranean for millennia before farming was established.

Piccolo è bello

The first time Ammerman took a leap into the unknown was as an undergraduate at the University of Michigan, Ann Arbor, in 1964, when he turned away from math and physics to literature. As the Vietnam War reached its apex, he put aside dreams of becoming a "rocket scientist" because, he says, he felt it would mean making weapons "in one way or another." A newly declared English major, he scooped up the university's top prizes for essay writing and for original poetry. By 1966, he was an editor at a New York literary company, producing recordings of readings by famous actors and actresses.

But in 1967, says Ammerman, "curiosity" drove him to jump again. He moved to England and enrolled in a Ph.D. program at the Institute of Archaeology, now part of University College London. "My friends told me I was crazy to consider being a student," Ammerman recalls. His employer had just agreed to make him the new editor in chief of their European operation, with "my own London office and two secretaries." Instead, Ammerman ended up "in Italy, searching for the origins of agriculture, living on $10 a day," he says. "Those were the great years."

In the late 1960s, Ammerman says he and a like-minded group of "young turks" believed in a theory called "indigenism," which held that crops were domesticated all over Europe by the people living there. The theory was wrong, Ammerman soon realized. But in searching for evidence to support it, he acquired a deep understanding of the continent's prehistoric landscape. According to Andrew Moore, an archaeologist at the Rochester Institute of Technology in New York state, Ammerman had "a knack for finding sites in areas that others had not thought worthy of exploration."

Ammerman demonstrated that the earliest signs of agriculture didn't overlap with late hunter-gatherer sites, and this was key evidence for a theory contrary to indigenism—the view that agriculture swept across Europe in a rapid revolution, imported by newcomers. But it would be nearly 2 decades before Moore and others proved definitively that Europe's crop plants were domesticated in the Near East.

To find evidence of a farmer mass-migration, Ammerman crossed disciplines again. While he was in Italy in the late 1960s, he teamed up with Luca Cavalli-Sforza, a geneticist now at Stanford University in Palo Alto, California, who was studying human migrations. "Theirs was the first collaboration between an archaeologist and a geneticist to put together two totally distinct forms of scientific knowledge," says Moore. Ammerman mapped out the location of the earliest known appearances of agriculture across Europe, while Cavalli-Sforza analyzed samples of blood from people living in Europe today, gauging genetic differences by comparing mutations in the genes for blood proteins.

> "Agriculture didn't spread along the coasts because **they were already frequented" by voyaging foragers.**
>
> —Albert Ammerman, Colgate University

When they compared notes, a striking pattern emerged. Agriculture appeared steadily later the farther west they looked, and the degree of genetic difference between populations also grew steadily greater. "The best explanation for those patterns is that agricultural people moved into Europe from the east, displacing and mixing with hunter-gatherers as they went," says Ammerman. By correlating geographic and genetic distance, the duo calculated the rate of the spread of agriculture across Europe at roughly 1 kilometer per year. "It created an entirely new field of archaeology," says Curtis Runnels, an archaeologist at Boston University in Massachusetts.

The next leap came in 1985 while Ammerman was holding a temporary position at the University of Parma in Italy. While working on a dig in Rome, Ammerman teamed up with geophysicists to use techniques then foreign to archaeology, such as radar imaging and computer modeling of landscape evolution. In retrospect, says Terrenato, "establishing the solid contours and the geology of a site as it was when human occupation started" is an "obvious first step." But archaeologists had rarely done so, "in part because of the difficulty of acquiring the necessary data," he says.

Ammerman wasn't the only archaeologist exploring these new methods, says John Cherry, an archaeologist at Brown University, "but he was one of the first, and his approach was very creative."

The geo-archaeological methods paid off well. From Rome, Ammerman went to ancient Athens and other cities, plying his quantitative methods. In Venice, says Moore, Ammerman produced "spectacular results, pushing back the date of the inception of the city and giving it a new founding history." This work has also embroiled him in debates over the future of coastal cities in the face of climate change (*Science*, 25 August 2000, p. 1301).

But staying out of the mainstream has often required Ammerman to work "as the proverbial army of one," says Terrenato, stringing together small grants to do field work either alone or in small collaborations. Unlike colleagues at big research universities with troops of graduate students, Ammerman drifted between universities in Italy and settled at a small liberal arts college, Colgate University in Hamilton, New York. But if he has an underdog reputation, Ammerman is sanguine about it. "Piccolo è bello," he says—small is beautiful.

Neolithic redux

In 2004, Ammerman spent a year as a Fulbright senior scholar in Cyprus. He was attracted to an archaeological mystery on the island.

Ammerman and Cavalli-Sforza's rate of 1 kilometer per year for the spread of agriculture works well on the European mainland, but the picture is confusing along the Mediterranean coast. Cyprus, as the first big island off the Near Eastern coast, partly visible from mountains in Turkey, should have been colonized by farmers relatively early. To get there, however, they would have needed boats to traverse 60 kilometers of open water, and evidence for ancient seafaring in the Mediterranean is scant.

Striking similarity. Ammerman found stone tools near a rocky outcrop on Cyprus that he says resemble Neolithic tools from the mainland.

Within the past decade, Edgar Peltenburg, an archaeologist at the University of Edinburgh, U.K., has pushed the date of Cypriot occupation back to 8200 B.C.E., making it one of the earliest arrivals of agriculture from the Near East. The discovery implies that seafaring technology must have been available by then, says Ammerman, and it also creates a paradox. "In a world of boats, agriculture should have spread far more quickly around the Mediterranean than on the mainland." But the opposite is true. Traveling west, the next big island, Crete, is only days away by boat, but farmers do not seem to have left their mark there until 7000 B.C.E. The toe of Italy seems to have been foreign to farming until 1000 years after that. "What took them so long?" Ammerman wonders.

A few months after arriving at Cyprus, Ammerman was strolling along the Aeolianite bluff at Nissi Bay when he saw something that stopped him in his tracks. He picked up a small, chipped stone and turned it over in his hand. It was a tool from before the Neolithic Period. "Then I started seeing them all over the place," he says. He teamed up with a fellow Fulbright senior scholar on Cyprus, Jay Noller, a geologist at Oregon State University in Corvalis, to map out other Aeolianite outcrops on the island. Sure enough, a similar part of the coast to the west is peppered with stone blades and scrapers typical of the mainland about 12,000 years ago.

Archaeologists have never noticed these sites, says Ammerman, "because no one would ever think of looking in such a place." The Aeolianite seems like an unpleasant place to make a living, he says. But after several summers of fieldwork, "I now appreciate that it's awful for agriculturalists but wonderful for hunter-gatherers." The Aeolianite's natural pits and shelves "are like Paleolithic furniture, perfect if you've got seafood you've captured down at the coast and need a sheltered place to process and cook it."

Ammerman believes he's found by far the oldest evidence of seafaring in the Mediterranean, and he thinks it could shed light on the agricultural transition itself. "The mistake that I think we have always made about the Neolithic is to assume that agriculture must have been perceived as a far superior lifestyle and was immediately embraced," he says. "Agriculture can support far higher population densities," and that is why the agriculturalists inevitably took over. But the coastal environment is not ideal for agriculture, says Ammerman, adding "I think agriculture didn't spread along the coasts because they were already frequented by a stable culture of voyaging foragers."

But Ammerman "desperately needs independent evidence to sustain the early dating of his sites," says Peltenburg. Ammerman's first shot at that—getting a carbon date on a sample of charcoal from the surface—was disappointing. The sample turned out to be no older than the days of Napoleon. Now he plans to get carbon dates from samples of shells at lower levels.

Back in the bungee cage, Ammerman decides to skip this plunge. But about his new research direction, he has no hesitation. "Sure, I could be wrong," he says. "But this sure is fun." That seems to be the motto of a scientist who has followed the beat of his own drum. **–JOHN BOHANNON**

CREDIT: A. AMMERMAN

Environment counts. Despite the highly genetic nature of autism, which researchers are now deciphering, specialized school programs help.

NEUROSCIENCE

Autism's Cause May Reside in Abnormalities at the Synapse

New genetic evidence is leading researchers to home in on the cleft separating neurons as the site where the disorder may originate

No one knows what causes autism, which in its broad definition affects about 1 in every 150 children. The impaired social interaction, communication deficits, and restricted and repetitive behaviors seen in people with the condition have confounded scientists since it was first identified in 1943. Because only a minority of autistic persons have severe intellectual disability, and some show exceptional cognitive talents, relatively subtle changes in the brain are probably responsible. Now a flurry of new discoveries is pointing to one possible site of autism's origin: the synapse.

Synapses are junctions across which neurons communicate. They are essential for sensory perception, movement coordination, learning, and memory—virtually all brain function. "The synapse is like the soul of the brain," says Huda Zoghbi, a pediatric neurologist at the Baylor College of Medicine in Houston, Texas. "It's at the root of everything."

Zoghbi was the first to propose, in 2003, that altered synapses might be responsible for autism. But direct evidence was thin. Now "there seems to be a confluence of data flowing," says Stephen Scherer, a geneticist at the Hospital for Sick Children in Toronto, Ontario.

Until the mid-1980s, experts considered autism a strictly environmental disorder, with most of the blame falling on faulty parenting. Now we know that "autistic spectrum disorder," the term specialists prefer, is overwhelmingly genetic. Based mostly on studies of fraternal and identical twins, University of Illinois at Chicago autism researcher Edwin Cook concludes that genetic factors contribute about 90% to autism, with environmental factors contributing no more than 10%. Autism is "the most heritable of neurodevelopmental disorders that are complex in origin," says Scherer. (Biology is not destiny, of course, because the environment affects the form any genetic disorder takes, and autistic children often improve if placed in the right learning setting.)

Abnormalities of chromosomes, many of them visible under the microscope, are thought to account for 10 to 20% of autism cases. The effect of multiple genes acting in combination probably accounts for most of the rest. Two groups recently reported that many autism patients have novel deletions and duplications in their genomes (*Science*, 20 April 2007, p. 445), probably arising when chromosomes cross over during meiosis. Researchers are honing in on the individual genes responsible.

Because autism is a spectrum of disorders, different gene combinations will play a role in different individuals. What's generating excitement now is the discovery of mutations in single genes that, in rare instances, seem able to cause autism. These genes may be pointing directly at a general mechanism for the disorder, at the synapse.

The first autism genes?

Zoghbi's provocative 2003 synapse hypothesis rested partly on work that year by a group led by Thomas Bourgeron at the Pasteur Institute in Paris, France, that found mutations in proteins called neuroligins in two pairs of Swedish brothers with autism spectrum disorder. Neuroligins are proteins expressed on the surface of the postsynaptic neuron that bind to proteins on the presynaptic neuron called neurexins, spanning the synapse and forming a physical tether. Together, neuroligins and neurexins are thought to play key roles in the formation and functioning of synapses.

Some researchers contested the Pasteur Institute findings, however, because no other reports of these mutations in other individuals with autism followed; some even questioned whether the Swedish brothers actually had autism. "If it wasn't [autism], it was pretty damn close," says Scherer.

These rare neuroligin mutations and other suggestive evidence linking some neuroligin-binding proteins to autism led Bourgeron to postulate a "neuroligin autism pathway" in which abnormalities in any of these dozen or more proteins could predispose their possessors to the disorder. Bourgeron buttressed his case this January, when his group identified mutations in one of these proteins, Shank3, in three autistic individuals. In such rare cases, mutations in this single gene seem to be sufficient to cause autism. Other groups, according to Scherer, are also reporting Shank3 mutations in autistic patients. "It's being replicated for sure," he says. In the one published study so far, Shank3 mutations appear to

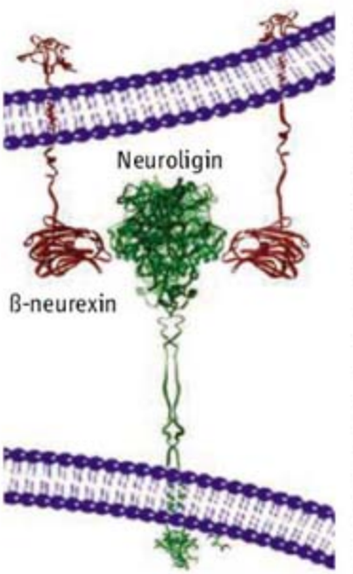

Critical connection. Neurexins and neuroligins coming together in the synapse. Alterations in these proteins could change how neurons communicate and lead to autism.

CREDITS (TOP TO BOTTOM): STEPHEN MCGEE/MCT/LANDOV; UNIVERSITY OF CALIFORNIA, SAN DIEGO/SKAGGS SCHOOL OF PHARMACY AND PHARMACEUTICAL SCIENCES

account for about 1% of autism cases.

Then, in March 2007, the Autism Genome Project Consortium, a group of over 50 institutions in North America and Europe, reported results of a 5-year study on the genetics of autism in 1600 families. In addition to several new chromosomal regions implicated in the disorder, the researchers found the neurexin-1 gene associated with autism. Since neurexins bind to neuroligins at the synapse, this finding boosted the neuroligin autism pathway idea, although the study's authors did not look for specific neurexin mutations. (Several groups are now sequencing the gene.) Shank3 abnormalities also turned up in some Autism Genome Project families, reports Scherer, the study's coprincipal investigator, again implicating the neuroligin pathway.

Bourgeron now feels vindicated. "People in the field are really accepting that this is a pathway which is associated with autism," he says. "When we published the neuroligin [report in 2003], nobody believed it."

Mutations in single synaptic genes, including neuroligins, neurexins, and Shank3, will probably explain only a small number of autism cases—5% at most, Scherer estimates. In the most convincing case so far, Shank3, "a single gene could cause this complex disease type," says Scherer. "That's tremendously important," Scherer explains, because it could provide clues to cellular defects underlying all autism. In Alzheimer's disease, for example, mutations in the ß-amyloid precursor protein (APP) account for a tiny fraction (less than 0.1%) of all cases yet were crucial in revealing the likely disease mechanism: the abnormal deposit of amyloid plaques in the brain. "This field, autism, is probably about 7 years behind the Alzheimer's story," says Scherer.

Orchestrating the synapse

Now the race is on to figure out how neuroligins and their binding proteins are contributing to autism. "What exactly do these proteins do at synapses?" asks Thomas Südhof, a neuroscientist at the University of Texas Southwestern in Dallas. "That's … crucial for understanding autism."

Südhof's lab discovered neurexins in 1992 and neuroligins in 1995. They have been studied intensely ever since, because they seemed to hold the key to how synapses form, and thus to brain development. At first their pairing was thought to physically tether the synapse, but it later became clear that they also promote the recruitment of neurotransmitter receptors and various structural molecules to the synapse—in fact, orchestrating a complete synapse. Neuroligins and neurexins "are unbelievably important proteins," says Südhof. "They're life or death."

Clues to their possible role in autism are now appearing. One theory is that an abnormal neuroligin pathway upsets the balance of excitatory and inhibitory synapses in neurons, thereby affecting learning and memory, and thus language and social communication. Broadly speaking, synapses can be either excitatory, when the neurotransmitter glutamate is released, or inhibitory, with release of the neurotransmitter gamma-aminobutyric acid (GABA). The ratio of excitatory and inhibitory synapses on a neuron determines whether it will fire in any given situation. In the 21 June issue of *Neuron*, Südhof reported that in experiments in cells, overexpressing neuroligin-1 leads to excitatory transmission at synapses, whereas neuroligin-2 overexpression leads to inhibition. Südhof speculates that an alteration in either neuroligin could change the excitatory-inhibitory balance, subtly changing the number of neurons that are firing during brain development. Such disruptions could eventually produce the lasting symptoms of autism, he explains, because synapses change with use, becoming more or less sensitive to stimuli depending on experience. This "synaptic plasticity" is the basis of learning and memory.

That's just one possibility. The synapse is extraordinarily complex, both chemically and structurally, and a lot could go wrong there as the brain develops. Studies in animals to understand the different components of the synapse and to determine mutation effects are just beginning.

Many research groups are now focusing on finding links between synapse genes and autism. Cook argues for a broader approach, including whole genome scans for other genes that might have less individual effect but may account for more autism cases. (Some such studies are in progress.) "To say one or the other approach … is the right way to go is, I think, at this point naïve," Cook says.

Few genes or many?

The hope is that most cases of autism are caused by just a few strongly acting genes, rather than many weak genes in concert. Simpler genetics would accelerate understanding of the disorder, as well as facilitate early diagnosis and genetic counseling, and provide more discrete targets for therapy. Bourgeron notes that a single abnormal gene—or even a single gene copy, as with Shank3—can, in rare instances, cause autism. But even Bourgeron doubts that altered synapses by themselves are enough to cause most cases. "Autism is not a single entity," he stresses.

He speculates that a combination of abnormal synapses and altered neural networks—the complex circuitry involving the billions of neurons that permits language and social interaction—could combine to cause most cases of autism. Factors that could alter neural networks include a global, as opposed to neuron-level, shift in the excitatory-inhibitory balance, increased neuron numbers (many autistic children have large heads), or high levels of the neurotransmitter serotonin, seen in about a quarter of autistic patients.

Besides synapse abnormalities, many causes of autism have been postulated, from altered neuron migration during early development to chronic inflammation in the brain. Imaging and post-mortem studies suggest that "underconnectivity" between brain regions is at the heart of the disorder (*Science*, 24 June 2005, p. 1856). Underconnectivity and altered synapses are not mutually exclusive. "If you have regionally different synapse dysfunction, you're going to have differences in connectivity between different brain regions," says Südhof. "That's exactly what you would predict."

In the end, it may all come down to the synapse. **–KEN GARBER**

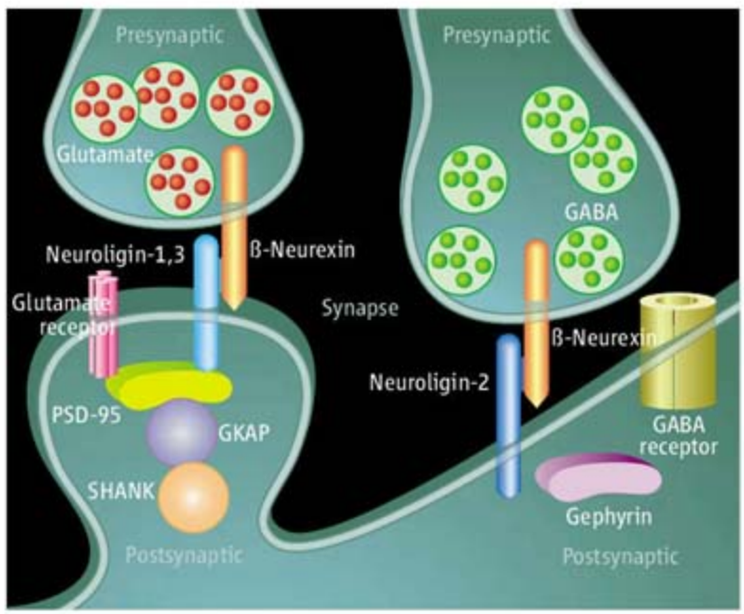

Autism's origin? Neuroligins and neurexins, proteins crucial for aligning and activating synapses, have now been implicated in autism, along with the Shank3 scaffolding protein. An altered balance between excitatory synapses (*left*) and inhibitory (*right*) could affect learning and memory during development.

CREDIT: P. HUEY/SCIENCE

Last-Gasp Effort to Save Borneo's Tropical Rainforests

One of the most ambitious attempts ever to safeguard tropical forests is taking shape in Southeast Asia. In February, the three nations—Brunei Darussalam, Indonesia, and Malaysia—that share Borneo agreed to conserve and jointly manage vast tracts of the world's third-largest island to protect its unparalleled biodiversity. At the meeting, scientists outlined their vision for the Heart of Borneo (HoB) initiative—to rave reviews. "It's phenomenal. A fantastic project," says terrestrial ecologist Nigel Stork, head of the School of Natural Resource Management at the University of Melbourne in Victoria, Australia. Yet with many details still to be worked out, some worry whether the partners will follow through on all that's been promised.

Under HoB, a third of the island—some 240,000 square kilometers straddling Brunei, Indonesia, and Malaysia—would be designated for varying degrees of protection, from conservation to uses ranging from tourism to sustainable logging. "This is the only place [in Southeast Asia] where tropical rainforest can still be conserved on a large-enough scale to remain permanently viable," says Rahimatsah Amat, chief technical officer for Borneo with the World Wide Fund for Nature (WWF) in Malaysia. Famed for its orangutans, Borneo is a biodiversity wonderland with three new species described each month, on average, over the past decade. The richness of tree diversity "is greater than anywhere else in the Old World," says Peter Ashton of Harvard University's Arnold Arboretum.

Ashton, who has conducted fieldwork in Brunei for 50 years, calls HoB "spectacular." The initiative, adds Carsten Brühl, an ecologist at the University Koblenz-Landau in Germany, is "the only chance that is left to do something meaningful to conserve the remaining forests of Borneo." As a cautionary tale, Brühl points to deforestation on nearby Sumatra. Without HoB, he says, Borneo's ecosystems "might be lost in 20 years."

Like those of Sumatra, Borneo's forests are under siege. Palm oil plantations are spreading as sales of the biofuel soar, invasive acacia trees are on a rampage, and wildfires ravage the island each year. The Heart of Borneo has come none too soon. "The project already appears to have been successful in deterring oil palm expansion in the HoB area, at least on paper," says conservation biologist Matthew Struebig of Queen Mary, University of London, U.K.

Withering heart. Although boundaries are not yet set, the Heart of Borneo initiative aims to keep remaining forests intact.

Although the three governments are still crafting implementation plans, the multimillion-dollar HoB would integrate management of national parks and other protected areas with adjoining landscapes to ensure contiguous forest cover. The HoB concept "is not a total lock-away of land," says the initiative's originator, WWF adviser Mikaail Kavanagh. Although about half of HoB land will continue to be utilized, the governments are expected to curtail unsustainable or damaging practices, such as clear-cutting and unbridled expansion of palm plantations. "We still have to provide livelihoods for people as well as protecting the biodiversity," says Stork, who is not involved with the initiative.

Scientists expect HoB will yield big, albeit vague, dividends in species protection. The project's scale "is very promising, since size does matter for biodiversity conservation in tropical forest habitats," says Brühl, who studies Borneo's ants. "I expect that such an ambitious project will provide a safeguard against biodiversity loss. But how will that be measured?" asks Myron Shekelle, an expert on tarsiers at the National University of Singapore.

Some scientists worry that the initiative could be detrimental to creatures outside project boundaries by distracting attention from them. "HoB looks like it would represent upland habitats in all states very well, but much of the diversity and the greatest conservation threats are in the lowlands," argues Struebig, who points out that substantial orangutan populations are outside HoB, in the peat swamps of Indonesia's Kalimantan provinces. Although HoB "can't cover all of Borneo," Struebig says, "it would be catastrophic if donor and government conservation interest was diverted from other flagship areas as a result."

The initiative's amorphousness also raises eyebrows. "Exactly what is covered and what commitments each country would take beyond publicity and tourism seem very uncertain at this stage," says Struebig. Experts are lobbying the three Borneo governments to take a rigorous approach to sustainable forest management. Timber extraction should be highly selective, using systems like helicopters or cables, says Brühl, who adds that such techniques have been tested in Borneo.

Despite the misgivings, experts laud WWF for conceiving HoB and persuading the politicians to adopt it. The initiative could become "a milestone in conservation," says Brühl. Or, he warns, "It could also become a piece of paper with a catchy title." The onus is now on Borneo's governments to carry the ball forward: to finalize HoB boundaries and lay out a mechanism for managing and funding it. A game plan is due by February 2008.

CREDIT: WWF GERMANY

Paradise Lost, Then Regained

A half-century ago, invaders overran Cousine Island. Feral pigs denuded the tiny outpost in the Seychelles archipelago, and alien plants ran riot. Many ecologists wrote off the island. "It was so degraded, so disturbed. It was in a very, very sad condition," says Michael Samways, an ecologist at the University of Stellenbosch in South Africa.

Samways didn't give up on Cousine, however. He has since become the chief architect of what appears to have been a stunning ecological recovery. At the meeting, Samways enthralled participants with a vivid description of the "landscape triage" his team has performed over the past 15 years to restore Cousine to a facsimile of what it was like before humans arrived. "We call it 'Paradise Gained,' " says Samways. "It's a marvelous story," says Paul Racey, a biologist at the University of Aberdeen, U.K.

In important ways, few islands compare to Cousine. It is privately owned, and the current owner bankrolled the restoration. Crucially to its ecology, Cousine appears never to have suffered a rodent infestation. That is probably because the island has no jetty, so boats cannot easily moor and introduce vermin stowaways, Samways says. Sans rats (egg fanciers), creatures like the lesser noddy, a seabird, hung on.

But ample devastation was inflicted by other mammals brought to Cousine in the first half of the 20th century. In 1977, Racey led a team to the island to assess its endangered brush warblers. They found no warblers—and "plenty of alien plants," he says. Subsequent surveys revealed that the Seychelles magpie robin also had vanished.

Ownership of Cousine changed hands, and in the early 1990s, Samways and Peter Hitchins, the island's manager, embarked on the restoration. First they enlisted "an army of people" to hunt down the feral pigs, cats, and chickens, Samways says. "There is nothing soft about conservation," he explains. "It has to be undertaken with military discipline rather than with poetic wonder."

After vanquishing the aliens, Samways's forces planted mapou trees to restore the canopy and released a couple of dozen tortoises that had been held in captivity elsewhere. Four Seychelles magpie robins brought to Cousine have since begat 40, and there are now around 200 brush warblers. Lesser noddy numbers have skyrocketed from a smattering to an estimated 90,000 pairs. "The noddy brings back a functioning ecosystem" by defecating and dropping food items, which add nutrients to impoverished soils, Samways says. One downside: The island's vitality could attract poachers—a "particular worry," he says, as they could be a conduit for rodents.

Primeval vision. The lesser noddy's recovery has helped revitalize Cousine's ecosystems.

The situation offshore is not so pretty. Cousine's coral reefs were hammered by the globe-girdling bleaching event of 1998. Since then, "there's been very little recovery," Samways says. Ten years ago, the reefs were alive with organ corals and butterfly fish. His team found neither on a survey earlier this year.

Although coral bleaching was beyond their control, Cousine's managers have implemented tough measures to safeguard the terrestrial revival. The approach might seem unorthodox: exclusive villas where celebrities and the superrich pay 400 euros and up for a night's stay. "All that money goes into the conservation efforts," Samways says. Guests are ferried in by helicopter and subjected to strict quarantine.

Cousine will serve as an ark for such endemic species like the Seychelles giant millipede that are under threat elsewhere in the archipelago. But to Samways, the deeper value of Cousine's renewal can only be fathomed by visiting the island. "The animals are so unafraid of people. You sit on the beach next to a bird with its egg, and it literally won't bat an eyelid." Many people, he says, have forgotten what it's like to truly experience nature. "Cousine rescues us from that extinction of experience."

Cousine may be exceptional, and "time will be the best judge of just what is in store for its natural systems," says Christopher Filardi, a biodiversity expert at the American Museum of Natural History in New York City. But it shows, he says, that "active intervention or restoration can reinvent a place that is richer and more reflective of its organic history than would exist if we did nothing." **–RICHARD STONE**

From Flying Foes to Fantastic Friends

The bell is tolling for Southeast Asia's bats. Pummeled by habitat erosion and hunting, some 20% of bat species may become extinct by the end of the century, experts predict. A concerted effort is now underway to save the furry critters with the establishment of a Southeast Asian Bat Conservation Research Unit.

Throughout the region, bats are an animal of ill repute. "People think bats are scary: they get stuck in your hair, they drink your blood," says Tigga Kingston, a biologist at Texas Tech University in Lubbock and head of the new research unit. "We want people to go from 'ugh' to 'aah.' " Since 2001, Kingston's team has reached out to Malaysian communities to publicize the high ecological value of the only mammals capable of powered flight. For starters, bats consume as much as their body weight in insects in a single night—"fantastic pest control," Kingston says. And some species pollinate fruit, including durian, a $1.5 billion commodity. "Bat conservation can be boiled down to: no bats, no durian, we can all go home." A chilling thought for fans of the pungent fruit.

Aah. The Horsfield's fruit bat (*Cynopterus horsfieldii*) is found across Southeast Asia.

Besides preaching the bat gospel, Kingston's research unit, bankrolled by the British American Tobacco Biodiversity Partnership, will fund science and conservation. One urgent need is to curb appetites for flying foxes, a delicacy in Malaysia and other countries. "They're under severe hunting pressure," Kingston says. A top research priority, meanwhile, is to establish a regional network of taxonomists. "There are more and more cryptic species being discovered," Kingston says. "You can't conserve what you can't identify." A taxonomy workshop is planned for the island of Java later this year.

Experts are thrilled. "It's an absolutely superb initiative," says University of Aberdeen, U.K., biologist Paul Racey, who studies bats on Madagascar. **–R.S.**

CREDITS (TOP TO BOTTOM): COURTESY OF MICHAEL SAMWAYS; TIGGA KINGSTON

A global warming
198

Climate change as an intergenerational issue
203

LETTERS | BOOKS | POLICY FORUM | EDUCATION FORUM | PERSPECTIVES

LETTERS

edited by Etta Kavanagh

Keeping the U.S. a World Leader in Science

JOHN MARBURGER'S RECENT, SOMEWHAT CRANKY STATEMENT THAT U.S. RESEARCHERS NEED TO rely more on private philanthropy and industry to expand the scientific enterprise ("U.S. science adviser tells researchers to look elsewhere," J. Mervis, News of the Week, 11 May, p. 817) provides a sobering revelation that the United States has begun to stumble as a world leader in science and technology. Failure to correct this situation will result in incalculable losses in terms of future U.S. economic well-being.

We at Research Corporation, America's first foundation for science advancement (begun in 1912), would like to say we stand ready to heed Marburger's marching orders. We'd like to boldly step forward to fund U.S. scientific research, so that the administration could continue to cut taxes for the rich and focus taxpayer dollars elsewhere, including the reported $9 billion or so it spends every month in Iraq. Alas, we can't.

Our $170 million endowment, even when combined with those of our sister science advancement foundations, isn't likely to meet all the needs of U.S. researchers left high and dry by flat federal funding. In 2004, the top 50 private U.S. foundations awarding science and technology grants distributed just under $456 million (*1*). This sum pales in comparison to the impact and importance of federal dollars.

Today's flat federal funding means that many bright young researchers will be forced out of promising science careers in the coming decade unless something is done. Eventually, some may choose to go elsewhere to do science; China, Korea, and India are grand examples of countries ramping up their basic research efforts. Young Americans with advanced degrees in physics, chemistry, and other hard sciences doubtless would be resilient enough to adapt to these intriguing cultures as they enriched their foreign corporate and government sponsors.

"[T]he technological fruits of scientific research have never been more important to economic development and national security."
—Gentile

These developments couldn't have come at a worse time. In today's world, where humanity's knowledge base continues to expand at a frenetic pace, the technological fruits of scientific research have never been more important to economic development and national security.

Last year, the Task Force on the Future of American Innovation reported survey results that indicated 70% of the public supports increasing federal funding by 10% a year for the next seven years for university research in science and engineering. The same survey showed that 49% of the electorate believes the United States' ability to compete economically in the world has grown worse over the past few years.

Unless we quickly come to an understanding that a simple-minded scheme to privatize scientific research, incrementally or otherwise, will not work, I fear that the nightmare of the United States as a scientifically developing-world nation could become a reality.

JAMES M. GENTILE

President, Research Corporation, 4703 E. Camp Lowell, Suite 201, Tucson, AZ 85712, USA.

Reference

1. The Foundation Center, Statistical Information Service (see http://foundationcenter.org/findfunders/statistics/pdf/04_fund_sub/2004/50_found_sub/f_sub_u_04.pdf).

Experimental Data for Structure Papers

We are writing to address the retraction of five papers on structural studies of ATP-binding cassette (ABC) transporters—three in *Science* (G. Chang *et al.*, "Retraction," Letters, 22 Dec. 2006, p. 1875), one in the *Proceedings of the National Academy of Sciences* (*1*), and one in the *Journal of Molecular Biology* (*2*). We have much sympathy for your readers but very little for the magazine. This is not the first time incorrect structures have been published in *Science* (*3*), and it will not be the last time. We and all of your readers make mistakes; crystallography is fortunate that by careful treatment of the experimental and derived data, most serious mistakes are caught and corrected before publication. The necessary tools and techniques are well described [for example, (*4*), and references therein] and widely used by our community. Inherent in structural analysis is a degree of subjectivity (*3*), which is particularly relevant in low-resolution studies such as those made by Chang and co-workers. Essentially correct structures have been built at 4.5 Å resolution, but it is not surprising that some of them turn out to be wrong upon further scrutiny.

For this scrutiny to take place, however, readers must be provided with the original experimental data, not only the derived atomic coordinates. Only armed with these data can an investigator conduct an independent evaluation that may result in a reinterpretation of the published structure.

The last time this happened, the structural community, with some prodding (most successfully from the major funding agencies) improved the frequency with which original experimental data (the so-called structure factors) are deposited at the Protein Data Bank. The response from and guidelines required by the publishing community, however, were very variable. Unfortunately, the higher the impact factor of the journal, the less likely it was that the experimental data were deposited. In *Science*, during the period from 1995 to 2002, only 38% of the deposited atomic models included the experimental data. *Nature* and *Cell* were only slightly better.

Depositing the experimental data does not

Computer viruses turn 25

210

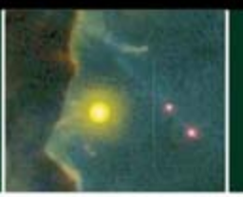

Water in the early solar system

211

guarantee that incorrect structures will not get published, but it does mean that an independent evaluation can be made of the experimental basis for the derived model. In the case of the ABC transporter structures, the serious errors in the atomic models could only have been corrected if the complete set of diffraction data (including the diffraction data from the single heavy atom derivative) had been deposited. No journal, as far as we know, demands this.

We call on *Science* and other journals to implement strict requirements for depositing original experimental data, both to forestall the publication of erroneous models in the future and to give readers the power to conduct independent evaluations of published models.

T. ALWYN JONES AND GERARD J. KLEYWEGT

Department of Cell and Molecular Biology, Uppsala University, BMC, Box 596, S-75124 Uppsala, Sweden.

References

1. C. Ma, G. Chang, *Proc. Natl. Acad. Sci. U.S.A.* **104**, 3668 (2007).
2. G. Chang, *J. Mol. Biol.* **369**, 596 (2007).
3. C.-I. Brändén, T. A. Jones, *Nature* **343**, 687 (1990).
4. G. J. Kleywegt, *Acta Crystallogr. Sect. D Biol. Crystallogr.* **D56**, 249 (2000).

PDB Improvement Starts with Data Deposition

A SMALL SOFTWARE FLAW RECENTLY TRIGGERED the retraction of a series of high-profile x-ray structures ["Retraction," Letters, 22 Dec. 2006, p. 1875; (*1*, *2*)]. Although in this case, the inaccurate protein structures were wrong and were promptly retracted, the Protein Data Bank (PDB) (*3*) still holds other structures that either are entirely wrong or are not correct enough to be used for the design or explanation of biological experiments.

In 1996, Hooft *et al.* (*4*) reported one million anomalies in the PDB, and we recently detected 10 times as many anomalies in a PDB that is 10 times as large. Most of these anomalies are of minor importance, and a small fraction are genuine discoveries that warrant further studies. However, a substantial number are serious errors. Using today's tools, we can correct many of the erroneous structures, provided that the original experimental x-ray data are available. We re-refined all 1195 PDB files that had a reported resolution of 2.0 Å and that were deposited after 1992 with the use of an experimental data file that included an R_{free} set. The details of the re-refinement procedure, the original and re-refined coordinate sets, structure validation reports for the original and TLS-refined coordinates, and all R and R_{free} values are available online (*5*).

The crystallographic community has long been advocating the deposition of experimental data. This has resulted in a clear policy by the International Union of Crystallography (IUCr) (*6*) and many scientific journals that the deposition of these data is required before publication. Unfortunately, 11% of the macromolecu-

MILLIPORE

CELL BIOLOGY

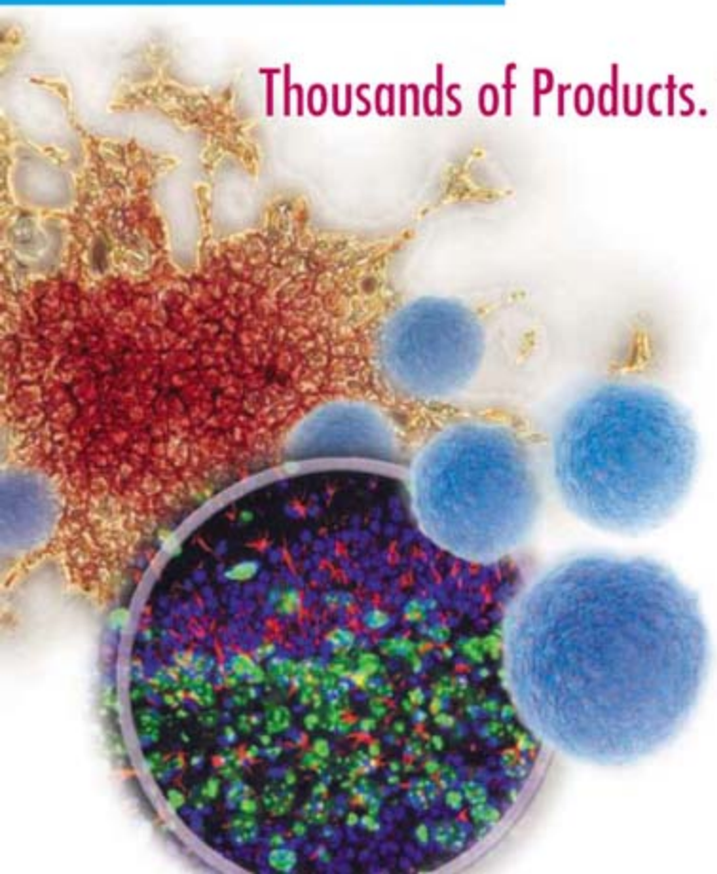

Thousands of Products. Hundreds of Techniques. Infinite Possibilities.

One Book.

The combination of Upstate®, Chemicon® and Millipore brings together all the leading tools for cell biology–including the most advanced stem cell products. All in one book. To see for yourself, request a copy of our new Cell Biology Application Guide today.

www.millipore.com/OneBook

upstate | CHEMICON

now part of Millipore

© 2007 Millipore Corporation

lar x-ray structures released in 2006 lacked the experimental data, and another 4% did not have a properly defined R_{free} set.

The re-refinement results (*5*) show that today's software can clearly improve the quality of most structures solved in the past. The vast majority of our test set clearly improved in terms of R_{free} and in terms of protein geometry. These results show the benefits of storing experimental x-ray data; these data allowed us to keep old protein structures relevant by means of re-refinement with the use of the latest insights and technologies. In anticipation of future improvements in refinement tools, we strongly urge journals and scientists to ever more rigorously strive for the deposition of all the original experimental x-ray data.

ROBBIE P. JOOSTEN AND GERT VRIEND

CMBI, NCMLS, UMC Nijmegen, Post Office Box 9101, 6500 HB Nijmegen, Netherlands.

References

1. C. Ma, G. Chang, *Proc. Natl. Acad. Sci. U.S.A.* **104**, 3668 (2007).
2. G. Chang, *J. Mol. Biol.* **369**, 596 (2007).
3. H. M. Berman *et al.*, *Nucleic Acids Res.* **28**, 235 (2000).
4. R. W. W. Hooft, G. Vriend, C. Sander, E. E. Abola, *Nature* **381**, 272 (1996).
5. PDB Redo (http://swift.cmbi.ru.nl/pdb_redo/).
6. International Union of Crystallography, Commission on Biological Macromolecules, *Acta Crystallgr. Sect. D Biol. Crystallogr.* **D55**, 2 (2000).

Editor's Note: Science seeks to enforce accepted community standards. With this motivation, we have required deposition of structure factors since 2002.

Permanent Reversal of Diabetes in NOD Mice

WE DISAGREE WITH HOW J. NISHIO *ET AL.* (*1*) represent our published data on the permanent reversal of type 1 diabetes in NOD mice (*2*). Nishio *et al.* state (*1*) that "a FCA alone control was not included in the report by Kodama *et al.*" (*3*). Further, in their response to our Technical Comment (*4*), they claim in numerous locations, including the abstract, that "[t]he experiments of Faustman *et al.* lack adequate controls," and "we continue to wonder why Faustman *et al.* have not performed the essential Freund's complete adjuvant alone control" (*4*). These statements in their papers are misrepresentations. These specific FCA (CFA)-alone controls were published in 2001 in our *Journal of Clinical Investigation* (JCI) paper (*5*). Nishio *et al.* cite our JCI paper that contains the numerous CFA control studies. The CFA-alone controls are present in eight locations in our manuscript: Fig. 1a; Fig. 1b; Fig. 2, Group D; Fig. 5, Group B; Fig. 6, Group D; Fig. 7c, Group B; Table 1, Group D; and Table 2, Group B.

DENISE L. FAUSTMAN

Massachusetts General Hospital and Harvard Medical School, Immunobiology Laboratories, Building 149, 13th Street, Boston, MA 02129, USA.

References

1. J. Nishio *et al.*, *Science* **311**, 1775 (2006).
2. D. Faustman *et al.*, *Science* **314**, 1243 (2006); www.sciencemag.org/ cgi/content/full/314/5803/1243a.
3. S. Kodama, W. Kühtreiber, S. Fujimura, E. A. Dale, D. Faustman, *Science* **302**, 1223 (2003).
4. J. Nishio *et al.*, *Science* **314**, 1243 (2006); www.sciencemag.org/ cgi/content/full/314/5803/1243c.
5. S. Ryu *et al.*, *J. Clin. Invest.* **108**, 63 (2001).

A Diver's Perspective on Coral Damage

I MUST TAKE EXCEPTION TO A COMMENT AND its implications in Richard Stone's otherwise excellent article "A world without corals?" (News Focus, 4 May, p. 678). Stone introduces the human toll on reefs by citing damage

inflicted by "divers clumsily breaking off chunks of coral." It is undeniable that recreational divers will, on occasion, inadvertently injure corals. However, I have been a certified SCUBA diver since 1992 and have logged over 150 ocean dives all over the world, and in that time I have seen only sporadic instances of divers impacting corals. Formal dive training by all major certification agencies includes instruction on reef protection, and the vast majority of dive tour operators repeatedly lecture divers about avoiding contact with coral and other marine life. It is undeniable that our coral reefs are threatened by human activities, but it is unfair to imply that sport divers at all popular reefs contribute significantly to this plight. Rather than a threat, I would argue that the growth of recreational diving is a major benefit to the future of our reefs: Divers are among the most environmentally conscious individuals I have met (note the "army of snorkeling and diving volunteers" described in the article), and this pastime depends on having beautiful, healthy corals to explore. As proof of this view, one need only visit Bonaire, a popular dive destination and the site of some of the world's healthiest coral reefs. Bonaire instituted strong legislation, including laws enacted in 1975 that made it illegal to break or sell coral. Subsequent efforts in cooperation with the World Wildlife Fund established a vast marine park that completely encompasses the island.

NORMAN KARIN

Pacific Northwest National Laboratory, Richland, WA 99352, USA.

Letters to the Editor

Letters (~300 words) discuss material published in *Science* in the previous 3 months or issues of general interest. They can be submitted through the Web (www.submit2science.org) or by regular mail (1200 New York Ave., NW, Washington, DC 20005, USA). Letters are not acknowledged upon receipt, nor are authors generally consulted before publication. Whether published in full or in part, letters are subject to editing for clarity and space.

TECHNICAL COMMENT ABSTRACTS

COMMENT ON "Maternal Oxytocin Triggers a Transient Inhibitory Switch in GABA Signaling in the Fetal Brain During Delivery"

Lionel Carbillon

Tyzio *et al.* (Reports, 15 December 2006, p. 1788) reported that maternal oxytocin triggers a transient excitatory-to-inhibitory switch of γ-aminobutyric acid (GABA) signaling during labor, thus protecting the fetal rat brain from anoxic injury. However, a body of evidence supports the possibility that oxytocin is released from the fetal pituitary during delivery, not only from the mother, particularly under conditions of hypoxic stress.

Full text at
www.sciencemag.org/cgi/content/full/317/5835/197a

RESPONSE TO COMMENT ON "Maternal Oxytocin Triggers a Transient Inhibitory Switch in GABA Signaling in the Fetal Brain During Delivery"

Roman Tyzio, Rosa Cossart, Ilgam Khalilov, Alfonso Represa, Yehezkel Ben-Ari, Rustem Khazipov

We tested the hypothesis that cortisol-induced release of fetal oxytocin triggers a perinatal inhibitory switch in γ-aminobutyric acid (GABA) signaling. The cortisol analog methylprednisolone did not modify GABA driving force and intracellular chloride concentration in 1-day-old rat hippocampal neurons. Together with the immaturity of the fetal rat hypothalamo-neurohypophysial system, these results suggest that oxytocin in the rat fetal brain is mainly provided by the mother.

Full text at
www.sciencemag.org/cgi/content/full/317/5835/197b

MILLIPORE

IMMUNODETECTION

Thousands of Biotools. Decades of Experience. Countless Options.

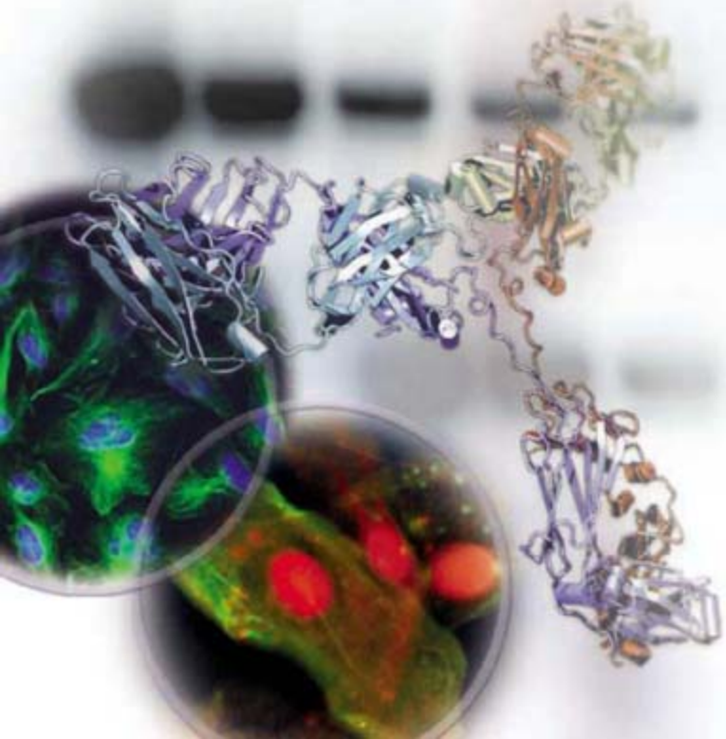

One Book.

The combination of Upstate®, Chemicon® and Millipore brings together all the leading tools for immunodetection–including the latest antibodies for life science research. All in one book. To see for yourself, request a copy of our new Immunodetection Application Guide today.

www.millipore.com/OneBook

upstate | CHEMICON
now part of Millipore

© 2007 Millipore Corporation

FILM: CLIMATE

Trying to Get Us to Change Course

Rush Holt

Scientists can learn much from *An Inconvenient Truth*, the widely viewed film and companion book of the same name, by former U.S. Vice President Al Gore. They are important works: Not for the science, although Gore does no injustice to that and no doubt through his presentation has taught some good science to many people. Nor for the visual images, although those too are well chosen, clear, and attractive. Rather, their importance lies in the author's successful attempt to do something even harder than modeling climate, deciphering ecological relationships, or designing low-carbon energy sources. What he has done is to help bring about a change of opinion in a resistant public. Scientists would be wise to take some of his methods to heart.

An Inconvenient Truth

Davis Guggenheim, Director

Paramount Classics, Hollywood, CA, 2006. 97 minutes. DVD, $29.99. www.climatecrisis.net/

An Inconvenient Truth
The Planetary Emergency of Global Warming and What We Can Do About It

by Al Gore

Rodale, New York, 2006. 328 pp. Paper, $21.95, C$28.95. ISBN 9781594865671.

As Gore reminds us, for more than two decades scientists have been issuing warnings that the release of greenhouse gases, principally carbon dioxide (CO_2), is probably altering Earth's climate in ways that will be expensive and even deadly (*1*, *2*). The American public yawned and bought bigger cars. Statements by the American Association for the Advancement of Science (*3*), American Geophysical Union (*4*), American Meteorological Society (*5*), Intergovernmental Panel on Climate Change (*6*), and others underscored the warnings and called for new government policies to deal with climate change. Politicians, presented with noisy statistics, shrugged, said there is too much doubt among scientists, and did nothing.

So, why is it that only recently the American public and their representative policymakers have begun to pay attention? How does conventional public opinion change? Is it a kind of phase change, where a seed can cause large crystals to drop out of solution, or maybe where a school of fish change direction almost at once from an indistinguishable signal? Whatever the metaphor, change has occurred. The public now widely believes that climate change is under way and that it is induced by humans (*7*). Those are two major conceptual shifts. The public has not yet crossed the conceptual barriers to the recognition that the present climatic changes present a serious threat and that solutions are possible, although they may be close to clearing those third and fourth hurdles as well.

Adding to our atmosphere.

CREDIT: © STEVE COLE/GETTY IMAGES

Gore can be given as much credit as anyone for these developments. The film earned over $24 million at the box office, the book has been a best seller (760,000 copies are in print), and 1.5 million DVDs have been sold. Students are being shown the film in school, and municipalities are scheduling viewings in public spaces. Word of mouth and this year's Academy Award for Best Documentary Feature have also fueled *An Inconvenient Truth*'s success.

It is instructive to consider how Gore did it. First, he worked for several years on the presentation, meeting with climate experts, energy engineers, and ecologists again and again. He collected some of the best images available, including time-lapse pictures of melting glaciers, schematics of ocean circulation, and newsreels of storm flooding. And he practiced his talk perhaps hundreds of times in front of many different audiences—politicians, scientists, business leaders, and a variety of others. I myself heard him give it several times in the years before he made the film.

I find Gore's science solid. More important, those who are expert in the relevant fields tell me that they are at least comfortable with his explanations of the science and in some cases admiring of his clarity and accuracy. Certainly, they say, he has the gist. Of course, critics will find points to dispute. They may note that he is wrong when he indicates diverted ocean currents will cause Europe to cool—although to be fair, it was only recent modeling that now shows the ocean cooling is insufficient to overwhelm the atmospheric warming. Gore makes provisional conclusions sound more definite than a practicing scientist might. He takes some worst-case outcomes (such as the catastrophic melt of all Greenland ice) and then presents the resulting effects, leaving the viewer to expect those results. Not what a scientist would do, perhaps, but recall that researchers had been trying for years to draw any attention to the matter.

Most significant, Gore structured the presentation with a shrewd recognition of how people learn and how they make decisions. He tells stories, personal stories. Scientists typically try to present their work to nonscientists by simplifying the life out of it. Simplification may be necessary, but that is not the key. Scientists should not simply distill their analysis. If they want their work to have any relevance beyond their specialty, they should create movement, present contests and conflicts, and develop personalities.

As Gore develops the story of scientific understanding of the effects of atmospheric CO_2, he shows graphs with hardly a mention of the numbers on the axes and uses animation of

The reviewer, U.S. Representative for New Jersey's 12th District, is at the U.S. House of Representatives, 1019 Longworth House Office Building, Washington, DC 20515, USA.

the graphs to move the story. It is, he says, just as predicted by his wise former professor Roger Revelle (*8*). Then, in a denouement worthy of a detective novel, he shows that the temperature record over 600,000 years matched the record of CO_2 concentration over the same period. "Aha!" concludes the viewer. CO_2 is exposed as the cause of the deadly hurricanes, the spreading disease vectors, and the vanishing landscapes. Gore leaves the viewer with the mistaken impression that CO_2 is the driver of climate change in that historic record. Nonetheless, it is true that climate models including the CO_2 concentration as a coupled feedback provide excellent retrospective fits, and it is reasonable to accept the models' prediction that a CO_2 concentration several times greater than recorded in that record will result in temperatures similarly off scale.

Gore identifies CO_2 as the cause, though not the culprit. Gore creates flesh-and-blood heroes and villains. Revelle is presented as a modern day Paul Revere sounding the alarm. For villains, Gore invokes comparisons with the tobacco companies, who by sowing doubt about the epidemiology of smoking caused the deaths of many people (*9*), including Gore's beloved sister. Similarly, he says, those who would ruin our planet are sowing doubt about climate change. The film and book present a compelling story reminiscent of Rachel Carson's *Silent Spring* (*10*), which by dramatizing science changed public perception and policy.

Using the conceptually simple "wedge model" of Robert Socolow and Stephen Pacala (*11*), Gore suggests that a half-dozen approaches to energy efficiency, alternative energy generation, and carbon capture could collectively pull our planet back from the brink of runaway climate change. The responses he calls for are not so much advanced technology as immediate, extensive, even bold, applications of methods currently available for reducing carbon in the energy mix: stop energy waste, choose efficient transportation, insulate buildings, use renewable energy, and capture and store CO_2. Gore has since gone on to propose an immediate freeze on new emissions, taxes on carbon emitters, a ban on incandescent lights, increased fuel efficiency requirements for American cars, and a mortgage association to help homeowners save energy (*12*). He tells the viewers that they are now part of the story. He intends to leave his audience with a sense of responsibility and empowerment, not despair.

Through *An Inconvenient Truth*, Gore has personalized the climate change debate and made it accessible in a way that has not only reversed public apathy but also motivated citizens to seek real policy changes. It is a lesson for all of us who believe science can serve public policy, giving us a clear understanding of how to engage people in a debate.

References and Notes

1. See for example, National Research Council, *Carbon Dioxide and Climate: A Scientific Assessment* (National Academy Press, Washington, DC, 1979).
2. J. T. Houghton, G. J. Jenkins, J.J. Ephraums, Eds., *Climate Change: The IPCC Scientific Assessment* (Cambridge Univ. Press, Cambridge, 1990).
3. www.aaas.org/news/press_room/climate_change/mtg_200702/.
4. www.agu.org/sci_soc/policy/climate_change_position.html.
5. www.ametsoc.org/POLICY/2007climatechange.html.
6. J. T. Houghton *et al.*, Eds., *Climate Change: The Scientific Basis* (Cambridge Univ. Press, Cambridge, 2001).
7. J. M. Broder, M. Connelly, *New York Times*, 27 April 2007, p. A20.
8. R. Revelle, H. Suess, *Tellus* **9**, 18 1957).
9. D. Kessler, *A Question of Intent: A Great American Battle with a Deadly Industry* (Public Affairs, New York, 2001).
10. R. Carson, *Silent Spring* (Houghton Mifflin, Boston, 1962).
11. S. Pacala, R. Socolow, *Science* **305**, 968 (2004).
12. F. Barringer, A. C. Revkin, *New York Times*, 22 March 2007, p. A18.

10.1126/science.1142810

WOMEN IN SCIENCE

Can Evidence Inform the Debate?

Marcia C. Linn

Almost everyone has an opinion about the relative dearth of women in science. *Why Aren't More Women in Science?* offers evidence to enrich, strengthen, question, or even refute commonly held views. The 15 essays bring to life recent findings on the involvement of women and men in science courses and careers. Editors Stephen Ceci and Wendy Williams, developmental psychologists at Cornell University, enticed 19 leading researchers on gender differences in ability to contribute succinct, informative essays summarizing their studies. The contributors present their strongest arguments, support those with their best data, and articulate their beliefs about the current participation of women in science. I encourage readers to note their views about the issue, read the essays, reflect on their own beliefs, and then take advantage of the editors' cogent introduction and thoughtful conclusions.

Why Aren't More Women in Science?
Top Researchers Debate the Evidence

Stephen J. Ceci and Wendy M. Williams, Eds.

American Psychological Association, Washington, DC, 2007. 274 pp. $59.95. ISBN 9781591474852.

My main quibbles with the book are the focus on exceptional scientific attainments (Ph.D. level) and the emphasis on small differences between males and females. Although important, these discussions overshadow the stunning increases in participation of women in science and may reinforce stereotypes that affect selection and career decisions.

In recent decades, the participation in science of women relative to men has increased dramatically. For example, in her essay Janet Hyde reports that, in 1966, women earned only 4.5% of the U.S. doctoral degrees in physical sciences but by 2000 this percentage had risen to 24.6%. For the biological sciences, women earned 12% of the doctoral degrees in 1966 and 42% in 2000. Similarly, Diane Halpern reports that in the biological sciences (including medicine, from which women were actively excluded not very long ago) the participation of men and women in Ph.D. and medical programs is now approximately equal. However, as Virginia Valian notes, women progress through the ranks less rapidly and get fewer of the most prestigious jobs and promotions after completing their final degree.

Against this encouraging backdrop of women's increasing participation in science, the essayists focus on three main areas of scholarship. They largely agree that subtle beliefs about who can participate in science—held both by those who instruct and select participants and by those who decide whether to participate—affect participation and persistence. They offer disparate interpretations of well-documented findings about cognitive abilities that might contribute to success in science, as indicated by mathematics test scores and spatial reasoning scores. They discuss the emerging methodologies and findings about a wide range of biological indicators, including prenatal hormones, brain development, brain lateralization, evolutionary processes, and brain activation patterns measured while individuals engage in science-related tasks.

Many essays showcase the role of subtle beliefs in decisions concerning the participation of men and women in science. A series of studies of selection decisions illustrates these phenomena. These studies provided respondents with a portfolio, a job application, an

The reviewer is at the Education in Mathematics, Science, and Technology Program, Graduate School of Education, University of California, Berkeley, 4611 Tolman Hall, Berkeley, CA 94720–1670, USA. E-mail: mclinn@berkeley.edu

BROWSING

AirCraft. The Jet as Art. Jeffrey Milstein. Abrams, New York, 2007. 104 pp. $29.95, C$35.95, £15.95. ISBN 9780810992856.
Photographer Milstein presents 60 precise digital images of current long-distance and regional airliners, air freighters, and corporate jets. Most of the photographs were taken looking directly up from the end of the runway at planes about to touch down. All are printed without any background, to emphasize the planes' engineering details and graphic designs. Many of the jets bear standard, if sometimes striking, airline paint schemes. Others display customized treatments—such as these Boeing 737-700s that Southwest Airlines patterned after state flags.

individual essay, or other information that was attributed to a male or a female. Whether the task is to admit someone to a graduate program, to select someone for tenure, or to assign a grade to an essay, the studies demonstrate that documents associated with a male name consistently get a higher rating than the same documents associated with a female name. For example, Elizabeth Spelke and Ariel Grace report on a study of a tenure decision for a candidate with an average record. When the dossier was associated with a male name, 70% of the reviewers recommended tenure; when it was attributed to a female name, only 45% recommended tenure. In their separate chapters, Carol Dweck and Jacquelynne Eccles discuss how subtle beliefs about who should participate in science affect admission, hiring, promotion, and funding decisions as well as career choices.

Several of the essays consider performance on competitive mathematics tests, such as the Scholastic Aptitude Test (SAT) and the Trends in International Mathematics and Science Study, often offering rather divergent interpretations of such evidence. Mean differences in performance of men and women on mathematics assessments have narrowed over the years, which leads Hyde to argue for gender similarities rather than differences. Many authors focus on the performance of males and females at the extremes of the distribution, where the gap is large but again narrowing. The chapter by David Lubinski and Camilla Benbow is one of several that mentions the 1980s talent search by Benbow and Julian Stanley, in which they recruited students under 14 to take the SAT and found that for scores over 700 (two standard deviations above the mean), the ratio was 13 boys to 1 girl. By 1997, the ratio had dropped to about 4 to 1 (*1*); it has recently fallen further to 2.8 to 1 (*2*). These large differences motivate some contributors to criticize others for ignoring the evidence for males' superior abilities in science. In the most dramatic statement, Doreen Kimura argues that giving special scholarships or grants exclusively to women "bribes them to enter fields they may neither excel in nor enjoy."

A number of essayists provide very provocative findings about sex differences in the level of prenatal hormones, brain architecture, and brain activity patterns—factors that may play roles in determining people's aptitudes and interests in science. These studies are, of necessity, conducted with relatively small samples and often reach conflicting conclusions. For example, Ruben Gur and Raquel Gur draw attention to the rapidly developing techniques and methodologies in neuroscience and conclude that "biology can only offer a limited perspective."

Through their efforts, Williams, Ceci, and the contributors offer readers the opportunity to explore important issues in the ongoing debates surrounding the participation and persistence of women in science. The volume provides thoughtful and lucid viewpoints from essayists who disagree with each other and differ in their interpretations of the same evidence. It also draws attention to neglected variables that may affect gender differences in science, such as the hours per week that individuals report in pursuing their careers and trade-offs between financial and intellectual rewards in career decision-making.

Despite the disagreements among the contributors, they all concur that scientific talent is desperately needed to address the challenges facing us. They express in delightful, thoughtful, and encouraging ways their commitment to the goal of attracting able and interested individuals to science. At the same time, they endorse research on the full range of factors that might contribute to success in science. *Why Aren't More Women in Science?* raises important questions. The volume will stimulate all readers to think more deeply about their own beliefs, commitments, and activities as they consider participation in science and how we can ensure that all individuals have the opportunities they deserve.

Increased participation. In 1997, the AAAS Board of Directors included (left to right) physicist and electrical engineer Mildred S. Dresselhaus (president-elect), microbiologist Rita R. Colwell (chair), and ecologist Jane Lubchenco (president).

References

1. J. C. Stanley, *Johns Hopkins Mag.* **49**(4), 6 (September 1997); www.jhu.edu/~jhumag/0997web/letters.html.
2. R. Monastersky, *Chron. High. Educ.* **51**(26), A1 (4 March 2005); http://chronicle.com/free/v51/i26/26a00102.htm.

10.1126/science.1141569

CREDITS: (TOP TO BOTTOM) JEFFREY MILSTEIN/COURTESY ABRAMS; AAAS ARCHIVES

ECONOMICS

Critical Assumptions in the Stern Review on Climate Change

The Stern Review's analysis of global-warming economics depends on an extreme view of economic discounting.

William Nordhaus

In November 2006, the British government presented a comprehensive study on the economics of climate change (*1*), the Stern Review. It painted a dark picture for the globe, "[I]f we don't act, the overall costs and risks of climate change will be equivalent to losing at least 5% of global GDP [gross domestic product] each year, now and forever. If a wider range of risks and impacts is taken into account, the estimates of damage could rise to 20% of GDP or more." The Stern Review recommended urgent, immediate, and sharp reductions in greenhouse-gas emissions.

These findings differ markedly from economic models that calculate least-cost emissions paths to stabilize concentrations or paths that balance the costs and benefits of emissions reductions. Mainstream economic models definitely find it economically beneficial to take steps today to slow warming, but efficient policies generally involve modest rates of emissions reductions in the near term, followed by sharp reductions in the medium and long term (*2*–*5*).

A standard way of showing the stringency of policies is to calculate the "carbon tax," or penalty on carbon emissions. A recent study by the author estimates an optimal carbon tax for 2005 of around $30 per ton carbon in today's prices, rising to $85 by the mid–21st century and further increasing after that (*5*). A similar carbon price has been found in studies that estimate the least-cost path to stabilize CO_2 concentrations at two times preindustrial levels (*2*). The sharply rising carbon tax reflects initially low, but rising, emissions-reduction rates. We call this the climate-policy ramp, in which policies to slow global warming increasingly tighten or ramp up over time. A $30 carbon tax may appear to be a modest target, but it is at least 10 times the current globally averaged carbon tax implicit in the Kyoto Protocol (shown as Stern assumptions).

What is the logic of the ramp? In a world where capital is productive and damages are far in the future (see chart above), the highest-return investments today are primarily in tangible, technological, and human capital. In the coming decades, damages are predicted to rise relative to output. As that occurs, it becomes efficient to shift investments toward more intensive emissions reductions and the accompanying higher carbon taxes. The exact timing of emissions reductions depends on details of costs, damages, learning, and the extent to which climate change and damages are nonlinear and irreversible.

The Stern Review proposes to move the timetable for emissions reductions sharply forward. It suggests global emissions reductions of between 30 and 70% over the next two decades, objectives consistent with a carbon tax of around $300 per ton today, or about 10 times the level suggested by standard economic models.

Given that the Stern Review embraces traditional economic techniques such as those described in (*2*–*5*), how does it get such different results and strategies? Having analyzed the Stern Review in (*6*) (which also contains a list of recent analyses), I find that the difference stems almost entirely from its technique for calculating discount rates and only marginally on new science or economics. The reasoning has questionable founda-

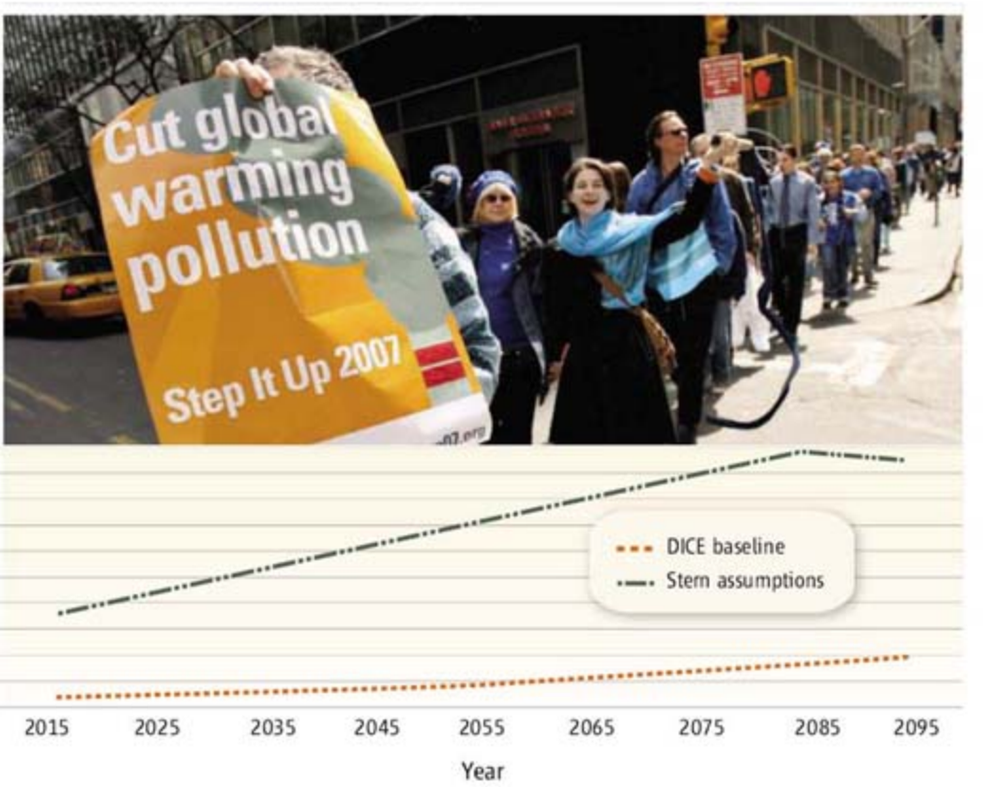

Comparing the optimal carbon tax under alternative discounting assumptions. The Dynamic Integrated model of Climate and the Economy (DICE model) (*5*) integrates the economic costs and benefits of greenhouse-gas (GHG) reductions with a simple dynamic representation of the scientific and economic links of output, emissions, concentrations, and climate change. The DICE model is designed to choose levels of investment in tangible capital and in GHG reductions that maximize economic welfare. It calculates the optimal carbon tax as the price of carbon emissions that will balance the incremental costs of abating carbon emissions with the incremental benefits of lower future damages from climate change. Using the DICE model to optimize climate policy leads to an optimal carbon tax in 2005 of around $30 per ton carbon (shown here as "DICE baseline"). If we substitute the Stern Review's assumptions about time discounting and the consumption elasticity into the DICE model, the calculated optimal carbon tax is much higher and rises much more rapidly (shown as "Stern assumptions").

PHOTO CREDIT: DIMA GAVRYSH/AP PHOTO

Department of Economics, Yale University, New Haven, CT 06511–8268, USA. E-mail: william.nordhaus@yale.edu

tions in terms of its ethical assumptions and also leads to economic results that are inconsistent with market data.

Some background on growth economics and discounting concepts is necessary to understand the debate. In choosing among alternative trajectories for emissions reductions, the key economic variable is the real return on capital, r, which measures the net yield on investments in capital, education, and technology. In principle, this is observable in the marketplace. For example, the real pretax return on U.S. corporate capital over the last four decades has averaged about 0.07 yr^{-1}. Estimated real returns on human capital range from 0.06 yr^{-1} to >0.20 yr^{-1}, depending on the country and time period (*7*). The return on capital is the "discount rate" that enters into the determination of the efficient balance between the cost of emissions reductions today and the benefit of reduced climate damages in the future. A high return on capital tilts the balance toward emissions reductions in the future, whereas a low return tilts reductions toward the present. The Stern Review's economic analysis recommended immediate emissions reductions because its assumptions led to very low assumed real returns on capital.

Where does the return on capital come from? The Stern Review and other analyses of climate economics base the analysis of real returns on the optimal economic growth theory (*8*, *9*). In this framework, the real return on capital is an economic variable that is determined by two normative parameters. The first parameter is the time discount rate, denoted by ρ, which refers to the discount on future "utility" or welfare (not on future goods, like the return on capital). It measures the relative importance in societal decisions of the welfare of future generations relative to that of the current generation. A zero discount rate means that all generations into the indefinite future are treated the same; a positive discount rate means that that the welfare of future generations is reduced or "discounted" compared with nearer generations.

Analyses are sometimes divided between the "descriptive approach," in which assumed discount rates should conform to actual political and economic decisions and prices, and the "prescriptive approach," where discount rates should conform to an ethical ideal, sometimes taken to be very low or even zero. Philosophers and economists have conducted vigorous debates about how to apply discount rates in areas as diverse as economic growth, climate change, energy, nuclear waste, major infrastructure programs, hurricane levees, and reparations for slavery.

The Stern Review takes the prescriptive approach in the extreme, arguing that it is indefensible to make long-term decisions with a positive time discount rate. The actual time discount rate used in the Stern Review is 0.001 yr^{-1}, which is vaguely justified by estimates of the probability of the extinction of the human race.

The second parameter that determines return on capital is the consumption elasticity, denoted as η. This parameter represents the aversion to the economic equality among different generations. A low (high) value of η implies that decisions take little (much) heed about whether the future is richer or poorer than the present. Under standard optimal growth theory, if time discounting is low and society cares little about income inequality, then it will save a great deal for the future, and the real return will be low. This is the case assumed by the Stern Review. Alternatively, if either the time discount rate is high or society is averse to inequality, the current savings rate is low and the real return is high.

This relation is captured by the "Ramsey equation" of optimal growth theory (*8*, *9*), in which the long-run equilibrium real return on capital is determined by $r = \rho + \eta g$, where g is the average growth in consumption per capita, ρ is the time discount rate, and η is the consumption elasticity. Using the Stern Review's assumption of $\rho = 0.001$ yr^{-1} and $\eta = 1$, along with its assumed growth rate ($g^* = 0.013$ yr^{-1}) and a stable population, yields an equilibrium real interest rate of 0.014 yr^{-1}, far below the returns to standard investments. It would also lead to much higher savings rates than today's. This low rate of return is used in the Stern Review without any reference to actual rates of return or savings rates.

The low return also means that future damages are discounted at a low rate, and this helps explain the Stern Review's estimate that the cost of climate change could represent the equivalent of a "20% cut in per-capita consumption, now and forever." When the Stern Review says that there are substantial losses "now," it does not mean "today." In fact, the Stern Review's estimate of the output loss "today" is essentially zero. We can illustrate this using the Stern Review's high-climate scenario with catastrophic and nonmarket impacts. For this case, the mean losses are 0.4% of world output in 2060, 2.9% in 2100, and 13.8% in 2200. This is reported as a loss in "current per capita consumption" of 14.4%.

How do damages that average around 1% over the next century turn into 14.4% cuts "now and forever"? The answer is that, with the low interest rate, the relatively small damages in the next two centuries get overwhelmed by the high damages over the centuries and millennia that follow 2200. In fact, if the Stern Review's methodology is used, more than half of the estimated damages "now and forever" occur after 2800.

What difference would it make if we used assumptions that are consistent with standard returns to capital and savings rates? For example, take the Stern Review's near-zero time discount rate with a high inequality aversion represented by a consumption elasticity of $\eta = 3$. This combination would yield real returns and savings rates close to those observed in today's economy and dramatically different from those shown in the Stern Review. The optimal carbon tax and the social cost of carbon decline by a factor of ~10 relative to these consistent with the Stern Review's assumptions, and the efficient trajectory looks like the policy ramp discussed above. In other words, the Stern Review's alarming findings about damages, as well as its economic rationale, rest on its model parameterization—a low time discount rate and low inequality aversion—that leads to savings rates and real returns that differ greatly from actual market data. If we correct these parameterizations, we get a carbon tax and emissions reductions that look like standard economic models.

The Stern Review's unambiguous conclusions about the need for urgent and immediate action will not survive the substitution of assumptions that are consistent with today's marketplace real interest rates and savings rates. So the central questions about global-warming policy—how much, how fast, and how costly—remain open.

References

1. N. Stern, *The Economics of Climate Change: The Stern Review* (Cambridge Univ. Press, Cambridge, UK, 2007).
2. J. Weyant, Ed., *Energy Econ.* **26** (4), Special Issue on EMF 19, pp. 501–755 (2004).
3. W. D. Nordhaus, J. Boyer, *Warming the World: Economic Modeling of Global Warming* (MIT Press, Cambridge, MA, 2000).
4. R. S. J. Tol, *Energy Policy*, **33**, 2064-2074 (2005).
5. W. D. Nordhaus, "The Challenge of Global Warming: Economic Models and Environmental Policy" (Yale Univ., New Haven, CT, 2007); available at http://nordhaus.econ.yale.edu/recent_stuff.html.
6. W. D. Nordhaus, *J. Econ. Lit.*, in press; available at http://nordhaus.econ.yale.edu/recent_stuff.html.
7. K. J. Arrow *et al. Climate Change 1995—Economic and Social Dimensions of Climate Change*, http://nordhaus.econ.yale.edu/stern_050307.pdf
8. F. Ramsey, *Econ. J.* **38**, 543 (1928).
9. T. C. Koopmans, *Acad. Sci. Scripta Varia* **28**, 1 (1965).

10.1126/science.1137316

ECONOMICS

Climate Change: Risk, Ethics, and the Stern Review

An optimal economic response to climate change requires consideration of discounting and value judgments.

Nicholas Stern and Chris Taylor

Any thorough analysis of policy on climate change must examine scientific, economic, and political issues and many other relationships and structures and must have ethics at its heart. In a Policy Forum in this issue of *Science*, Nordhaus (*1*) suggests that our results as described in the Stern Review (*2*) stem almost entirely from ethical judgments. This is not correct. In addition to revisiting the ethics, we also incorporated the latest science, which tells us that, for a given change in atmospheric concentration, the worst impacts now appear more likely. Further, the science also now gives us a better understanding of probabilities, so we could incorporate explicit risk analysis, largely overlooked in previous studies. It is risk plus ethics that drive our results.

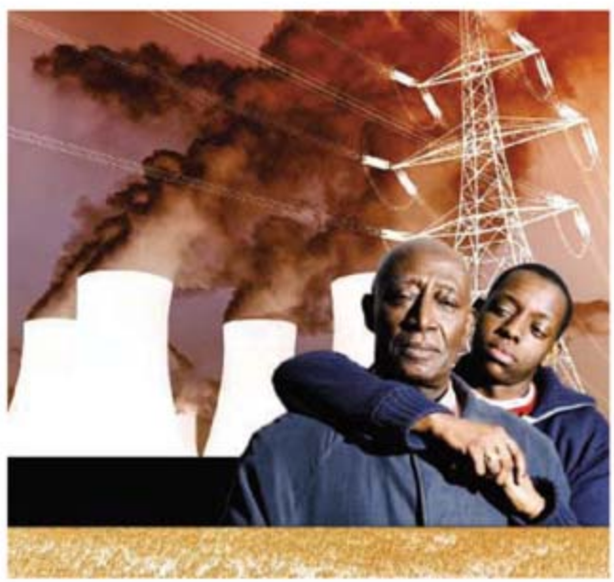

The most direct way to look at the problem of constructing an economic response to climate change is to look at the individual impacts of climate change alongside the cost of reducing emissions and then to ask whether it is worth paying for mitigation. However, we do not have the kind of information that would enable formally attaching numbers to all consequences, weighting them, and adding them all up with any plausibility. Thus, economists attempt aggregations of impacts and costs using very simplified aggregate modeling and, in the process, throw away much that is of fundamental importance to a balanced judgment.

The central estimate of mitigation costs for stabilizing emissions below 550 ppm CO_2 equivalent is 1% of gross domestic product (GDP) per annum (*2*). The basic question is thus whether it is worth paying 1% of GDP to avoid the additional risks of higher emissions. The modeling in the Stern Review is valuable in identifying some key drivers of costs and benefits in terms of economic modeling approaches, scientific variables, and ethical considerations. However, excessive focus on the narrow aspects of these simplistic models distorts and often exaggerates their role in policy decisions. They cannot substitute for the detailed risk and cost analysis of key effects.

Our sensitivity analysis shows that our main conclusions—that the costs of strong action are less than the costs of the damage avoided by that action—are robust to a range of assumptions. These assumptions concern (i) model structure and inputs (including population, structure of the damage function, aversion to irreversible consequences, future conditions, and the rise in price of environmental goods relative to consumption goods) and (ii) value judgments (attitudes to risk and inequality, the extent to which future generations matter, and intragenerational income distribution and/or regional equity weighting).

Some credible assumptions about the rate at which climate change will result in damage would lead to cost estimates that are much higher; our modeling approach has been cautious. Some modelers are very optimistic about economic growth and social rates of return for the next centuries. However, they appear to overlook that such rapid growth is likely to lead to greater emissions and, hence, the more rapid onset of climate change.

The ethical approach adopted in our analysis focuses on the ethics of allocation between richer and poorer people and between those born at different times. Ramsey (*3*) developed the standard social welfare discounting formula $r = \eta g + \rho$, where r is the consumption discount rate, η is the elasticity of the social benefits attained (also called the social marginal utility), g is per-capita consumption growth rate, and ρ is the time discount rate (also called the pure rate of time preference). The equation arises from comparing the social value of a bit of consumption in the future with a unit now and asking how it falls over time, the definition of a discount rate.

Traditionally, the discount rate has been applied to policies and projects involving small changes with direct benefits and costs over less than one generation (say a few decades at most), which means that people are feeling the impact of their decisions in their own lives. However, climate change is an intergenerational policy issue, and thus, we must see ρ as a parameter capturing discrimination by date of birth. For example, applying a 2% pure time discounting rate ($\rho = 2$) gives half the ethical weight to someone born in 2008 relative to someone born in 1973. Surely, many would find this difficult to justify.

In addition, the discounting formula described above depends on the path of future growth in consumption. Climate change involves potentially very large changes and can reduce future growth in consumption, so the discount rate applied in a world with climate change will be less than that in a world without, all else being equal. Moreover, this logic can be extended so that the uncertainty around climate impacts is taken into account. For every possible scenario of future climate change, there will be a specific average discount rate, depending on the growth rate of consumption in that scenario (*4*). Thus, to speak of "the discount rate" is misguided.

Using $\eta = 1$ implies that a given social benefit will be valued more highly by a factor of five for someone with one-fifth the resources of someone else. Some commentators have suggested that higher values should be used. Using $\eta = 2$ would mean that an extra benefit to the person who is poorer by a factor of five would have a value 25 times that to a richer person. In a transfer from the richer

PHOTO CREDITS (MAIN): GETTY IMAGES; (INSET) CORBIS

individual to the poorer one, how much would you be prepared to lose in the process and still regard it as a beneficial transfer? In the case of $\eta = 2$, as long as less than 96% is lost, it would be seen as beneficial and, for $\eta = 1$, less than 80%. Although it is a tenable ethical position, those who argue for η as high as 2 should be advocating very strong redistribution policies.

In the case of $\eta = 3$ in Nordhaus' example, over 99% could be lost and a transfer would still be beneficial. Does he advocate huge increases in transfers from rich to poor in the current generation?

A value of unity for η is quite commonly invoked, but higher values of ρ are sometimes used in cost-benefit analysis. Indeed, there are a number of reasons why a smaller-scale project such as a new road or railway may not be as valuable—or relevant at all—in several years time as circumstances change. However, avoiding the impacts of climate change (the value of a stable climate, human life, and ecosystems) is likely to continue to be relevant as long as the planet and its people exist.

Further, as people become richer and environmental goods become scarcer, it seems likely that, rather than fall, their value will rise very rapidly, which was an issue raised in chapter 2 of our review and has been investigated in later analyses (*5*). And the flow-stock nature of greenhouse gas accumulation, plus the powerful impact of climate change, will render many consequences irreversible. Thus, investing elsewhere and using the resources to compensate for any later environmental damage may be very cost-ineffective.

Many of the comments on the review have suggested that the ethical side of the modeling should be consistent with observable market behavior. As discussed by Hepburn (*6*), there are many reasons for thinking that market rates and other approaches that illustrate observable market behavior cannot be seen as reflections of an ethical response to the issues at hand. There is no real economic market that reveals our ethical decisions on how we should act together on environmental issues in the very long term.

Most long-term capital markets are very thin and imperfect. Choices that reflect current individual personal allocations of resource may be different from collective values and from what individuals may prefer in their capacity as citizens. Individuals will have a different attitude to risk because they have a higher probability of demise in that year than society. Those who do not feature in the market place (future generations) have no say in the calculus, and those who feature in the market less prominently (the young and the poor) have less influence on the behaviors that are being observed.

The issue of ethics should be tackled directly and explicitly through discussion (*7*). No discussion of the appropriateness of particular value judgments can be decisive. Alternative ethical approaches should be explored: Within the narrow confines of the modeling, sensitivity analysis does this. There is also scope for further work attempting to disentangle the roles of risk aversion and inequality aversion that are conflated (via η) in this modeling. Furthermore, we should go beyond the narrow framework of social welfare functions to consider other ethical approaches, including those involving rights and sustainability.

We note briefly that Nordhaus misrepresents the Stern Review on the subject of taxes. He argues that we propose a tax of $85 per ton of carbon dioxide, which equates to $312 per ton of carbon. This was our estimate of the marginal environmental cost of each extra carbon emission (the "social cost of carbon," hereafter SCC) under business-as-usual, with no policies to reduce emissions. To identify this with a recommended tax makes two mistakes. First, any estimate of the SCC is path-dependent. In chapter 13 of the Stern Review, we justify our proposed policy goal of stabilizing emissions between 450 and 550 ppm CO_2 equivalent. In this range, we estimate the social cost of carbon to be between $25 per ton of carbon dioxide (450 ppm) and $30 per ton (550 ppm), and so the proposed package of policies should be broadly consistent with this range. Second, in distorted and uncertain economies, any tax should be different from an SCC (*8*). Stabilization between 450 and 550 ppm is equivalent to reductions of around 25 to 70% in 2050. Nordhaus claims erroneously that the review suggests reductions on this scale over the next two decades. The Stern Review is also clear that prices should increase over time, although perhaps not as sharply as Nordhaus suggests.

The ethical approach in Nordhaus' modeling helps drive the initial low level of action and the steepness of his policy ramp. As future generations have a lower weight they are expected to shoulder the burden of greater mitigation costs. This could be a source of dynamic inconsistency, because future generations will be faced with the same challenge and, if they take the same approach, will also seek to minimize short-term costs but expect greater reductions in the future as they place a larger weight on consumption now over the effects on future generations (thus perpetuating the delay for significant reductions).

We have argued strongly for an assessment of policy on climate change to be based on a disaggregated approach to consequences—looking at different dimensions, places, and times—and a broad ethical approach. Nevertheless, our modeling sensitivity analysis demonstrates that the treatment of risk and uncertainty and the extent to which the model responds to progress in the scientific literature, are of roughly similar importance in shaping damage estimates as our approach to ethics and discounting. It is these three factors that explain higher damage estimates than those in the previous literature.

Given the centrality of risk, scientific advance, and ethics, in our view, the question should really be why, with some important exemptions, did the previous literature pay inadequate attention to these issues?

There was much structural caution in our approach. We left out many risks that are likely to be important, for example, the possibility of strong disruption of carbon cycles by changes to oceans and forests. It is possible that risks and damages are higher than we estimated. But one thing is clear: however unpleasant the damages from climate change are likely to appear in the future, any disregard for the future, simply because it is in the future, will suppress action to address climate change.

References and Notes

1. W. Nordhaus, *Science* **317**, 201 (2007).
2. N. Stern, *The Economics of Climate Change: The Stern Review* (Cambridge Univ. Press, Cambridge, 2006).
3. F. P. Ramsey, *Econ. J.* **38**, 543 (1928).
4. In the review's modeling, the *g* in the discount rate is specific to the growth path in each of the thousands of model runs in the Monte Carlo analysis of aggregated-impact cost estimates.
5. T. Sterner, U. M. Persson, "An even sterner review: Introducing relative prices into the discounting debate," Working draft, May 2007; www.hgu.gu.se/files/nationalekonomi/personal/thomas%20sterner/b88.pdf
6. C. Hepburn, "The economics and ethics of Stern discounting," presentation at the workshop the Economics of Climate Change, 9 March 2007, University of Birmingham, Birmingham, UK; www.economics.bham.ac.uk/maddison/Cameron%20Hepburn%20Presentation.pdf
7. N. Stern, "Value judgments, welfare weights and discounting," Paper B of "After the Stern Review: Reflections and responses," 12 February 2007, Working draft of paper published on Stern Review Web site; www.sternreview.org.uk
8. N. Stern, "The case for action to reduce the risks of climate change," Paper A of "After the Stern Review: Reflections and responses," working draft of paper published on Stern Review Web site, 12 February 2007; www.sternreview.org.uk.

10.1126/science.1142920

BIOCHEMISTRY

Toward Methylmercury Bioremediation

A strategy for facile cleavage of carbon-mercury bonds in chemical compounds may help in cleaning up environmental contamination by methylmercury.

James G. Omichinski

Human activities such as coal burning have produced many tons of ionic mercury, which is readily converted to methylmercury by microbes in sediments (*1*). This contamination is dangerous, because methylmercury accumulates in living tissues, where it is highly toxic. Specialized bacteria can grow naturally in methylmercury-contaminated environments, because they produce the methylmercury-degrading enzyme MerB (*2*). Because of its unique ability to cleave carbon-mercury bonds, MerB is crucial to efforts to clean up methylmercury from contaminated waterways. Unfortunately, little is known about the enzymatic mechanism of MerB at the atomic level, limiting its applications in remediation efforts. On page 225 of this issue, Melnick and Parkin (*3*) provide insights into the reaction catalyzed by MerB by demonstrating cleavage of a carbon-mercury bond by compounds whose structures closely resemble the active site of MerB.

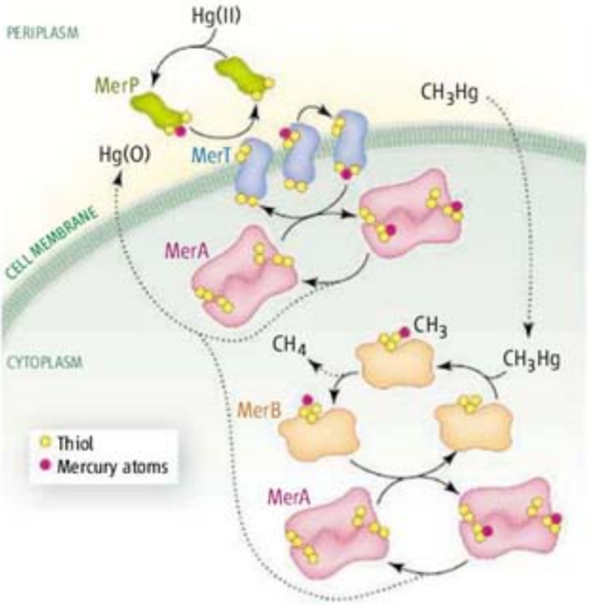

The mer system. The proteins of the mer system depend on thiols for high-affinity binding to mercury compounds. Ionic mercury [Hg(II)] is bound in the periplasmic space by MerP and then transferred to MerT for transport across the membrane. In the cytosol, Hg(II) is transferred from MerT to MerA. MerA reduces Hg(II) to elemental mercury [Hg(0)], which is expired. Methylmercury (CH_3Hg) directly enters the cytosol, where it binds to MerB. MerB uses thiols to cleave the carbon-mercury bond by a mechanism similar to that proposed by Melnick and Parkin. This cleavage generates methane and Hg(II). The latter remains bound to MerB until it is transferred to MerA for reduction to Hg(0).

Methylmercury toxicity was first observed on a large scale in Japan in the 1950s due to the consumption of contaminated fish from Minamata Bay (*4*). The contamination was caused by a nearby chemical factory discharging high concentrations of ionic mercury, which was converted to methylmercury and bioaccummulated in the fish.

Select strains of bacteria are resistant to mercury compounds through the acquisition of a transferable genetic element known as the mer operon. The mer operon is a dedicated set of mercury-resistant genes that are self-regulated by the DNA-binding protein MerR. Bacteria resistant to both ionic mercury and methylmercury code for proteins that regulate mercury transport (MerA, MerP, MerT) and mercury degradation (MerA and MerB) (see the first figure).

Mercury compounds are toxic because they bind very strongly to thiol groups in proteins. The mer system exploits this property by binding to mercury compounds with high affinity through thiol-containing cysteine residues. These thiols are critical not only for the enzymatic reactions by MerA and MerB (*5*, *6*), but also for the direct transfer of ionic mercury between members of the mer system (*7*–*9*), thus minimizing the opportunity for mercury compounds to bind other cellular proteins leading to toxicity.

The active site of MerB encoded by *Escherichia coli* (R831b) contains three cysteines (*10*). To emulate the environment in this active site, Melnick and Parkin prepared a series of alkyl-mercury compounds that contain three sulfurs (*3*). Following a reaction with a second thiol-containing compound, a subgroup of the alkyl-mercury compounds spontaneously cleaved their carbon-mercury bond. In the most active compounds, mercury can simultaneously bind to three thiols. The authors suggest that the three cysteines in the MerB active site create similar structures that facilitate cleavage of carbon-mercury bonds.

The results are consistent with earlier mechanistic studies of MerB (*11*). However, their model for MerB differs slightly from other models, which suggest that carbon-mercury bond cleavage requires two thiols and either a carboxylate (*12*) or possibly a phenolic group (*5*), rather than a third thiol. Phylogenetic analysis of MerB sequences indicates that only two of the three active-site cysteines are strictly conserved (*5*). All three cysteines are essential for resistance in vivo (*6*), but replacing the nonconserved cysteine with a serine hydroxyl group only moderately reduces MerB activity in vitro (*5*). Hence, either the third cysteine is not required for cleavage, or the hydroxyl group of serine is a suitable substitute. But even if the work by Melnick and Parkin does not exactly model MerB, the authors provide an elegant atomic-level description for the facile cleavage of a carbon-mercury bond (*3*).

There have been considerable efforts to develop bioremediation systems to deal with methylmercury contamination using MerB

MerB-expressing plants. Transgenic cottonwood plants expressing MerB (**right**) grow roots readily on concentrations of phenylmercury acetate that severely inhibit wild-type root growth (**left**).

The author is in the Département de Biochimie, Université de Montréal, Montréal, QC, H3C 3J7 Canada. E-mail: jg.omichinski@umontreal.ca

CREDITS (TOP TO BOTTOM): ADAPTED BY P. HUEY/SCIENCE; R. MEAGHER/UNIVERSITY OF GEORGIA, USA; S. MERKLE/UNIVERSITY OF GEORGIA, USA; AND R. KIM/PHYGEN, INC., KOREA

and MerA. The results of Melnick and Parkin help such efforts by providing atomic-level insight into the basic mechanisms of carbon-mercury bond cleavage by thiols. In a highly innovative approach, Meagher and co-workers have engineered MerA and MerB into plants to remediate methylmercury contamination (*13*). Remediation using plants is potentially more robust than bacterial remediation, because plants use solar energy, have roots that penetrate contaminated sediments, and accumulate a large aboveground biomass; furthermore, a few well-characterized plant species may be used to clean up contaminated wetland ecosystems (*13*). When they modified plants such as cottonwood trees (*14*) and tobacco (*15*) to express either MerB (see the second figure) or both MerB and MerA, the plants converted methylmercury to ionic mercury or elemental mercury, respectively. However, the elemental mercury was released into the atmosphere, where it may still pose a risk. Future studies must also evaluate the risks and benefits of introducing genetically modified MerB-expressing plants with respect to the dangers associated with methylmercury contamination.

Considerable work remains to be done to increase the efficiency and safety of current bioremediation systems for methylmercury involving MerB. Atomic-level knowledge of the carbon-mercury bond cleavage, such as the results of Melnick and Parkin, is essential to efforts to reengineer MerB to improve its catalytic efficiency for the bioremediation of methylmercury.

References and Notes

1. T. Barkay, S. M. Miller, A. O. Summers, *FEMS Microbiol. Rev.* **27**, 355 (2003).
2. A. O. Summers, *Annu. Rev. Microbiol.* **40**, 607 (1986).
3. J. G. Melnick, G. Parkin, *Science* **317**, 225 (2007).
4. P. A. D'Itri, F. M. D'Itri, *Environ. Manag.* **2**, 3 (1978).
5. K. E. Pitts, A. O. Summers, *Biochemistry* **41**, 10287 (2002).
6. M. J. Moore, M. D. Distefeno, L. D. Zydowsky, R. T. Cummings, C. T. Walsh, *Acc. Chem. Res.* **23**, 301 (1990).
7. A. P. Morby, J. L. Hobman, N. L. Brown, *Mol. Microbiol.* **17**, 25 (1995).
8. E. Rossy *et al.*, *FEBS Lett.* **575**, 86 (2004).
9. G. C. Benison *et al.*, *Biochemistry* **43**, 8333 (2004).
10. P. Di Lello *et al.*, *Biochemistry* **43**, 8322 (2004).
11. T. P. Begley, A. E. Walts, C. T. Walsh, *Biochemisty* **25**, 7192 (1986).
12. E. Gopinath, T. C. Bruice, *J. Am. Chem. Soc.* **109**, 7903 (1987).
13. R. B. Meagher, *Curr. Opin. Plant Biol.* **3**, 153 (2000).
14. S. Lyyra *et al.*, *Plant Biotechnol. J.* **5**, 254 (2007).
15. A. C. P. Heaton, C. L. Rugh, N.-J. Wang, R. B. Meagher, *Water Air, Soil Pollut.* **161**, 137 (2005).

16. I am supported by the National Science and Engineering Council of Canada. I thank R. Meagher for many stimulating discussions.

10.1126/science.1145810

BIOCHEMISTRY

PI3K Charges Ahead

Structural information about an enzyme implicated in numerous cancers provides insights into to how certain mutations promote cancer cell growth and survival.

Jennifer Y. Lee, Jeffrey A. Engelman, Lewis C. Cantley

The phosphoinositide 3-kinase (PI3K) signaling pathway is crucial to the viability of many cancers (*1*–*3*). PI3K inhibitors block cancer cell growth and survival, and some genetic alterations, such as loss of the *PTEN* tumor suppressor, increase PI3K activity in cancer cells. After the seminal discovery that *PIK3CA*—the gene encoding the PI3K catalytic subunit (p110α)—is mutated in cancers (*4*), these mutant p110α proteins were found to have constitutive PI3K activity and the capacity to transform normal cells into cancer cells (*5*). Mutations in *PIK3CA* occur throughout p110α, but two hotspot regions—the helical and kinase domains—comprise more than 80% of the mutations. However, the molecular mechanisms by which these mutations increase PI3K activity have remained a mystery. On page 239 of this issue, Miled *et al.* (*6*) elucidate how one of the hotspot mutations increases PI3K activity. The findings reveal a new mechanism for activating PI3K and suggest new possibilities for therapeutic agents that target this enzyme.

PI3K (specifically, class I_A PI3K) is a heterodimer consisting of a p85 regulatory subunit and a p110 catalytic subunit (*1*, *7*). Normally, PI3K, which resides in the cytoplasm, is activated upon binding to either a receptor tyrosine kinase at the cell surface (for example, the platelet-derived growth factor receptor) or to adaptor molecules (such as insulin receptor substrate–1, which is phosphorylated by activated insulin receptor). The p85 regulatory subunit mediates these binding events through two Src homology 2 (SH2) domains that interact with phosphorylated tyrosine residues on the receptor or adaptor protein. As a result, PI3K localizes to the plasma membrane, where it phosphorylates the membrane lipid phosphatidylinositol 4,5-bisphosphate (PIP_2) to produce phosphatidylinositol 3,4,5-trisphosphate (PIP_3). This leads to activation of downstream signaling pathways that control cell growth and survival.

The p85-p110α interaction is remarkably strong, and p110α is stable only when it is bound to p85 (*8*). This heterodimer is formed by the binding of the p85 inter-SH2 (iSH2) domain to the p110α adaptor-binding domain (ABD) (see the figure). However, the structure of this interaction had remained unknown until Miled and colleagues crystallized the p110α ABD bound to the p85 iSH2 domain. They found that the ABD forms a ubiquitin-like domain that contacts the antiparallel coiled-coil region of iSH2. However, previous data implied additional interactions between p85 and p110α—the p85 N-terminal SH2 domain (nSH2) inhibits purified p110α in vitro (*9*). This suggested that binding of the p85 nSH2 domain to a receptor or adaptor releases p110α from this inhibitory interaction with p85, without disrupting the iSH2-ABD interaction (see the figure).

In light of these structural findings, the authors examined two classes of p110α oncogenic mutations: the prevalent helical domain mutations and the less common ABD mutations. Several mutations in the helical domain result in an amino acid of opposite charge, such as a glutamic acid (negative charge) to lysine (positive charge) change at position 545 (E545K). Through biochemical studies, the authors found that, unlike wild-type p110α, the E545K mutant is not inhibited by p85 nSH2. Thus, this region of the p110α helical domain likely binds to p85 nSH2, an interaction that normally maintains wild-type PI3K in a low-activity state. The authors hypothesized that important charge-charge interactions occur between the p110α helical domain and p85 nSH2 domain, and they mutated all nSH2 basic residues to acidic ones. They identified two important residues in p85 (Lys^{379} and Arg^{340}) that are required to inhibit p110α. When they reversed the charge on these basic residues by mutating to glutamates, the mutant p85 nSH2 domains effectively inhibited p110α E545K but not wild-type p110α. Thus, the authors propose that p110α E545K is oncogenic

The authors are in the Department of Systems Biology, Harvard Medical School, and in the Division of Signal Transduction, Beth Israel Deaconess Medical Center, Boston, MA 02115, USA. J. A. Engelman is also at Massachusetts General Hospital Cancer Center, Boston, MA 02115, USA. E-mail: lewis_cantley@hms.harvard.edu

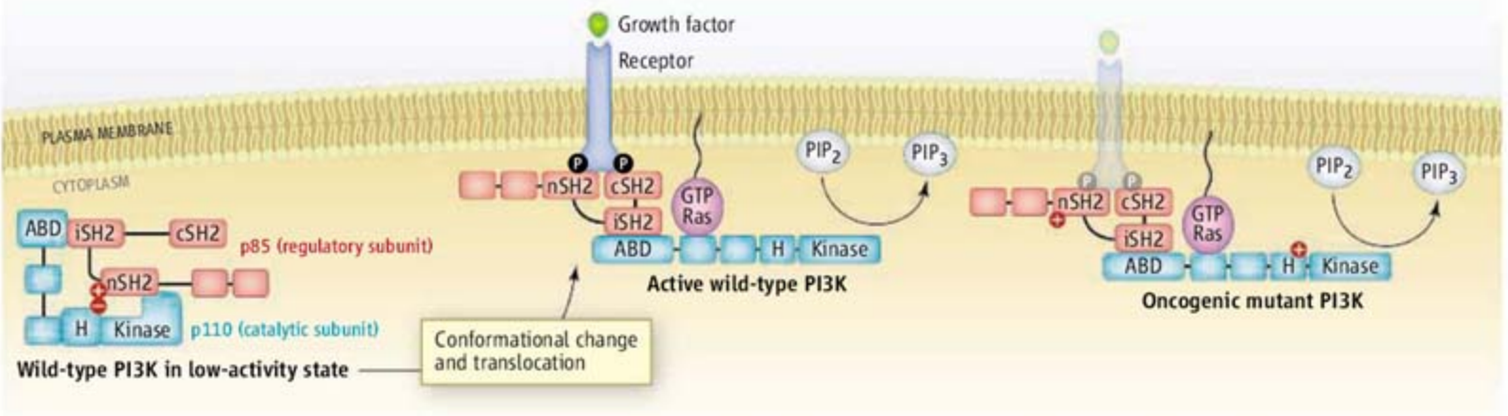

A cancer-linked mutation in PI3K. The major stabilizing interaction in PI3K involves the p85 iSH2 and p110α ABD domains. Inhibition of PI3K is mediated by a charge-charge interaction (shown as plus and minus signs) between the p85 nSH2 domain and the helical (H) domain of p110α. PI3K localizes to the membrane where interaction with an activated receptor relieves the inhibition. In PI3K with an oncogenic p110α charge-reversal mutation in the helical domain (E545K), the inhibitory interactions are abrogated, resulting in constitutive PI3K activation.

because it is not inhibited by the p85 nSH2 domain (see the figure).

It is less clear how the ABD mutations activate PI3K. Although the ABD binds to p85, ABD mutations are located on the exposed surface oriented away from the iSH2 domain, suggesting that ABD mutations do not directly interfere with p85-p110α interaction. Instead, they may distort orientation of the ABD with respect to the catalytic core, affecting the intrinsic enzymatic activity of p110α or its interactions with other proteins.

How does the E545K mutant promote cell growth and survival in the absence of growth factors? Although the mutation abrogates intermolecular inhibition, it does not explain its membrane localization. The p85 nSH2 domain, unencumbered by interaction with the p110α helical domain, might remain more tightly associated with receptors and adaptors, protecting critical tyrosine residues from dephosphorylation and thereby prolonging PIP_3 production. It is also possible that the mutant PI3K localizes to the membrane through membrane-bound Ras protein (p110α has a Ras-binding domain) or random encounters with membrane lipid substrate. The research by Miled *et al.* will hopefully spur efforts to crystallize the holoenzyme with both the wild-type and mutant p110α proteins.

PI3K inhibitors are now being evaluated in clinical trials. Analogous to the success of drugs that block kinases—trastuzumab in *HER2*-amplified breast cancers, imatinib in Philadelphia-chromosome chronic myelogenous leukemia, and gefitinib in *EGFR*-mutant lung cancers—cancers with genetic activation of PI3K signaling could be susceptible to PI3K inhibitors. Thus, cancers with *PIK3CA* mutations (or *PTEN* loss) will be carefully investigated for sensitivity to PI3K inhibitors. The p110α E545K mutant may be susceptible to compounds that bind to its unique helical domain surface. Such a specific therapy would be expected not to inhibit wild-type PI3K, thus reducing unwanted side effects. Moreover, different *PIK3CA* mutations may be functionally distinct and their effects on cellular responses to inhibitors could also be variable. Thus, we are reminded not to necessarily group all cancers with *PIK3CA* mutations together when analyzing cancers and their response to targeted therapies.

References

1. J. A. Engelman, J. Luo, L. C. Cantley, *Nat. Rev. Genet.* **7**, 606 (2006).
2. L. C. Cantley, *Science* **296**, 1655 (2002).
3. A. G. Bader, S. Kang, L. Zhao, P. K. Vogt, *Nat. Rev. Cancer* **5**, 921 (2005).
4. Y. Samuels *et al.*, *Science* **304**, 554 (2004).
5. P. K. Vogt, S. Kang, M. A. Elsliger, M. Gymnopoulos, *Trends Biochem. Sci.* 10.1016/j.tibs.2007.05.005 (2007).
6. N. Miled *et al.*, *Science* **317**, 239 (2007).
7. R. Katso *et al.*, *Annu. Rev. Cell Dev. Biol.* **17**, 615 (2001).
8. J. Yu *et al.*, *Mol. Cell. Biol.* **18**, 1379 (1998).
9. J. Yu, C. Wjasow, J. M. Backer, *J. Biol. Chem.* **273**, 30199 (1998).

10.1126.science.1146073

CLIMATE CHANGE

A Changing Climate for Prediction

Standard climate model projections, which have shown the significance of global warming, must be redesigned to inform climate change adaptation and mitigation policy.

Peter Cox and David Stephenson

The latest report by the Intergovernmental Panel on Climate Change (IPCC) makes it clear that recent global warming is significant in the context of natural climate variations, and that human activities are very likely to be the cause of this climate change. As a result, businesses, policy-makers, and members of the public are seeking the advice of climate scientists on what they should do to prepare for the inevitable further climate change over the next few decades (adaptation) and how they can help to avoid dangerous climate change in the longer term (mitigation).

Current climate change projections produce a wide range of estimates of global warming by 2100. These projections are useful for stressing the consequences of different greenhouse gas emission scenarios, but too long-term and uncertain to guide regional adaptation to climate change. Standard climate projections are also insufficiently focused on quantifying the risk of dangerous climate change to properly inform mitigation policy under the United Nations Framework Convention on Climate Change. (The UNFCCC is an international treaty joined by most countries; the Kyoto Protocol is an addendum to that treaty.) How can projections be designed so that they better inform policy?

Uncertainties in climate predictions vary with the averaging period over which the climate is defined and with the lead time of the prediction. Consider, for example, the prediction of the global mean decadal temperature over the next century, with forecast lead times

The authors are in the School of Engineering, Computing and Mathematics, University of Exeter, Exeter EX4 4QF, UK. E-mail: p.m.cox@exeter.ac.uk

CREDIT: P. HUEY/SCIENCE

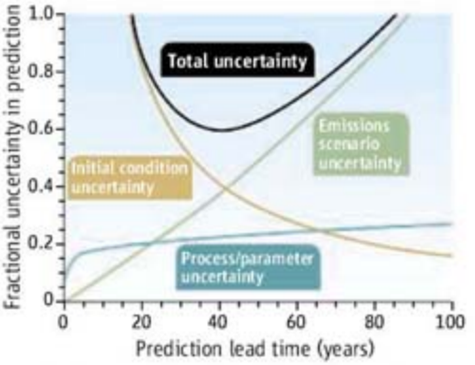

Minimizing uncertainties. Contributions to uncertainty in the predicted decadal mean temperature vary with the lead time of the prediction. Here the fractional uncertainty is defined as the prediction error divided by its central estimate. Climate predictions focusing on lead times of ~30 to 50 years have the lowest fractional uncertainty. This schematic is based on simple modeling.

varying between 1 and 100 years. On lead times of less than 10 years, the signal of anthropogenic climate change is relatively small compared to natural decadal climate variability, and uncertainties in initial conditions dominate the overall uncertainty of the prediction (see the first figure) (*1*).

By contrast, climate predictions on time scales of a century are much less sensitive to initial conditions, because the signal of anthropogenic climate change is typically much larger at longer time scales and because most elements of the climate system have a "memory" of past climate-forcing factors that is shorter than a few decades. The major source of uncertainty here lies in the future anthropogenic emissions of greenhouse gases and aerosols (see the first figure) (*2*). This uncertainty can be seen as humankind's free will concerning future climate change.

The parameters used to specify climate processes in climate models are also a source of uncertainty. These parameters determine, for example, the behavior of clouds and the strength of atmospheric convection in the models. They have a large impact on the sensitivity of the modeled climate to a doubling of the carbon dioxide (CO_2) concentration (*3*, *4*). The net effect of all these uncertainties is that the fractional uncertainty is smallest when lead times are between 30 and 50 years (see the first figure). Fortunately, this is also the time scale over which most longer-term policy and business planning is carried out.

Mitigation, as defined by the UNFCCC, is concerned with even longer time scales. The UNFCCC aims to stabilize greenhouse gases at a concentration that avoids dangerous interference in the climate system. The convention, therefore, focuses on the risk of dangerous climate change as a function of the concentration of greenhouse gases and on the relation between CO_2 emissions and increases in atmospheric CO_2 concentrations through climate–carbon cycle feedbacks (*5*, *6*).

These issues are not easily addressed with the model simulations currently used by the IPCC (see the second figure, left panel). In the IPCC approach, scenarios of possible future emissions of greenhouse gases and aerosols are generated with socioeconomic models that take into account a range of "story lines" covering global population growth, economic development, energy use, and a variable mix of future energy sources. These emission scenarios are used to drive atmospheric chemistry and carbon cycle models that simulate changes in the concentration of greenhouse gases and aerosols. The resulting concentration scenarios are put into general circulation models (GCMs) of the climate system, which generate climate change scenarios that in turn drive models of the impacts on human and natural systems.

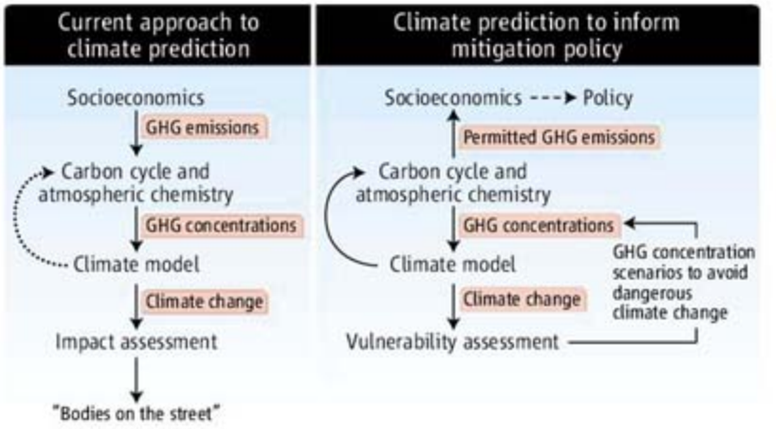

Models for informing policy. The design of climate model studies must change to inform climate change mitigation policy. (**Left**) Current IPCC process. (**Right**) Proposed new experimental design (*7*). GHG, greenhouse gas.

Mitigation policy requires a different, less linear structure, beginning with an assessment of the vulnerability of natural and human systems to climate change as a function of the magnitude of global warming and ending with scenarios of greenhouse gas emissions that avoid the most damaging impacts (see the second figure, right panel). Given the emphasis on avoiding dangerous change in the light of inevitable uncertainty, the UNFCCC also requires a reliable probabilistic risk assessment to inform emission-reduction targets. The mitigation policy agenda, as defined by the UNFCCC, therefore demands an overhaul of the design of climate change assessments (*7*).

Climate change adaptation and climate change mitigation may at first sight appear to require different modeling strategies. Observations of the contemporary Earth system are the key that must tie these modeling strands together. Informing adaptation on decadal time scales requires data on the slower climate system components (especially the ocean) to initialize high-resolution climate predictions (*8*). The interpretation of observations in a manner consistent with the model (through "model-data fusion" or "data assimilation") is common in numerical weather prediction and seasonal to decadal prediction (*9*), but is not yet used to constrain the climate projections of the IPCC.

For climate change mitigation, the dominant uncertainties are associated with climate system processes and feedbacks, rather than uncertainties in initial conditions. However, the major constraints on these processes and feedbacks also come from observations of the historical and contemporary climate. We can therefore envisage a climate diagnosis and prediction system that assimilates data into a climate model not only to define the initial conditions for decadal projections, but also to refine estimates of the key internal model parameters that influence climate sensitivity (*10*). Such a system would provide data-constrained estimates of the range of possible future climate changes on decadal to century time scales, which could be updated on the basis of new observations.

Climate projections have been instrumental in convincing many of the need for action to limit future climate change. It is now time for modelers to turn their expertise toward developing forecasting systems better suited for active management of the climate system.

References

1. T. C. K. Lee *et al.*, *J. Clim.* **19**, 5305 (2006).
2. M. O. Andreae, C. D. Jones, P. M. Cox, *Nature* **435**, 1187 (2005).
3. J. M. Murphy *et al.*, *Nature* **430**, 768 (2004).
4. D. A. Stainforth *et al.*, *Nature* **430**, 403 (2005).
5. P. Friedlingstein *et al.*, *J. Clim.* **19**, 3337 (2006).
6. C. D. Jones, P. M. Cox, C. Huntingford, *Tellus B* **58**, 603 (2006).
7. K. A. Hibbard, G. A. Meehl, P. M. Cox, P. Friedlingstein, *Eos* **88**, 217 (2007).
8. A. Ganachaud, C. Wunsch, *J. Clim.* **16**, 696 (2003).
9. M. A. Liniger, H. Mathis, C. Appenzeller, F. J. Doblas-Reyes, *Geophys. Res. Lett.* **34**, L04705 (2007).
10. P. Rayner *et al.*, *Global Biogeochem. Cycles* **19**, GB2026 (2005).

10.1126/science.1145956

MOLECULAR BIOLOGY

How and When the Genome Sticks Together

Cells respond to DNA damage by strengthening chromosome cohesion across the entire genome independently of DNA replication.

Erwan Watrin and Jan-Michael Peters

Before a eukaryotic cell divides, it generates a copy of its genome by DNA replication. As a result, each chromosome in a postreplicative cell contains two identical DNA molecules, the sister chromatids. These DNA molecules are physically connected to each other, a phenomenon known as sister-chromatid cohesion. Cohesion is essential for the symmetrical segregation of chromosomes during cell division (*1*). Not surprisingly, cohesion is normally established when sister chromatids are synthesized during S phase of the cell division cycle (see the figure). But cohesion also helps to repair damaged DNA after S phase has been completed (*2*). Two papers in this issue, by Ström *et al.* (*3*) on page 242 and Ünal *et al.* (*4*) on page 245, show that cohesion can be established in response to DNA damage independently of DNA replication. This overturns a long-held belief that cohesion is strictly coupled to DNA synthesis. The papers also imply that DNA damage may have a broader impact than previously thought, triggering genome-wide protection of chromosome integrity.

Sister-chromatid cohesion is thought to be mediated by ring-shaped protein structures called cohesin complexes (*1*). In normal cells, cohesin can connect sister chromatids only in S phase, even though newly synthesized cohesin complexes can associate with DNA in the subsequent G_2 phase (*5*, *6*). Until recently, it was generally assumed that sister-chromatid cohesion can only be generated at replication forks where DNA is synthesized. This view was first challenged by the finding that cohesion can also occur in G_2 phase if DNA is damaged by double-strand breaks (*7*, *8*). In this case, large amounts of cohesin are recruited to the damaged DNA, forming new connections between the sister chromatids (*7*, *9*). However, repair of damaged DNA also typically depends on DNA, synthesis. It therefore remained quite possible that establishment of cohesion after DNA damage is also mechanistically coupled to DNA synthesis, just as the two processes are linked during S phase.

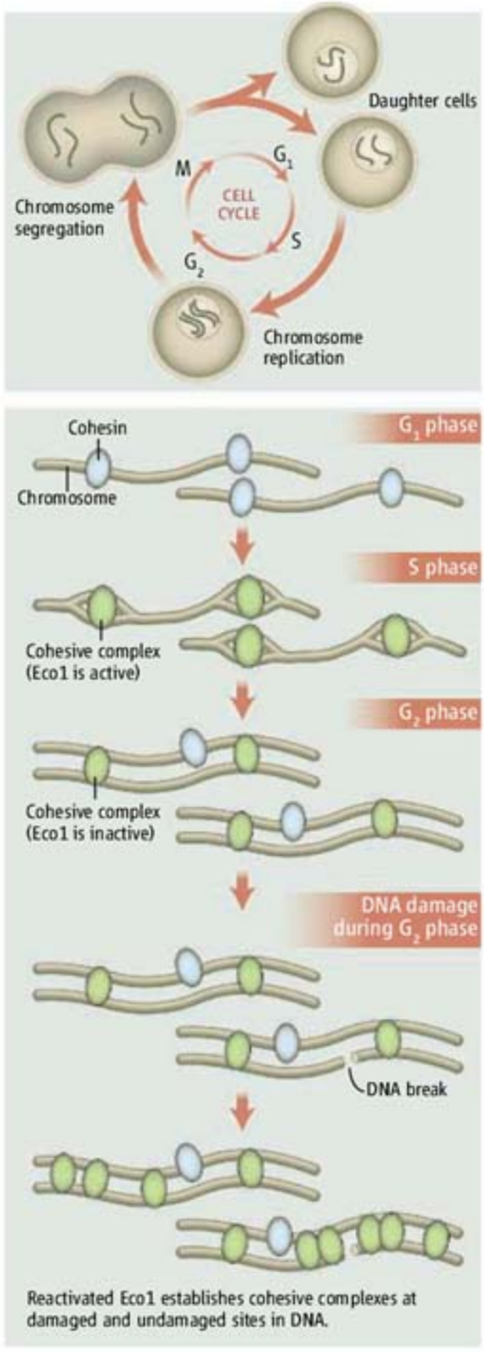

Forging cohesion. (**Top**) Chromosome dynamics during the four phases (S, G_2, M, and G_1) of the cell division cycle. (**Bottom**) Cohesin protein (blue) is loaded onto chromosomes before DNA replication begins in S phase. In S phase, the acetyltransferase Eco1 converts cohesin into cohesive complexes (green) that hold sister chromatids together. A DNA double-strand break in G_2 can also trigger cohesin loading and cohesion establishment both at the break site and on undamaged chromosomes.

To address this issue, Ström *et al.* and Ünal *et al.* analyzed budding yeast mutants that are deficient in an enzyme (Rad52) that is needed for DNA synthesis, specifically during DNA repair. Both groups observed cohesion even if the DNA of these mutant cells was damaged during G_2 phase, indicating that cohesion can be fully uncoupled from DNA synthesis. Beyond this surprise, the discovery could also prove technically useful to address another long-standing question: Do DNA replication factors also function in sister-chromatid cohesion? Replication defects inevitably lead to the absence of cohesion. The discovery that cohesion can, under certain conditions, occur without DNA replication may enable reinvestigation of this question.

Ünal *et al.* and Ström *et al.* made a second unexpected discovery when they analyzed yeast cells in which only one chromosome had been damaged by a double-strand break. Surprisingly, cohesin complexes could establish cohesion on both damaged and undamaged chromosomes during G_2 phase. This implies that the presence of DNA double-strand breaks somehow reactivates the molecular machinery that normally forges cohesion only during S phase.

What could this machinery be? Ünal *et al.* speculate that part of it could be Eco1 (also known as Ctf7), an enzyme that is needed to generate cohesion in S phase but not for its subsequent maintenance throughout G_2 phase (*10*, *11*). Indeed, both Ünal *et al.* and Ström *et al.* found that Eco1 is required for de novo establishment of cohesion in DNA-damaged G_2-phase cells, but more surprisingly, Ünal *et al.* discovered that overexpression of Eco1 induces the de novo establishment of cohesion in undamaged cells. Eco1 may therefore be rate-limiting for cohesion in G_2-phase cells, perhaps, as Ünal *et al.* speculate, because it becomes inactivated by an unknown mechanism at the end of DNA replication in S phase, whereas Eco1 may be specifically reactivated in response to DNA damage (see the figure). These results imply that Eco1 may have a key role in regulating cohesion.

The studies raise a number of question about Eco1: How is it regulated during S and G_2 phases? How does it contribute to generating cohesion? Eco1 is an an enzyme that

The authors are at the Research Institute of Molecular Pathology (IMP), Dr. Bohr-Gasse 7, A-1030 Vienna, Austria. E-mail: peters@imp.univie.ac.at

CREDIT: P. HUEY/SCIENCE

attaches acetyl residues to proteins, thereby possibly modifying their properties (*12*). Other enzymes of this class are famous for their ability to change chromatin structure by acetylating histone proteins, but the physiological substrates of Eco1 are unknown. More strangely, its acetyltransferase activity is required for de novo establishment of cohesion in G_2 phase (*4*), but is not essential when cohesion is generated during S phase (*13*). To explain this conundrum, Ünal *et al*. speculate that acetyltransferase activity may only be required to reactivate Eco1 after DNA damage, but more work is needed to resolve the mystery surrounding the role of this enzymatic activity. Finally, it will be interesting to determine why yeast cells "strengthen" their preexisting cohesion on chromosomes in a genome-wide manner after DNA damage, and to understand how a single chromosome break triggers cohesion across the entire genome.

References

1. K. Nasmyth, C. H. Haering, *Annu. Rev. Biochem.* **74**, 595 (2005).
2. E. Watrin, J. M. Peters, *Exp. Cell Res.* **312**, 2687 (2006).
3. L. Ström *et al.*, *Science* **317**, 242 (2007).
4. E. Ünal, J. M. Heidinger-Pauli, D. Koshland, *Science* **317**, 245 (2007).
5. F. Uhlmann, K. Nasmyth, *Curr. Biol.* **8**, 1095 (1998).
6. C. H. Haering *et al.*, *Mol. Cell* **15**, 951 (2004).
7. L. Ström, H. B. Lindroos, K. Shirahige, C. Sjögren, *Mol. Cell* **16**, 1003 (2004).
8. L. Ström, C. Sjögren, *Cell Cycle.* **4**, 536 (2005).
9. E. Ünal *et al.*, *Mol. Cell* **16**, 991 (2004).
10. R. V. Skibbens, L. B. Corson, D. Koshland, P. Hieter, *Genes Dev.* **13**, 307 (1999).
11. A. Toth *et al.*, *Genes Dev.* **13**, 320 (1999).
12. D. Ivanov *et al.*, *Curr. Biol.* **12**, 323 (2002).
13. A. Brands, R. V. Skibbens, *Curr. Biol.* **15**, R50 (2005).

10.1126/science.1146072

COMPUTER SCIENCE

Happy Birthday, Dear Viruses

The first computer virus was created 25 years ago, but there is no end in sight to malicious software.

Richard Ford and Eugene H. Spafford

Birthdays and other anniversaries are often a time for celebration, as we reflect on milestones passed. In the world of computing, we have quite a few happy anniversaries: for example, the first computer (arguably, Babbage's design of 1822) and the first e-mail message sent (1965).

Some remembrances, however, are less positive, and 2007 marks the silver anniversary of a darker sort—the genesis of malicious computer viruses (*1*–*3*). In 1982, a virus written by a high-school student in Pittsburgh began appearing on Apple II systems. This virus—known as "Elk Cloner"—infected the operating system, copied itself to floppy discs, and displayed bad poetry. Primarily intended to be irritating, the virus came and went with little notice. Few people spent time worrying about the beastie, and almost nobody predicted that it was a harbinger of the current multibillion dollar antivirus industry.

From such humble beginnings, computer viruses—and, more broadly, "malware" programs—are now so ingrained in popular culture that they've become the butt of jokes in ads and talk shows. Although the malware problem grew slowly in the early 1980s, not much time passed before it really made the news. In 1988, the infamous "Morris Worm" spread worldwide, causing outages across the fledgling Internet. There was also the media storm surrounding the Michelangelo virus, which was set to trigger on 6 March 1992, threatening to destroy data on infected machines. Since then, SQL.Slammer, Code Red, Nimda, Concept, and Melissa all had their 15 minutes of fame and, in the process, collectively caused billions of dollars in damage.

The most talked-about risks from today's malware have a distinctly financial flavor. If the viruses and worms of the past decade were the online equivalent of graffiti artists, malware is now like criminals who wish to steal your wallet and forge your checks. This has led to much quieter attacks, because too much visibility would cut down on profits. Instead of displaying a message or erasing your hard drive, modern malware is more insidious, turning your machine into a relay for spam, a staging ground to attack other systems, or a spy capturing your bank account and credit card information—or all three.

Spyware, phishing, rootkits, and bots — the cutting-edge malware of today—are truly nasty, and considerable effort has been invested in their creation. It has become a significant criminal enterprise and supports a thriving underground economy.

Surely the scientific community has simply been too preoccupied to deal with this challenge and a good solution is available. Sadly, even after decades, it appears that no end is in sight. This stems partly from a subtle computational twist: Building a computer program that can tell with absolute certainty whether any other program contains a virus is equivalent to a famous computer science conundrum called the "halting problem." It has no solution in the general case and has no approximate solution for our current computing environments without also generating too many false results (*4*).

Popular opinion holds that malware is a Microsoft-only problem. Macs, for example, don't seem to suffer from malware as much as Windows, so perhaps everyone should switch to Macs. Linux and Unix, too, are often touted as obvious solutions. However, no system is fully immune.

Windows has suffered for a variety of reasons; Microsoft must take some responsibility for the problem. They made some architectural decisions that, in retrospect, left Microsoft products more vulnerable. Backwards compatibility meant that later releases kept old weaknesses. And Microsoft products have undergone intense scrutiny: It is the obvious software to attack as it is the dominant player in the desktop

CREDIT: PETER HOEY

R. Ford is at the College of Engineering and Computer Sciences, Florida Institute of Technology, Melbourne, FL 32901–6975, USA. E-mail: rford@se.fit.edu E. H. Spafford is at the Center for Education and Research in Information Assurance and Security, Purdue University, West Lafayette, IN 47907–2086, USA. E-mail: spaf@ cerias.purdue.edu

market. Macs and Unix systems would undoubtedly be more frequently attacked if they were dominant, although their underlying architecture and maturity might result in less (but not zero) success for attackers. It is definitely not the case that malware is a problem only because of consumers' choice of operating system (the "platform"). The truth is much more complicated and far more worrisome.

Diversity of platform is a double-edged solution in that it solves some problems neatly but creates new ones. For example, if we want some machines always running, diversity makes it very difficult for one attack to wipe out all available computers—some machines are always immune. The flipside is that diversity may actually increase the "attack surface": Although some machines are safe and secure, diversity may increase the chances that other machines are vulnerable to some other attack. Diversity is a boon for survivability but a potential risk in terms of network penetration.

There is one basic fact in security: The more functionality, the more opportunities a developer has to make a mistake. The simple truth is that modern computers are anything but simple—their increasing complexity is driven by consumers' thirst for functionality. Furthermore, computers are almost ubiquitous: For most people, the cell phones in their pockets are as much computers as are their laptops. Virulent cell-to-cell malware is not far off; researchers have already seen some limited "proof of concept" efforts. Personal digital assistants, music players, "smart" appliances, and more are all increasingly making use of available connectivity. Consumers and producers alike need to understand that more functionality means more risk. Unfortunately, no change is likely in the near term, and vendors will continue to add poorly thought-out code to their products.

Despite the best efforts of researchers, malware is not going to vanish any time soon. Computers are extremely difficult to secure, and humans are often the weakest link. For example, in one hoax users were encouraged to delete a particular file from their computers. Many users did exactly that and carefully followed the instructions to forward the warning message to all their friends. The file they deleted was critical to the system; the "virus" was executing in their minds. There is no obvious "fix" for human nature—that has not changed in many hundreds of years. Because of this, it seems likely that in another 25 years time, we will all be lifting our glasses to (or because of) malware once again.

References

1. D. Ferbrache, *A Pathology of Computer Viruses* (Springer, Berlin, 1991).
2. E. H. Spafford, in *The Encyclopedia of Software Engineering*, J. Marciniak, Ed. (Wiley, New York, 1994).
3. P. Szor, *The Art of Computer Virus Research* (Addison-Wesley, Boston, MA, 2005).
4. F. B. Cohen, *A Short Course on Computer Viruses* (Wiley, New York, 1994).

10.1126/science.1140909

GEOCHEMISTRY

Strange Water in the Solar System

Analysis of a primitive meteorite offers clues about the environment in which the solar system formed.

Edward D. Young

Cosmochemists use isotope ratios to understand the stellar environment in which our solar system formed. The most pronounced and mysterious of these ratios involve the three stable isotopes of oxygen, ^{16}O, ^{17}O, and ^{18}O. Normally, ^{17}O and ^{18}O separate partially from the more abundant ^{16}O according to their relative mass differences. Variations in the $^{17}O/^{16}O$ ratio are thus about half those of $^{18}O/^{16}O$. But many rocky materials in the solar system violate this expectation, exhibiting variations in isotope ratios that are independent of mass. This is most apparent in chondrite meteorites, which are remnants of primitive rocks accreted during the earliest stages of solar system formation.

This anomalous distribution of oxygen isotopes produces a distinctive line with slope equal to 1 on a plot of $\delta^{17}O$ versus $\delta^{18}O$ (*1*) rather than a slope of ~ ½ typical of oxygen reservoirs on Earth (see the figure). The cause of this "^{16}O anomaly" has been a mystery for three decades (*2*). Water, it seems, was a key player in the origin of the ^{16}O anomaly, and on page 231 of this issue, Sakamoto *et al.* (*3*) report evidence for the original isotopic composition of water in the early solar system. From this discovery come insights into the origin of the ^{16}O isotope anomaly and clues to the nature of the stellar nursery that gave birth to the Sun (*4*).

Many mechanisms have been proposed for producing the ^{16}O anomaly in the solar system. Perhaps we have simply inherited the isotope abundances as they evolved in our Galaxy (*5*). Or possibly the isotope ratios stem from chemically induced mass-independent fractionation, analogous to what happens during ozone production in Earth's atmosphere (*6*, *7*).

Researchers have recently looked to light-induced destruction of CO as the cause. About half of the total oxygen in a protoplanetary disk like the one that produced our solar system resides in CO. Another third exists in the form of H_2O with the remainder as oxides of other elements (*8*, *9*). Carbon monoxide absorbs ultraviolet (UV) light emanating from stars and is dissociated to C and O. In regions of the right gas density, UV absorption cleaves $C^{16}O$, $C^{17}O$, and $C^{18}O$ molecules in proportions inverse to their relative abundances, a process referred to as "self-shielding."

Because $C^{16}O$ is the most abundant of these isotope varieties, the oxygen liberated by CO photodissociation is ^{17}O and ^{18}O rich and ^{16}O poor. Clayton (*10*) suggested that CO self-shielding at the inner annulus of the solar protoplanetary disk might be the cause of the slope = 1 line on the $\delta^{17}O$ versus $\delta^{18}O$ plot (see the figure). Yurimoto and Kuramoto (*11*) suggested that CO photodissociation and self-shielding in the molecular cloud precursor to the solar system could have caused the ^{16}O anomaly. Lyons and Young (*12*) suggested that CO photodissociation at the surfaces of the protoplanetary disk might have been the cause (see the figure).

A key prediction of the CO self-shielding models is that O liberated by CO photodestruction reacted with H to form ^{16}O-poor H_2O (*11*–*14*). We know that water in the early solar system was depleted in ^{16}O relative to rocks, but the extreme depletions predicted by the CO self-shielding models were not observed. Estimates of the original oxygen isotope ratios of solar system water relied on inferences from the measured oxygen isotope ratios of "secondary minerals"

The author is in the Department of Earth and Space Sciences and the Institute of Geophysics and Planetary Physics, University of California, Los Angeles, Los Angeles, CA 90095, USA. E-mail: eyoung@ess.ucla.edu

like carbonate, iron oxides, and clay minerals in chondrites (see the figure) (*15*, *16*).

These minerals grew by reactions between water and rocks in hydrologically active planetesimals, vestiges of which are found today among asteroids. Meteorite parent bodies were hydrologically active, unlike the asteroids of today, because heat from short-lived radioisotopes melted ice within the bodies, leading to the formation of carbonate, iron oxide, and clay minerals.

But there is a problem with using minerals produced by reactions between rocks and waters to infer the original oxygen isotopic composition of solar system H_2O: These secondary minerals take time to grow, whereas isotope exchange between water and rock can be rapid. As a result, new minerals generally grew from waters that had already exchanged oxygen isotopes with rock, diluting or even erasing the original isotopic composition of the water. Secondary minerals therefore generally do not have the original isotopic composition of pristine water. Instead, they inherit a mixture of rock and water isotopic compositions.

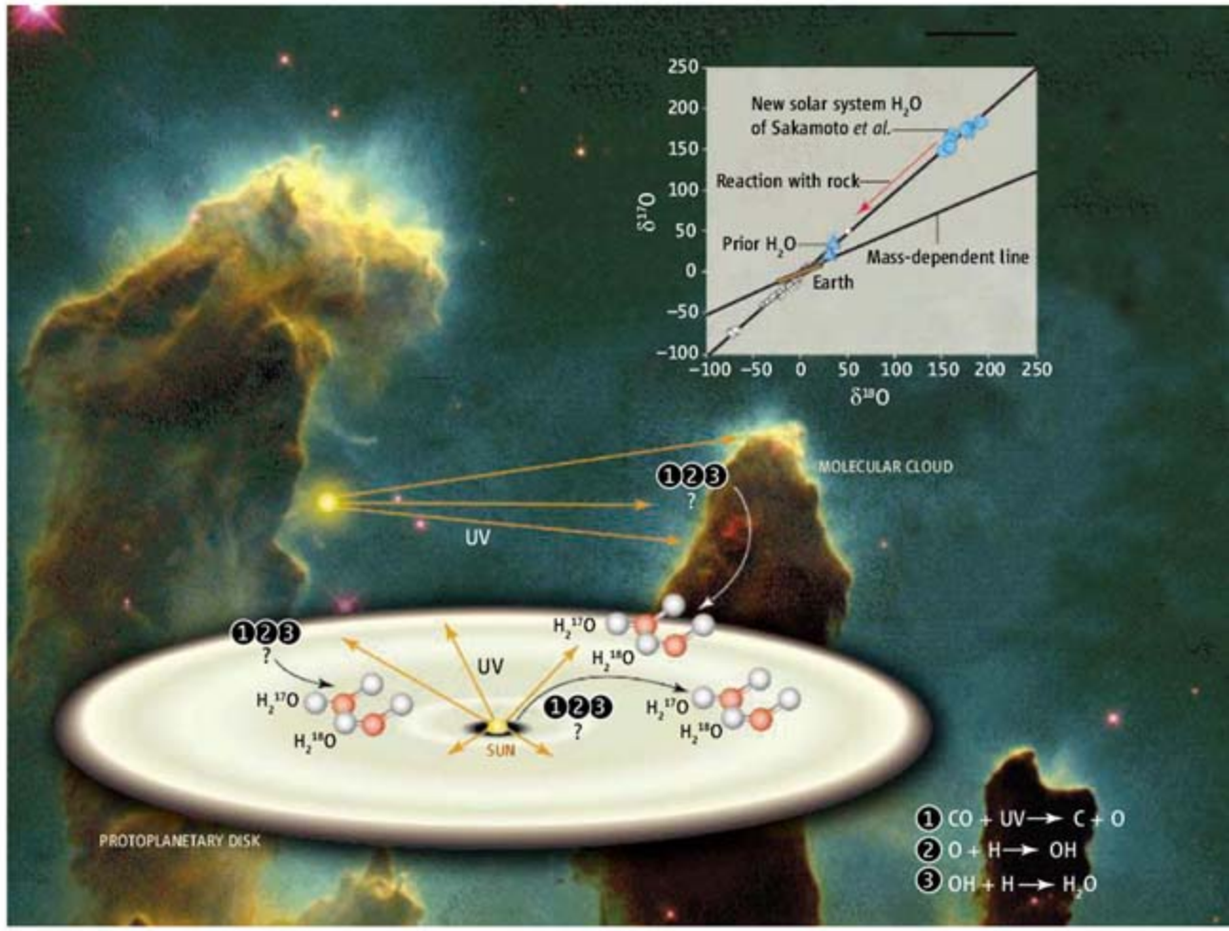

Oxygen isotope anomalies. Oxygen isotope ratios of water may record photochemical reactions in the solar protoplanetary disk. Three possible sources of ^{16}O-poor and ^{17}O- and ^{18}O-rich H_2O are produced by photochemical dissociation of CO molecules (reactions 1 to 3): (i) the inner annulus of the solar protoplanetary disk (*9*); (ii) the molecular cloud core that collapsed to form the disk (*10*); and (iii) the surfaces of the protoplanetary disk (*11*). The $\delta^{17}O$-$\delta^{18}O$ plot compares the new estimates of pristine solar system H_2O from Sakamoto *et al.* (blue circles) with previous estimates (blue triangles). Change in water isotope ratios expected as a result of reactions with rock are shown by the red arrow. Also shown are representative meteorite and lunar soil data (white circles), the slope-1 line, and the "normal" slope-½ mass-dependent line.

The discovery by Sakamoto *et al.* avoids this problem. They find hints of alteration of a primitive meteorite rock by reactions between water and rock that occurred before exchange of oxygen changed the composition of the water. In these earliest reaction products, Sakamoto *et al.* find ^{16}O depletions approaching 20%, by far the least ^{16}O seen in any solar system material to date.

Moreover, the oxygen reservoir identified by Sakamoto *et al.* lies on the extension of the line of slope 1 on the graph of $\delta^{17}O$ versus $\delta^{18}O$. This line is postulated to represent the primitive oxygen reservoir of the solar system. These extremely depleted ^{16}O oxygen abundances along the slope-1 line are consistent with the predictions of CO self-shielding models.

Sakamoto *et al.* do not prove that self-shielding was the origin of the ^{16}O anomaly. However, they appear to verify a key prediction of the models, that H_2O in the early solar system was depleted by tens of percent in ^{16}O. If CO self-shielding were verified as the origin of ^{16}O anomalies, it would show that UV light was important in the chemistry of the early solar system. The UV source could have been nearby giant stars or the Sun itself. The UV flux responsible for the ^{16}O anomaly might then indicate whether the Sun formed in a cluster of young stars or in relative isolation.

The next step will be to search for signs of CO self-shielding going on today in other protoplanetary disks. One observation suggests $C^{16}O$ overabundance (implying ^{16}O depletion): Brittain *et al.* (*17*) presented infrared spectra of the disk surrounding the young star HL Tau that imply a $C^{16}O$ enrichment of several tens of percent. Ultimately, observations on scales ranging from the width of a human hair in meteorites to protoplanetary disks many millions of kilometers away will be required to settle the origin of the solar system ^{16}O anomaly.

References and Notes

1. Differences in oxygen isotope ratios are given in δ notation where $\delta^{17}O$ and $\delta^{18}O$ refer to per thousandth differences in $^{17}O/^{16}O$ and $^{18}O/^{16}O$ from their values in standard mean ocean water. A slope of 1 in $\delta^{17}O$ versus $\delta^{18}O$ signifies changes in ^{16}O relative to ^{17}O and ^{18}O.
2. R. N. Clayton, L. Grossman, T. K. Mayeda, *Science* **182**, 485 (1973).
3. N. Sakamoto *et al.*, *Science* **317**, 231 (2007); published online 14 June 2007 (10.1126/science.1142021).
4. J. J. Hester, S. J. Desch, K. R. Healy, L. A. Leshin, *Science* **304**, 1116 (2004).
5. D. D. Clayton, *Astrophys. J.* **334**, 191 (1998).
6. M. H. Thiemens, H. E. Heidenreich III, *Science* **219**, 1073 (1983).
7. R. A. Marcus, *J. Chem. Phys.* **121**, 8201 (2004).
8. E. Anders, N. Grevesse, *Geochim. Cosmochim. Acta* **53**, 197 (1989).
9. B. Fegley, *Space Sci. Rev.* **92**, 177 (2000).
10. R. N. Clayton, *Nature* **415**, 860 (2002).
11. H. Yurimoto, K. Kuramoto, *Science* **305**, 1763 (2004).
12. J. R. Lyons, E. D. Young, *Nature* **435**, 317 (2005).
13. H. Yurimoto, K. Kuramoto, paper 5149 presented at the 65th Annual Meteoritical Society Meeting, Los Angeles, CA, 21 to 26 July 2002.
14. E. D. Young, J. R. Lyons, paper 1923 presented at the 34th Lunar and Planetary Science Conference, Houston, TX, 17 to 21 March 2003.
15. R. N. Clayton, T. K. Mayeda, *Earth Planet. Sci. Lett.* **67**, 151, (1984).
16. E. D. Young, *Philos. Trans. R. Soc. London A* **359**, 2095 (2001).
17. S. D. Brittain, T. W. Rettig, T. Simon, C. Kulesa, *Astrophys. J.* **626**, 283 (2005).

Published online 14 June 2007;
10.1126/science.1145055
Include this information when citing this paper.

PHOTO CREDIT: NASA

FREE with registration

Science Alerts in Your Inbox

Get daily and weekly E-alerts on the latest breaking news and research!

This Week in *Science*
Summaries of research content

***Science* Magazine TOC**
Weekly table of contents

***Science* News This Week**
Brief summaries of the journal's news content

***Science* Posting Notification**
Alert when weekly issue is posted

***Science*NOW Daily Alert**
Daily headline summary

***Science* Express Notification**
Articles published in advance of print

***Science*NOW Weekly Alert**
Weekly headline summary

Editors' Choice
Highlights of the recent literature

STKE TOC
Weekly table of contents

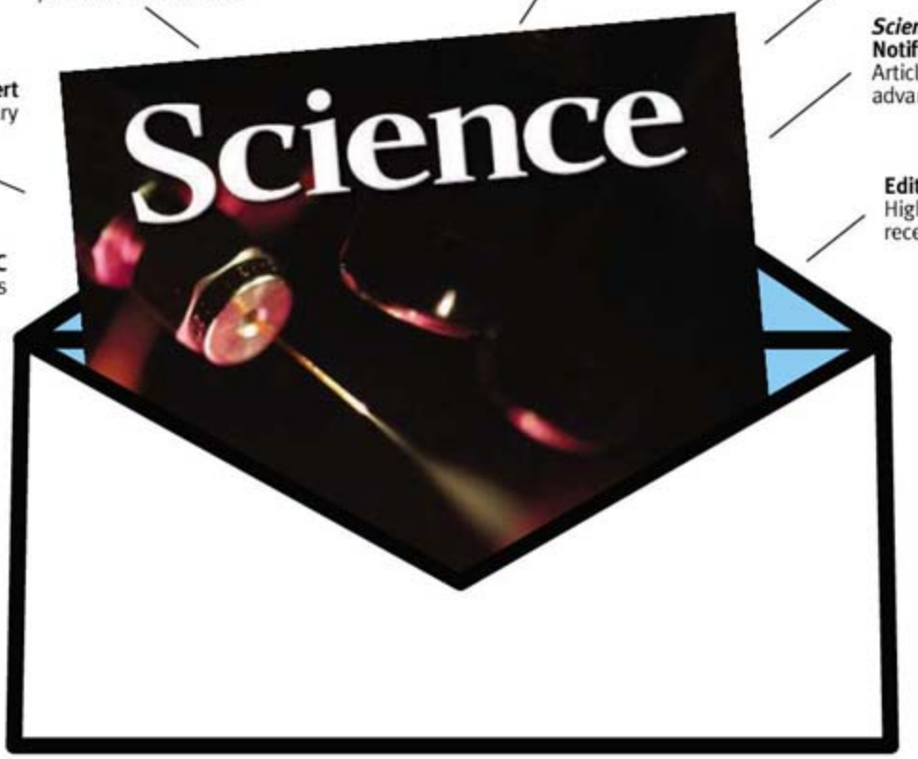

Get the latest news and research from *Science* as soon as it is published. Sign up for our e-alert services and you can know when the latest issue of *Science* or *Science* Express has been posted, peruse the latest table of contents for *Science* or *Science*'s Signal Transduction Knowledge Environment, and read summaries of the journal's research, news content, or Editors' Choice column, all from your e-mail inbox. To start receiving e-mail updates, go to:

http://www.sciencemag.org/ema

Science
AAAS

Extraordinary Flux in Sex Ratio

Sylvain Charlat,[1,2]* Emily A. Hornett,[1] James H. Fullard,[3] Neil Davies,[2] George K. Roderick,[4] Nina Wedell,[5] Gregory D. D. Hurst[1]

The ratio of males to females within a species is central to many aspects of its biology, from mating frequency (*1*) to population growth and disease spread. Forty years ago, Hamilton (*2*) noted that the evolutionary arms race engaged between "selfish" sex-ratio distorters and counteracting suppressor genes has the potential to produce rapid flux in sex ratio. Here we document this process in action in a tropical butterfly and report a transition from 99% females to parity within 10 generations.

The butterfly *Hypolimnas bolina* is infected by a maternally inherited *Wolbachia* bacterium that selectively kills male embryos. Extreme population sex ratio bias associated with high prevalence of the male killer has been recorded in Polynesian populations, most notably on the Samoan islands Upolu and Savaii, where males represented only 1% of individuals in 2001 (*3*). In May and June 2005, informal observations revealed substantial numbers of males at three different locations on Upolu, suggesting a dramatic alteration of the sex ratio. At the same time, the sex ratio on neighboring Savaii remained at >99% female, with no males observed (~100 individuals were observed on each island).

We carried out a formal survey of *H. bolina* sex ratio in 2006 and also scored male-killing efficiency via the sex ratio produced by wild caught females (Fig. 1). On Upolu, where males were very rare in 2001 but common in 2005, we collected 20 males and 33 females in total in 2006 from two sites within the island. We reared progeny from 14 females, and all produced sons. This represents a marked difference from the 2001 data, where only 3 of 64 females gave rise to any male offspring ($\chi^2 = 55.76$, df = 1, $P < 0.0001$). Overall, the sex ratio produced by Upolu females was near 1:1 (83 females to 75 males), with no heterogeneity within or between sampling sites. Lack of male killing was also corroborated by high egg hatch rates.

The 2006 data from Savaii showed a similar transformation: Barely 10 generations after extreme female bias was reported, 21 males and 33 females were collected from Savaii. At Salelologa, close to Upolu, the shift to a 1:1 sex ratio was nearly complete: All females produced sons, there was no heterogeneity between broods, and the overall sex ratio produced was consistent with 1:1. High egg hatch rate also indicates loss of male killing. In contrast, at Sagone (more distant from Upolu), the shift to a 1:1 sex ratio was incomplete: Three of six females produced no sons, and sex ratio was heterogeneous between broods. Consistent with retention of male killing, the median egg hatch rate was 71% (Fig. 1).

Polymerase chain reaction (PCR) assay of the butterflies revealed that all individuals from Upolu and Savaii, male and female, carry *Wolbachia*, and sequence identity at six *Wolbachia* loci confirmed that the previously present strain had not been replaced (*4*). Thus, the change in *H. bolina* sex ratios arose because of a loss of male-killing efficiency in the existing *Wolbachia* rather than either loss of infection or displacement by a new strain. We tested whether loss of efficiency was caused by the evolution of suppressor genes in the butterfly host, as previously observed (*5*). Introgressing the Samoan *Wolbachia* onto a nonsuppressor *H. bolina* nuclear background (*4*) restored full male-killing ability after three generations of introgression, demonstrating that the shift in sex ratio was caused by the spread of host suppressor genes (table S1 and fig. S1).

These results establish that conflicts associated with cytoplasmic sex ratio distorters can generate very rapid shifts in local population sex ratio, in our case from 100:1 to near 1:1 in fewer than 10 generations. The nature of the processes targeted by sex ratio distorters (for example, sex determination) suggests that intense selection for suppression could drive the evolution of core developmental traits that otherwise remain stable over time. With *Wolbachia* being just one of many widespread sex ratio distorters, it is probable that such phenomena occurred in the past on many branches of the tree of life.

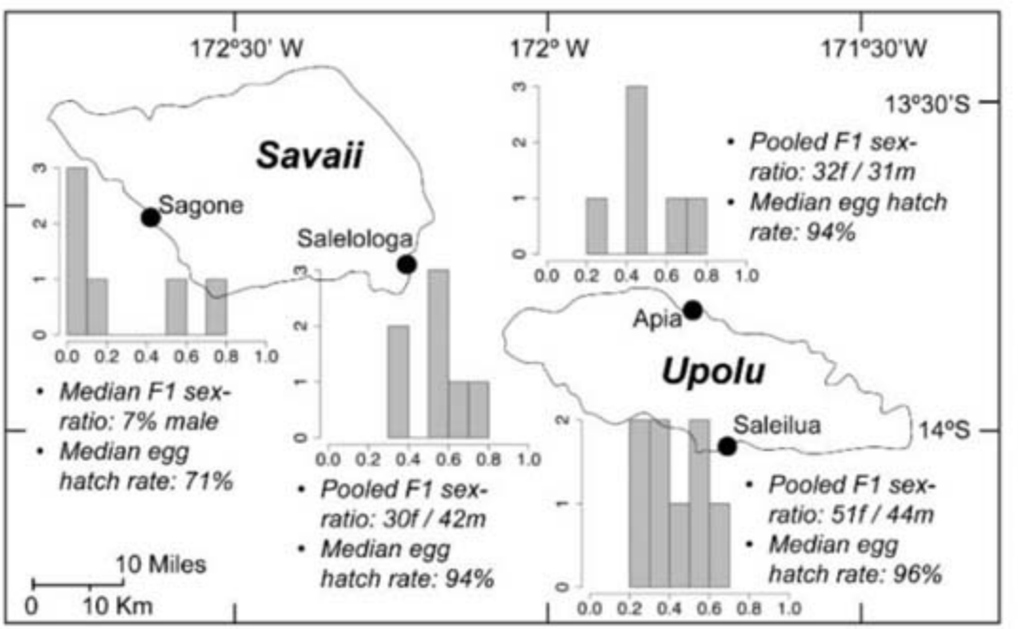

Fig. 1. F_1 sex ratio and egg hatch rate in 2006. Histograms give the distribution of F_1 sex ratios (*x* axis, proportion of males; *y* axis, number of broods). Sex ratios are homogeneous within sites at Apia ($\chi^2 = 7.59$, df = 5, $P = 0.18$), Saleilua ($\chi^2 = 5.68$, df = 7, $P = 0.58$), and Salelologa ($\chi^2 = 4.89$, df = 6, $P = 0.56$) and are compatible with a 1:1 sex ratio (Upolu pooled $\chi^2 = 0.41$, df = 1, $P = 0.52$; Salelologa $\chi^2 = 2$, df = 1, $P = 0.16$). Sex ratios are heterogeneous at Sagone ($\chi^2 = 18.27$, df = 5, $P < 0.003$). Breeding is as described in (*1*).

References and Notes

1. S. Charlat *et al.*, *Curr. Biol.* **17**, 273 (2007).
2. W. D. Hamilton, *Science* **156**, 477 (1967).
3. E. A. Dyson, G. D. D. Hurst, *Proc. Natl. Acad. Sci. U.S.A.* **101**, 6520 (2004).
4. Materials and methods are available on *Science* Online.
5. E. A. Hornett *et al.*, *PLoS Biol.* **4**, e283 (2006).

6. We thank C. Vermenot and A. Duplouy for assistance and O. Duron and M. Reuter for comments. Funded by NSF (USA, no. 0416268), Natural Environment Research Council (UK, no. NE/B503292/1), and Natural Sciences and Engineering Research Council (Canada). Sequences were deposited in GenBank with accession numbers EF589952 to EF589956.

Supporting Online Material

www.sciencemag.org/cgi/content/full/317/5835/214/DC1
Materials and Methods
Fig. S1
Table S1
References and Notes

3 April 2007; accepted 16 May 2007
10.1126/science.1143369

[1]Department of Biology, University College London, 4 Stephenson Way, London NW1 2HE, UK. [2]Gump South Pacific Research Station, University of California, Berkeley, BP 244 Maharepa, 98728 Moorea, French Polynesia. [3]Department of Biology, University of Toronto at Mississauga, 3359 Mississauga Road N, Mississauga, ON L5L 1C6, Canada. [4]Environmental Science (ESPM), University of California, Berkeley, CA 94720–3114, USA. [5]School of Biosciences, University of Exeter, Cornwall Campus, Tremough, Penryn TR10 9EZ, UK.

*To whom correspondence should be addressed. E-mail: s.charlat@ucl.ac.uk

Prefrontal Regions Orchestrate Suppression of Emotional Memories via a Two-Phase Process

Brendan E. Depue,[1,2]* Tim Curran,[1,2,3] Marie T. Banich[1,2,3,4]

Whether memories can be suppressed has been a controversial issue in psychology and cognitive neuroscience for decades. We found evidence that emotional memories are suppressed via two time-differentiated neural mechanisms: (i) an initial suppression by the right inferior frontal gyrus over regions supporting sensory components of the memory representation (visual cortex, thalamus), followed by (ii) right medial frontal gyrus control over regions supporting multimodal and emotional components of the memory representation (hippocampus, amygdala), both of which are influenced by fronto-polar regions. These results indicate that memory suppression does occur and, at least in nonpsychiatric populations, is under the control of prefrontal regions.

One of the most controversial issues in psychology over the past 100 years is the degree to which memories can be manipulated, both whether they can be falsely created (*1*) and whether they can be suppressed. Although some researchers have provided initial evidence for memory suppression (*2*, *3*), others claim that memory repression or suppression is a clinical myth in search of scientific support (*4*).

We hypothesized that evidence for memory suppression would be provided by activation below a fixation baseline in brain regions processing components of memory representation (*5*). We used the Think/No-Think paradigm (T/NT) of Anderson and colleagues, in which individuals attempt to elaborate a memory by repetitively thinking of it (T condition) or to suppress a memory by repetitively not letting it enter consciousness (NT condition) (*2*, *3*). Our recent T/NT work, using faces as cues and pictures as targets, suggests that the impact of exerting control is larger for emotional than for nonemotional information (*6*). Because of these findings, as well as the clinical relevance of intrusive negative images in posttraumatic stress disorder (PTSD) and obsessive-compulsive disorder (OCD) (*7*–*9*), we used negative pictures known to activate the visual cortex as memory targets (*10*). In both monkeys (*11*) and humans (*10*), retrieval of memories involves the same regions of the brain that are involved in encoding a memory (*12*, *13*). Thus, we used the degree of activation in the hippocampus, amygdala, and visual processing areas that are known to be involved in the creation and retrieval of emotional memories (*14*, *15*)—to determine whether memory suppression involves inhibition of the neural machinery underlying memory processing.

Two aspects of our version of the T/NT paradigm were important (Fig. 1A). First, the experimental phase included fixation items that acted as a low-level baseline of brain activity to

[1]Department of Psychology, University of Colorado, Boulder, CO 80309, USA. [2]Center for Neuroscience, University of Colorado, Boulder, CO 80309, USA. [3]Institute of Cognitive Science, University of Colorado, Boulder, CO 80309, USA. [4]Department of Psychiatry, University of Denver Health Sciences, Denver, CO 80208, USA.

*To whom correspondence should be addressed. E-mail: depue@colorado.edu

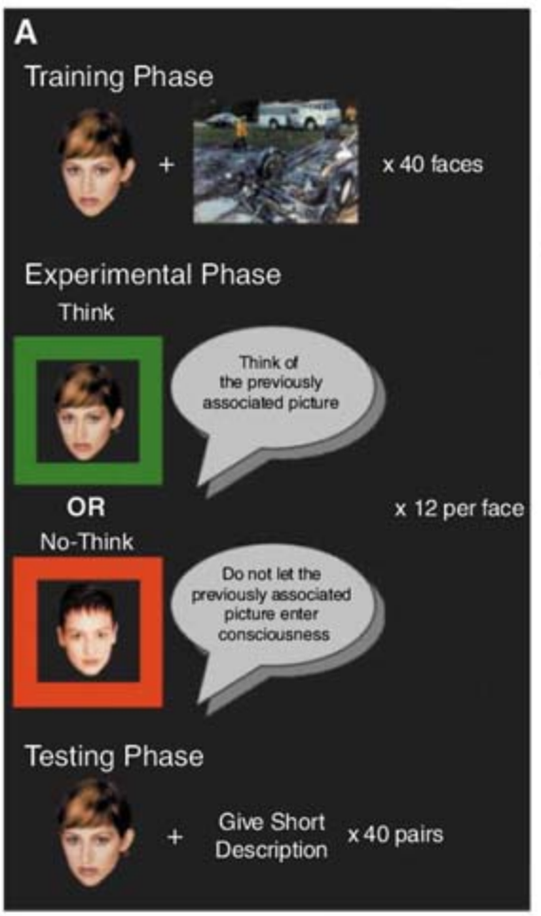

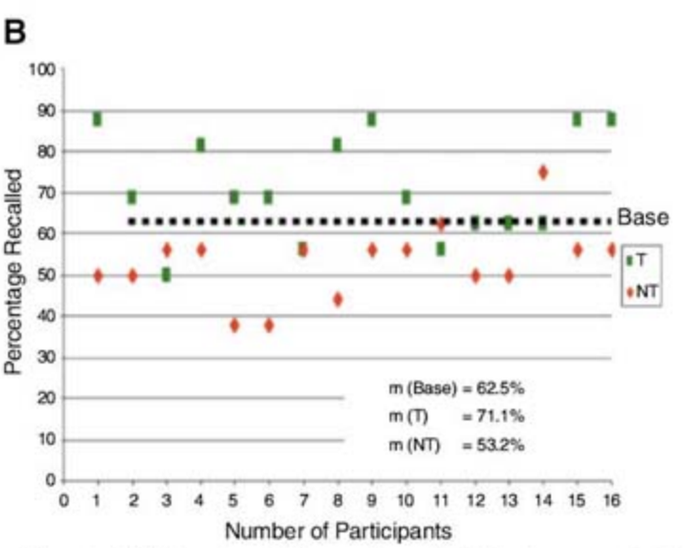

Fig. 1. (**A**) Experimental procedure. Individuals were first trained during structural scanning to associate 40 cue-target pairs. During the experimental phase, brain activity was recorded using fMRI while individuals viewed only the face (16 faces per condition, 12 repetitions per face; 3.5 s per face). On some trials they were instructed to think of the previously learned picture; on other trials they were instructed not to let the previously associated picture enter consciousness. The presentation of only the cue (i.e., the face) ensures that individuals manipulate the memory of the target picture. The additional faces (8 items) not shown during this phase acted as a behavioral baseline. During the test phase, the individuals were shown the 40 faces and asked to describe the previously associated picture. (**B**) Behavioral results: percentage recall for each participant for T trials (green) and NT trials (red), with the dotted line indicating baseline recall for items not viewed in the experimental phase. Recall differed for T and NT items [$t(15) = -4.29$, $P = 0.0006$] because of a trend for greater recall in the T condition [$t(15) = 1.49$, $P = 0.07$] and a significant reduction in recall in the NT condition [$t(15) = -2.28$, $P = 0.02$], calculated relative to baseline.

determine whether activity in the regions of interest (ROIs) actually decreased (*5*). Although Anderson and colleagues (*2*) demonstrated the involvement of prefrontal regions in cognitive control over memory, they examined the contrast between activation on NT and T trials without reporting fixation baseline contrasts, making it difficult to associate activity with a specific condition (e.g., T or NT).

Second, in the experimental phase, each face was shown 12 times with the presentation of the faces pseudo-randomly intermixed. Although in our previous study (*6*) memory increased linearly with the number of times cognitive control was exerted for T trials, this was not the case for NT trials. Hence, we divided our data into quartiles (three repetitions per cue during each quartile) to determine whether the neural mechanisms involved in memory suppression change with repeated attempts.

The behavioral results shown in Fig. 1B indicated that individuals effectively suppressed memory. To investigate the neural basis of this effect, we first analyzed the functional magnetic resonance imaging (fMRI) data for instances of NT > T—that is, significantly greater activity for NT trials than for T trials—irrespective of recall accuracy (*5*). Additionally, because we were specifically interested in effective control over memory, we examined this same contrast only for NT trials in which the picture was forgotten (NTf) and on T trials in which it was remembered (Tr). Brain areas are discussed according to their putative functional roles: (i) cognitive control, (ii) sensory representation of memory, and (iii) memory processes and emotional components of memory.

Sources and sites of cognitive control. Prefrontal regions, right-sided and spanning BA 8, 9/46, 47, and BA 10, exhibited NT > T contrast. A conjunction analysis indicated that these differences resulted from an increase in activity for NT trials rather than a decrease in activation for T trials relative to baseline (Fig. 2A), which suggests that these regions are specifically involved in controlling the suppression of emotional memories.

Next, we sought to determine which regions support components of the memory representation. These regions showed condition-specific changes, which we defined as yielding not only a significant difference for the NT > T contrast but also a negative signal change for NT trials and, conversely, a positive signal change for T trials, relative to baseline. Brain areas underlying the sensory representation of memory that showed such an effect were the visual cortex, including bilateral BA17, BA18, and BA37 [fusiform gyrus (FG)], and the pulvinar nucleus of the thalamus (Pul; Fig. 2B). Suppression of emotional memories thus involved decreased activity in sensory cortices that are normally active when memories are being retrieved, as well as in regions (i.e., Pul) that play a role in gating and modulating attention toward or away from visual stimuli (*16*, *17*).

Brain areas involved in memory processes and emotional components of memory representation that exhibited significant condition-specific activity were the hippocampal complex (Hip) and the amygdala (Amy; Fig. 2C), which are strongly involved in emotional learning and memory (*18*, *19*), as would be required by the face-picture association in our paradigm. Hence, the suppression of emotional memory also involved suppression of memory processes and emotional aspects of the memory representation.

Two phases of memory suppression. We next examined how brain activity changed with

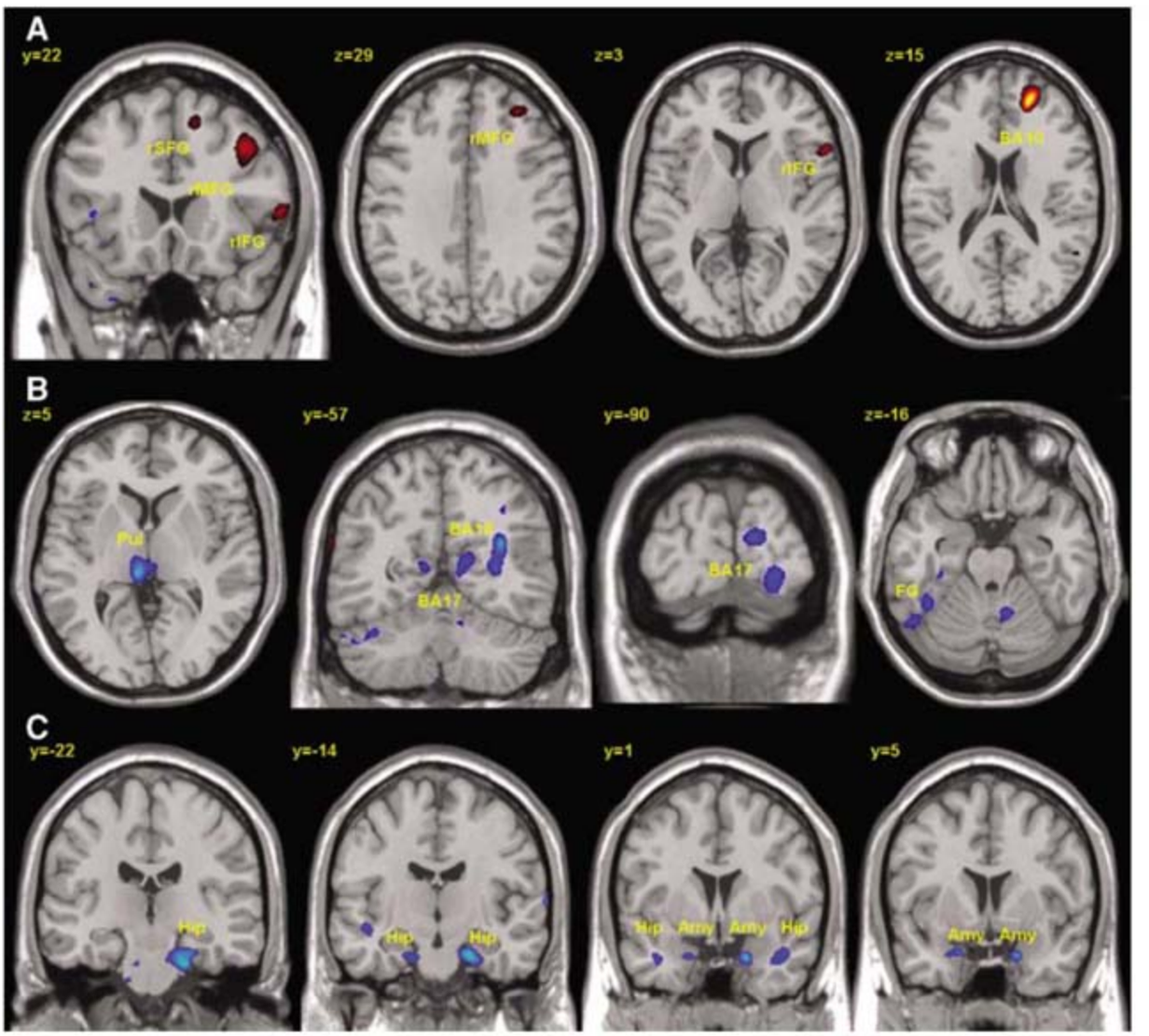

Fig. 2. Functional activation of brain areas involved in (**A**) cognitive control, (**B**) sensory representations of memory, and (**C**) memory processes and emotional components of memory (rSFG, right superior frontal gyrus; rMFG, right middle frontal gyrus; rIFG, right inferior frontal gyrus; Pul, pulvinar; FG, fusiform gyrus; Hip, hippocampus; Amy, amygdala). fMRI data were analyzed using a hemodynamic response function–convolved epoch; statistical parameter maps (SPMs) were thresholded on a voxelwise basis at $Z = 2.81$, $P = 0.005$. To adjust for false positive errors on an area-of-activation basis, we set a clusterwise threshold at $P = 0.05$ (cluster size of 120) as determined by the Analysis of Functional NeuroImages program AlphaSim. Red indicates greater activity for NT trials than for T trials; blue indicates the reverse. Conjunction analyses revealed that areas seen in blue are the culmination of increased activity for T trials above baseline as well as decreased activity of NT trials below baseline.

increased attempts at cognitive control, over trials, as well as covariation of prefrontal activation and the two putative sets of posterior cortex (sensory areas, Amy-Hip complex). This was accomplished by dividing the 12 attempts at cognitive control into quartiles (three repetitions per quartile). We then plotted percent signal change (ΔS) across the quartiles of each brain area that showed differential activation for NT trials relative to T trials (*5*).

Two patterns of temporal change in activation were observed, each associated with different groupings of prefrontal and posterior brain areas. The two groupings were composed of (i) right inferior frontal gyrus (rIFG), Pul, and FG, and (ii) right middle frontal gyrus (rMFG), Hip, and Amy. Unique temporal patterns of prefrontal cortex (PFC) influence on posterior brain regions were observed for each group. rIFG showed early activation in the time course of suppression, which lasted through the second quartile of repetitions, and then a decreased level of activation during the last two quartiles (Fig. 3A). Activity of Pul and FG followed a similar time course of ΔS, which lagged behind that for rIFG. To express quantitatively the relationship in activation between these brain areas as a function of time, we plotted the correlations of activation of rIFG with Pul and FG, respectively, as a function of quartile (Fig. 3C). Greater activity in rIFG in the second quartile was significantly associated with decreased activity in Pul and FG during the second quartile, but showed no significant relation for later quartiles (*20*). This correlation pattern is consistent with the temporal pattern of ΔS: The apparent rIFG inhibition of its associated brain regions begins early, in the first quartile, reaches maximum in the second quartile, and is greatly reduced thereafter.

In contrast to rIFG, rMFG activation increased later and remained active. Activity in Hip and Amy appeared to follow that of rMFG in reverse: In the first quartile, activity was significantly above baseline, but it decreased steadily to reach significance below baseline by the fourth quartile (Fig. 3B). Increased activity in rMFG did not predict activity in Hip and Amy in the first or second quartiles, but did so significantly in the third and fourth quartiles (Fig. 3C). This covariation pattern suggests that rIFG and rMFG suppress different aspects of memory processing during different temporal phases.

To assess the linkage between Hip activation and memory, we performed a subsequent memory analysis (remembered versus forgotten) on Hip activation during the fourth quartile, when the effects of cognitive control were largest. We found a linear decrease of activity in Hip: Tr > Tf > baseline > NTr > NTf (*5*), with only that of NT trials below baseline. Further analyses showed that activity of rMFG and Hip correlated with behavioral success at suppression (*5*). Taken together with the previous data, these findings suggest that rMFG modulates activity in Hip, which is directly related to behavioral success. These data replicated the finding of Anderson and colleagues, so the relationship between prefrontal and hippocampal regions may well be involved in suppressing memory recall.

Higher-order orchestration of memory suppression. Only one prefrontal region, BA 10, exhibited activity across the entire experimental phase (Fig. 4A). Because this region receives minimal sensory input and is predominantly connected with other prefrontal areas, we inspected its relationship with rIFG and rMFG for each quartile. The maximal correlation between BA10 and each of the prefrontal regions was observed in the quartile preceding the maximal correlation between rIFG and rMFG and their respectively associated brain regions (Fig. 4, B to D). This pattern suggests that activity in BA10 modulates activity in rIFG and rMFG, which in turn modulates activity in posterior regions. This result is consistent with recent research suggesting that activity in BA10 increases with task complexity and is involved in other aspects of higher-order cognition, such as monitoring of internal states, memory retrieval, emotional processes, coordination of higher-level goals, and modulating other areas of PFC to attain these goals (*21*, *22*).

Conclusion. Our finding of below-baseline activation in brain areas related to sensory representation (Pul, FG) and memory (Hip, Amy) for emotional stimuli during NT trials is consistent with the operation of an active process of suppression. Furthermore, our findings are less consistent with two sets of alternative interpretations of responses in behavior and brain activation that we observe on NT trials. One alternative explanation is replacement, in which participants think of a new cue-target association or substitute an alternate memory to create distraction from the target memory (*23*). However, the generation of a new associate would be associated with activation, not deactivation below baseline of sensory and memory representations to represent and encode the new association. In essence, replacement would manifest functionally in brain activations as in T trials.

A second alternative suggests that reduced recall on NT trials involves disengagement with the stimuli (e.g., momentary mind-wandering or introspection), because in some studies BA10 activation has been correlated with internally fo-

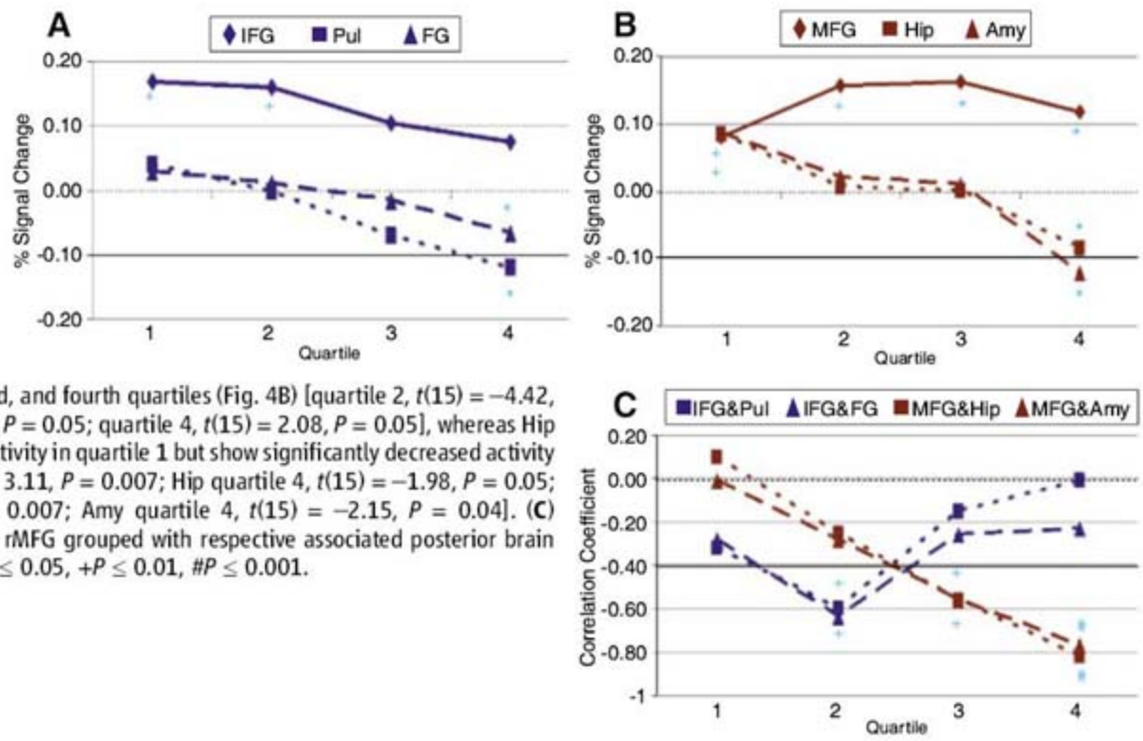

Fig. 3. Time course of percentage signal change (ΔS) relative to baseline for the two regional groupings. (**A**) rIFG shows significantly increased activity only for the first and second quartiles [quartile 1, $t(15) = 3.65$, $P = 0.001$; quartile 2, $t(15) = 2.66$, $P = 0.01$], whereas the activities of Pul and FG decrease to significantly below baseline during quartile 4 [Pul, $t(15) = -2.11$, $P = 0.05$; FG, $t(15) = -1.96$, $P = 0.05$]. (**B**) rMFG displays significantly elevated activity during the second, third, and fourth quartiles (Fig. 4B) [quartile 2, $t(15) = -4.42$, $P = 0.0005$; quartile 3, $t(15) = 2.10$, $P = 0.05$; quartile 4, $t(15) = 2.08$, $P = 0.05$], whereas Hip and Amy initially exhibit increased activity in quartile 1 but show significantly decreased activity by quartile 4 [Hip quartile 1, $t(15) = 3.11$, $P = 0.007$; Hip quartile 4, $t(15) = -1.98$, $P = 0.05$; Amy quartile 1, $t(15) = 3.11$, $P = 0.007$; Amy quartile 4, $t(15) = -2.15$, $P = 0.04$]. (**C**) Correlation coefficients for rIFG and rMFG grouped with respective associated posterior brain regions as a function of quartile. $^*P \leq 0.05$, $^+P \leq 0.01$, $^\#P \leq 0.001$.

cused attention. However, we found that BA10 activity precedes and covaries with the activity of two separate prefrontal areas that are initiated at different temporal points in the process of suppressing activation in two different sets of posterior brain regions. This time-phased, region-specific activity pattern of BA10 is more complex than that expected for simple mind-wandering during NT trials, and is more consistent with BA10's proposed role of orchestration of multiple prefrontal processes involved in guiding complex tasks (*21*, *22*).

Our findings suggest that the suppression of emotional memory involves at least two pathways with staggered phases of their modulatory influence. The first pathway involves cognitive control by rIFG over sensory components of memory representation, as evidenced by reduced activity in FG and Pul. This finding is consistent with computational models that posit that activation and inhibition of the thalamus is a critical means of gating working memory information (*24*). A second pathway involves cognitive control by rMFG over memory processes and emotional components of memory representation via modulation of Hip and Amy (*2*, *25*). The overall timing of these suppression effects appears to be orchestrated by a modulatory influence of BA10, first over rIFG, then over rMFG. Further research is needed to determine the extent to which the two pathways act independently or interactively.

Our findings also provide insight into the potential neurocognitive mechanisms by which emotional memories are suppressed. Our data are consistent with the idea that initial memory suppression is most readily accomplished by prefrontal modulation of activity in sensory cortices that is likely to recreate the sensory percept. This process, however, does not predict subsequent behavioral recall and may be a "late-correction" mechanism (*26*) to suppress prepotent activity in sensory cortices generated as a result of viewing the cue. In contrast, activity of rMFG (over all quartiles) and Hip (during the last quartile) predicts behavioral suppression (*5*). This suppression process may reduce access to the memory itself, by blocking Hip and Amy activity needed for retrieval of the emotional memory. However, this mechanism becomes effective only after repeated attempts at control, as shown by the increased correlation in activity between rMFG-Hip and rMFG-Amy over quartiles (Fig. 3C). Once successful suppression of hippocampal activity is achieved, the need to invoke the "late-correction" process apparently decreases, as reflected in the decreased rIFG-Pul and rIFG-FG correlations.

Our data also provide an intriguing hint that, as suggested in clinical practice, it is necessary to "revisit" an emotionally distressing memory before it can be controlled. We found that early in the course of suppression (during quartiles 1 and 2), greater Hip activity was observed for NTf trials than NTr trials, as was also found by Anderson *et al.* in nontemporal analyses (*2*, *5*). We speculate that memories that activate Hip to a greater degree are more amenable to cognitive control because they are more elaborated and may provide increased access. By the fourth quartile, activation in Hip for NTf trials (but not NTr trials) is significantly below baseline, indicating that Hip activity has been effectively suppressed.

At a broader level, our findings extend research suggesting that prefrontal brain areas associated with inhibitory mechanisms (BA 10 and superior, inferior, and middle FG) are lateralized predominantly to the right hemisphere (*27*, *28*). We have shown the involvement of these areas in the suppression of emotional memories, which replicates current literature suggesting that these areas are active in the suppression of emotional reactivity (*29*, *30*). Activity in these brain areas, along with inhibition over Hip and Amy, suggests that suppression of emotional memories may use mechanisms similar to those used in emotion regulation. Thus, various right-lateralized PFC areas may be involved in coordinating suppression processes across many behavioral domains, including memory retrieval, motor processes, feelings of social rejection, self motives, and state emotional reactivity (*27*–*32*).

Our findings may have implications for therapeutic approaches to disorders involving the inability to suppress emotionally distressing memories and thoughts, including PTSD, phobias, ruminative depression/anxiety, and OCD. They provide the possibility for approaches to controlling memories by suppressing sensory aspects of memory and/or by strengthening cognitive control over memory and emotional processes through repeated practice. Refinement of therapeutic procedures based on these distinct means of manipulating emotional memory might be an exciting and fruitful development in future clinical research.

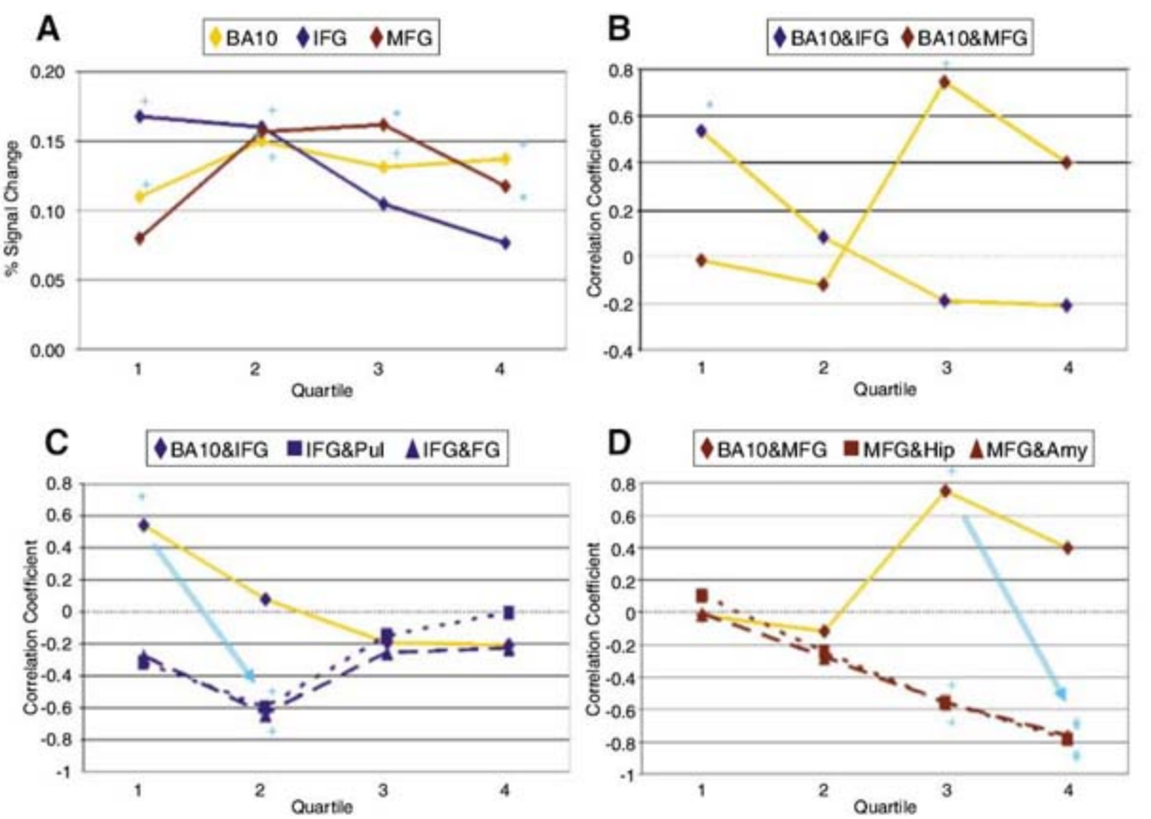

Fig. 4. (**A**) Time course of percent signal change for BA10, rIFG, and rMFG. (**B**) Correlations of rBA10 with rIFG and rMFG as a function of quartiles of suppression repetitions. (**C**) Correlations of BA10 with rIFG, rIFG with Pul, and rIFG with FG as a function of quartiles of suppression repetitions. (**D**) Correlations of BA10 with rMFG, rMFG with Hip, and rMFG with Amy as a function of suppression repetitions. Arrows in (C) and (D) indicate a preceding orchestration of control. For the quartile in which the correlation was maximal, greater activity in BA10 was associated with significantly increased activity in rIFG ($r = 0.56$, $P = 0.03$) and rMFG ($r = 0.77$, $P = 0.001$), but not with other brain areas [Pul, $r = -0.16$; FG, $r = -0.16$; Hip, $r = -0.22$; Amy, $r = -0.09$; $Ps > 0.40$ (*5*)]. $^*P \leq 0.05$, $^+P \leq 0.01$, $^\#P \leq 0.001$.

Our results suggest that effective voluntary suppression of emotional memory only develops with repeated attempts to cognitively control posterior brain areas underlying instantiated memories. In this sense, memory suppression may best be conceived as a dynamic process in which the brain acquires multiple modulatory influences to reduce the likelihood of retrieving unwanted memories.

References and Notes

1. E. Loftus, *Neuroscience* **4**, 231 (2003).
2. M. C. Anderson *et al.*, *Science* **303**, 232 (2004).
3. M. C. Anderson, C. Green, *Nature* **410**, 366 (2001).
4. J. F. Kihlstrom, *Trends Cognit. Sci.* **6**, 502 (2002).
5. See supporting data on *Science* Online.
6. B. E. Depue, M. T. Banich, T. Curran, *Psychol. Sci.* **17**, 441 (2006).
7. B. A. van der Kolk, J. A. Burbridge, J. Suzuki, *Ann. N.Y. Acad. Sci.* **821**, 99 (1997).
8. B. A. van der Kolk *et al.*, *Am. J. Psychiatry* **153**, 83 (1996).
9. C. Purdon, *Behav. Res. Ther.* **37**, 1029 (1999).
10. P. J. Lang *et al.*, *Psychophysiology* **35**, 199 (1998).
11. E. T. Rolls, *Hum. Neurobiol.* **3**, 209 (1984).
12. S. M. Kosslyn, W. L. Thompson, in *The New Cognitive Neurosciences*, M. S. Gazzaniga, Ed. (MIT Press, Cambridge, MA, ed. 2, 2000), pp. 975–985.
13. C. L. Raye *et al.*, *Cortex* **43**, 135 (2007).
14. A. D. Wagner *et al.*, *Neuroimage* **14**, 1337 (2001).
15. J. L. McGaugh, *Science* **287**, 248 (2000).
16. S. Kastner *et al.*, *J. Neurophysiol.* **91**, 438 (2004).
17. S. Kastner *et al.*, *Science* **282**, 108 (1998).
18. S. Hamann, *Trends Cognit. Sci.* **5**, 394 (2001).
19. E. A. Phelps, *Curr. Opin. Neurobiol.* **14**, 198 (2004).
20. Our activation of FG has been established to be different (more posterior/medial) from the activation of the fusiform face area (FFA) commonly observed in face perception studies (*33*).
21. K. Sakai, R. E. Passingham, *J. Neurosci.* **26**, 1211 (2006).
22. N. Ramnani, A. M. Owen, *Nat. Rev. Neurosci.* **5**, 184 (2004).
23. P. T. Hertel, G. Calcaterra, *Psychonom. Bull. Rev.* **12**, 484 (2005).
24. R. C. O'Reilly, *Science* **314**, 91 (2006).
25. M. Beauregard, J. Lévesque, P. Bourgouin, *J. Neurosci.* **21**, RC165 (2001).
26. L. L. Jacoby, C. M. Kelley, B. D. McElree, in *Dual-Process Theories in Social Psychology*, S. Chaiken, Y. Trope, Eds. (Guilford, New York, 1999), pp. 383–400.
27. H. Garavan, T. J. Ross, E. A. Stein, *Proc. Natl. Acad. Sci. U.S.A.* **96**, 8301 (1999).
28. A. R. Aron, T. W. Robbins, R. A. Poldrack, *Trends Cognit. Sci.* **8**, 170 (2004).
29. K. N. Ochsner *et al.*, *J. Cognit. Neurosci.* **14**, 1215 (2002).
30. N. I. Eisenberger, M. D. Lieberman, K. D. Williams, *Science* **302**, 290 (2003).
31. H. L. Urry *et al.*, *J. Neurosci.* **26**, 4415 (2006).
32. D. Knoch, A. Pascual-Leone, K. Meyer, V. Treyer, E. Fehr, *Science* **314**, 829 (2006); published online 4 October 2006 (10.1126/science.1129156).
33. I. Gautier *et al.*, *Nat. Neurosci.* **3**, 191 (2000).

34. We thank Y. Du, D. Singel, and R. Freedman for assistance in functional imaging, and three anonymous reviewers for their critical insights. Supported by the Graduate School, the Vice-Chancellor for Research, and the Institute of Cognitive Science at the University of Colorado at Boulder (M.T.B.).

Supporting Online Material

www.sciencemag.org/cgi/content/full/317/5835/215/DC1
Materials and Methods
Figs. S1 to S5
Tables S1 to S4
References

4 January 2007; accepted 6 June 2007
10.1126/science.1139560

REPORTS

Scattering and Interference in Epitaxial Graphene

G. M. Rutter,[1] J. N. Crain,[2] N. P. Guisinger,[2] T. Li,[1] P. N. First,[1]* J. A. Stroscio[2]*

A single sheet of carbon, graphene, exhibits unexpected electronic properties that arise from quantum state symmetries, which restrict the scattering of its charge carriers. Understanding the role of defects in the transport properties of graphene is central to realizing future electronics based on carbon. Scanning tunneling spectroscopy was used to measure quasiparticle interference patterns in epitaxial graphene grown on SiC(0001). Energy-resolved maps of the local density of states reveal modulations on two different length scales, reflecting both intravalley and intervalley scattering. Although such scattering in graphene can be suppressed because of the symmetries of the Dirac quasiparticles, we show that, when its source is atomic-scale lattice defects, wave functions of different symmetries can mix.

Built of a honeycomb of sp^2-bonded carbon atoms, graphene has a linear, neutrino-like energy spectrum near the Fermi energy, E_F. This results from the intersection of electron and hole cones in the graphene band structure at the Dirac energy, E_D. The linear energy dispersion and concomitant topological constraints give rise to massless Dirac quasiparticles in graphene, with energy-independent propagation speed $v_F \approx 10^6$ m/s (where v_F is the Fermi velocity). Distinctive symmetries of the graphene wave functions lead to unusual quantum properties, such as an anomalous integer quantum Hall effect (*1*, *2*) and weak antilocalization (*3*, *4*), that have spurred an intense scientific interest in graphene (*5*). Bilayer graphene (*5*–*7*) is equally distinctive: Quasiparticle states are chiral (*6*) with Berry's phase 2π for the bilayer versus π for the monolayer (*6*). High carrier mobilities, chemical inertness, and the two-dimensional (2D) nature of graphene make it a promising candidate for future electronic-device applications (*1*, *2*, *5*, *8*, *9*). In particular, graphene grown epitaxially on SiC substrates and patterned via standard lithographic procedures has been proposed as a platform for carbon-based nanoelectronics and molecular electronics (*8*, *9*).

Epitaxial graphene was grown on the silicon-terminated (0001) face of high-purity semi-insulating 4H-SiC by thermal desorption of silicon at high temperatures (*8*, *10*). This method produces an electron-doped graphene system, with the Fermi level 200 to 400 meV above E_D. The data that we present were obtained from a region identified as bilayer graphene (*11*). Scanning tunneling microscopy (STM) measurements were performed in a custom-built ultrahigh-vacuum, low-temperature instrument. We measured the scanning tunneling spectroscopy (STS) differential conductance dI/dV (where I is current and V is voltage) with lock-in detection by applying a small modulation to the tunnel voltage at ≈500 Hz. Differential conductance maps were obtained by recording an STS spectrum at each spatial pixel in the topographic measurement. All measurements reported here were taken at 4.3 K.

STM topographic images (Fig. 1) show the atomic structure and different types of disorder for epitaxial graphene on SiC(0001). At the atomic scale, the graphene is imaged as a triangular lattice (Fig. 1B), characteristic of imaging only one of the two graphene sublattices. Superimposed on this atomic structure is a modulation period of ≈2 nm caused by a reconstruction of the SiC interface beneath the graphene: a SiC "6 × 6" superstructure (*12*). Survey images reveal two categories of defects. Type A defects, such as mounds (red arrow in Fig. 1A), have an unperturbed graphene structure that is continuous, akin to a blanket. These defects are due to irregularities in the interface layer between graphene and the SiC bulk. In contrast, type B defects are atomic defects within the graphene lattice itself (Fig. 1, A, C, and D) and are accompanied by strong distortions in the local lattice images. These distortions are of electronic origin and are accompanied by large increases in the local density of states (LDOS) at the defect site (*13*, *14*). Quasiparticle scattering from type B defects gives rise to spectacular patterns in the topographic images (Fig. 1, C and D) resulting

[1]School of Physics, Georgia Institute of Technology, Atlanta, GA 30332, USA. [2]Center for Nanoscale Science and Technology, National Institute of Standards and Technology, Gaithersburg, MD 20899, USA.

*To whom correspondence should be addressed. E-mail: joseph.stroscio@nist.gov (J.A.S.); first@physics.gatech.edu (P.N.F.)

from the symmetry of the graphene Bloch states (*15*–*17*).

Detailed information on scattering from both types of defects is obtained from STS maps of dI/dV (Fig. 2), which is determined by the LDOS. By comparing the topographic and spectroscopic images, we find that type B defects in the graphene lattice are the dominant scattering centers. Over much of the energy range studied, these atomic-scale defects have a large central density of states surrounded by a strong reduction in the LDOS that appears to pin the phase of the scattering pattern nearby. For example, the type B defects labeled by blue arrows in Fig. 2 show a bright central spot encircled by a dark region and a bright ring (Fig. 2, B to E). In contrast, the dI/dV maps show that type A defects, over which the graphene is continuous (red arrows in Fig. 2), have dramatically less influence on the LDOS.

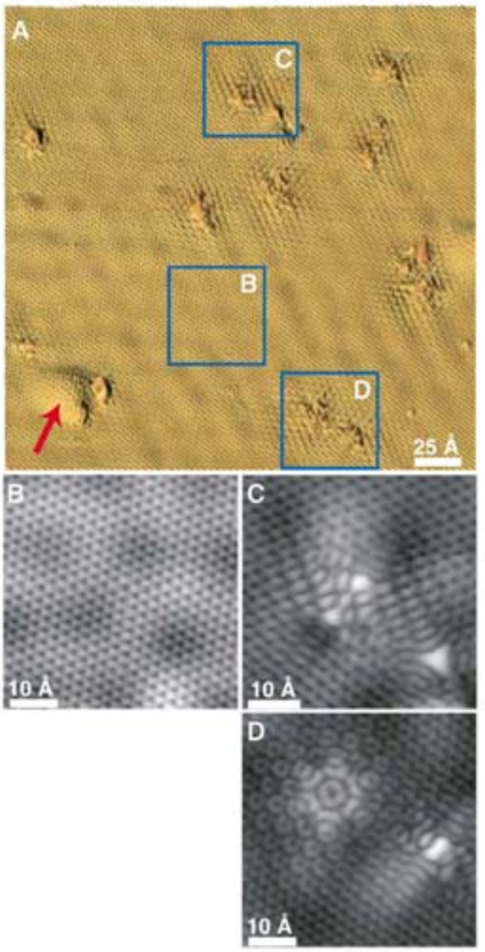

Fig. 1. STM topographic images of defects in the bilayer epitaxial graphene sample. (**A**) Large field of view showing a variety of defects. Type A defects (red arrow) are subsurface irregularities blanketed by graphene. The defect indicated by the red arrow has a height of 2 Å. Type B defects are atomic-scale defects in the graphene lattice. Higher-magnification images from the boxed regions in (A) are shown: a defect-free region (**B**) and complex scattering patterns around type B defects [(**C**) and (**D**)]. Tunneling setpoint: I = 100 pA, V = 300 mV.

Over large length scales, the dI/dV maps exhibit long-wavelength fluctuations that change with sample bias voltage (Fig. 2, B to E). As the sample voltage increases from −100 to +100 mV, the dominant wavelength decreases correspondingly from 9 to 5 nm. Fluctuations of much shorter wavelength are also present in these dI/dV maps, but they are not apparent over such a large displayed area. Figure 3 shows the short-wavelength modulations in dI/dV maps taken with atomic-scale spatial resolution. The interference patterns in these maps display a local $(\sqrt{3} \times \sqrt{3})$R30° structure (Fig. 3, B to E) with respect to the graphene lattice, with a superimposed long-wavelength modulation. Both the long-wavelength standing-wave modulations and the $\sqrt{3} \times \sqrt{3}$ periodicity are due to quasiparticle scattering from type B defects through wave vectors determined by the electronic structure of epitaxial graphene.

The 2D constant-energy contours in reciprocal space (Fig. 4A) are used to understand the scattering vectors that define the interference patterns observed in the STS maps of Figs. 2 and 3 (*18*). For graphene, the constant-energy contours near E_F cut through the electron or hole conical sheets, resulting in small circles of radius κ, centered at the wave vectors $\mathbf{K}_+$ and $\mathbf{K}_-$, that each locate three symmetry-equivalent corners of the 2D Brillouin zone. The scattering wave vectors $\mathbf{q}$ connect different points on the constant-energy contours (Fig. 4A). Two dominant families of scattering vectors, labeled $\mathbf{q_1}$ and $\mathbf{q_2}$, give rise to the patterns observed in the spectroscopic conductance maps. Wave vectors $\mathbf{q_1}$ connect points on a single constant-energy circle (intravalley scattering) and determine the observed long-wavelength patterns. Wave vectors $\mathbf{q_2}$ connect constant-energy circles at adjacent $\mathbf{K}_+$ and $\mathbf{K}_-$ points (intervalley scattering), yielding scattering wave vectors close in length to that of $\mathbf{K}_\pm$. $\mathbf{K}_+$ ($\mathbf{K}_-$) is related to the reciprocal lattice vectors $\mathbf{G}$ by a rotation of 30° (−30°) and a length that is shorter by $1/\sqrt{3}$ in reciprocal space. This relationship gives rise to the $(\sqrt{3} \times \sqrt{3})$R30° real-space superstructures observed in the high-resolution maps (Fig. 3, B to E). The vectors $\mathbf{q_2}$ will differ from the exact $\mathbf{K}_\pm$ wave vector because of the finite size of the constant-energy circles. The combination of different lengths contributing to $\mathbf{q_2}$ leads to the modulation of the $\sqrt{3} \times \sqrt{3}$ scattering patterns in Fig. 3.

To quantify the observed interference patterns and deduce the local band structure, we obtain $\mathbf{q}$-space images of the scattering vectors (Fig. 4B) from Fourier transform power spectra of the spectroscopic dI/dV maps (*19*, *20*). In Fig. 4B, $\mathbf{q_1}$ scattering appears as a bright ring centered at $\mathbf{q} = 0$. The ring is a consequence of the enhanced phase space for scattering near the spanning vectors of the constant-energy circle. Circular disks appear centered at the $\mathbf{K}_+$ and $\mathbf{K}_-$ points because of the distribution of $\mathbf{q_2}$ wave vectors. We determined ring radii for the central ring (Fig. 4C) and the $\mathbf{K}_\pm$ point disks using angular averages to maximize the signal-to-noise ratio. Both features change radius as a function of bias voltage because of dispersion in the graphene electronic states, and for these extremal $\mathbf{q}$ values, the scattering geometry determines $|\mathbf{q}| = 2\kappa$ or $|\mathbf{q} \pm \mathbf{K}_\pm| = 2\kappa$. The resulting κ values vary linearly with energy (Fig. 4D), with $v_F = (9.7 \pm 0.6) \times 10^5$ m/s (*18*). The $\kappa = 0$ energy intercept gives the Dirac energy, $E_F - E_D = 330 \pm 20$ meV. This local measurement of $E(\kappa)$ agrees well with photoemission studies of bilayer epitaxial graphene (*7*), and the parameters are close to those reported from transport studies on epitaxial graphene grown on SiC$(000\bar{1})$ (*9*). Similar results are found for a single monolayer of graphene (fig. S1) (*18*).

In addition to states localized on defect sites, sharp conductance peaks, ≈5 meV in width, are found several nanometers from the nearest type B defect (Fig. 3). The peaks are clearly associated with the $\mathbf{q_2}$-induced $\sqrt{3} \times \sqrt{3}$ LDOS modulation, as can be seen in the dI/dV maps (Fig. 3, B

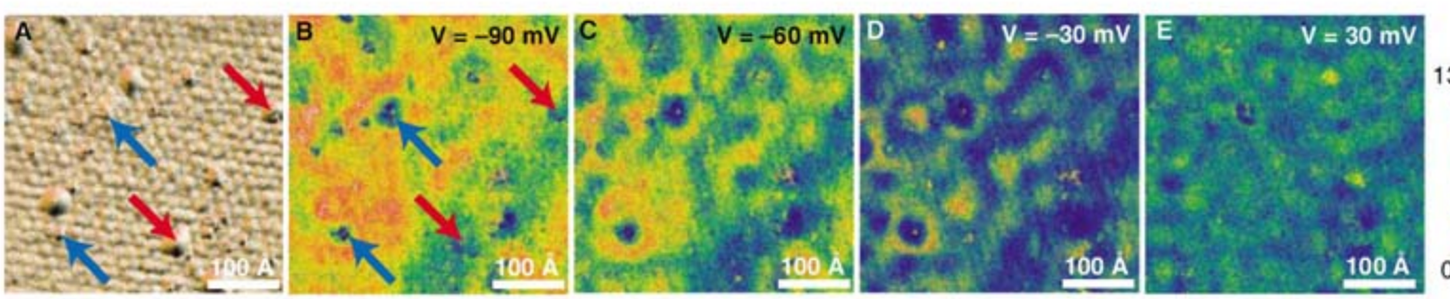

Fig. 2. Defect scattering in bilayer epitaxial graphene. (**A**) STM topography and (**B** to **E**) simultaneously acquired spectroscopic dI/dV maps. Type A defects (mounds) and type B defects are labeled with red and blue arrows, respectively. Sample biases are: (B) −90 mV, (C) −60 mV, (D) −30 mV, and (E) 30 mV. I = 500 pA, V = 100 mV, $\Delta V = 1$ mV$_{rms}$ where ΔV is the modulation voltage.

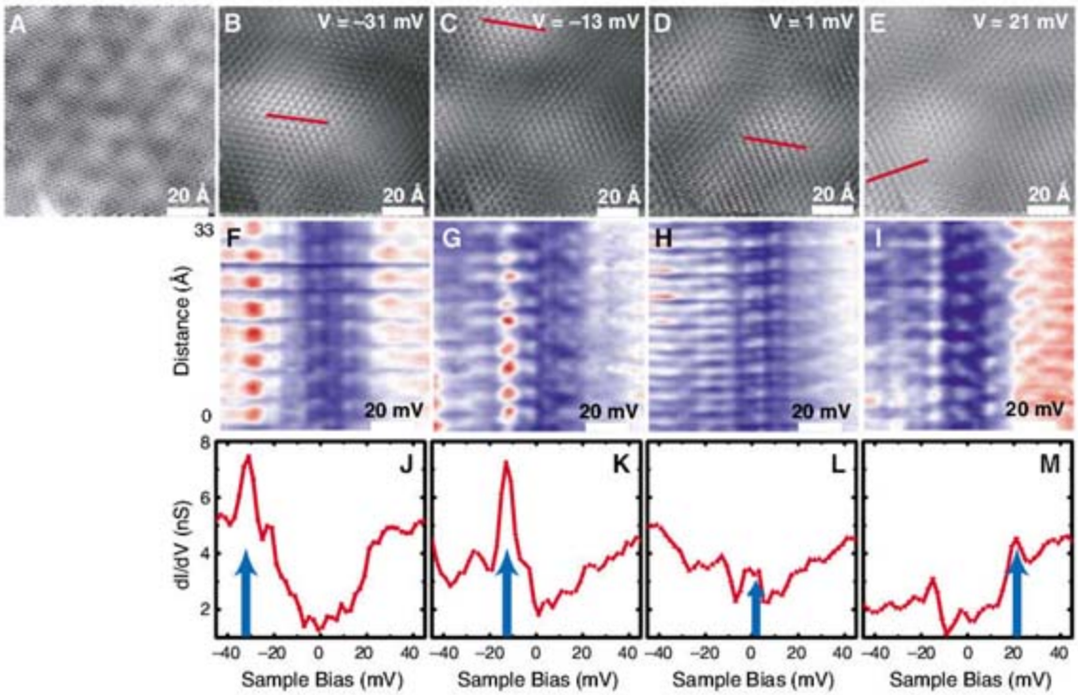

Fig. 3. Bilayer graphene topography (**A**) and simultaneous *dI/dV* maps at sample bias voltages of (**B**) −31 mV, (**C**) −13 mV, (**D**) 1.0 mV, and (**E**) 21 mV. The type B scattering centers lie outside the image region [see lower left corner of (A)]. (**F** to **I**) *dI/dV* (color scale) versus sample bias (horizontal axis) and distance (vertical axis) along corresponding red lines in (B) to (E). The blue-white-red color scale spans the conductance values observed in (J) to (M). (**J** to **M**) Line-averaged *dI/dV* spectra obtained from regions marked by red lines in (B) to (E). The spectra are averages of nine curves acquired at positions of the $\sqrt{3} \times \sqrt{3}$ interference maxima in the region of the red lines. Peaks in the *dI/dV* spectra correlate with maxima in the long-wavelength modulation of the $\sqrt{3} \times \sqrt{3}$ interference pattern. Blue arrows indicate the bias (energy) position of the corresponding conductance images in (B) to (E). I = 500 pA, V = 100 mV, ΔV = 0.7 mV_{rms}.

to E) and the spectral line profiles (Fig. 3, F to I). Furthermore, the data show that these conductance peaks are spatially localized, with maximum intensity in regions of constructive interference (i.e., over broad maxima modulating the $\sqrt{3} \times \sqrt{3}$ pattern in Fig. 3, B to E). We attribute these conductance peaks to scattering resonances, which localize quasiparticles because of constructive interference in scattering from the random arrangement of defects found within a phase coherence length (*18*).

In support of these conclusions, Fig. 3, F to I, displays sequences of *dI/dV* spectra taken along the red lines shown in Fig. 3, B to E (the red lines are in regions of maximum intensity modulation for the four different energies of the *dI/dV* maps in panels B through E). Each of the figures shows a very prominent $\mathbf{q_2}$ modulation along the vertical (distance) axis at the energy of the corresponding *dI/dV* map (B to E). The lower set of panels (J to M) shows *dI/dV* spectra obtained at positions of the $\sqrt{3} \times \sqrt{3}$ maxima, in the general areas of constructive interference (i.e., near the red lines). Clearly, the energy-dependent standing-wave patterns are associated with conductance peaks of different energies. Across the series of maps and spectra, resonances decrease in intensity as new ones acquire increased spectral strength, each corresponding to a particular spatial location of constructive interference in panels B to E. Resonances are seen at –31 mV (Fig. 3, F and J), at –13 mV (Fig. 3, G and K), straddling the Fermi energy at ±1 mV (Fig. 3, H and L), and at several energies above the Fermi level (Fig. 3, I and M). Many more spectral peaks are observed for different spatial locations in the data set in Fig. 3, with equally narrow line widths.

Of particular interest is the influence of the observed scattering centers on the transport properties of epitaxial graphene. For perfect monolayer graphene, the lattice A-B site symmetry and the $\mathbf{K}_\pm$ valley symmetry give rise to wave functions with distinct values of pseudospin and chirality (*3*, *21*, *22*). Both quantities are tied directly to the group velocity of the quasiparticle wave function, and their near-conservation in the presence of weak potentials is equivalent to a suppression of backscattering. Our measurements of both $\mathbf{q_1}$ and $\mathbf{q_2}$ scattering processes show very directly that in-plane atomic defects are a dominant source of both intravalley (pseudospin-flip) and intervalley (chirality-reversal) backscattering. This result may explain the observation of weak localization in similar samples (*8*, *18*). The related phenomenon of weak antilocalization was recently confirmed in epitaxial graphene grown by a

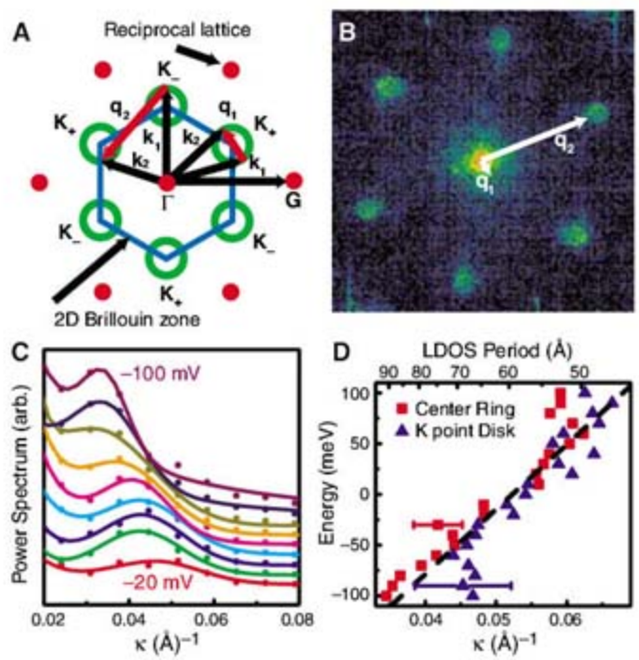

Fig. 4. (**A**) Schematic of the 2D Brillouin zone (blue lines), constant-energy contours (green rings) at the $\mathbf{K}_\pm$ points, and the two dominant classes of scattering vectors that create the interference patterns. $\mathbf{k_1}$ and $\mathbf{k_2}$ denote the wave vectors of incident and scattered carriers. Scattering wave vectors $\mathbf{q_1}$ (short red arrow) are seen to connect points on a single constant-energy circle, and wave vectors $\mathbf{q_2}$ (long red arrow) connect points on constant-energy circles between adjacent $\mathbf{K}_+$ and $\mathbf{K}_-$ points. Red circles indicate graphene reciprocal lattice points with origin Γ. (**B**) **q**-space map of scattering amplitudes, obtained from the Fourier transform power spectrum of the *dI/dV* map in Fig. 2D. $\mathbf{q_1}$ scattering forms the small ring at $\mathbf{q} = 0$, whereas $\mathbf{q_2}$ events create the six circular disks at $\mathbf{K}_\pm$ points. (**C**) Angular averages of the central $\mathbf{q_1}$ ring from the **q**-space maps, at bias voltages from −100 to −20 mV shown in 10-mV increments. arb., arbitrary units. (**D**) Energy dispersion as a function of κ for bilayer graphene determined from the **q**-space profiles in (C) and similar data. Values shown are derived from the radii of the central $\mathbf{q_1}$ scattering rings (red squares) and from the angle-averaged radii of the scattering disks at $\mathbf{K}_+$ and $\mathbf{K}_-$ (blue triangles). Dashed line shows a linear fit to the data with $v_F = (9.7 \pm 0.6) \times 10^5$ m/s and an energy intercept of −330 ± 20 meV. Similar results are found for a single monolayer of graphene (fig. S2D) (*18*). The error bars represent the typical combined statistical and systematic uncertainties estimated for each data set.

different method on carbon-terminated SiC$(000\bar{1})$ substrates (*4*), indicating a very low density of in-plane atomic scattering centers in those samples. Thus, the transport properties in epitaxial graphene are critically influenced by the microscopic properties of the sample, determined (at least) by the substrate and growth conditions. For carbon-based electronics, this work highlights the need for further microscopic studies that are correlated closely with macroscopic transport measurements.

References and Notes

1. K. S. Novoselov *et al.*, *Nature* **438**, 197 (2005).
2. Y. B. Zhang, Y. W. Tan, H. L. Stormer, P. Kim, *Nature* **438**, 201 (2005).
3. E. McCann *et al.*, *Phys. Rev. Lett.* **97**, 146805 (2006).
4. X. Wu *et al.*, *Phys. Rev. Lett.* **98**, 136801 (2007).
5. A. K. Geim, K. S. Novoselov, *Nat. Mater.* **6**, 183 (2007).
6. E. McCann, V. I. Fal'ko, *Phys. Rev. Lett.* **96**, 086805 (2006).
7. T. Ohta *et al.*, *Science* **313**, 951 (2006).
8. C. Berger *et al.*, *J. Phys. Chem. B* **108**, 19912 (2004).
9. C. Berger *et al.*, *Science* **312**, 1191 (2006).
10. E. Rollings *et al.*, *J. Phys. Chem. Solids* **67**, 2172 (2006).
11. The identification of monolayer and bilayer graphene is made from counting the number of atomic steps from the SiC substrate layer combined with STS measurements. Layers are also differentiated by the appearance of Si adatom interface states visible on monolayer graphene (*18*).
12. F. Owman, P. Martensson, *Surf. Sci.* **369**, 126 (1996).
13. V. M. Pereira *et al.*, *Phys. Rev. Lett.* **96**, 036801 (2006).
14. T. O. Wehling *et al.*, *Phys. Rev. B* **75**, 125425 (2007).
15. H. A. Mizes, J. S. Foster, *Science* **244**, 559 (1989).
16. K. F. Kelly, N. J. Halas, *Surf. Sci.* **416**, L1085 (1998).
17. P. Ruffieux *et al.*, *Phys. Rev. Lett.* **84**, 4910 (2000).
18. Additional text and data are available on *Science* Online.
19. L. Petersen, P. Hofmann, E. W. Plummer, F. Besenbacher, *J. Electron Spectrosc. Relat. Phenom.* **109**, 97 (2000).
20. J. E. Hoffman *et al.*, *Science* **297**, 1148 (2002).
21. T. Ando, T. Nakanishi, R. Saito, *J. Phys. Soc. Jpn.* **67**, 2857 (1998).
22. P. L. McEuen *et al.*, *Phys. Rev. Lett.* **83**, 5098 (1999).

23. We thank M. Stiles, E. Jarvis, W. de Heer, X. Wu, C. Berger, and F. Guinea for valuable comments and discussions and S. Blankenship, F. Hess, A. Band, and N. Brown for their technical assistance. This work was supported in part by the Office of Naval Research, by Intel Research, and by NSF grant ECS-0404084.

Supporting Online Material

www.sciencemag.org/cgi/content/full/317/5835/219/DC1
Materials and Methods
Figs. S1 and S2
References

22 March 2007; accepted 22 May 2007
10.1126/science.1142882

Efficient Tandem Polymer Solar Cells Fabricated by All-Solution Processing

Jin Young Kim,[1,2] Kwanghee Lee,[1,2]* Nelson E. Coates,[1] Daniel Moses,[1] Thuc-Quyen Nguyen,[1] Mark Dante,[1] Alan J. Heeger[1]

Tandem solar cells, in which two solar cells with different absorption characteristics are linked to use a wider range of the solar spectrum, were fabricated with each layer processed from solution with the use of bulk heterojunction materials comprising semiconducting polymers and fullerene derivatives. A transparent titanium oxide (TiO_x) layer separates and connects the front cell and the back cell. The TiO_x layer serves as an electron transport and collecting layer for the first cell and as a stable foundation that enables the fabrication of the second cell to complete the tandem cell architecture. We use an inverted structure with the low band-gap polymer-fullerene composite as the charge-separating layer in the front cell and the high band-gap polymer composite as that in the back cell. Power-conversion efficiencies of more than 6% were achieved at illuminations of 200 milliwatts per square centimeter.

Polymer solar cells based on conjugated polymer and fullerene composites offer special opportunities as renewable energy sources because they can be fabricated to extend over large areas by means of low-cost printing and coating technologies that can simultaneously pattern the active materials on lightweight flexible substrates (*1*–*4*). Although encouraging progress has been made with power-conversion efficiencies (η_e) of 5% having been reported (*5*–*9*), the limited efficiency has hindered the path toward commercialization.

The "tandem cell" architecture, a multilayer structure that is equivalent to two photovoltaic cells in series, offers a number of advantages. Because the two cells are in series, the open-circuit voltage (V_{oc}) is increased to the sum of the V_{oc}'s of the individual cells. The use of two semiconductors with different band gaps enables absorption over a broad range of photon energies within the solar emission spectrum; the two cells typically use a wide band-gap semiconductor for the first cell and a smaller band-gap semiconductor for the second cell (*10*). Because the electron-hole pairs generated by photons with energies greater than that of the energy gap rapidly relax to the respective band edges, the power-conversion efficiency of the two cells in series is inherently better than that of a single cell made from the smaller band-gap material. Moreover, because of the low mobility of the charge carriers in the polymer-fullerene composites, an increase in the thickness of the active layer increases the internal resistance of the device, which reduces both the V_{oc} and fill factor (*FF*) (*11*). Thus, the tandem cell architecture can have a higher optical density over a wider fraction of the solar emission spectrum than that of a single cell without increasing the internal resistance. The tandem cell architecture can therefore improve the light harvesting in polymer-based photovoltaic cells.

Tandem structures have been investigated for small-molecule heterojunction organic solar cells (*12*–*15*) and for hybrid organic solar cells in which the first cell uses an evaporated small-molecule material and the second cell uses a conjugated polymer; the two cells are separated by a semitransparent metal layer (*16*). Recently, polymer-fullerene composite tandem cells were reported (*17*–*20*). In these devices, a thermally evaporated metal layer is used as a charge-recombination layer and as a protection layer (to prevent interlayer mixing) during the spin-casting of the second cell (*17*–*19*). These polymer-based tandem cells exhibit a high V_{oc}, close to the expected sum of the V_{oc}'s of the two subcells, but the short-circuit current (J_{sc}) is lower than that of either single cell. When the same polymer was used for the front and back cells, the small J_{sc} was attributed to the absorption spectra being identical, so that the back cell absorbs less incident light and thus limits the photocurrent (because the two cells are in series, the current through the multilayer device is determined by that from the back cell). Moreover, because the interfacial metal layer is only semitransparent, the additional absorption also reduces the intensity of the light incident on the back cell. Thus, even when two different polymers are used, the photocurrent is correspondingly reduced.

We report here that we have successfully demonstrated the application of polymer-based bulk heterojunction tandem cells, with each layer processed from solution. A transparent TiO_x layer is used to separate and connect the front cell and the back cell. The TiO_x layer serves as an electron transport and collecting layer for the first cell and as a stable foundation that enables the fabrication of the second cell to complete the tandem cell architecture. In earlier work on tandem cells fabricated with organic semiconductors, the analogous intermediate layer was formed by the evaporative deposition of a semitransparent metal layer in high vacuum. This increases the complexity of device fabrication and causes unwanted loss of light intensity (due to absorption) to the back cell (*14*). For the tandem cells reported here, the TiO_x intermediate layer was deposited from solution (by means of sol-gel chemistry) with no substantial interlayer mixing. The performance of the polymer tandem solar cell is summarized as follows: $J_{sc} = 7.8$ mA/cm^2, $V_{oc} = 1.24$ V, $FF = 0.67$, and $\eta_e = 6.5\%$.

[1]Center for Polymers and Organic Solids, University of California, Santa Barbara, CA 93106–5090, USA. [2]Department of Materials Science and Engineering, Gwangju Institute of Science and Technology, Gwangju 500-712, Korea.

*To whom correspondence should be addressed. E-mail: klee@gist.ac.kr

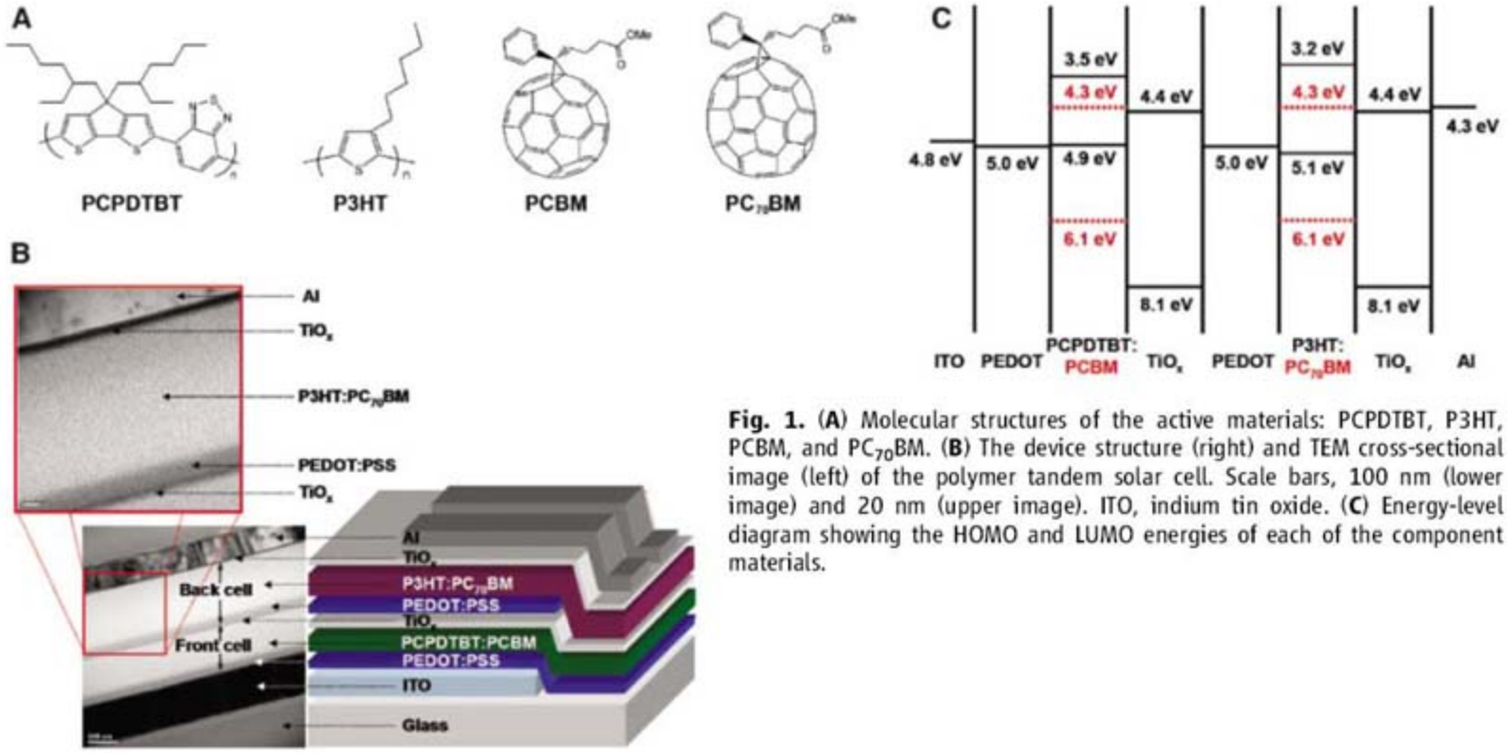

Fig. 1. (**A**) Molecular structures of the active materials: PCPDTBT, P3HT, PCBM, and $PC_{70}BM$. (**B**) The device structure (right) and TEM cross-sectional image (left) of the polymer tandem solar cell. Scale bars, 100 nm (lower image) and 20 nm (upper image). ITO, indium tin oxide. (**C**) Energy-level diagram showing the HOMO and LUMO energies of each of the component materials.

Figure 1 shows the structure of the multilayer polymer tandem solar cell together with the chemical structure of its components. The charge-separation layer for the front cell is a bulk heterojunction composite of poly[2,6-(4,4-bis-(2-ethylhexyl)-4*H*-cyclopenta[2,1-b;3,4-b'] dithiophene)-*alt*-4,7-(2,1,3-benzothiadiazole)] (PCPDTBT) and [6,6]-phenyl-C_{61} butyric acid methyl ester (PCBM). The charge-separation layer for the back cell is a bulk heterojunction composite of poly(3-hexylthiophene) (P3HT) and [6,6]-phenyl-C_{71} butyric acid methyl ester ($PC_{70}BM$). The two polymer-fullerene layers are separated by a transparent TiO_x layer and a highly conductive hole transport layer, poly(3,4-ethylenedioxylenethiophene)-polystylene sulfonic acid (PEDOT:PSS) (Baytron PH500 from H. C. Starck, Newton, Massachusetts, USA). Electrons from the first cell combine with holes from the second cell at the TiO_x-PEDOT:PSS interface.

The TiO_x layer is deposited by means of sol-gel chemistry, as described in (*9*). The TiO_x layer serves five separate functions. First, hydrophilic TiO_x separates the PEDOT:PSS that is cast on it from aqueous solution, from the underlying hydrophobic PCPDTBT:PCBM charge-separating layer of the front cell; the hydrophobic TiO_x precursor becomes hydrophilic after conversion to TiO_x. Second, the TiO_x layer breaks the symmetry in the front cell and thereby creates the open-circuit voltage. Third, the TiO_x functions as an electron transport layer. Fourth, the TiO_x functions as a hole blocking layer because the top of the valence band of TiO_x is sufficiently electronegative, 8.1 eV below the vacuum, to block holes (*9*). Finally, the top TiO_x layer (i.e., between the P3HT:$PC_{70}BM$ charge-separating layer of the back cell and the aluminum electrode) acts as an optical spacer that redistributes the light intensity to optimize the efficiency of the back cell (*9*).

Cross-sectional images of the polymer tandem solar cells taken with high-resolution transmission electron microscopy (TEM) show the individual layers clearly (Fig. 1B) (*21*). Perhaps more important, the various interfaces are very sharp; there is no interlayer mixing.

The energy-level diagram (Fig. 1C) indicates the highest occupied molecular orbital (HOMO) energies and the lowest unoccupied molecular orbital (LUMO) energies of the individual component materials. As noted, the V_{oc} of the tandem cell is equal to the sum of the V_{oc} of each subcell because the front and back cells are connected in series (*12*).

The absorption bands of the PCPDTBT and P3HT (Fig. 2A) complement each other and make these two materials appropriate for use in the two subcells of a spectrum-splitting tandem cell device. The absorption spectrum of a film of the bulk heterojunction composite of each subcell and that of a bilayer film of PCPDTBT:PCBM and P3HT:$PC_{70}BM$ are shown in Fig. 2B. The absorption of the PCPDTBT:PCBM film is weak in the visible spectral range but has two strong bands: one in the near-infrared (near-IR) between 700 and 850 nm that arises from the interband π-π^* transition of the PCPDTBT (*22*) and one in the ultraviolet (UV) that arises primarily from the HOMO-LUMO transition of the PCBM. The absorption of the P3HT:$PC_{70}BM$ film falls in the "hole" in the PCPDTBT:PCBM spectrum and covers the visible spectral range. The electronic absorption spectrum of the tandem structure can be described as a simple superposition of the absorption spectra of the two com-

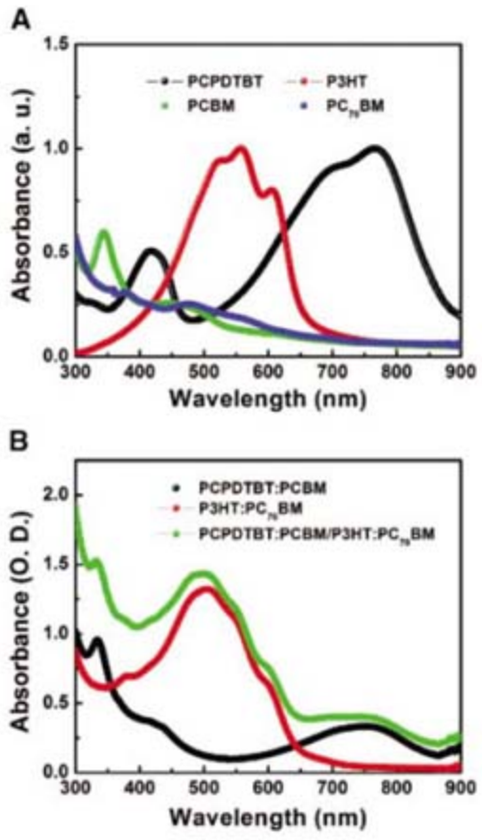

Fig. 2. (**A**) Absorption spectra of films of each material. The absorption band of the P3HT complements the absorption of PCPDTBT in visible range. a.u., arbitrary units. (**B**) Absorption spectra of a PCPDTBT:PCBM bulk heterojunction composite film, a P3HT:$PC_{70}BM$ bulk heterojunction composite film, and a bilayer of the two as relevant to the tandem device structure. O.D., optical density.

plementary composites. Therefore, the PEDOT:PSS and TiO_x layers have negligible absorption in the tandem device structure.

Tandem cells generally use a wide band-gap material as the first charge-separation layer and a narrow band-gap material as the second charge-separation layer with a thinner front cell than the back cell so that the photocurrents generated in each subcell are balanced. In our case, because of the non-optimum phase morphology of the PCPDTBT:PCBM composite, increasing the film thickness of this layer above 130 nm leads to reduced values for both J_{sc} and *FF* in single cells (*22*). However, the J_{sc} of a P3HT:PC_{70}BM single cell increases as the film thickness increases up to 200 nm, beyond which the *FF* is reduced. Because of these material characteristics, we have chosen an "inverted tandem cell" structure with the low band-gap bulk heterojunction composite (PCPDTBT:PCBM) as the front cell and the higher band-gap bulk heterojunction composite (P3HT:PC_{70}BM) as the back cell (Fig. 1B) (*21*).

We have measured the incident photon-to-current collection efficiency (IPCE) spectra of both the single cells and of the tandem cell, using a bias light on the tandem cell to confirm the series connection of the subcells and to extend the data over the full spectral coverage (Fig. 3A) (*16*, *21*, *23*). Each single cell shows the known spectral response of its bulk heterojunction composite, which is in excellent agreement with the absorption spectra of the two composites (Fig. 2B): The P3HT:PC_{70}BM composite gives a maximum IPCE of ~78% at 500 nm, and the PCPDTBT:PCBM composite has two dominant peaks (~35% at 750 to 800 nm and over 32% below 440 nm). When carrying out the measurements on the tandem cell, we find that biasing the device with 530-nm blue light and with 730-nm red light selectively excites the front and back cells, respectively, showing that (i) the device harvests photons from the UV to the near-IR, and (ii) each subcell functions individually (*23*).

The current density versus voltage (*J-V*) characteristics of single solar cells and the tandem solar cell with PCPDTBT:PCBM and P3HT:PC_{70}BM composites under Air Mass 1.5 Global (AM1.5G) illumination from a calibrated solar simulator with irradiation intensity of 100 mW/cm^2 are shown in Fig. 3B. The single devices show a typical photovoltaic response with device performance comparable to that reported in previous studies (*9*, *22*); the PCPDTBT:PCBM single cell yields J_{sc} = 9.2 mA/cm^2, V_{oc} = 0.66 V, *FF* = 0.50, and η_e = 3.0%, and the P3HT:PC_{70}BM single cell yields J_{sc} = 10.8 mA/cm^2, V_{oc} = 0.63 V, *FF* = 0.69, and η_e = 4.7%.

With two subcells stacked in series, the current that is extracted from the tandem cell is determined by the current generated in either the front or back cell, whichever is smaller (*23*). Accordingly, when there is greater carrier generation in either subcell, these excess charges cannot contribute to the photocurrent and so compensate for the built-in potential across that subcell. This compensation leads to a reduced V_{oc} in the tandem cell (*19*).

To optimize and balance the current in each subcell, we tried all possible variations of the tandem cell architecture: by changing the order of the active materials, by varying the concentration and ratio of each component in the composite solutions, and by varying the thicknesses of the two bulk heterojunction materials. Because of the high extinction coefficient of the PCPDTBT:PCBM composite, the P3HT:PC_{70}BM back cell has the smaller J_{sc} of the two subcells and is thus the limiting cell (*23*). The *FF* of the

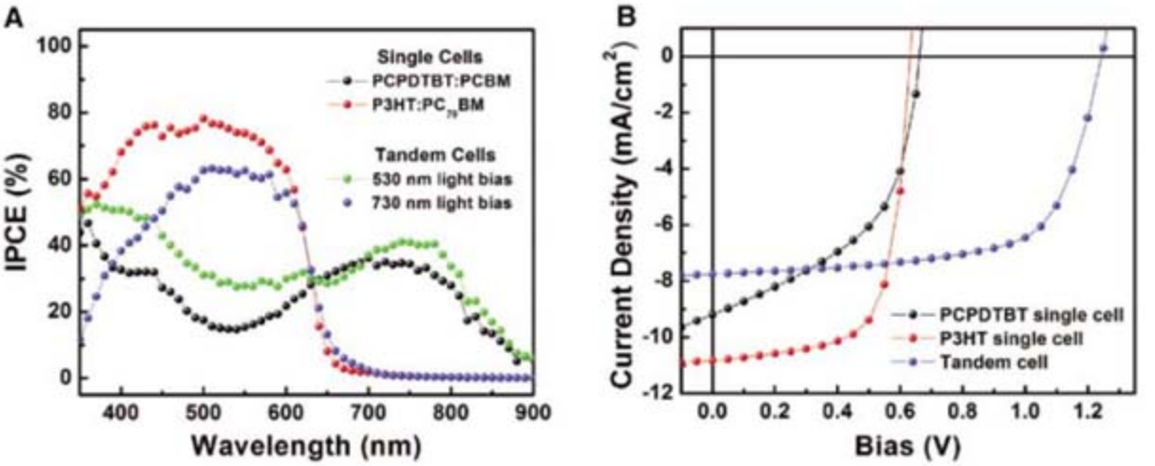

Fig. 3. (**A**) IPCE spectra of single cells and a tandem cell with bias light. We carried out the IPCE measurements using modulation spectroscopy with a lock-in amplifier for the single cells and for the tandem cell without light bias. For the tandem cell measurements made with bias light, unmodulated monochromatic light with an intensity of ~2 mW/cm^2 was used. (**B**) *J-V* characteristics of single cells and tandem cell with PCPDTBT:PCBM and P3HT:PC_{70}BM composites under AM1.5G illumination from a calibrated solar simulator with irradiation intensity of 100 mW/cm^2 (about one sun) are presented. The power-conversion efficiency of a solar cell is given as $\eta_e = (J_{sc} \cdot V_{oc} \cdot FF) \cdot 100/P_{inc}$, where P_{inc} is the intensity of incident light. The device performance is summarized as follows: The PCPDTBT:PCBM single cell shows J_{sc} = 9.2 mA/cm^2, V_{oc} = 0.66 V, *FF* = 0.50, and η_e = 3.0%; the P3HT:PC_{70}BM single cell shows J_{sc} = 10.8 mA/cm^2, V_{oc} = 0.63 V, *FF* = 0.69, and η_e = 4.7%; and the tandem cell shows J_{sc} = 7.8 mA/cm^2, V_{oc} = 1.24 V, *FF* = 0.67, and η_e = 6.5%.

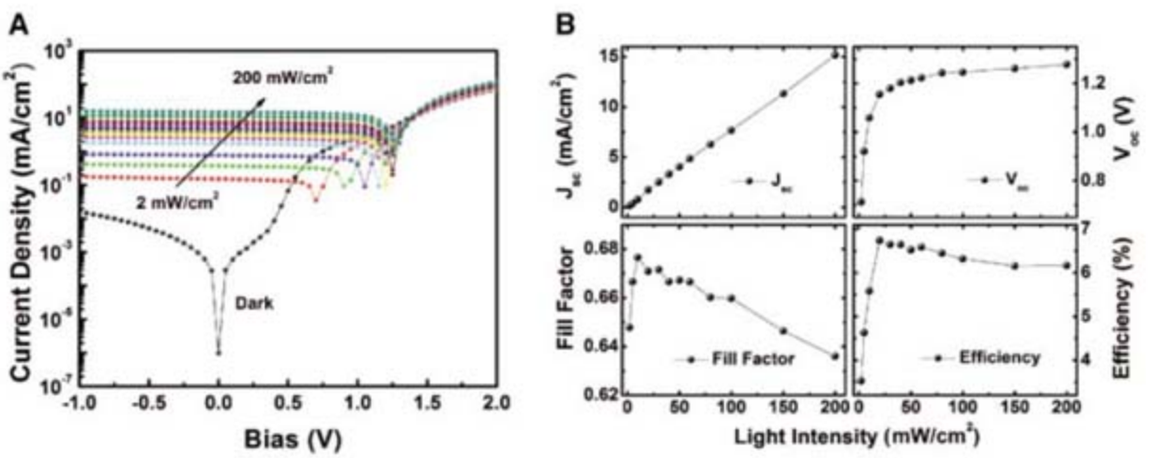

Fig. 4. (**A**) *J-V* characteristics of the optimized tandem cell measured with different incident light intensities from 0 to 200 mW/cm^2 (AM1.5G solar spectrum). (**B**) J_{sc}, V_{oc}, *FF*, and η_e of the tandem cell are plotted as functions of the incident light intensities. The η_e of the optimized tandem cell reaches its maximum of η_e = 6.7% at 20 mW/cm^2.

tandem cell can be very near the *FF* of the limiting cell. Thus, we use the P3HT:$PC_{70}BM$ as the back cell to obtain a higher *FF*.

More than 200 individual tandem cells were made in order to optimize the fabrication procedure and device architecture (*24*). This optimization led to the inverted tandem cell device depicted in Fig. 1B. Using this inverted structure, we fabricated more than 20 tandem cells with efficiencies above 6.2%. Performance parameters for a typical device are as follows: J_{sc} = 7.8 mA/cm^2, V_{oc} = 1.24 V, *FF* = 0.67, and η_e = 6.5%. The J_{sc} in the tandem cell is consistent with the IPCE measurements because the photocurrent in the back cell from IPCE is 72% of that of the P3HT:$PC_{70}BM$ single cell, confirming that the back cell is the limiting cell for J_{sc} as well as for *FF*.

Initial measurements of the stability of the tandem cell yield promising results. After storing the tandem cell in N_2 for 3500 hours (fig. S2A), its efficiency decreased from η_e = 6.5 to 5.5%. This relatively small decrease after nearly half a year confirms the robustness of the tandem cell architecture. Moreover, the tandem solar cells showed reasonable stability under continuous illumination. When exposed continuously to irradiation with an intensity of one sun (AM1.5G), the tandem cell retained ~70% of its original efficiency after 40 hours and over 60% even after 100 hours (fig. S2B) (*21*). Clearly, more extensive measurements on the degradation of packaged devices are required in future work.

The *J-V* characteristics of the optimized inverted tandem cell, measured with different incident light intensity from 0 to 200 mW/cm^2, are shown in Fig. 4A. In Fig. 4B, the performance parameters of the tandem cell (J_{sc}, V_{oc}, *FF*, and η_e) are plotted as functions of the incident light intensity. Because J_{sc} is linear with illuminated light intensity, there is no substantial space charge buildup in the tandem device. The V_{oc} also increases monotonically with an increase in the light intensity and approaches 1.3 V under AM1.5G conditions at 200 mW/cm^2, the sum of V_{oc} of the two subcells. The *FF* approaches 0.68 at 10 mW/cm^2, a value near the *FF* of the limiting P3HT:$PC_{70}BM$ back cell, and exceeds 0.63 at 200 mW/cm^2. The power-conversion efficiency of the optimized tandem cell reaches its maximum of η_e = 6.7% at 20 mW/cm^2, whereas η_e = 3.5% at 2 mW/cm^2 and η_e = 6.1% at 200 mW/cm^2. With these performance parameters, it is evident that the subcells in our tandem cell are connected in series and provide enhanced coverage of the solar spectrum.

References and Notes

1. N. S. Sariciftci, L. Smilowitz, A. J. Heeger, F. Wudl, *Science* **258**, 1474 (1992).
2. G. Yu, J. Gao, J. C. Hemmelen, F. Wudl, A. J. Heeger, *Science* **270**, 1789 (1995).
3. C. J. Brabec, *Sol. Energy Mater. Sol. Cells* **83**, 273 (2004).
4. K. M. Coakley, M. D. McGehee, *Chem. Mater.* **16**, 4533 (2004).
5. W. Ma, C. Y. Yang, X. Gong, K. Lee, A. J. Heeger, *Adv. Funct. Mater.* **15**, 1617 (2005).
6. M. Reyes-Reyes, K. Kim, D. L. Carroll, *Appl. Phys. Lett.* **87**, 083506 (2005).
7. G. Li *et al.*, *Nat. Mater.* **4**, 864 (2005).
8. Y. Kim *et al.*, *Nat. Mater.* **5**, 197 (2006).
9. J. Y. Kim *et al.*, *Adv. Mater.* **18**, 572 (2006).
10. M. W. Wanlass *et al.*, *Sol. Cells* **27**, 191 (1989).
11. I. Riedel, V. Dyakonov, *Phys. Status Solidi A* **201**, 1332 (2004).
12. M. Hiramoto, M. Suezaki, M. Yokoyama, *Chem. Lett. (Jpn.)* **19**, 327 (1990).
13. A. Yakimov, S. R. Forrest, *Appl. Phys. Lett.* **80**, 1667 (2002).
14. J. Xue, S. Uchida, B. P. Rand, S. R. Forrest, *Appl. Phys. Lett.* **85**, 5757 (2004).
15. J. Drechsel *et al.*, *Appl. Phys. Lett.* **86**, 244102 (2005).
16. G. Dennler *et al.*, *Appl. Phys. Lett.* **89**, 073502 (2006).
17. V. Shrotriya, E. H.-E. Wu, G. Li, Y. Yao, Y. Yang, *Appl. Phys. Lett.* **88**, 064104 (2006).
18. K. Kawano, N. Ito, T. Nishimori, J. Sakai, *Appl. Phys. Lett.* **88**, 073514 (2006).
19. A. Hadipour *et al.*, *Adv. Funct. Mater.* **16**, 1897 (2006).
20. J. Gilot, M. M. Wienk, R. A. J. Janssen, *Appl. Phys. Lett.* **90**, 143512 (2007).
21. Materials and methods are available as supporting material on *Science* Online.
22. D. Mühlbacher *et al.*, *Adv. Mater.* **18**, 2884 (2006).
23. J. Burdick, T. Glatfelter, *Sol. Cells* **18**, 301 (1986).
24. All the solar cell devices were fabricated by J.Y.K., who also measured their performance. The IPCE measurements were performed by J.Y.K. and N.E.C. The TEM images were obtained by M.D.

25. The research was supported by Konarka Technologies (Lowell, MA), by the U.S. Department of Energy (under grant DE-FGO2-06ER46324), and by the Ministry of Science & Technology of Korea under the International Cooperation Research Program (Global Research Laboratory Program: K.L. and A.J.H., Principal Investigators). The PCPDTBT, PCBM, P3HT, and $PC_{70}BM$ materials were supplied for our use by Konarka Technologies. We thank W. Ma for contributions during the early phase of this work.

Supporting Online Material

www.sciencemag.org/cgi/content/full/317/5835/222/DC1
Materials and Methods
Figs. S1 and S2
References

23 February 2007; accepted 16 May 2007
10.1126/science.1141711

Cleaving Mercury-Alkyl Bonds: A Functional Model for Mercury Detoxification by *MerB*

Jonathan G. Melnick and Gerard Parkin*

The extreme toxicity of organomercury compounds that are found in the environment has focused attention on the mechanisms of action of bacterial remediating enzymes. We describe facile room-temperature protolytic cleavage by a thiol of the Hg-C bond in mercury-alkyl compounds that emulate the structure and function of the organomercurial lyase *MerB*. Specifically, the tris(2-mercapto-1-*t*-butylimidazolyl)hydroborato ligand [Tm^{Bu^t}], which features three sulfur donors, has been used to synthesize [Tm^{Bu^t}]HgR alkyl compounds (R = methyl or ethyl) that react with phenylthiol (PhSH) to yield [Tm^{Bu^t}]HgSPh and RH. Although [Tm^{Bu^t}]HgR compounds exist as linear two-coordinate complexes in the solid state, ^{1}H nuclear magnetic resonance spectroscopy indicates that the complexes exist in rapid equilibrium with their higher-coordinate [κ^2-Tm^{Bu^t}]HgR and [κ^3-Tm^{Bu^t}]HgR isomers in solution. Facile access to a higher-coordinate species is proposed to account for the exceptional reactivity of [Tm^{Bu^t}]HgR relative to that of other two-coordinate mercury-alkyl compounds.

The extreme toxicological problems associated with mercury and its compounds (*1*) are largely a consequence of the high affinity of mercury for sulfur. As such, mercury binds readily to the thiol groups of cysteine residues in proteins and enzymes and may displace Zn(II) from cysteine-rich structural and catalytic zinc sites (*2*). For example, Hg(II) inhibits the Fpg DNA repair protein by a mechanism that is believed to involve replacement of Zn(II) in the Cys_4 zinc finger binding site (*3*–*6*). Mercury alkyls, in particular, are potent neurotoxins because they bind so strongly to protein residues and are capable of crossing the blood-brain barrier. Indeed, methyl-mercury compounds are responsible for Minamata disease, so-called because it caused the death of almost 2000 people around Minamata Bay (Japan) in the late 1950s when the residents consumed fish that was contaminated with methyl-mercury compounds (*1*). Although the initial outbreak of the disease was a result of toxic release from a nearby chemical plant, methyl-mercury compounds are also introduced into the environment by biomethylation of naturally occurring Hg(II) in an aquatic environment (*7*, *8*). The Hg-CH_3 bond is kinetically stable toward protolytic cleavage in aqueous solution, with the result that methyl-mercury compounds accumulate in predatory fish and may be consumed by humans (*1*, *7*).

Detoxification of organomercury compounds is therefore of critical importance. In nature, this is achieved by the combined action of two enzymes. Specifically, bacterial organomercurial lyase (*MerB*) achieves protolytic cleavage of the

Department of Chemistry, Columbia University, New York, NY 10027, USA.

*To whom correspondence should be addressed. E-mail: parkin@columbia.edu

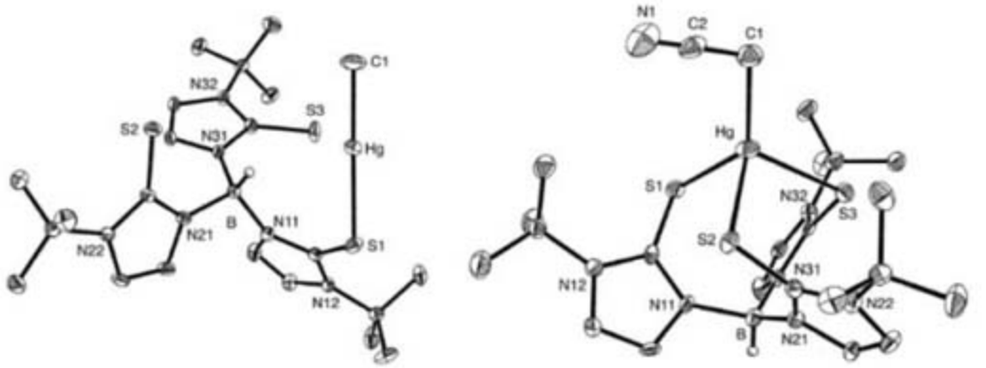

Fig. 1. Molecular structures of $[Tm^{Bu^t}]HgMe$ (left) and $[Tm^{Bu^t}]HgCH_2CN$ (right).

otherwise inert Hg-C bond while a second enzyme, mercuric ion reductase (*MerA*), reduces Hg(II) to less toxic elemental mercury, Hg(0) (*1*, *9*). Here, we provide evidence relevant to the mechanism of action of *MerB* by investigation of a synthetic analog system.

MerB obtained from *Escherichia coli* (R831b) has four cysteine residues that are crucial for enzymatic activity. Of these, one cysteine (Cys^{117}) is considered to play only a structural role, whereas the other three (Cys^{96}, Cys^{159}, and Cys^{160}) are believed to serve the combined roles of binding the organomercury substrate and protolytically cleaving the mercury-carbon bond (*9*–*12*). Other than this general description of the reaction sequence, however, the coordination mode of the organomercury substrate in *MerB* and the intimate details of the reaction mechanism are unknown. Therefore, to provide a more thorough understanding of the mechanism of action of *MerB*, it is pertinent to investigate the bioorganometallic chemistry of mercury in a sulfur-rich coordination environment. For this purpose, we have used the tris(2-mercapto-1-*t*-butylimidazolyl)hydroborato ligand $[Tm^{Bu^t}]$, which features three sulfur donors, to synthesize mercury-alkyl compounds that emulate aspects of the structure and function of *MerB* (*13*, *14*).

The mercury-alkyl compounds $[Tm^{Bu^t}]HgMe$ and $[Tm^{Bu^t}]HgEt$ are readily synthesized via the reaction of $[Tm^{Bu^t}]K$ with MeHgI and EtHgCl, respectively (Scheme 1) (*15*). The molecular structures of $[Tm^{Bu^t}]HgMe$ (Fig. 1) and $[Tm^{Bu^t}]HgEt$ have been determined by x-ray diffraction, thereby demonstrating that the $[Tm^{Bu^t}]$ ligand coordinates primarily in a κ^1 manner (i.e., coordination via a single sulfur atom), with a linear S-Hg-C geometry and Hg-S bond lengths of 2.396(2) and 2.405(1) Å, respectively (*16*). This κ^1 coordination mode is quite distinct from the κ^3 mode (i.e., coordination via three sulfur atoms) that is observed for other $[Tm^R]HgX$ derivatives in the solid state (*17*, *18*); nonetheless, it does correspond closely to the means by which the protein coordinates to the metal in the mercury-dithiothreitol complex of *MerB* (*19*). In contrast to the κ^1 coordination observed for $[Tm^{Bu^t}]HgMe$ and $[Tm^{Bu^t}]HgEt$, the cyanomethyl complex $[Tm^{Bu^t}]HgCH_2CN$ (*20*) adopts κ^3 coordination of the $[Tm^{Bu^t}]$ ligand, giving a four-coordinate pseudotetrahedral mercury center (Fig. 1). Of these two geometries, the linear coordination mode is most prevalent for mercury-alkyl compounds (*21*–*23*); $[\{\kappa^3\text{-}[9]aneS_3\}HgMe]^+$ (*24*), $\{[\kappa^3\text{-}N(CH_2CH_2PPh_2)_3]HgMe\}^+$ (*25*), and $[\kappa^3\text{-}Tp^{Ph_2}]HgEt$ (*26*) are illustrative of the few pseudotetrahedral mercury-alkyl compounds previously characterized (*27*, *28*).

Prior efforts to emulate *MerB* have examined protolytic cleavage with the use of strong Brønsted oxo acids such as CF_3SO_3H (*24*). However, because *MerB* uses a cysteine S-H group to effect cleavage of the Hg-C bond, we considered that a better model for cysteine would be simple thiols (*29*). It is therefore noteworthy that each of the alkyl compounds $[Tm^{Bu^t}]HgR$ (R = Me, Et, CH_2CN) reacts with PhSH rapidly at room temperature (*30*) to yield pseudotetrahedral $[Tm^{Bu^t}]HgSPh$ (*31*) and liberate RH, thereby demonstrating facile Hg-C bond cleavage by a thiol in a sulfur coordination environment (Scheme 2).

With respect to the mechanism of cleavage of the Hg-C bond, it is well known that two-coordinate monoalkyl-mercury compounds of the type X-Hg-R (*15*) are notoriously inert toward cleavage of the Hg-C bond under physiological conditions (*32*–*34*). As such, the high reactivity of $[Tm^{Bu^t}]HgMe$ and $[Tm^{Bu^t}]HgEt$ may be attributed to the ability to access κ^2 or κ^3 isomers (*35*, *36*). In this regard, variable-temperature ^1H nuclear magnetic resonance (NMR) spectroscopic studies on $[Tm^{Bu^t}]HgR$ (R = Me, Et) indicate that the molecules are highly fluxional. At –60°C, the spectrum is consistent with a $[\kappa^3\text{-}Tm^{Bu^t}]HgR$ pseudotetrahedral structure, whereas at intermediate temperatures, both κ^1 and κ^3 isomers are observed. A two-dimensional exchange spectroscopy experiment confirms that these isomers are in rapid equilibrium at –20°C and a three-coordinate $[\kappa^2\text{-}Tm^{Bu^t}]HgR$ intermediate is implied in this process (*37*).

The observed fluxionality of $[Tm^{Bu^t}]HgR$ provides excellent evidence that the role of one of the cysteine ligands in the active site of *MerB* is to activate a two-coordinate mercury-alkyl compound toward protolytic cleavage by an

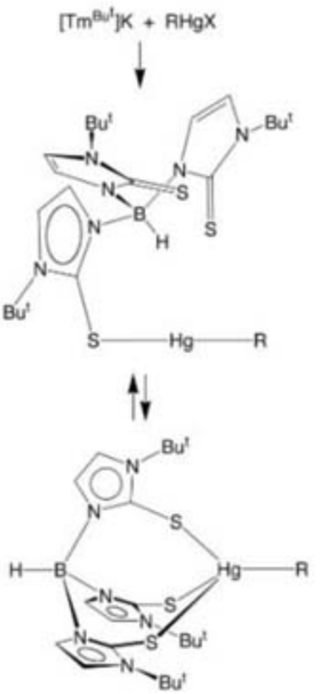

Scheme 1.

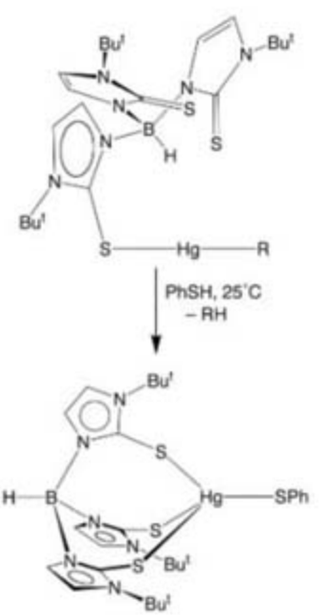

Scheme 2.

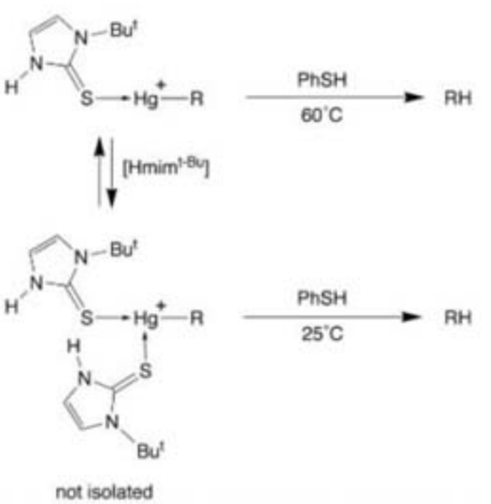

Scheme 3.

additional cysteine S-H group. To address further the impact of coordination number on the ability to cleave the Hg-C bond, we examined the corresponding reactivity of strictly two-coordinate mercury-alkyl compounds that bear a close relationship to $[\kappa^1\text{-Tm}^{Bu^t}]HgR$. Specifically, we investigated the 1-*t*-butylimidazole-2-thione derivatives $\{[Hmim^{Bu^t}]HgR\}^+$ (*37*) in which the $Hmim^{Bu^t}$ ligand emulates the κ^1 coordination mode of the $[Tm^{Bu^t}]$ ligand, as determined by x-ray diffraction studies on $\{[Hmim^{Bu^t}]HgEt\}[BF_4]$ (*38*, *39*).

Interestingly, whereas $[Tm^{Bu^t}]HgMe$ and $[Tm^{Bu^t}]HgEt$ react rapidly with PhSH at room temperature, the two-coordinate compounds $\{[Hmim^{Bu^t}]HgMe\}^+$ and $\{[Hmim^{Bu^t}]HgEt\}^+$ are stable under comparable conditions; protolytic cleavage and liberation of RH are nonetheless observed at elevated temperatures (Scheme 3) (*40*). The lower reactivity of $\{[Hmim^{Bu^t}]HgR\}^+$ relative to $[Tm^{Bu^t}]HgR$ supports the proposal that access to coordination numbers greater than 2 promotes protolytic cleavage of the Hg-C bond (*41*). In support of this suggestion, addition of $Hmim^{Bu^t}$ to a mixture of $\{[Hmim^{Bu^t}]HgEt\}[BF_4]$ and PhSH causes elimination of ethane at room temperature, an observation consistent with the formation of a higher-coordinate species $\{[Hmim^{Bu^t}]_nHgEt\}^+$ that is more susceptible to Hg-C protolytic cleavage than is two-coordinate $\{[Hmim^{Bu^t}]HgEt\}^+$ (*42*).

In view of the low reactivity of two-coordinate $\{[Hmim^{Bu^t}]HgR\}^+$ toward PhSH, we attribute the high reactivity of $[Tm^{Bu^t}]HgMe$ and $[Tm^{Bu^t}]HgEt$ to the accessibility of a higher-coordinate mercury alkyl by κ^2 or κ^3 binding of the $[Tm^{Bu^t}]$ ligand. Thus, of the three nonstructural cysteine residues of *MerB* that are crucial for enzymatic activity, it is evident that one cysteine is required to coordinate $[HgR]^+$ in a linear manner, a second cysteine is required to activate the Hg-alkyl group toward protolytic cleavage, and the third cysteine is required to effect the cleavage reaction (*43*, *44*).

References and Notes

1. T. W. Clarkson, L. Magos, *Crit. Rev. Toxicol.* **36**, 609 (2006).
2. H. C. Tai, C. Lim, *J. Phys. Chem. A* **110**, 452 (2006).
3. A. Hartwig *et al.*, *Food Chem. Toxicol.* **40**, 1179 (2002).
4. For other examples of Hg(II) binding to zinc finger proteins, see (*5*, *6*).
5. M. Razmiafshari, J. Kao, A. d'Avignon, N. H. Zawia, *Toxicol. Appl. Pharmacol.* **172**, 1 (2001).
6. A. Witkiewicz-Kucharczyk, W. Bal, *Toxicol. Lett.* **162**, 29 (2006).
7. W. F. Fitzgerald, C. H. Lamborg, C. R. Hammerschmidt, *Chem. Rev.* **107**, 641 (2007).
8. T. Barkay, S. M. Miller, A. O. Summers, *FEMS Microbiol. Rev.* **27**, 355 (2003).
9. M. J. Moore, M. D. Distefano, L. D. Zydowsky, R. T. Cummings, C. T. Walsh, *Acc. Chem. Res.* **23**, 301 (1990).
10. K. E. Pitts, A. O. Summers, *Biochemistry* **41**, 10287 (2002).
11. P. Di Lello *et al.*, *Biochemistry* **43**, 8322 (2004).
12. Cys^{96}, Cys^{117}, and Cys^{159} are highly conserved in *MerB* from other sources and are essential for activity; Cys^{160} is only weakly conserved and is not essential (*10*).
13. $[Tm^R]$ ligands have recently been effectively used to provide compounds that mimic aspects of the chemistry relevant to the active sites of sulfur-rich zinc enzymes and proteins. See, for example, (*14*).
14. G. Parkin, *Chem. Rev.* **104**, 699 (2004).
15. Abbreviations: Me = methyl, Et = ethyl, Ph = phenyl, Bu^t = *t*-butyl, R = alkyl or aryl, X = monovalent inorganic ligand, $Hmim^{Bu^t}$ = 1-*t*-butylimidazole-2-thione.
16. There is also a long-range Hg···S secondary interaction (3.3 Å) that is perpendicular to the two primary Hg-C and Hg-S bonds.
17. J. L. White, J. M. Tanski, D. Rabinovich, *J. Chem. Soc. Dalton Trans.* **2002**, 2987 (2002).
18. I. Cassidy *et al.*, *Eur. J. Inorg. Chem.* **2002**, 1235 (2002).
19. G. C. Benison *et al.*, *Biochemistry* **43**, 8333 (2004).
20. $[Tm^{Bu^t}]HgCH_2CN$ is obtained from the reaction of $[Tm^{Bu^t}]K$, EtHgCl, and KBH_4 in MeCN.
21. C. E. Holloway, M. Melník, *J. Organomet. Chem.* **495**, 1 (1995).
22. Two-coordination at mercury is also common for thiolate compounds (*23*).
23. J. G. Wright, M. J. Natan, F. M. MacDonnell, D. M. Ralston, T. V. O'Halloran, *Prog. Inorg. Chem.* **38**, 323 (1990).
24. M. Wilhelm *et al.*, *Eur. J. Inorg. Chem.* **2004**, 2301 (2004).
25. P. Barbaro *et al.*, *Inorg. Chem.* **33**, 6163 (1994).
26. G. Gioia Lobbia, C. Santini, F. Giordano, P. Cecchi, K. Coacci, *J. Organomet. Chem.* **552**, 31 (1998).
27. Intermediate three-coordinate "T-shaped" geometries are also known. For example, the approximately linear coordination observed for [pzTp]HgMe [169(2)°] is supplemented by a secondary Hg···N interaction (*28*).
28. A. J. Canty, B. W. Skelton, A. H. White, *Aust. J. Chem.* **40**, 1609 (1987).
29. $\{[\kappa^3\text{-N}(CH_2CH_2PPh_2)_3]HgPh\}^+$ reacts with ArSH, but the reaction has been proposed to involve initial dissociation of $N(CH_2CH_2PPh_2)_3$ and subsequent formation of $[HN(CH_2CH_2PPh_2)_3]^+$, which is the active reagent in the protolytic cleavage, rather than the thiol (*25*).
30. Half-life ≈ 15 min for $[Tm^{Bu^t}]HgEt$ with [PhSH] = 0.1 M.
31. D. Rabinovich, *Struct. Bonding* **120**, 143 (2006).
32. M. M. Kreevoy, *J. Am. Chem. Soc.* **79**, 5927 (1957).
33. Thus, whereas Me_2Hg reacts slowly with certain biologically related thiols to cleave one of the Hg-C bonds, cleavage of the second Hg-CH_3 bond could not be achieved (*34*).
34. H. Strasdeit, A. von Döllen, W. Saak, M. Wilhelm, *Angew. Chem. Int. Ed.* **39**, 784 (2000).
35. Calculations suggest that the increased facility of protolytic cleavage of the Hg-C bond upon increasing coordination number is a consequence of an associated increase in negative charge on the carbon (*36*).
36. B. Ni, J. R. Kramer, R. A. Bell, N. H. Werstiuk, *J. Phys. Chem. A* **110**, 9451 (2006).
37. See supporting material on *Science* Online.
38. The related methimazole complex $[(Hmim^{Me})HgMe](NO_3)$ has been reported (*39*).
39. A. R. Norris, S. E. Taylor, E. Buncel, F. Bélanger-Gariépy, A. L. Beauchamp, *Can. J. Chem.* **61**, 1536 (1983).
40. The nature of the final mercury product has not been identified.
41. The positive charge on the complex could also inhibit protolytic cleavage. In this regard, the corresponding reaction of neutral $[mim^{Bu^t}]HgR$ with PhSH was also investigated, but the reaction yielded PhSHgR as a result of preferential protonation of the nitrogen atom of the $[mim^{Bu^t}]$ ligand. Moreover, the two-coordinate neutral compound PhSHgR is inert to excess PhSH at room temperature.
42. Addition of $Hmim^{Bu^t}$ to $\{[Hmim^{Bu^t}]HgR\}^+$ in the absence of PhSH does not result in cleavage of the Hg-C bond. Rather, the ^1H NMR spectrum shows that $Hmim^{Bu^t}$ merely binds reversibly, as indicated by the observation that the mercury-methyl signal for $\{[Hmim^{Bu^t}]HgMe\}^+$ shifts from δ 0.48 to 0.62 in the presence of $Hmim^{Bu^t}$.
43. Although *MerB* obtained from *E. coli* (R831b) has three cysteines at the active site, only two of these are highly conserved in *MerB* from other sources (*10*). It is therefore possible that a residue other than cysteine could also facilitate the protolytic cleavage. In this regard, studies on a model system indicate that carboxylate bases may also serve to promote protolytic cleavage of Hg-C bonds (*44*).
44. E. Gopinath, T. C. Bruice, *J. Am. Chem. Soc.* **109**, 7903 (1987).

45. Supported by NSF grant CHE-0619638, which enabled the acquisition of an x-ray diffractometer, and by NIH grant GM046502. Complete crystallographic data have been deposited in the Cambridge Crystallographic Database Centre (accession numbers 648324 to 648331).

Supporting Online Material

www.sciencemag.org/cgi/content/full/317/5835/225/DC1
SOM Text
Figs. S1 to S9
Table S1
References

26 April 2007; accepted 31 May 2007
10.1126/science.1144314

Magmatic Gas Composition Reveals the Source Depth of Slug-Driven Strombolian Explosive Activity

Mike Burton,[1]* Patrick Allard,[1,2] Filippo Muré,[1] Alessandro La Spina[1,3]

Strombolian-type eruptive activity, common at many volcanoes, consists of regular explosions driven by the bursting of gas slugs that rise faster than surrounding magma. Explosion quakes associated with this activity are usually localized at shallow depth; however, where and how slugs actually form remain poorly constrained. We used spectroscopic measurements performed during both quiescent degassing and explosions on Stromboli volcano (Italy) to demonstrate that gas slugs originate from as deep as the volcano-crust interface (~3 kilometers), where both structural discontinuities and differential bubble-rise speed can promote slug coalescence. The observed decoupling between deep slug genesis and shallow (~250-meter) explosion quakes may be a common feature of strombolian activity, determined by the geometry of plumbing systems.

Strombolian explosive activity, named after Stromboli volcano, is commonly observed on volcanoes fed by low to moderate viscosity magmas. It consists of periodic jets or explosions throwing molten lava fragments tens to hundreds of meters above open vents, which are driven by the fast up-rise of gas slugs through magma-filled conduits (*1*–*5*). It is widely agreed that gas slugs form by coalescence of smaller bubbles at depth and keep sufficient overpressure

upon ascent to disrupt their skin and the upper magma column when they burst at the surface. However, both the depth at which slugs form and the mechanism of slug coalescence—be it differential bubble-rise rate in conduits (*2*, *3*) or bubble foam accumulation at structural discontinuities (*4*, *5*)—remain poorly constrained. Shallow source depths for strombolian explosions are estimated from associated seismic (*6*–*10*) and acoustic (*9*–*12*) signals, but whether these coincide with the slug source depth is unknown.

We provide quantitative constraints for the depth of slug genesis producing strombolian activity, based on spectroscopic measurements of the magmatic gas phase driving explosions at Stromboli volcano. Stromboli island, in the Aeolian archipelago, is the emerged upper part of a ~3-km-high stratovolcano erupting a volatile-rich high-potassium (HK) arc basalt (*13*–*15*). Its standard activity consists of quiescent magma degassing through crater vents located at 750 m above sea level and brief (10- to 15-s) explosions that, every 10 to 20 min, launch crystal-rich scoriae and lava blocks to 100- to 200-m height. According to geophysical signals (*6*–*8*, *11*, *12*), these periodic explosions originate at shallow depth (~250 m) below the vents. Although spectacular, they contribute little of the bulk volatile discharge, most of which is supplied by quiescent degassing (*16*, *17*). Episodically, the volcano also produces more powerful, deeper-derived explosions (*14*, *18*) that have no clear warning signal [apart from recent observations of precursory changes in gas composition (*19*)] and constitute a major hazard for the thousands of visitors and volcanologists alike. Therefore, improved understanding of the processes controlling the different types of explosions at Stromboli is also a high priority for civil defense.

Between mid-2000 and September 2002, we repeatedly measured the chemical composition of Stromboli magmatic gases between and during explosions, using open-path Fourier transform infrared (OP-FTIR) spectroscopy. With this remote sensing tool, recently used by volcanologists (*20*–*23*), magmatic gases issuing from the crater vents could be analyzed from a safe distance and with high temporal resolution (~4-s period). Here, we present and discuss one representative data set obtained on 9 April 2002, during 3.2 hours of passive and explosive degassing at the southwest vent that was most active at the time. Our spectrometer overlooked this vent from a slant distance of 240 m. We acquired double-sided interferograms, which we subsequently Fourier transformed, using the infrared radiation emitted from the hot crater floor and/or molten lava ejecta. The obtained FTIR absorption spectra allowed simultaneous retrieval of the path amounts (in molecules cm^{-2}) of major volcanic gas species (H_2O, CO_2, SO_2, and HCl) and minor volcanic gas species (CO and COS), with an accuracy ranging from ±4 to 6% for the purely volcanic species to, respectively, ±10% and 20 to 25% for CO_2 and H_2O, the amounts of which had to be corrected for air background (*22*). Details of the operating conditions and data retrieval procedures are given in (*24*).

The observed variations in radiating source temperature, volcanic gas amounts (Fig. 1), and derived molar gas compositions (Table 1) revealed the following features: (i) Quiescent gas release between the explosions has a well-defined, quite steady mean composition. It contains ~83 mol % of water vapor; it has mean CO_2/SO_2 and SO_2/HCl ratios of ~8 and 1.0 to 1.5, respectively; and according to its CO/CO_2 ratio, it last equilibrates at 630° to 760°C even though it was at close-to-ambient temperature (17° to 30°C) when measured. (ii) Each explosion is marked by sharp increases in the IR source temperature and the volcanic gas temperature and amounts. At the very onset of an explosion, the gas is as hot as the radiating ejecta (up to 970°C),

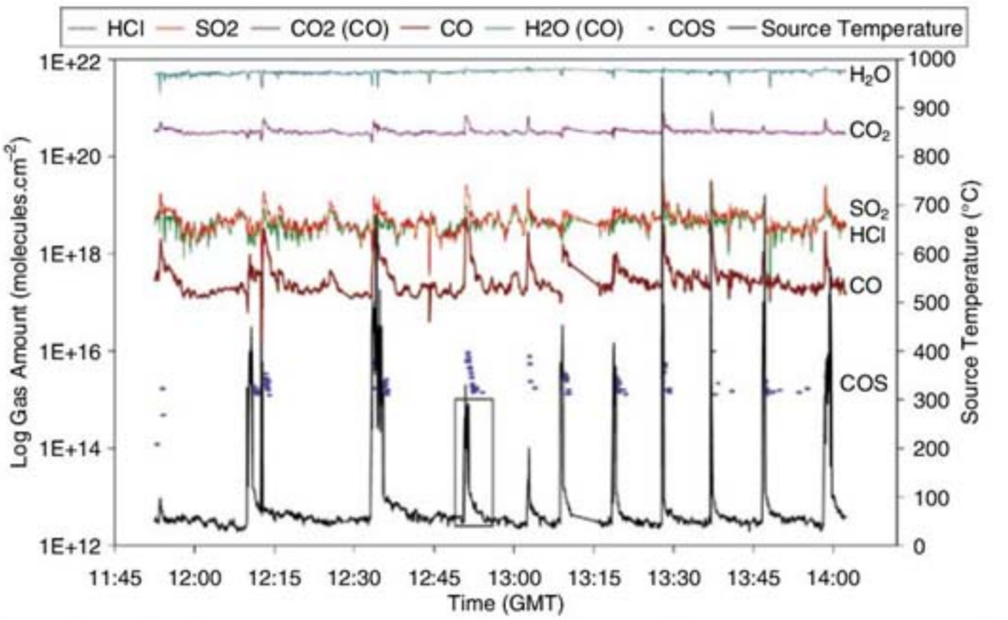

Fig. 1. Time series of volcanic gas amounts (molecules cm^{-2}) and radiating source temperature measured during quiescent and explosive degassing on Stromboli (9 April 2002). Quiescent emissions produce a background composition over which sharp bursts of gas, enriched in CO_2, SO_2, CO, and COS, are measured during explosions. These bursts coincide with peaks in radiation source temperature due to the ejection of molten lava clots. The third explosion, whose gas composition is reported in Table 1, is boxed and shown in greater detail in fig. S1.

Table 1. Molar gas compositions during quiescent and explosive crater degassing at Stromboli volcano, measured with OP-FTIR spectroscopy. "Typical explosion" shows the gas composition during the explosion shown in Fig. 2 and the average gas ratios (±1σ) for similar such explosions. "Smaller explosions" shows the average gas composition for smaller, CO_2-poorer explosions. The equilibrium gas temperatures (Equil. temp.) were computed from measured CO/CO_2 ratios and thermodynamic data for the reaction $2CO + O_2 = 2CO_2$, assuming ideal gas behavior and redox buffering by Stromboli basalt [$\log fO_2$ ~ NNO + 0.3 (*34*); NNO, nickel-nickel oxide buffer]. Source pressures were inferred from the modeled degassing of Stromboli basalt during decompression (Fig. 3). b.d., below detection limit.

Gas features	Quiescent degassing	Typical explosion	Smaller explosions
H_2O %	82.9	64.4	79.3
CO_2 %	13.6	33.1	19.0
SO_2 %	1.7	1.8	1.15
HCl %	1.7	0.33	0.43
CO %	0.03	0.44	0.15
COS %	b.d.	0.008	b.d.
H_2O/CO_2	6.1	2.3 ± 0.8	4.5 ± 2.3
CO_2/S	7.8	20.7 ± 2.1	16.8 ± 1.9
S/Cl	1.0–1.5	4.7 ± 0.8	2.5 ± 0.8
CO/SO_2 (10^{-2})	1.8	24.0 ± 0.9	14.6 ± 0.4
CO/CO_2 (10^{-2})	0.21	1.14 ± 0.09	0.9 ± 0.08
Equil. temp. (°C)	700	1020–1130	1000–1060
Source pressure (MPa)	≤0.3–4	~70–80	~20–50

[1]Istituto Nazionale di Geofisica e Vulcanologia, Catania, Italy. [2]Groupe des Sciences de la Terre, Laboratoire Pierre Süe, CNRS-CEA, Gif-sur-Yvette, France. [3]Dipartimento di Chimica e Fisica della Terra ed Applicazioni, Palermo University, Palermo, Italy.

*To whom correspondence should be addressed. E-mail: burton@ct.ingv.it

which prevents its analysis. Sudden expansion of the eruptive cloud produces an apparent drop in background gas amounts (Fig. 1), due to shorter beam path length. After a few seconds, however, the explosive gas phase rapidly cools through expansion and air dilution, whereas the radiation source (fresh lava clots on the crater floor) cools more slowly, providing a large temperature contrast and simple absorption spectra. Subtracting the background gas amount measured immediately before each explosion from the amount produced by the explosion allowed us to determine the chemical composition of the pure slug gas. Once cooled enough, the latter displays a stable composition (Fig. 2) that can be observed for a minute or so before the eruptive cloud gradually dissipates. We find that the slug gas markedly differs from the quiescent emissions: It is less hydrous, richer in CO_2, SO_2, CO, and COS, and its CO_2/SO_2, SO_2/HCl, and CO/CO_2 ratios are three to five times as high. Moreover, its computed equilibrium temperature (1000° to 1140°C) closely matches that of the molten basalt (Table 1). Therefore, the gas phase driving the explosions preserves the memory of hotter but also deeper source conditions, as shown by its enrichment in early exsolving volatile species such as CO_2.

Similar observations made for explosions at different periods suggest a reproducible source process. However, the explosions separated by "standard" repose intervals of ~15 to 20 min (such as the second to fifth peaks in Fig. 1) were generally found to display more reproducible and higher CO_2/SO_2, CO/SO_2, and SO_2/HCl ratios but a lower H_2O/CO_2 ratio than smaller explosions succeeding at shorter intervals (Table 1). Accordingly, the smaller explosions may have a more shallow origin, consistent with their higher frequency and lower energy, or they may be powered by smaller and hence slower slugs that suffer greater contamination by gas—present in the shallow conduit—that is poor in CO_2-S and richer in Cl-H_2O.

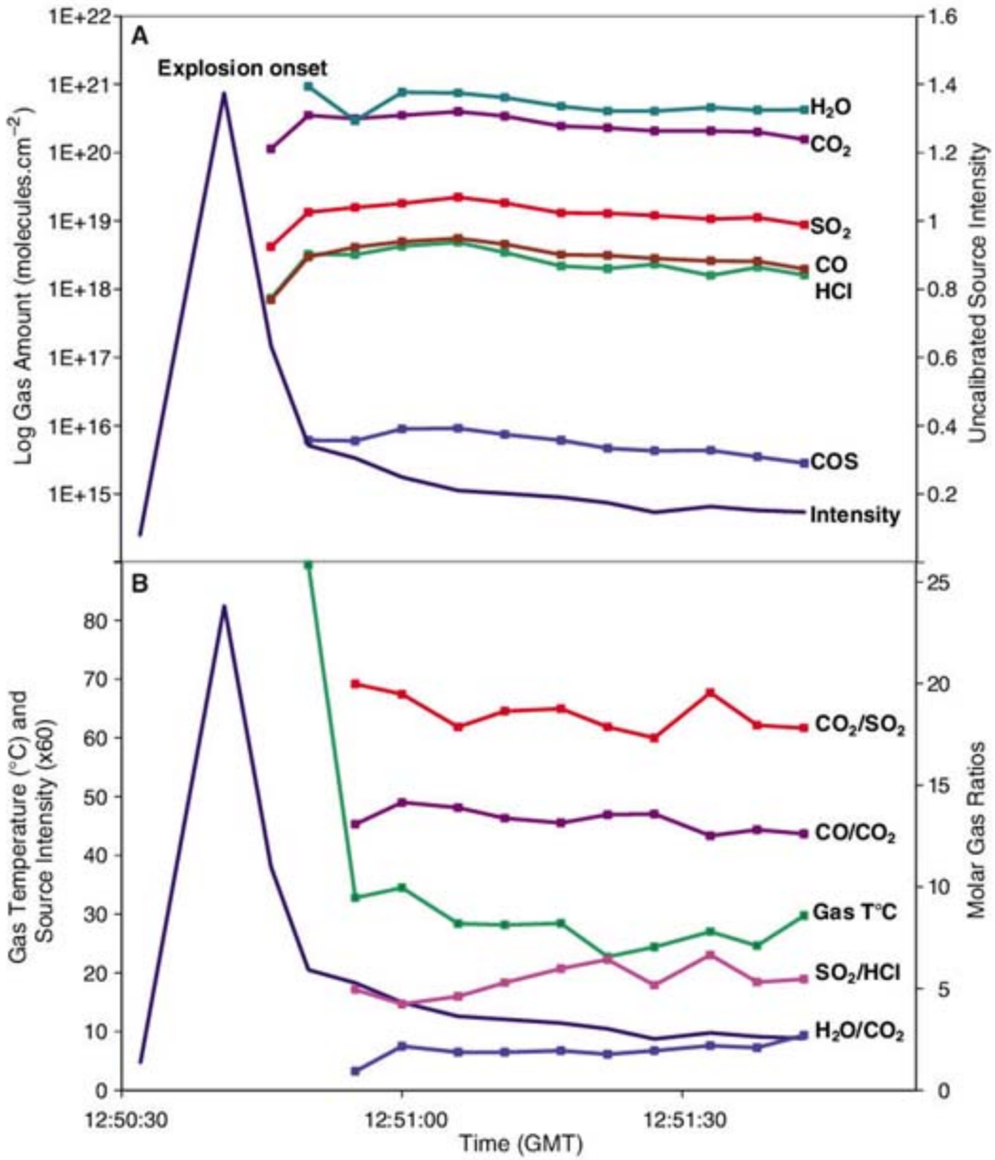

Fig. 2. (**A**) Gas amounts and (**B**) molar gas ratios of the pure slug phase driving one illustrative Strombolian explosion (which occurred at 12:50:41 GMT). At the explosion onset, marked by a peak in radiative intensity, the gas is as hot as the radiation source, preventing detection. As the gas cools, the thermal contrast between the radiation source (molten lava clots) and the gas increases until its stable composition is observed.

Melt inclusion studies of volatiles dissolved in Stromboli HK-basalt (*11*–*13*) provide the key information to interpret our results. Primitive inclusions of the basaltic melt entrapped in olivine at about 280 MPa (~10-km depth) contain on average 3.0 weight (wt) % H_2O, 0.12 wt % CO_2, and 0.17 wt % of S and Cl (*13*–*15*). At that pressure, the basalt already coexists with ~2.5 wt % of CO_2-rich gas formed by early exsolution of the abundant CO_2 contained in Stromboli parental magma (*25*). Starting from these data and using the VolatileCalc software (*26*), we computed the pressure-related evolution of H_2O and CO_2 in the melt and the gas phase during closed-system ascent and differentiation (tracked by K_2O) of the HK-basalt from 280 MPa to the surface. The amounts of S and Cl degassed during this process were then estimated from the best fit of their dissolved content with respect to H_2O and K_2O in melt inclusions (*13*–*15*). The main sources of uncertainty in our modeling arose from the sparse number of melt inclusions recording intermediate pressures and, to a lesser degree, from intrinsic limitations of VolatileCalc in simulating the degassing of water-rich basalt (*26*). Notwithstanding these issues, the modeled degassing trends reproduced fairly well both petrologic observations and the FTIR-measured gas compositions. Figure 3 shows the variations of H_2O/CO_2, CO_2/S, and S/Cl molar ratios in the equilibrium gas phase as a function of pressure between 100 and 0.1 MPa [S and Cl here refer to the exsolved amounts of bulk elemental sulfur and chlorine which, in surface emissions, predominantly occur as SO_2 and HCl, as shown here and in (*16*, *17*)].

We highlight two conclusions. (i) The chemical composition of quiescent emissions is well reproduced by complete degassing of the uprising basalt, with a transition from closed- to open-system conditions in the shallow volcanic conduits. This is consistent with a steady-state process of magma ascent, degassing, and convective overturn that contributes the bulk of the volcanic gas output (*16*, *17*). The emitted gas only diverges from the modeled composition in its higher water content and slightly lower S/Cl ratio (Table 1 and Fig. 3). We attribute these discrepancies to both spectroscopic interferences from low-temperature, water- and Cl-rich crater rim fumaroles (*27*, *28*) and probable entrainment of meteoric steam from the shallow hydrothermal system. (ii) The gas slugs driving Strombolian explosions cannot have a shallow origin. Instead, their measured compositions correspond to those achieved by the equilibrium gas phase under confining pressures of ~70 to 80 MPa (most energetic explosions) to ~20 MPa (smallest explosions). To preserve these compositions at the surface, the slugs must then rise separately from the magma from depths between ~2.7 and

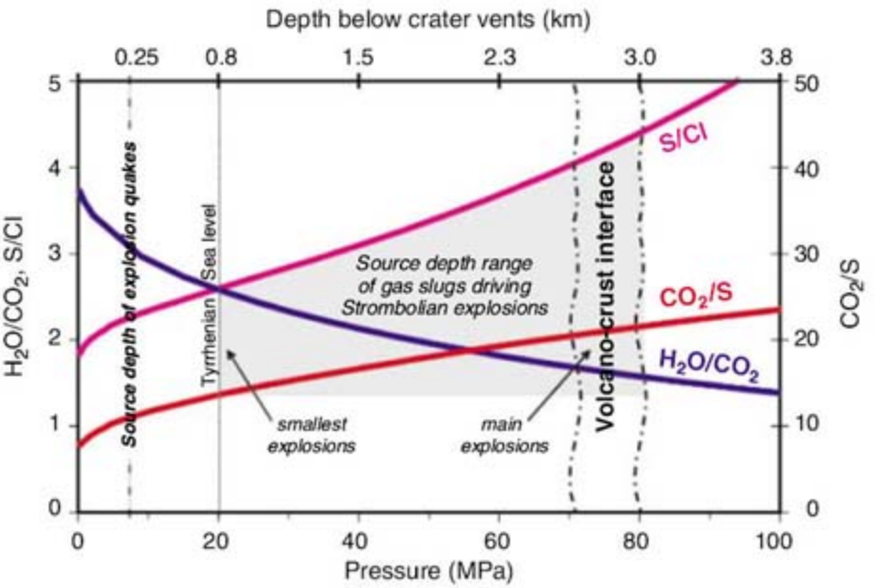

Fig. 3. Pressure-related modeled evolution of H_2O/CO_2, CO_2/S, and S/Cl molar ratios in the magmatic gas phase during closed-system ascent, differentiation, and degassing of Stromboli HK-basalt (100 to 0.1 MPa) and inferred source depths of gas slugs driving Strombolian explosions. Gas modeling was performed using (i) the chemistry and dissolved volatile content of olivine-hosted melt inclusions representative of the primitive and evolved basalt (*13*–*15*); (ii) the original CO_2 content of Stromboli parental magma (*25*); and (iii) VolatileCalc software (*26*). The VolatileCalc software was used to compute the step-by-step evolution of H_2O and CO_2 in the melt and the gas phase from initial boundary conditions of P = 280 MPa, T = 1140°C, and melt SiO_2 = 48.5 wt %. Partial sulfur exsolution during genesis of Stromboli HK-basalt (*13*) has been taken into account. The measured CO_2/S and S/Cl ratios of gas slugs driving Strombolian explosions require their separate ascent from pressures of ~80 to 70 MPa to 20 MPa, or ~3- to 0.8-km depth below the vents (i.e., from between the volcano-crust interface and the Tyrrhenian Sea level). This is much deeper than the source depth (~250 m) of explosion quakes (*6*–*8*). H_2O/CO_2 ratios suggest somewhat lower but more uncertain source depths, owing to larger analytical uncertainty on emitted H_2O and probable entrainment of hydrothermal meteoric steam during shallow slug ascent.

0.8 km below the vents (for a rock density of 2700 kg m^{-3})—that is, from between about the base of the volcanic pile and the Tyrrhenian Sea level (Fig. 3). In that depth interval, the melt vesicularity increases rapidly from ~0.35 to ~0.7, promoting a transition from closed- to open-system degassing (*29*). At the volcano-crust interface, slug genesis could thus result either from bubble accumulation and foam growth at structural discontinuities (*4*, *5*) or from the coalescence of bubbles with different sizes and rise speeds (*2*, *3*). Discriminating between these two processes is challenging, even though the former should be favored by increased flow rate of gas-rich magma and could thus explain increases in tremor (*30*), explosion-quake frequency, and gas flux (*31*) that are observed during periods of elevated activity. Increasing magma permeability in the shallow volcanic conduits would rather inhibit slug coalescence. Therefore, unless another geometrical discontinuity exists at ~1 km below the vents, the most shallow gas compositions associated with the weakest explosions may reflect greater incorporation of shallow bubbles into slowly rising, smaller slugs, which formed at the volcano-crust interface.

We demonstrate here that Stromboli's recurrent explosions have much deeper roots than previously inferred from geophysical data (*6*–*8*, *11*, *12*). The shallow (~250-m) source depth of explosion quakes and associated acoustic signals do not signify a shallow origin of the rising gas slugs. Instead, these signals are the result of a permanent structural discontinuity at the base of the upper conduits, where deeper-derived gas slugs undergo an abrupt flow-pattern change (*32*) before bursting at the surface. This conclusion is supported by the unchanged source location of explosion quakes during the 2002-2003 lava flow eruption (*31*), despite lateral drainage of the upper magma column. We thus reveal a strong decoupling between geophysical signals of the explosions, controlled by structural discontinuity, and the true process of slug genesis. Such an observation may apply to several other volcanoes (such as Villarica, Erebus, Masaya, Yasur, and Arenal) displaying comparable persistent explosive activity, depending on their magma volatile content and the geometry of their plumbing system. Recent FTIR measurements on Yasur (*23*) detected weak CO_2 enrichment of gas driving explosions, but the lack of constraints from seismic or petrological data prevented quantitative assessment of the slug source depth. Improved understanding of the mechanisms controlling strombolian explosive activity clearly requires multidisciplinary investigations. As shown here, spectroscopic measurement of the driving magmatic gas phases is a powerful tool in such studies.

References and Notes

1. R. S. J. Sparks, *J. Volcanol. Geotherm. Res.* **3**, 1 (1978).
2. L. Wilson, J. W. Head III, *J. Geophys. Res.* **86**, 2971 (1981).
3. E. A. Parfitt, *J. Volcanol. Geotherm. Res.* **134**, 77 (2004).
4. C. Jaupart, S. Vergniolle, *Nature* **331**, 58 (1988).
5. C. Jaupart, S. Vergniolle, *J. Fluid Mech.* **203**, 347 (1989).
6. B. Chouet *et al.*, *J. Geophys. Res.* **102**, 15129 (1997).
7. B. Chouet *et al.*, *J. Geophys. Res.* **108**, 2019 (2003).
8. M. Ripepe, S. Diliberto, M. D. Schiava, *J. Geophys. Res.* **106**, 8713 (2001).
9. C. A. Rowe, R. C. Aster, P. R. Kyle, R. R. Dibble, J. W. Schlue, *J. Volcanol. Geotherm. Res.* **101**, 105 (2000).
10. M. T. Hagerty, M. Protti, S. Y. Schwartz, M. A. Garces, *J. Volcanol. Geotherm. Res.* **101**, 27 (2000).
11. S. Vergniolle, G. Brandeis, J.-C. Marechal, *J. Geophys. Res.* **101**, 20449 (1996).
12. M. Ripepe, A. J. L. Harris, R. Carniel, *J. Volcanol. Geotherm. Res.* **118**, 285 (2002).
13. N. Métrich, A. Bertagnini, P. Landi, M. Rosi, *J. Petrol.* **42**, 1471 (2001).
14. A. Bertagnini, N. Métrich, P. Landi, M. Rosi, *J. Geophys. Res.* **108**, 2336 (2003).
15. P. Landi, N. Métrich, A. Bertagnini, M. Rosi, *Contrib. Mineral. Petrol.* **147**, 213 (2004).
16. P. Allard, J. Carbonnelle, N. Métrich, H. Loyer, P. Zettwoog, *Nature* **368**, 326 (1994).
17. P. Allard *et al.*, *Geophys. Res. Lett.* **27**, 1207 (2000).
18. F. Barberi, M. Rosi, A. Sodi, *Acta Vulcanol.* **3**, 173 (1993).
19. A. Aiuppa, C. Federico, *Geophys. Res. Lett.* **31**, L14607 (2004).
20. T. Mori *et al.*, *Earth Plan. Sci. Lett.* **134**, 219 (1995).
21. P. W. Francis, M. Burton, C. Oppenheimer, *Nature* **396**, 567 (1998).
22. P. Allard, M. Burton, F. Muré, *Nature* **433**, 407 (2005).
23. C. Oppenheimer, P. Bani, J. Calkins, M. Burton, G. M. Sawyer, *Appl. Phys. B* **85**, 453 (2006).
24. Data were collected with a Bruker OPAG-22 FTIR spectrometer, working at 0.5 cm^{-1} resolution. Single-scan, double-sided interferograms were collected every ~4 s and were Fourier transformed offline with the use of Norton-Beer medium apodization. Spectral analysis was performed with a nonlinear least-squares fitting program and an adapted forward model based around the Reference Forward Model (*33*). The different physical conditions of atmospheric and volcanic gases were taken in account using a two-layer atmospheric model. Volcanic gas temperature was retrieved by fitting this parameter during analysis of the SO_2 $\nu_1 + \nu_3$ combination band at 2500 cm^{-1}, whose rotational line envelope is highly temperature dependent. Source temperatures were determined from the ratio of the observed signal at 4400 and 4460 cm^{-1} and fitting to a Planck curve. Quiescent degassing compositions between the explosions were determined with the use of linear fits to correlation plots of volcanic gas amounts.
25. P. Allard, abstract GMPV7-8044, presented at the European Geophysical Union General Assembly, Vienna, Austria, 16 to 20 April 2007.
26. S. Newman, J. B. Lowenstern, *Comput. Geosci.* **28**, 597 (2002).
27. M. Chaigneau, *C. R. Acad. Sci. Paris* **261**, 2241 (1965).
28. M. L. Carapezza, C. Federico, *J. Volcanol. Geotherm. Res.* **95**, 227 (2000).
29. M. Burton, H. Mader, M. Polacci, P. Allard, *Eos* **86** (Fall Meeting Suppl.), 52 (abstr. V13G-01) (2005).
30. H. Langer, S. Falsaperla, *Pure Appl. Geophys.* **147**, 57 (1996).
31. M. Ripepe *et al.*, *Geology* **33**, 273 (2005).
32. M. R. James, S. J. Lane, B. A. Chouet, *J. Geophys. Res.* **111**, B05201 (2006).
33. A. Dudhia, University of Oxford, www.atm.ox.ac.uk/RFM.
34. N. Métrich, R. Clocchiatti, *Geochim. Cosmochim. Acta* **60**, 4151 (1996).

35. We gratefully acknowledge the Dipartimento di Protezione Civile of Italy for helicopter support that proved essential for OP-FTIR measurements on Stromboli and for support via project V2: Stromboli. We thank A. Bonaccorso, S. Calvari, and E. Boschi for their continuous support and N. Métrich (LPS, Saclay, France) for helpful discussions on melt inclusion data.

Supporting Online Material

www.sciencemag.org/cgi/content/full/317/5835/227/DC1
Fig. S1

28 February 2007; accepted 16 May 2007
10.1126/science.1141900

Remnants of the Early Solar System Water Enriched in Heavy Oxygen Isotopes

Naoya Sakamoto,[1] Yusuke Seto,[1] Shoichi Itoh,[1] Kiyoshi Kuramoto,[2] Kiyoshi Fujino,[1] Kazuhide Nagashima,[3] Alexander N. Krot,[3] Hisayoshi Yurimoto[1,4]*

Oxygen isotopic composition of our solar system is believed to have resulted from mixing of two isotopically distinct nebular reservoirs, ^{16}O-rich and ^{17,18}O-rich relative to Earth. The nature and composition of the ^{17,18}O-rich reservoir are poorly constrained. We report an in situ discovery of a chemically and isotopically unique material distributed ubiquitously in fine-grained matrix of a primitive carbonaceous chondrite Acfer 094. This material formed by oxidation of Fe,Ni-metal and sulfides by water either in the solar nebula or on a planetesimal. Oxygen isotopic composition of this material indicates that the water was highly enriched in ^{17}O and ^{18}O ($\delta^{17,18}O_{SMOW}$ = +180‰ per mil), providing the first evidence for an extremely ^{17,18}O-rich reservoir in the early solar system.

Oxygen isotopic variations in chondrites provide important constraints on the origin and early evolution of the solar system (*1*). Oxygen isotope ratios in chondrites change not only by mass-dependent isotope fractionation law (isotope fractionation depending on mass differences among isotopes) but also by large mass-independent isotope fractionation (MIF) that keeps $^{17}O/^{18}O$ ratio nearly constant. It is generally accepted that MIF recorded by meteorites resulted from mixing of two isotopically distinct nebular reservoirs, ^{16}O-rich and ^{17,18}O-rich (*2*). The composition of the ^{16}O-rich reservoir has been recently constrained from isotopic compositions of nebular condensates (*3*) and of a unique chondrule (*4*). The nature and composition of an ^{17,18}O-rich nebular reservoir are still poorly constrained (*5*, *6*). According to the currently favorite self-shielding models (*7*–*11*), nebular water is hypothesized to have been highly enriched in ^{17,18}O (5 to 20%) relative to Earth, which is, however, yet to be verified by isotope measurements. Here we report an in situ discovery of a chemically and isotopically unique material in the primitive carbonaceous chondrite Acfer 094. This material is mainly composed of iron, oxygen, and sulfur, and is highly enriched in ^{17}O and ^{18}O (up to +18%) relative to Earth's ocean. Mineralogical observations and thermodynamic analysis suggest that this material resulted from oxidation of iron metal and/or iron sulfide by water in the solar nebula or on a planetesimal. We infer that the extreme oxygen isotopic composition of this material recorded composition of this primordial water that corresponds to an ^{17,18}O-rich nebular reservoir in the early solar system, in agreement with the self-shielding models (*7*–*12*).

During our ongoing in situ survey (*13*–*16*) of presolar grains of primitive meteorites (*17*), we discovered isotopically anomalous regions of oxygen in matrix of the ungrouped carbonaceous chondrite Acfer 094 in addition to isotopically anomalous spots corresponding to presolar grains (Fig. 1). The oxygen isotopic compositions of the regions are uniform and enriched in ^{17}O and ^{18}O relative to ^{16}O (Fig. 2). The data seem to be plotted along the slope-1 line (*18*) rather than the carbonaceous chondrite anhydrous mineral mixing (CCAM) line (*2*) (Fig. 3). The representative values of $\delta^{17}O_{SMOW} = \delta^{18}O_{SMOW}$ are about +180 per mil (‰); SMOW is standard mean ocean water (*19*). These are the heaviest oxygen isotopic compositions of the solar system materials reported so far. The less ^{17}O- and ^{18}O-rich compositions ($\delta^{17,18}O_{SMOW}$ = +50‰) of unknown origin have been recently reported in the surface layers of metal grains from lunar regolith (*20*).

The chemical compositions of the isotopically anomalous regions determined by an energy-dispersive x-ray spectrometer (EDS) attached to a field-emission scanning electron microscope (FE-SEM) (*16*) show that they are homogeneous and mainly composed of Fe, Ni, O and S (representatively, in weight percent, Fe, 61.6; Ni, 5.4; O, 19.3; S, 9.6; Mg, 0.1; Si, 0.2). In addition, analytical transmission electron microscopy (ATEM) (*16*) reveals that the regions consist of aggregates of nanocrystals with a size range of 10 to 200 nm (fig. S1). The electron diffraction patterns from ~100-nm-sized individual crystals show that the main spots of the crystals are similar to those of magnetite (Fe_3O_4; space group *Fd3m*); the corresponding cell parameter *a* is 0.83 nm. In addition, there are weak extra spots suggesting a threefold superstructure. Characteristic x-ray spectra from individual crystals show that they consist of the same elements determined by the FE-SEM-EDS study. These observations indicate that the crystals have a magnetite-like structure and may represent a new Fe-O-S–bearing mineral; more detailed characterization is necessary to identify it. Although this mineral consists of the same elements as a poorly characterized phase (PCP) commonly observed in aqueously altered CM chondrites and largely composed of tochilinite or tochilinite-cronstedtite intergrowths (*21*, *22*), its O/S atom ratios are about 4 times as large as those in tochilinite. Hereafter, we refer to this mineral as a new-PCP.

The chemically unique and isotopically anomalous new-PCPs are ubiquitous and scattered randomly throughout the Acfer 094 matrix. Twenty-two new-PCPs (the largest is 160 μm^2) were identified in about an 11-mm^2 area of the matrix using elemental mapping with a 7-μm^2 spatial resolution. This corresponds to 94 ± 20 (σ) parts per million (ppm) by volume. Because the number of the new-PCP grains increases exponentially with decreasing size, the grain numbers below 7 μm^2 are dominant and the actual abundance of new-PCP must be larger than the estimate.

The new-PCP often coexists with troilite (FeS) (Fig. 2), which is considered to be a reaction product between Fe, Ni-metal and H_2S gas (*23*, *24*).

$$Fe + H_2S = FeS + H_2 \qquad (1)$$

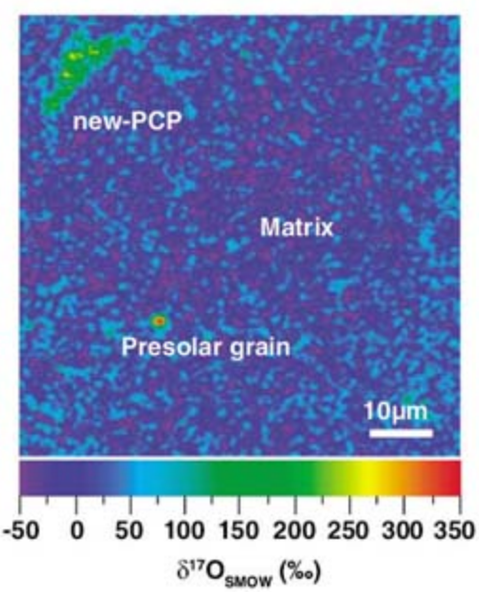

Fig. 1. Spatial distribution of $^{17}O/^{16}O$ in matrix of the ungrouped carbonaceous chondrite Acfer 094 measured with isotopography (*16*). An isotopically anomalous 10 μm-sized region ($\delta^{17}O_{SMOW}$ = +180‰) and a spot ($\delta^{17}O_{SMOW}$ = +400‰) are surrounded by the isotopically normal matrix materials. The spot corresponds to a presolar silicate grain, whereas the isotopically anomalous region corresponds to a new-PCP.

[1]Department of Natural History Sciences, Hokkaido University, Sapporo 060-0810, Japan. [2]Department of Cosmosciences, Hokkaido University, Sapporo 060-0810, Japan. [3]Hawai'i Institute of Geophysics and Planetology, School of Ocean and Earth Science and Technology, University of Hawai'i at Manoa, Honolulu, HI 96822, USA. [4]Isotope Imaging Laboratory, Creative Research Initiative "Sousei," Hokkaido University, Sapporo, 001-0021, Japan.

*To whom correspondence should be addressed. E-mail: yuri@ep.sci.hokudai.ac.jp

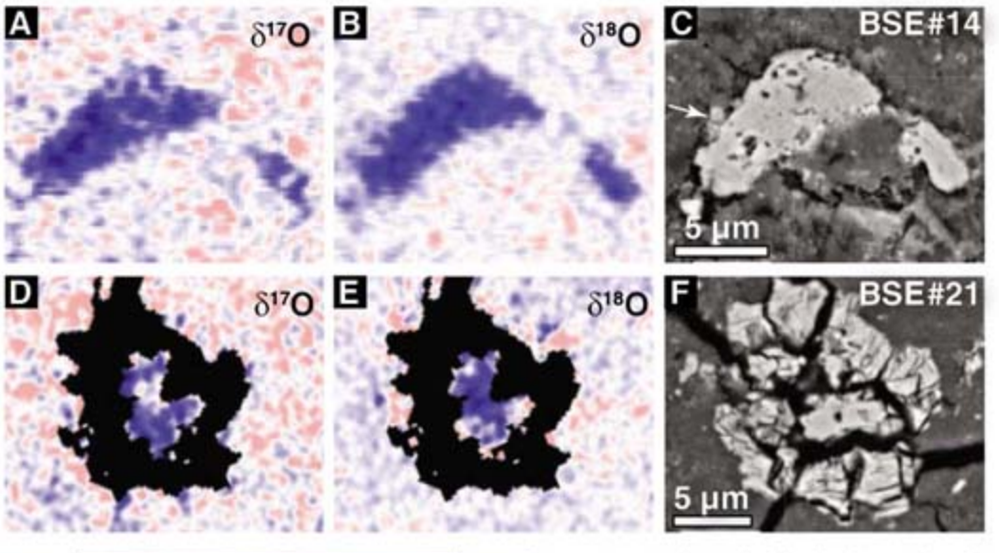

Fig. 2. Oxygen isotopic distribution and grain shape for new-PCP embedded in chondrite matrix. $\delta^{17}O_{SMOW}$ (**A** and **D**), $\delta^{18}O_{SMOW}$ (**B** and **E**), and backscattered electron (**C** and **F**) images for new-PCP #14 [(A) to (C)] and #21 [(D) to (F)] in the Acfer 094 matrix. Arrow in (A) indicates small troilite grains attached to the new-PCP #14. The new-PCP #21 is surrounded by troilite. Because troilite contains no oxygen, the troilite area in (D) and (E) is masked by black color. The new-PCPs are highly enriched in ^{17}O and ^{18}O isotopes relative to the matrix.

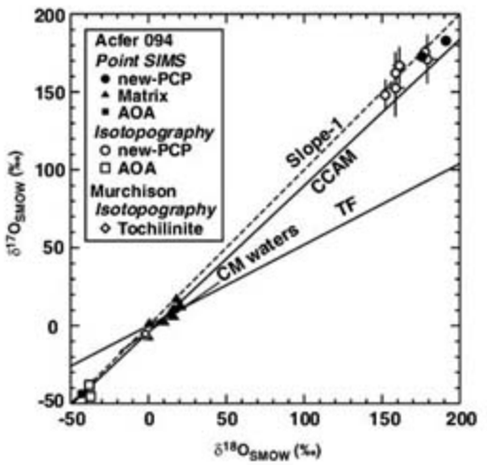

Fig. 3. Oxygen isotopic compositions of the new-PCP from the Acfer 094 matrix. Oxygen isotopic compositions of matrix and amoeboid olivine aggregate (AOA) from Acfer 094 and tochilinite from Murchison are also plotted. The new-PCPs are plotted on extrapolation of slope-1 line or carbonaceous chondrite anhydrous mineral mixing (CCAM) line. The compositions of the Murchison tochilinite are plotted near the terrestrial fractionation (TF) line, along an aqueous alternation line [CM waters (*26*)]. Isotopography: analyzed by precise isotopic imaging with an isotope microscope (*16*). Point SIMS: analyzed by conventional point analysis by secondary ion mass spectrometry (*16*). The data are listed in table S1.

Because new-PCP has magnetite-like diffraction patterns, magnetite can be used as its proxy. Magnetite can be formed by oxidation of Fe, Ni-metal (*23*, *25*), or troilite.

$$3Fe + 4H_2O = Fe_3O_4 + 4H_2 \quad (2)$$

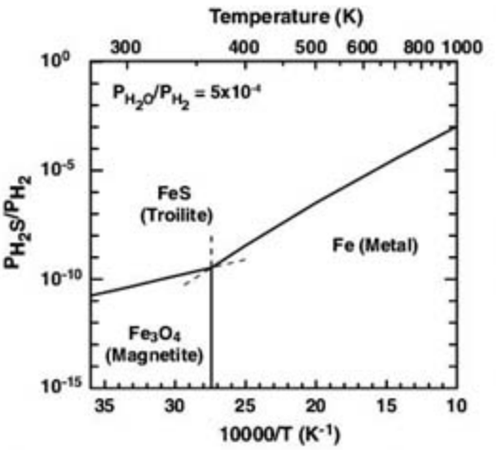

Fig. 4. Calculated equilibrium temperatures for Fe-metal, troilite (FeS) and magnetite (Fe_3O_4) as a function of P_{H2S}/P_{H2} ratio. The magnetite phase boundary is calculated assuming canonical solar nebular H_2O/H_2 ratio of 5×10^{-4} (*30*). Magnetite is considered as a proxy of a new-PCP. Thermodynamic data from JANAF tables (*31*) were used for calculations.

$$3FeS + 4H_2O = Fe_3O_4 + 3H_2S + H_2 \quad (3)$$

Oxidation of troilite or metal to form new-PCP would occur below 360 K, independent of total pressure of the solar nebula (Fig. 4). If the nebular P_{H2O}/P_{H2} ratio increases from a characteristic value for a gas of solar composition (*25*), formation of new-PCP occurs at higher temperature. Although the complete chemical equilibrium would not be expected in the cool solar nebula (*23*), the new-PCP would be formed inside the water sublimation front (snowline) of the solar nebula, because water vapor is the major oxidant in the solar nebula and the sublimation temperature of water ice is below 200K even in the several-fold H_2O-enriched nebula (*23*).

Alternatively, new-PCP may have been formed by aqueous alteration of metal and troilite on the Acfer 094 parent body, like tochilinite in the aqueously altered CM chondrites (*22*). To test this hypothesis, we analyzed oxygen isotopic compositions of tochilinite in the CM chondrite Murchison. In contrast to the Acfer 094 new-PCP, oxygen isotopic composition of the Murchison tochilinite is plotted near the terrestrial fractionation line, along the "CM waters" line (*26*) (Fig. 3), that is considered to be a reaction path between aqueous solution and matrix silicates toward the isotope equilibrium (*26*). These observations and the lack of mineralogical and petrographical evidence of aqueous alteration of Acfer 094 (*27*) exclude formation of new-PCP by the aqueous alteration previously observed in chondrites. If new-PCP resulted from oxidation of troilite or metal in a planetesimal setting, a plausible oxidant would be water vapor or aqueous solution that originated from accreted nebular ice and did not experience oxygen isotope exchange with the matrix silicates. In contrast, the inferred oxygen isotopic compositions (*26*, *28*) and the observed chondrite parent body water composition richest in $^{17,18}O$ (*29*) may have recorded equilibration of aqueous solutions with the chondrite matrix silicates.

We conclude that oxygen isotopic compositions of new-PCP in Acfer 094 represent composition of the primordial water of the solar system and the previously hypothesized ^{17}O- and ^{18}O-rich reservoir in the early solar system. The wide oxygen isotopic variations of at least $-80‰ < \delta^{17,18}O < +180‰$ found from hot and cold origin materials must provide new guidelines for the origin of oxygen isotope anomalies in the solar system.

References and Notes

1. R. N. Clayton, *Science* **313**, 1743 (2006).
2. R. N. Clayton, *Annu. Rev. Earth Planet. Sci.* **21**, 115 (1993).
3. A. N. Krot, K. D. McKeegan, L. A. Leshin, G. J. MacPherson, E. R. D. Scott, *Science* **295**, 1051 (2002).
4. S. Kobayashi, H. Imai, H. Yurimoto, *Geochem. J.* **37**, 663 (2003).
5. H. Yurimoto, M. Ito, H. Nagasawa, *Science* **282**, 1874 (1998).
6. A. N. Krot *et al.*, *Astrophys. J.* **622**, 1333 (2005).
7. R. N. Clayton, *Nature* **415**, 860 (2002).
8. H. Yurimoto, K. Kuramoto, *Meteorit. Planet. Sci.* **37**, A153 (2002).
9. H. Yurimoto, K. Kuramoto, *Science* **305**, 1763 (2004).
10. J. R. Lyons, E. D. Young, *Nature* **435**, 317 (2005).
11. H. Yurimoto *et al.*, in *Protostars and Planets V*, B. Reipurth, D. Jewitt, K. Keil, Eds. (Univ. of Arizona Press, Tucson, AZ, 2007) pp. 849–862.
12. E. D. Young, *Lunar Planet. Sci.* **XXXVII**, abstr. no. 1790 (2006).
13. H. Yurimoto, K. Nagashima, T. Kunihiro, *Appl. Surf. Sci.* **203-204**, 793 (2003).
14. S. Itoh, H. Yurimoto, *Nature* **423**, 728 (2003).

15. T. Kunihiro, K. Nagashima, H. Yurimoto, *Geochim. Cosmochim. Acta* **69**, 763 (2005).
16. Materials and methods are available as supporting material on *Science* Online.
17. K. Nagashima, A. N. Krot, H. Yurimoto, *Nature* **428**, 921 (2004).
18. E. D. Young, S. S. Russell, *Science* **282**, 452 (1998).
19. $\delta^{i}O_{SMOW}$ (‰) = $[(^{i}O/^{16}O)_{sample}/(^{i}O/^{16}O)_{SMOW} - 1] \times 1000$, where $i = 17$ or 18.
20. T. R. Ireland, P. Holden, M. D. Norman, J. Clarke, *Nature* **440**, 776 (2006).
21. L. H. Fuchs, E. Olsen, K. J. Jensen, *Smithson. Contrib. Earth Sci.* **10**, 1 (1973).
22. K. Tomeoka, P. R. Buseck, *Geochim. Cosmochim. Acta* **49**, 2149 (1985).
23. B. Fegley Jr., *Space Sci. Rev.* **92**, 177 (2000).
24. D. S. Lauretta, D. T. Kremser, B. Fegley Jr., *Icarus* **122**, 288 (1996).
25. Y. Hong, B. Fegley Jr., *Meteorit. Planet. Sci.* **33**, 1101 (1997).
26. R. N. Clayton, T. K. Mayeda, *Geochim. Cosmochim. Acta* **63**, 2089 (1999).
27. A. Greshake, *Geochim. Cosmochim. Acta* **61**, 437 (1997).
28. E. D. Young, *Philos. Trans. R. Soc. London A* **359**, 2095 (2001).
29. B.-G. Choi, K. D. McKeegan, A. N. Krot, J. T. Wasson, *Nature* **392**, 577 (1998).
30. A. N. Krot, B. Fegley Jr., K. Lodders, H. Palme, in *Protostars and Planets IV*, V. Mannings, A. P. Boss, S. S. Russell, Eds. (Univ. of Arizona Press, Tucson, AZ, 2000) pp. 1019–1054.
31. J. M. W. Chase, *NIST-JANAF Thermochemical Tables, Fourth edition, Journal of Physical and Chemical Reference Data, Monograph 9, Parts I and II* (American Institute of Physics, New York, 1998).

32. We thank Y. Matsuhisa for providing a magnetite standard, T. Kaito and I. Nakatani for assistance with focused ion beam sample preparation, K. Tomeoka for indicating Murchison tochilinite, and E. D. Scott and G. R. Huss for discussion. This work was partly supported by Monkasho (H.Y.) and NASA (A.N.K.).

Supporting Online Material

www.sciencemag.org/cgi/content/full/1142021/DC1
Materials and Methods
Fig. S1
Tables S1 and S2
References

2 March 2007; accepted 17 May 2007
Published online 14 June 2007;
10.1126/science.1142021
Include this information when citing this paper.

How Much More Rain Will Global Warming Bring?

Frank J. Wentz,* Lucrezia Ricciardulli, Kyle Hilburn, Carl Mears

Climate models and satellite observations both indicate that the total amount of water in the atmosphere will increase at a rate of 7% per kelvin of surface warming. However, the climate models predict that global precipitation will increase at a much slower rate of 1 to 3% per kelvin. A recent analysis of satellite observations does not support this prediction of a muted response of precipitation to global warming. Rather, the observations suggest that precipitation and total atmospheric water have increased at about the same rate over the past two decades.

In addition to warming Earth's surface and lower troposphere, the increase in greenhouse gas (GHG) concentrations is likely to alter the planet's hydrologic cycle (*1*–*3*). If the changes in the intensity and spatial distribution of rainfall are substantial, they may pose one of the most serious risks associated with climate change. The response of the hydrologic cycle to global warming depends to a large degree on the way in which the enhanced GHGs alter the radiation balance in the troposphere. As GHG concentrations increase, the climate models predict an enhanced radiative cooling that is balanced by an increase in latent heat from precipitation (*1*, *2*). The Coupled Model Intercomparison Project (*4*) and similar modeling analyses (*1*–*3*) predict a relatively small increase in precipitation (and likewise in evaporation) at a rate of about 1 to 3% K^{-1} of surface warming. In contrast, both climate models and observations indicate that the total water vapor in the atmosphere increases by about 7% K^{-1} (*1*–*3*, *5*, *6*).

More than 99% of the total moisture in the atmosphere is in the form of water vapor. The large increase in water is due to the warmer air being able to hold more water vapor, as dictated by the Clausius-Clapeyron (C-C) relation under the condition that the relative humidity in the lower troposphere stays constant. So according to the current set of global coupled ocean-atmosphere models (GCMs), the rate of increase in precipitation will be several times lower than that for total water. This apparent inconsistency is resolved in the models by a reduction in the vapor mass flux, particularly with respect to the Walker circulation, which reinforces the trade winds (*3*, *7*). Whether a decrease in global winds is a necessary consequence of global warming is a complex question that is yet to be resolved (*8*).

Using satellite observations from the Special Sensor Microwave Imager (SSM/I), we assessed the GCMs' prediction of a muted response of rainfall and evaporation to global warming. The SSM/I is well suited for studying the global hydrologic cycle in that it simultaneously measures precipitation (P), total water vapor (V), and also surface-wind stress (τ_0), which is the principal term in the computation of evaporation (E) (*8*, *9*).

The SSM/I data set extends from 1987 to 2006. During this time Earth's surface temperature warmed by 0.19 ± 0.04 K decade^{-1}, according to the Global Historical Climatology Network (*10*, *11*). Satellite measurements of the lower troposphere show a similar warming of 0.20 ± 0.10 K decade^{-1} (*12*). The error bars are at the 95% confidence level. This warming is consistent with 20th-century climate-model runs (*13*) and provides a reasonable, albeit short, test bed for assessing the impact of global warming on the hydrologic cycle.

When averaged globally over monthly time scales, P and E must balance except for a negligibly small storage term. This $E = P$ constraint provides a useful consistency check with which to evaluate our results. However, the constraint is valid only for global averages. Accordingly, the first step in our analysis was to construct global monthly maps of P and E at a 2.5° spatial resolution for the period 1987 to 2006.

The SSM/I retrievals used here are available only over the ocean. To supplement the SSM/I over-ocean rain retrievals, we used the land values from the Global Precipitation Climatology Project data set, which is a blend of satellite retrievals and rain gauge measurements (*14*, *15*). Satellite rain retrievals over land were less accurate than their ocean counterparts, but this drawback was compensated by the fact that there are abundant rain gauges over land for constraining the satellite retrievals. Likewise, global evaporation was computed separately for oceans and land. Because 86% of the world's evaporation comes from the oceans (*16*), ocean evaporation was our primary focus. We computed evaporation over the oceans with the use of the bulk formula from the National Center for Atmospheric Research Community Atmospheric Model 3.0 (*8*, *17*). Evaporation over land cannot be derived from satellite observations, and we resorted to using a constant value of 527 mm year^{-1} for all of the continents, excluding Antarctica (*16*). For Antarctica and sea ice, we used a value of 28 mm year^{-1} (*8*, *16*).

The GCMs indicate that E should increase about 1 to 3% K^{-1} of surface warming. However, according to the bulk formula (eq. S1) (*8*), evaporation increases similarly to C-C as the surface temperature warms, assuming that the other terms remain constant. For example, a global increase of 1 K in the surface air temperature produces a 5.7% increase in E (*8*). To obtain the muted response of 1 to 3% K^{-1}, other variables in the bulk formula need to change with time. The air-sea temperature difference and the near-surface relative humidity are expected to remain nearly constant (*8*), and this leaves τ_0 as the one variable that can reduce evaporation to the magnitude required to balance the radiation budget in the models. To bring the bulk formula into agreement with the radiative cooling constraint, $\sqrt{\tau_0}$

Remote Sensing Systems, 438 First Street, Santa Rosa, CA 95401, USA.

*To whom correspondence should be addressed. E-mail: frank.wentz@remss.com

would need to decrease by about 4% K^{-1}. Thus, a muted response of precipitation to global warming requires a decrease in global winds (*2*, *3*, *7*).

To evaluate the GCMs' prediction of a decrease in winds, we looked at the 19 years of SSM/I wind retrievals. These winds are expressed in terms of an equivalent neutral-stability wind speed (W) at a 10-m elevation, which is proportional to $\sqrt{\tau_0}$ (*8*, *16*). Figure 1 shows a decadal trend map of W. For each 2.5° grid cell, a least-squares linear fit to the 19-year time series was calculated after removing the seasonal variability. The wind trends from the International Comprehensive Ocean-Atmosphere Data Set (ICOADS) are also shown, but just for comparison. They were not used in our analysis. Although the ICOADS trend map is very noisy because of sampling and measurement deficiencies, it shows trends similar to those from the SSM/I in the northern Atlantic and Pacific, where the ICOADS ship observations are more abundant. The North Atlantic Oscillation (NAO) is apparent in both trend maps as a tripole feature with increasing winds between 30°N and 40°N and decreasing winds to the north and south (*18*). This feature is consistent with the observed decrease in the NAO index since 1987. When averaged over the tropics from 30°S to 30°N, the winds increased by 0.04 m s^{-1} (0.6%) $decade^{-1}$, and over all oceans the increase was 0.08 m s^{-1} (1.0%) $decade^{-1}$. The SSM/I wind retrievals were validated by comparisons with moored ocean buoys and satellite scatterometer wind retrievals (fig. S1). On the basis of this analysis, the error bar on the SSM/I wind trend is estimated to be ±0.05 m s^{-1} $decade^{-1}$ at the 95% confidence level (*8*). This observed increase in the SSM/I winds is opposite to the GCM results, which predict that the 1987-to-2006 warming should have been accompanied by a decrease in winds on the order of (0.19 K $decade^{-1}$)(4% K^{-1}) = 0.8% $decade^{-1}$.

We then looked at the variability of global precipitation and evaporation during the past two decades. Figure 2A shows the time series for P and E. Also shown is the over-ocean SSM/I retrieval of V. To generate the time series, the seasonal variability was first removed, and then the variables were low-pass filtered by convolution with a Gaussian distribution that had a ±4-month width at half-peak power. The major features apparent in the time series are the 1997–1998 El Niño and the 1986–1987 El Niño, followed by the strong 1988–1989 La Niña. It is noteworthy that E, P, and V all exhibited similar magnitudes for interannual variability and decadal trends (Table 1). After applying the ±4-month smoothing, the correlation of E versus P was 0.68. Because global precipitation and evaporation must balance, the observed differences in the derived values of P and E provided an error estimate that we used to estimate the uncertainty in the decadal trend. The estimated error bar at the 95% confidence level for E and P is ±0.5% $decade^{-1}$ (*8*).

Also shown in Fig. 2A is the ensemble mean of nine climate-model simulations smoothed in

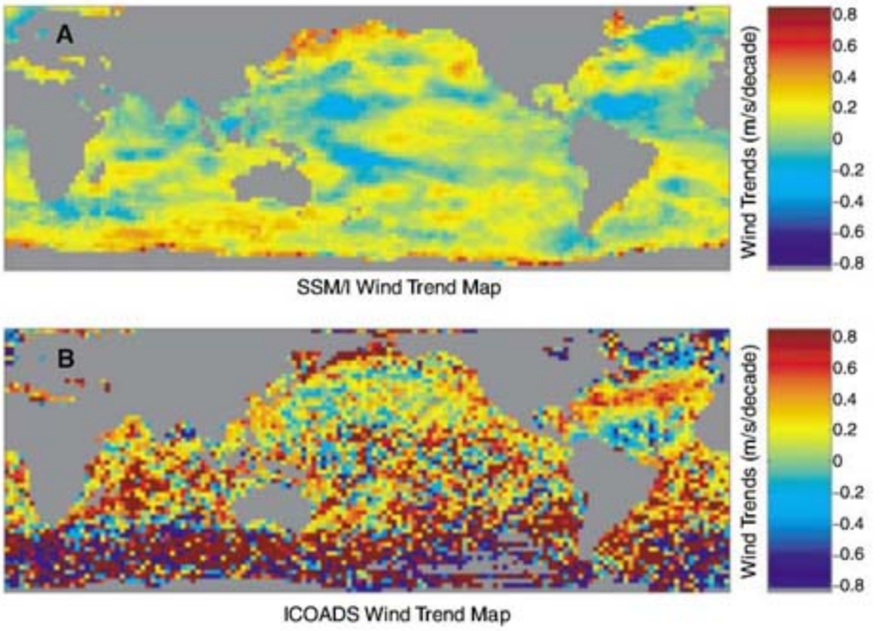

Fig. 1. Surface-wind trends for the period July 1987 through August 2006 computed at a spatial resolution of 2.5°. (**A**) SSM/I wind trends. (**B**) ICOADS wind trends. In the North Pacific and North Atlantic where ICOADS ship observations are more abundant, the two data sets show similar trends. The tripole feature in the North Atlantic is consistent with the recent decrease in the NAO index.

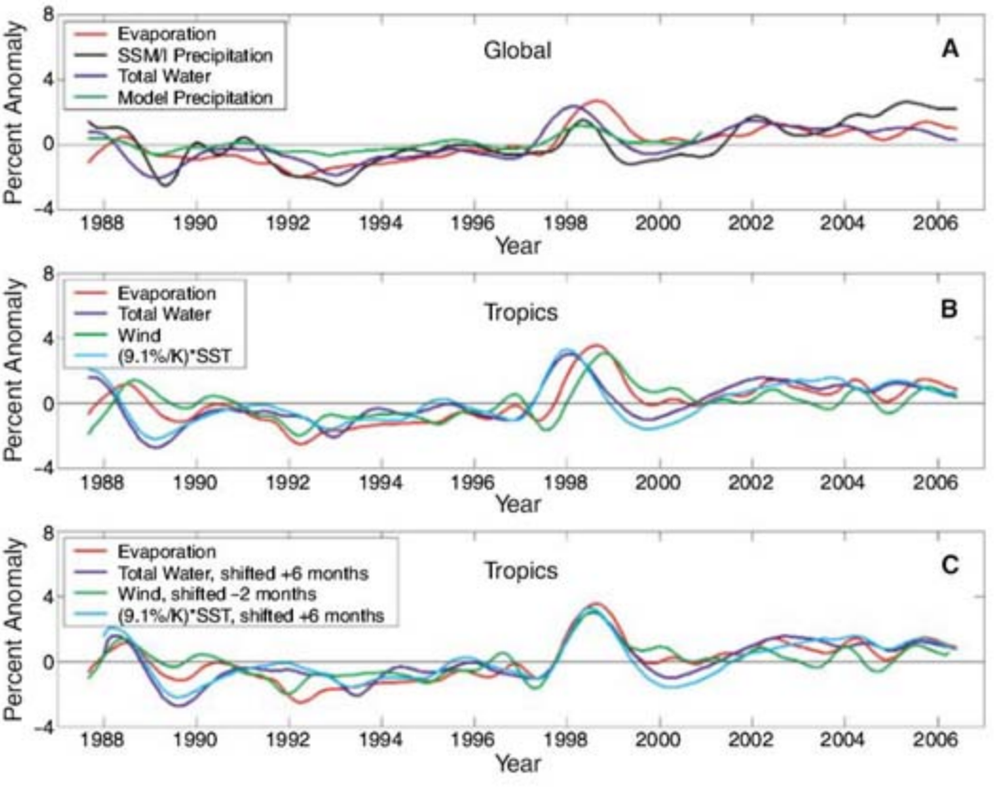

Fig. 2. Anomaly time series of the hydrologic variables. (**A**) Global results for the observed precipitation and evaporation and over-ocean results for total water vapor. The average model precipitation predicted by AMIP simulations is also shown. (**B**) Tropical ocean results for evaporation, total water vapor, surface-wind speed, and SST. The SST time series has been scaled by 9.1% K^{-1}. During the El Niños, evaporation and wind were not in phase with vapor and SST. At the end of 1996, SST and vapor began to increase while the winds began to decrease, with no net effect on evaporation. About 8 months later (mid-1997), the winds in the tropics began to recover and then increased sharply, reaching a maximum value in late 1998. All four variables remained at elevated values thereafter. (**C**) Same as (B), except that the water vapor and SST curves have been shifted forward in time by 6 months, and the wind curve has been shifted backward by 2 months. The statistics on the global time series, including error bars, are given in Table 1.

the same way as in the satellite observations. These climate runs, for which the sea-surface temperature (SST) is prescribed from observations, are from the Atmospheric Model Intercomparison Project II (AMIP-II) (*19*, *20*). There is a pronounced difference between the precipitation time series from the climate models and that from the satellite observations. The amplitude of the interannual variability, the response to the El Niños, and the decadal trends are all smaller by a factor of 2 to 3 in the climate-model results, as compared with the observations. This characteristic of the models to underpredict the amplitude of precipitation changes to El Niño–Southern Oscillation events has been reported previously (*21*), and the results presented here suggest that the climate models are also underestimating the decadal variability.

The similarity in the satellite-derived time series became more pronounced when the analysis was limited to the tropical oceans (30°S to 30°N), where most of the evaporation occurs. Although the condition $E = P$ was no longer valid for this regional analysis, the coupling of evaporation with the other variables was more apparent. Figure 2B shows the tropical time series of E, V, *SST*, and W. The variables V and *SST* exhibited a high correlation [correlation coefficient (r) = 0.96], and their scaling relation of 9.1% K^{-1} was equal to the C-C rate (6.5% K^{-1}) times a moist adiabatic lapse rate (MALR) factor of 1.4 (*5*). The MALR factor is the ratio of change in the lower tropospheric temperature to the change in *SST*. This strong coupling between V and *SST* is another confirmation that the total atmospheric water increases with temperature at the C-C rate.

During the two El Niños, evaporation and wind speed were not in phase with vapor and *SST*. The increase in evaporation lagged the increase in vapor by 6 months, and the increase in winds lagged by 8 months (Fig. 2B). When a 6-month lag was applied, the correlation between E and V was 0.84 in the tropics and 0.88 globally.

Figure 3 shows a trend map of $P - E$. The most striking feature is in the tropical Western Pacific Warm Pool, where $\Delta(P - E)$ is about 400 mm $year^{-1}$ $decade^{-1}$, and Δ represents change. This is a region of maximum $P - E$ (1500 to 2000 mm $year^{-1}$). Simple hydrologic models predict that $\Delta(P - E)$ should vary similarly to $P - E$ (*3*). That is to say, wet regions should get wetter and dry regions should get drier. This seems to be the case over the Warm Pool, but elsewhere this direct proportionality is not as apparent.

During the past two decades, the hydrologic parameters E, P, and V exhibited similar responses to the two El Niños (apart from a 6-month lag), similar magnitudes of interannual variability (1.0 to 1.3%), and similar decadal trends (1.2 to 1.4% $decade^{-1}$). Earth's surface warmed by 0.2 K $decade^{-1}$ during this period, and hence the observed changes in E and P suggest an acceleration in the hydrologic cycle of about 6% K^{-1}, close to the C-C value. In addition, ocean winds exhibited a small increase of 1.0% $decade^{-1}$. There is no evidence in the observations that radiative forcing in the troposphere is inhibiting the variations in E, P, and W. Rather, E and P seem to simply vary in unison with the total atmospheric water content.

The reason for the discrepancy between the observational data and the GCMs is not clear. One possible explanation is that two decades is too short of a time period, and thus we see internal climate variability that masks the limiting effects of radiative forcing. However, we would argue that although two decades may be too short for extrapolating trends, it may indeed be long enough to indicate that the observed scaling relations will continue on a longer time scale. Another possible explanation is that there are errors in the satellite retrievals, but the consistency among the independent retrievals and validation of the winds with other data sets suggests otherwise. Lastly, there is the possibility that the climate models have in common a compensating error in characterizing the radiative balance for the troposphere and Earth's surface. For example, variations in modeling cloud radiative forcing at the surface can have a relatively large effect on the precipitation response (*4*), whereas the temperature response is more driven by how clouds affect the radiation at the top of the troposphere.

The difference between a subdued increase in rainfall and a C-C increase has enormous impact, with respect to the consequences of global warming. Can the total water in the atmosphere increase by 15% with CO_2 doubling but precipitation only increase by 4% (*1*)? Will warming really bring a decrease in global winds? The observations reported here suggest otherwise, but clearly these questions are far from being settled.

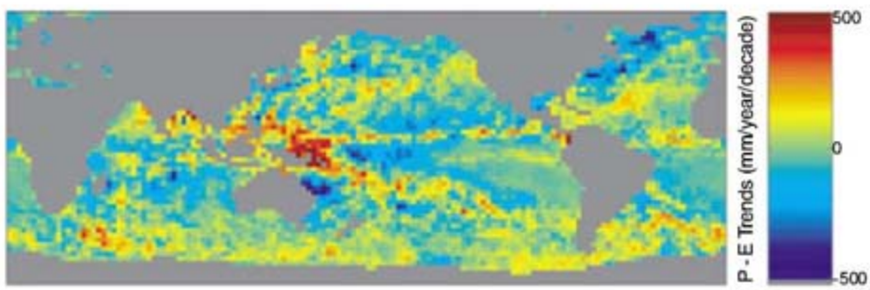

Fig. 3. Trends in satellite-derived $P - E$ for the period July 1987 through August 2006. The largest change was over the warm pool in the western Pacific: a wet area that became wetter.

Table 1. Statistics on the variation of global evaporation, global precipitation, and over-ocean water vapor for the period July 1987 through August 2006. The error bars on the trends are given at the 95% confidence level. The values in parentheses are in terms of percentage change, rather than absolute change.

Parameter	Mean	Standard deviation	Trend
Evaporation	961 mm $year^{-1}$	10.1 mm $year^{-1}$ (1.1%)	12.6 ± 4.8 mm $year^{-1}$ $decade^{-1}$ (1.3 ± 0.5% $decade^{-1}$)
Precipitation	950 mm $year^{-1}$	12.7 mm $year^{-1}$ (1.3%)	13.2 ± 4.8 mm $year^{-1}$ $decade^{-1}$ (1.4 ± 0.5% $decade^{-1}$)
Total water	28.5 mm	0.292 mm (1.0%)	0.354 ± 0.114 mm $decade^{-1}$ (1.2 ± 0.4% $decade^{-1}$)

References and Notes

1. M. R. Allen, W. J. Ingram, *Nature* **419**, 224 (2002).
2. J. F. B. Mitchell, C. A. Wilson, W. M. Cunnington, *Q. J. R. Meteorol. Soc.* **113**, 293 (1987).
3. I. M. Held, B. J. Soden, *J. Clim.* **19**, 5686 (2006).
4. C. Covey *et al.*, *Global Planet. Change* **37**, 103 (2003).
5. F. J. Wentz, M. Schabel, *Nature* **403**, 414 (2000).
6. K. E. Trenberth, J. Fasullo, L. Smith, *Clim. Dyn.* **24**, 741 (2005).
7. G. A. Vecchi *et al.*, *Nature* **441**, 73 (2006).
8. See supporting material on *Science* Online.
9. F. J. Wentz, *J. Geophys. Res.* **102**, 8703 (1997).
10. T. M. Smith, R. W. Reynolds, *J. Clim.* **18**, 2021 (2005).
11. Data are posted at www.ncdc.noaa.gov/oa/climate/research/ghcn/ghcngrid.html.
12. C. A. Mears, F. J. Wentz, *Science* **309**, 1548 (2005); published online 11 August 2005 (10.1126/science.1114772).
13. G. A. Meehl *et al.*, *Science* **307**, 1769 (2005).
14. R. F. Adler *et al.*, *J. Hydrometeorol.* **4**, 1147 (2003).
15. The satellite-gauge combined precipitation product V2 was downloaded from ftp://precip.gsfc.nasa.gov/pub/gpcp-v2/psg/.
16. J. P. Peixoto, A. H. Oort, in *Physics of Climate* (Springer, New York, 1992), pp. 170–172, 228–237.
17. W. D. Collins *et al.*, *NCAR Technical Note TN-464+STR* (National Center for Atmospheric Research, Boulder, CO, 2004).
18. J. W. Hurrell, Y. Kushnir, G. Ottersen, M. Visbeck, Eds., *The North Atlantic Oscillation: Climate Significance and Environmental Impact* (Geophysical Monograph Series, American Geophysical Union, Washington, DC, 2003), pp. 1–35.
19. W. L. Gates *et al.*, *Bull. Am. Meteorol. Soc.* **73**, 1962 (1998).
20. The more recent AMIP-II simulations were obtained from www-pcmdi.llnl.gov/projects/amip.
21. B. J. Soden, *J. Clim.* **13**, 538 (2000).

22. This work was supported by NASA's Earth Science Division.

Supporting Online Material

www.sciencemag.org/cgi/content/full/1140746/DC1
Materials and Methods
SOM Text
Fig. S1
References

2 February 2007; accepted 21 May 2007
Published online 31 May 2007;
10.1126/science.1140746
Include this information when citing this paper.

Food Web–Specific Biomagnification of Persistent Organic Pollutants

Barry C. Kelly,[1] Michael G. Ikonomou,[2] Joel D. Blair,[1] Anne E. Morin,[1] Frank A. P. C. Gobas[1]*

Substances that accumulate to hazardous levels in living organisms pose environmental and human-health risks, which governments seek to reduce or eliminate. Regulatory authorities identify bioaccumulative substances as hydrophobic, fat-soluble chemicals having high octanol-water partition coefficients (K_{OW}) (≥100,000). Here we show that poorly metabolizable, moderately hydrophobic substances with a K_{OW} between 100 and 100,000, which do not biomagnify (that is, increase in chemical concentration in organisms with increasing trophic level) in aquatic food webs, can biomagnify to a high degree in food webs containing air-breathing animals (including humans) because of their high octanol-air partition coefficient (K_{OA}) and corresponding low rate of respiratory elimination to air. These low K_{OW}–high K_{OA} chemicals, representing a third of organic chemicals in commercial use, constitute an unidentified class of potentially bioaccumulative substances that require regulatory assessment to prevent possible ecosystem and human-health consequences.

The Stockholm Convention on Persistent Organic Pollutants was endorsed by 131 nations in 2004 to eliminate the world's most persistent bioaccumulative and toxic substances (*1*). Such substances include polychlorinated biphenyls (PCBs) and dichlordiphenyltrichloroethanes (DDTs), which are highly accumulative and can cause adverse health effects in fish, wildlife, and humans (*2*–*6*). Brominated flame retardants and certain perfluorinated chemicals have recently emerged as new contaminants of concern (*7*, *8*). Governments worldwide are currently evaluating all commercial chemicals, with the goal to identify substances that can biomagnify in food chains and achieve harmful concentrations in high–trophic level organisms including human beings.

To identify bioaccumulative substances, regulatory authorities rely on the chemical's K_{OW} or, when available, on organism/water chemical concentration ratios measured in laboratory tests [bioconcentration factors (BCFs)] or in the field (bioaccumulation factors) (*9*). These criteria were derived from laboratory tests in fish, which revealed correlations between the K_{OW} and the BCF of organic chemicals and showed that bioconcentration could be explained and predicted by lipid-water partitioning (*10*). Studies in real food webs demonstrated that bioaccumulation in food webs is not solely a lipid-water partitioning process. Dietary accumulation or biomagnification can cause additional bioaccumulation, resulting in an increase in chemical concentration with increasing trophic level in food webs (*11*). This apparent chemical transport against the thermodynamic gradient is due to food digestion and absorption, which concentrate ingested chemicals in the gastrointestinal tract (*12*, *13*). Poorly metabolizable, hydrophobic substances with $K_{OW} \geq 10^5$ have proven particularly susceptible to biomagnification in fish (*14*), whereas chemicals with lower K_{OW} do not generally biomagnify in fish.

However, less hydrophobic chemicals (e.g., chlorobenzenes and lindane), with $K_{OW} < 10^5$ and with BCFs in fish-based experiments below the regulatory criterion of 5000, were found to biomagnify in lichen-caribou-wolf food chains in northern Canada (*15*, *16*). Also, perfluorinated sulfonic acids such as perfluorooctane sulfonate, which (with a calculated $K_{OW} < 10^5$) do not biomagnify in laboratory tests with fish (*17*), show a high degree of biomagnification in birds and mammals (*8*, *18*, *19*). These findings indicate that very hydrophobic chemicals with a $K_{OW} \geq 10^5$ are not the only chemicals with biomagnification potential and that lipid-water partitioning cannot serve as a universal model for identifying bioaccumulative substances in wildlife and humans.

To test the applicability of current regulatory criteria for identifying bioaccumulative substances, we measured and compiled concentrations of organic contaminants of varying hydrophobicity and K_{OW} in a piscivorous food web (water-respiring organisms only), a terrestrial food web (air-breathing organisms only), and a combined marine mammalian food web (including water-respiring and air-breathing organisms) from northern Canada (*20*) (fig. S2). We also used mechanistic food web bioaccumulation models to determine the influence of

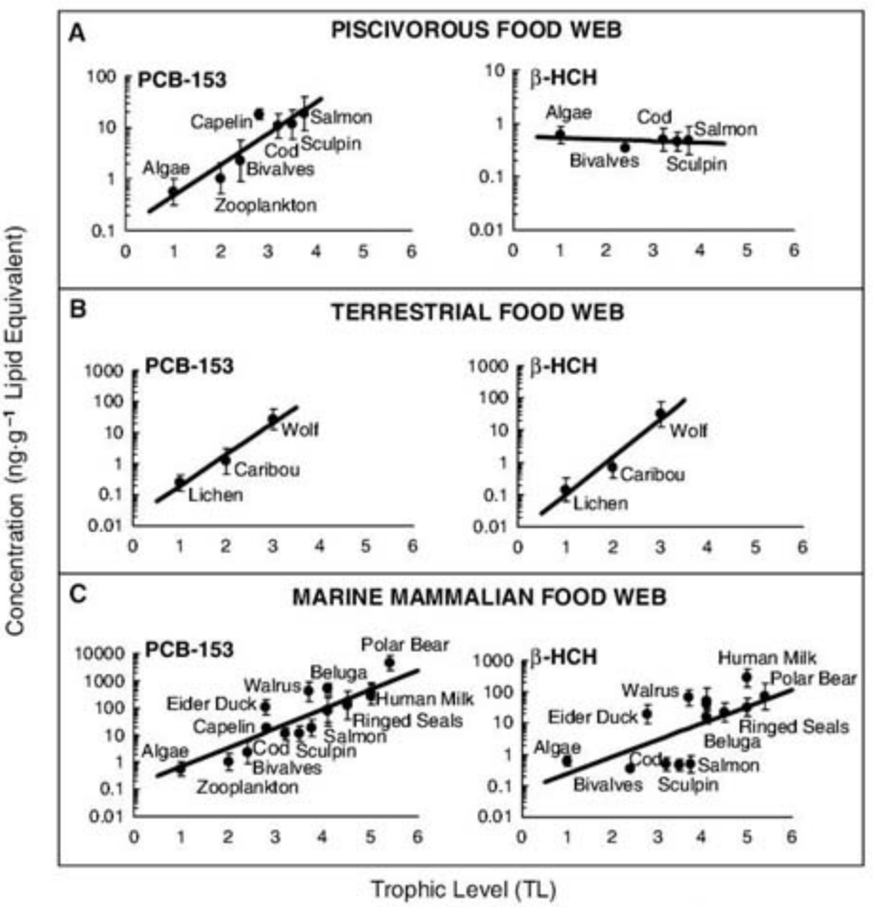

Fig. 1. Relationship between observed tissue residue concentrations (ng·g^{-1} lipid equivalent) and trophic level for PCB 153 (a high K_{OW}–high K_{OA} compound) and β-HCH (a low K_{OW}–high K_{OA} compound) in Arctic organisms of the piscivorous (**A**), terrestrial (**B**), and marine mammalian (**C**) food webs. Data represent geometric means ± 1 SD.

[1]School of Resource and Environmental Management, Simon Fraser University, 8888 University Drive, Burnaby, British Columbia, V5A 1S6, Canada. [2]Fisheries and Oceans Canada, Institute of Ocean Sciences, Ocean Sciences Division, 9860 West Saanich Road, Sidney, British Columbia, V8L 4B2, Canada.

*To whom correspondence should be addressed. E-mail: gobas@sfu.ca

K_{OW} on chemical bioaccumulation in these food chains (*20*, *21*).

In field studies, we observed strong positive relationships ($r^2 > 0.8$, $P < 0.001$) between trophic level and concentrations of recalcitrant PCB congeners 138, 180, and 153; mirex; hexachlorobenzene (HCBz); dieldrin; and DDTs in all three food webs (Fig. 1 and fig. S4, A to C). These and related findings (*22*–*24*) support the current regulatory and scientific paradigm that very hydrophobic organic chemicals with a $K_{OW} \geq 10^5$ can biomagnify in food webs. However, although less hydrophobic compounds ($K_{OW} < 10^5$) such as α, β, and γ hexachlorocyclohexanes (HCHs) ($K_{OW} = 10^{3.8}$), tetrachlorobenzenes (TeCBz) ($K_{OW} = 10^{4.1}$), and endosulfans ($K_{OW} = 10^{3.7}$) did not biomagnify in the piscivorous food web, they showed a high degree of biomagnification in the lichen-caribou-wolf food chain and in air-breathing organisms of the marine mammalian food web (Fig. 1 and fig. S4, D to F). The predator-prey biomagnification factors or BMFs (*25*) of β-HCH in ringed seals of 20 and in beluga whales of 50 exceed the BMFs of PCB 180 in those animals. These findings demonstrate that although substances with a K_{OW} below 10^5 cannot biomagnify in fish, they can biomagnify in birds and mammals.

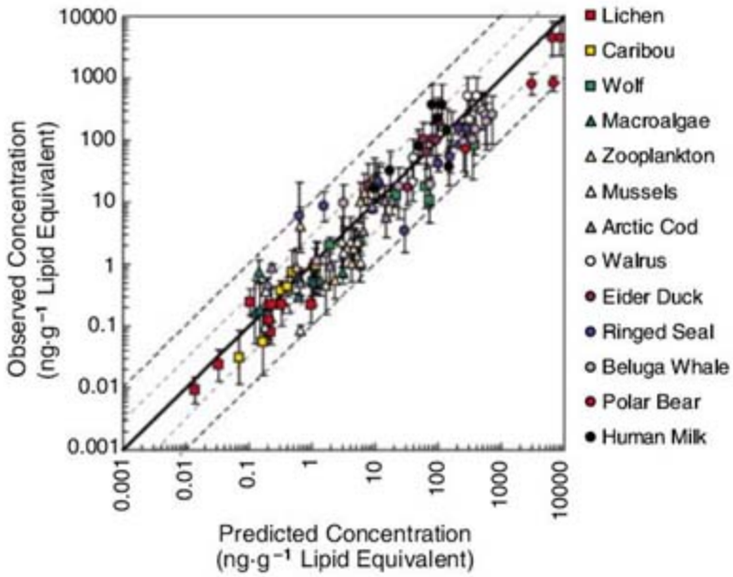

Fig. 2. Model predicted versus observed concentrations (ng·g^{-1} lipid equivalent) in various organisms of the Canadian Arctic terrestrial and marine ecosystems. Observed data represent geometric mean ± 1 SD. The solid black line represents an ideal model fit (1:1 predicted:observed line). Dashed lines represent a factor of 3 (gray dashes) and 10 (black dashes) above and below the ideal fit.

Bioaccumulation modeling studies (*20*) showed good agreement between calculated and observed concentrations of recalcitrant substances in all three food webs (Fig. 2). The model shows that air-breathing organisms in this analysis exhibit higher BMFs than those in water-respiring organisms because of their greater ability to absorb and digest their diet (Table 1), which is related to differences in digestive tract physiology and body temperature. The model also shows that the relationship between the BMF and chemical properties is controlled by the rate of elimination. In water-respiring or air-breathing organisms because of efficient respiratory elimination to air and water. Low K_{OW} (log K_{OW} ~2 to 5)–high K_{OA} (log K_{OA} ~6 to 12) chemicals exhibit no biomagnification in water-respiring organisms but biomagnify in air-breathing organisms. High K_{OW}–high K_{OA} chemicals biomagnify in water-respiring and air-breathing organisms.

Table 1. Calculated BMFs (*25*) of selected industrial chemicals in aquatic invertebrates, fish, reptiles, amphibians, birds, nonhuman mammals, and humans for organic chemicals varying in molecular weights (M_W, g·mol^{-1}), log K_{OW}, and log K_{OA}. No metabolic transformation was assumed. Biomagnification occurs if BMF > 1. Low K_{OW}–low K_{OA} chemicals show no biomagnification in

Chemical*	M_W (g·mol^{-1})†	Log K_{OW}†	Log K_{OA}†	Water-respiring organisms			Air-breathing organisms						
				Zooplankton	Forage fish	Predatory fish	Reptile	Amphibian	Seabird	Marine mammal	Terrestrial herbivore	Terrestrial carnivore	Human
Low K_{OW}–low K_{OA}													
1,4 butadiene	145	1.9	2.9	<1	<1	<1	<1	<1	<1	<1	<1	<1	<1
1,3,5 TriCBz	182	3.5	4.7	<1	<1	<1	<1	<1	<1	<1	<1	<1	<1
Hexachlorobutadiene	261	4.5	3.9	<1	<1	<1	<1	<1	<1	<1	<1	<1	<1
Styrene	150	2.5	4.9	<1	<1	<1	<1	<1	<1	<1	<1	<1	<1
Low K_{OW}–high K_{OA}													
Dicofol	371	3.5	8.9	<1	<1	<1	6.1	12	16	42	3.9	76	76
β-endosulfan	391	3.7	7.1	<1	<1	<1	4.9	11	10	22	2.5	28	23
β-HCH	291	3.8	8.9	<1	<1	<1	7.5	12	17	45	4.0	85	84
Musk xylene	297	4.1	8.9	<1	<1	<1	8.5	12	18	47	4.1	90	89
Trifluralin	350	4.4	7.2	<1	<1	<1	6.2	11	12	26	2.8	34	28
Tetradifon	356	4.6	11.4	<1	<1	<1	9.4	12	19	49	4.1	97	97
1,2,4,5 TeCBz	247	4.7	6.3	<1	<1	<1	2.4	7.3	3.9	7.3	1.0	7.6	5.9
High K_{OW}–high K_{OA}													
PeCBz	247	5	6.9	<1	<1	<1	4.8	10	8.4	17	2.1	21	16
Dieldrin	381	5.4	8.8	1.7	2.4	2.3	9.6	12	19	48	4.1	94	93
HCBz	285	5.5	7.7	1.8	2.7	2.7	8.4	12	16	38	3.6	62	55
PCB 153	361	7.5	9.6	2.5	5.0	7.7	9.6	12	18	49	3.3	97	96
PCB 180	381	7.5	10.9	2.5	5.1	8.0	9.3	12	18	47	2.4	95	95
PBDE 47	308	6.0	9.8	2.2	4.0	5.1	9.7	12	19	49	4.1	98	98
PBDE 99	342	6.8	11.2	2.5	4.9	7.5	9.7	12	19	49	3.6	98	98
Mirex	546	8.1	9.6	1	1	2	8.2	10	14	16	1	82	82
PBDE 209	600	9.9	13.1	1	1	1	1	1	1	3	1	8	8

*Chemical abbreviations not provided in the text include TriCBz (trichlorobenzene), PeCBz (pentachlorobenzene), PCB 153 (2,2′,4,4′,5,5′ hexachlorobiphenyl), PCB 180 (2,2′,3,4,4′,5,5′ heptachlorobiphenyl), PBDE 47 (2,2′,4,4′ tetrabromodiphenyl ether), PBDE 99 (2,2′,4,4′,5 pentabromodiphenyl ether), and PBDE 209 (2,2′,3,3′,4,4′,5,5′,6,6′ decabromodiphenyl ether). †See supporting online material for physical-chemical properties.

respiring organisms, elimination becomes sufficiently slow to cause biomagnification if the K_{OW} of the chemical exceeds ~10^5. In the air-breathing organisms of this study, this occurs for chemicals with a high K_{OA} ($\geq 10^6$), which causes slow respiratory elimination, and a $K_{OW} > 10^2$, causing slow elimination in urine or nitrogenous wastes (Table 1). The difference in biomagnification behavior between air-breathing and water-respiring organisms implies that, for substances with a $K_{OA} \geq 10^6$ and a $K_{OW} > 10^2$, K_{OW} and the BCF in fish are not good predictors of biomagnification in air-breathing animals.

Application of the bioaccumulation model to identify potentially bioaccumulative substances among commercial chemicals reveals distinct differences in the biomagnification behavior of chemicals in different food webs (Fig. 3). In the piscivorous food web, concentrations of non-metabolizing chemicals with K_{OW} between 10^5 and 10^8 biomagnify in top-level predatory fish up to 100-fold (Fig. 3A). No biomagnification occurs for less hydrophobic chemicals with $K_{OW} < 10^5$, which are efficiently eliminated by respiration, or for superhydrophobic organic substances with $K_{OW} > 10^8$, which are absorbed at very slow rates (*26*–*28*). However, in the marine mammalian food web (Fig. 3B), which includes water-respiring invertebrates and fish and air-breathing birds and mammals, poorly metabolizing chemicals with a $K_{OW} \geq 10^5$ and $K_{OA} \geq 10^6$ biomagnify, attaining concentrations in top predators (polar bears) up to 10,000 times the concentrations in primary producers. Less hydrophobic chemicals with $K_{OW} < 10^5$ and $K_{OA} \geq 10^6$ also biomagnify strongly, with concentrations in polar bears exceeding those in primary producers up to 3000-fold. Chemicals with $K_{OW} < 10^2$ do not biomagnify in this food web regardless of their high K_{OA} because air-breathing animals eliminate them through urinary excretion. In terrestrial food webs, chemicals with a K_{OW} between 10^2 and 10^{10} and a $K_{OA} \geq 10^6$ can biomagnify up to 400-fold if not metabolized (Fig. 3C). Chemicals with a K_{OW} between ~10^3 and 10^9 achieve a similar degree of biomagnification, given the same K_{OA}.

Simulations, representing human dietary exposure of contaminants to the indigenous Inuit population of northern Canada, show that chemical amplifications can reach ~4000-fold for chemicals with a log $K_{OW} \geq 5$ and a log $K_{OA} \geq 6$ and 2000-fold for chemicals with a log K_{OW} between 2 and 5 and a log K_{OA} above 6 (Fig. 3D). The modeling results are consistent with empirical observations for PCBs, chlordanes, HCBz, dieldrin, and DDTs, which have both a high log $K_{OW} \geq 5$ and a high log $K_{OA} \geq 6$ and biomagnify in all three Arctic food webs studied (fig. S4). The results are also consistent with observations of HCHs, TeCBz, and endosulfans, which have a low log $K_{OW} < 5$ but a high log $K_{OA} \geq 6$ and exhibit no biomagnification in the piscivorous food web but biomagnify in air-breathing organisms.

Organic chemicals with a $K_{OW} > 10^2$ and a $K_{OA} \geq 10^6$ (i) have an inherent biomagnification potential in air-breathing organisms of terrestrial, marine mammalian, and human food chains and (ii) include almost two-thirds of all organic chemicals used in commerce (*29*) (fig. S6). About 40% of chemicals with these properties have a $K_{OW} > 10^5$ and are currently recognized as potentially bioaccumulative because of their high degree of lipid-water partitioning. The remaining 60% of these chemicals, which include substances with a K_{OW} between 10^2 and 10^5 and a $K_{OA} \geq 10^6$, should also be considered for their bioaccumulative potential because of their high degree of lipid-air partitioning. These low K_{OW}–high K_{OA} chemicals are susceptible to biomagnification in air-breathing animals, including humans, because of their slow rate of respiratory elimination. Metabolic transformation can reduce or eliminate the anticipated biomagnification potential but only if the metabolic transformation rate is sufficiently high. In those cases, the bioaccumulation behavior of resulting metabolites should also be considered.

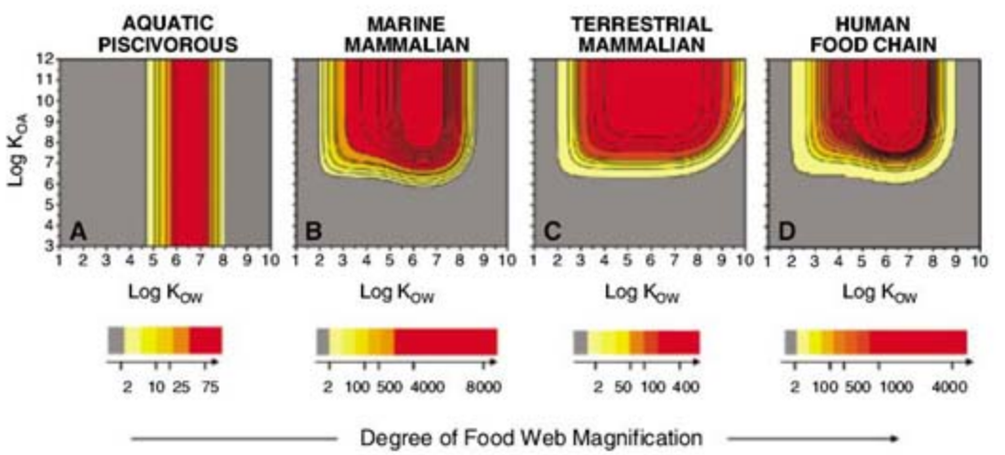

Fig. 3. Contour plots illustrating the relationship between chemical K_{OW} (*x* axis), K_{OA} (*y* axis), and food web magnification (*z* dimension represented as contours) in the aquatic piscivorous food web (**A**), marine mammalian food web (**B**), terrestrial mammalian food chain (**C**), and Arctic indigenous human food chain (**D**). The data represent the combined magnification of the chemical concentrations (ng·g^{-1} lipid equivalent) in the top predator over the concentrations at the base of the food web [e.g., primary producers at trophic level (TL) = 1 to polar bear at TL = 5.4]. A matrix table was generated with ~30,000 K_{OW}-K_{OA} combinations over a log K_{OW} range of 1 to 10 and a log K_{OA} range of 3 to 12. These data demonstrate the combined effect of K_{OW} and K_{OA} on chemical bioaccumulation.

References and Notes

1. United Nations Environment Program (UNEP), *Final Act of the Conference of Plenipotentiaries on The Stockholm Convention on Persistent Organic Pollutants*, Stockholm, Sweden, 22 to 23 May 2001 (UNEP, Geneva, Switzerland, 2001).
2. P. M. Cook *et al.*, *Environ. Sci. Technol.* **37**, 3864 (2003).
3. D. A. Ratcliffe, *Nature* **215**, 208 (1967).
4. G. M. Woodwell, *Sci. Am.* **216**, 24 (1967).
5. B. C. Gladen *et al.*, *J. Pediatr.* **113**, 991 (1988).
6. Y. C. Chen, Y. L. Guo, C. C. Hsu, W. J. Rogan, *JAMA* **268**, 3213 (1992).
7. M. G. Ikonomou, S. Rayne, R. F. Addison, *Environ. Sci. Technol.* **36**, 1886 (2002).
8. J. P. Giesy, K. Kannan, *Environ. Sci. Technol.* **35**, 1339 (2001).
9. J. A. Arnot, F. A. P. C. Gobas, *Environ. Rev.* **14**, 257 (2006).
10. D. Mackay, *Environ. Sci. Technol.* **16**, 274 (1982).
11. J. P. Connolly, C. J. Pedersen, *Environ. Sci. Technol.* **22**, 99 (1988).
12. F. A. P. C. Gobas, X. Zhang, R. Wells, *Environ. Sci. Technol.* **27**, 2855 (1993).
13. F. A. P. C. Gobas, J. B. Wilcockson, R. W. Russel, G. D. Haffner, *Environ. Sci. Technol.* **33**, 133 (1999).
14. A. T. Fisk, R. J. Norstrom, C. D. Cymbalisty, D. C. G. Muir, *Environ. Toxicol. Chem.* **17**, 951 (1998).
15. B. C. Kelly, F. A. P. C. Gobas, *Environ. Sci. Technol.* **35**, 325 (2001).
16. B. C. Kelly, F. A. P. C. Gobas, *Environ. Sci. Technol.* **37**, 2966 (2003).
17. J. W. Martin, S. A. Mabury, K. R. Solomon, D. C. G. Muir, *Environ. Toxicol. Chem.* **22**, 189 (2003).
18. G. T. Tomy *et al.*, *Environ. Sci. Technol.* **38**, 6475 (2004).
19. K. Kannan *et al.*, *Environ. Sci. Technol.* **35**, 1593 (2001).
20. Materials and methods are available as supporting material on *Science* Online.
21. "Food web" is defined as the network of organisms and species-specific feeding relationships that control the flow of energy and contaminants in the ecosystems studied. In some cases, we use the term "food chain" to represent the overall transfer of contaminants from primary producers to top predators of a given food web (e.g., marine mammalian food chain: phytoplankton to invertebrate to fish to mammal).
22. H. Hop, K. Borga, G. W. Gabrielsen, L. Kleivane, J. U. Skaare, *Environ. Sci. Technol.* **36**, 2589 (2002).
23. A. T. Fisk, K. A. Hobson, R. J. Norstrom, *Environ. Sci. Technol.* **35**, 732 (2001).
24. P. F. Hoekstra *et al.*, *Environ. Pollut.* **124**, 509 (2003).
25. BMFs represent the ratio of lipid equivalent chemical concentrations in an organism and in its prey.
26. A. Morck, H. Hakk, U. Orn, E. Klasson Wehler, *Drug Metab. Dispos.* **31**, 900 (2003).
27. H. M. Stapleton, M. Alaee, R. J. Letcher, J. E. Baker, *Environ. Sci. Technol.* **38**, 112 (2004).
28. A. Kierkegaard, L. Balk, U. Tjarnlund, C. A. De Wit, B. Jansson, *Environ. Sci. Technol.* **33**, 1612 (1999).
29. F. A. P. C. Gobas, B. C. Kelly, J. A. Arnot, *Quant. Struct.-Act. Relat. Comb. Sci.* **22**, 329 (2003).

30. We thank M. Kwan, S. Sang, B. Doidge, D. Muir, J. Arnot, J. Armitage, M. Fischer, N. Crewe, and M. Gibbs. We acknowledge the Natural Sciences and Engineering Research Council of Canada and Environment Canada's Northern Ecosystems Initiative for financial support, Fisheries and Oceans Canada for chemical analysis support, and northern Quebec Inuit communities of Umiujaq and Inukjuaq for assistance with collection of field samples.

Supporting Online Material
www.sciencemag.org/cgi/content/full/317/5835/236/DC1
Materials and Methods
Figs. S1 to S6
Tables S1 to S11
References

1 December 2006; accepted 8 June 2007
10.1126/science.1138275

Mechanism of Two Classes of Cancer Mutations in the Phosphoinositide 3-Kinase Catalytic Subunit

Nabil Miled,[1]*† Ying Yan,[2]* Wai-Ching Hon,[1] Olga Perisic,[1] Marketa Zvelebil,[3] Yuval Inbar,[4] Dina Schneidman-Duhovny,[4] Haim J. Wolfson,[4] Jonathan M. Backer,[2]‡ Roger L. Williams[1]‡

Many human cancers involve up-regulation of the phosphoinositide 3-kinase PI3Kα, with oncogenic mutations identified in both the p110α catalytic and the p85α regulatory subunits. We used crystallographic and biochemical approaches to gain insight into activating mutations in two noncatalytic p110α domains—the adaptor-binding and the helical domains. A structure of the adaptor-binding domain of p110α in a complex with the p85α inter–Src homology 2 (inter-SH2) domain shows that oncogenic mutations in the adaptor-binding domain are not at the inter-SH2 interface but in a polar surface patch that is a plausible docking site for other domains in the holo p110/p85 complex. We also examined helical domain mutations and found that the Glu^{545} to Lys^{545} (E545K) oncogenic mutant disrupts an inhibitory charge-charge interaction with the p85 N-terminal SH2 domain. These studies extend our understanding of the architecture of PI3Ks and provide insight into how two classes of mutations that cause a gain in function can lead to cancer.

Phosphoinositide 3-kinases and their lipid product, phosphatidylinositol-(3,4,5)-trisphosphate [PtdIns(3,4,5)P_3], play key roles in a variety of cellular processes (*1*–*3*). Aberrations in PtdIns(3,4,5)P_3 levels, either through activation of PI3Ks or through inactivation of lipid phosphatase PTEN, occur frequently in numerous forms of cancers. For example, recent data suggest that at least 50% of human breast cancers involve mutations in either PI3Kα or PTEN (*4*, *5*). Broad-spectrum PI3K inhibitors such as LY294002 or wortmannin result in increased apoptosis, decreased proliferation, and reduced metastasis in vitro and in tumor models [reviewed in (*6*–*8*)]. Understanding the structural mechanisms of PI3K regulation may facilitate development of isozyme-specific therapeutics.

The class IA PI3Ks are obligate heterodimers (*9*), consisting of a p110 catalytic subunit and a regulatory subunit. Any of the three class IA catalytic subunits (p110α, p110β, and p110δ) can bind any of the p85-related regulatory subunits. Regulatory subunits have multiple roles in the function of PI3K: down-regulation of the basal activity, stabilization of the catalytic subunit, activation downstream of receptor tyrosine kinases, and sequential activation by tyrosine kinases and Ras (*10*–*13*). Common to all regulatory subunits are two SH2 domains (nSH2 and cSH2) that flank an intervening domain (iSH2), and common to all catalytic subunits are the N-terminal adaptor-binding domain (ABD), the Ras-binding domain (RBD), the putative membrane-binding domain (C2), and the helical and catalytic domains (Fig. 1A). The iSH2 domain is responsible for tight binding to the ABD (*14*). The nSH2 and cSH2 domains bind phosphorylated tyrosines in Tyr-X-X-Met motifs found in activated receptors and adaptor proteins, and this interaction activates the heterodimeric PI3K. The nSH2-iSH2 unit constitutes the minimal fragment capable of regulating the PI3K activity (*15*): It both inhibits the basal activity and facilitates activation by binding phosphotyrosine peptides. In contrast, the isolated iSH2 only minimally affects the PI3K activity, although it tightly binds the p110 subunit.

A number of studies have identified a high frequency of somatic point mutations in the gene encoding the p110α catalytic subunit in different human cancers (*16*, *17*). An increased lipid kinase activity in vitro and the ability to induce oncogenic transformation in vivo were shown both for the most frequently mutated, "hotspot" residues (*16*, *18*–*20*) and for 14 rare cancer-specific mutations in p110α (*21*). The cancer-specific mutations can be grouped into four classes defined by the four domains of the catalytic subunit in which they occur—the ABD, C2, helical, and catalytic domains—and it has been proposed that these classes may increase PI3K activity by different mechanisms (*21*, *22*). Hotspot mutations in the catalytic domain cluster around the "activation loop" involved in substrate recognition (*23*) and are likely to share a common mechanism (*21*). The ABD binds tightly to the regulatory subunit, the C2 domain is thought to interact with the plasma membrane, and the helical domain appears to act as a rigid scaffold around which the RBD, C2, and catalytic domains are mounted (*24*). The catalytic and C2 domain mutations may up-regulate PI3K by increasing the affinity for substrate-containing membranes. However, it is not immediately clear what might be the mechanism of helical domain mutations. We used structural and biochemical approaches to understand the basis for gain-of-function mutations in the ABD and helical domains of p110α. Because the ABD is the only p110 domain for which there is no known structure, we crystallized it in a complex with the iSH2 domain from p85. This structure suggested a rough preliminary model for the p110/p85 heterodimer, which led us to hypothesize that the nSH2 domain might contact the helical domain. To understand how helical domain oncogenic mutations function, we created a series of site-specific mutations in the nSH2 domain, resulting in an adaptor subunit that specifically counteracts the p110 helical domain hotspot E545K mutant.

We determined the crystal structure of a complex between the bovine p110α ABD (residues 1 to 108) and the human p85α iSH2 domain (residues 431 to 600) at 2.4 Å resolution (*25*), revealing the interaction of the small, globular ABD (35 by 25 by 15 Å) with one end of the long, rodlike iSH2 (115 Å long) (Fig. 1B). The ABD is similar to many ubiquitin-like domains: It superimposes on ubiquitin with a root mean square deviation of 1.4 Å for 60 out of 76 residues (Fig. 1C). The β-grasp fold of both the ABD and ubiquitin is a common fold, and neither sequence nor function suggests a common origin for the ABD and ubiquitin. The ABD ranks as one of the least conserved domains among class I catalytic subunits. Conversely, the iSH2 domain is highly conserved in vertebrates, sharing >90% sequence similarity from human to zebrafish (fig. S1). Despite a lack of sequence similarity, secondary and tertiary structure predictions for the class IB p110γ ABD are consistent with a ubiquitin-like fold, similar to the class IA p110 ABD. However, the greater sequence divergence of the p110γ ABD makes it

[1]Medical Research Council Laboratory of Molecular Biology, Hills Road, Cambridge CB2 2QH, UK. [2]Department of Molecular Pharmacology, Albert Einstein College of Medicine, Bronx, NY 10461, USA. [3]Ludwig Institute for Cancer Research, University College London, London W1W 7BS, UK. [4]School of Computer Science, The Raymond and Beverly Sackler Faculty of Exact Sciences, Tel Aviv University, Tel Aviv 69978, Israel.

*These authors contributed equally to this work.
†Present address: Laboratoire de Biochimie et de Génie Enzymatique des Lipases, Ecole Nationale d'Ingenieurs Sfax, Route Soukra BPW, 3038 Sfax, Tunisia.
‡To whom correspondence should be addressed. E-mail: rlw@mrc-lmb.cam.ac.uk (R.L.W.); backer@aecom.yu.edu (J.M.B.)

unable to bind the iSH2 domain. Consistent with previous studies (*26*), the p85α iSH2 domain consists of two helices, α1 and α2, that form a long, antiparallel coiled coil followed by the short α3 helix (Fig. 1B).

The ABD/iSH2 interface is large, burying 2284 Å^2 surface area, with the concave face of the ABD β sheet interacting with the coiled-coil helices of the iSH2 (Fig. 1, B and E). Most of the interactions with the ABD are formed by the iSH2 helix α1, which contacts the ABD with seven of its turns, whereas only three turns of iSH2 helix α2 interact with the ABD. Central to the ABD/iSH2 interface is the surface encompassing the strands β1 to β2 of the ABD, which contains the conserved 25-Leu-Leu-Pro-X-Gly-ϕϕ-31 motif, where ϕ denotes a hydrophobic residue (Fig. 1, D and E). This motif forms a loop that through both its side chains and backbone contacts two conserved iSH2 residues, Gln^{497} and Asn^{527}, one on each long helix of the domain. Among all residues at the interface, the side chains of these two polar iSH2 residues engage in the greatest number of intersubunit contacts. Overall, about three-quarters of the ABD/iSH2 interactions are van der Waals contacts, and most of them involve exposed hydrophobic side chains (fig. S1). At the periphery of the interface are two salt links, Glu$^{23}{}_{ABD}$/Arg$^{534}{}_{iSH2}$ and Arg$^{79}{}_{ABD}$/Glu$^{496}{}_{iSH2}$; however, site-specific mutagenesis of the individual charged residues to Ala did not eliminate binding in vitro. This is consistent with the very high affinity of the iSH2 domain for the ABD (*14*, *27*). Other iSH2-contacting sites include the α1/β3, the β3/β4, and the β4/β5 loops of ABD.

Among rare cancer-specific mutations in p110, there are three residues that map to the ABD—Arg^{38}, Arg^{88}, and Pro^{104}. Recently, it was shown the R38H (*28*) mutation induces oncogenic transformation of avian cells, although with weak efficiency (*21*). None of these residues are at the interface between the ABD and the iSH2 domain. Analysis with ConSurf (*29*) shows that there is a highly conserved ABD surface patch outside the conserved ABD/iSH2 interface (Fig. 2A). This patch, formed by the β4/h3 region and the β2/α1 loop in the ABD (Fig. 2 and fig. S1), consists predominately of polar residues, including two of the three ABD residues whose mutation is linked with cancer, Arg^{38} and Arg^{88}. It represents a plausible docking site for other domains in the rest of the p110/p85 complex. Mutations in this surface may affect the relationship of the ABD with respect to the catalytic core. This could reorient the adaptor subunit with respect to the p110 subunit or change the orientation of the enzyme on the membrane.

A minimal regulatory p85 fragment consisting of nSH2 and iSH2 (p85ni) readily inhibits activity of the wild-type p110α (Fig. 3A), suggesting an undefined inhibitory p85-p110 contact (*30*). Hypothesizing that the helical domain might be a good candidate for the inhibitory nSH2 binding, we looked at the effect of oncogenic mutants in the helical domain. We found that the p85ni regulatory fragment does not inhibit p110α helical domain oncogenic mutants E542K, E545K, or Q546K in vitro (Fig. 3A). Because all of these helical domain mutations increase the positive charge on the surface of the

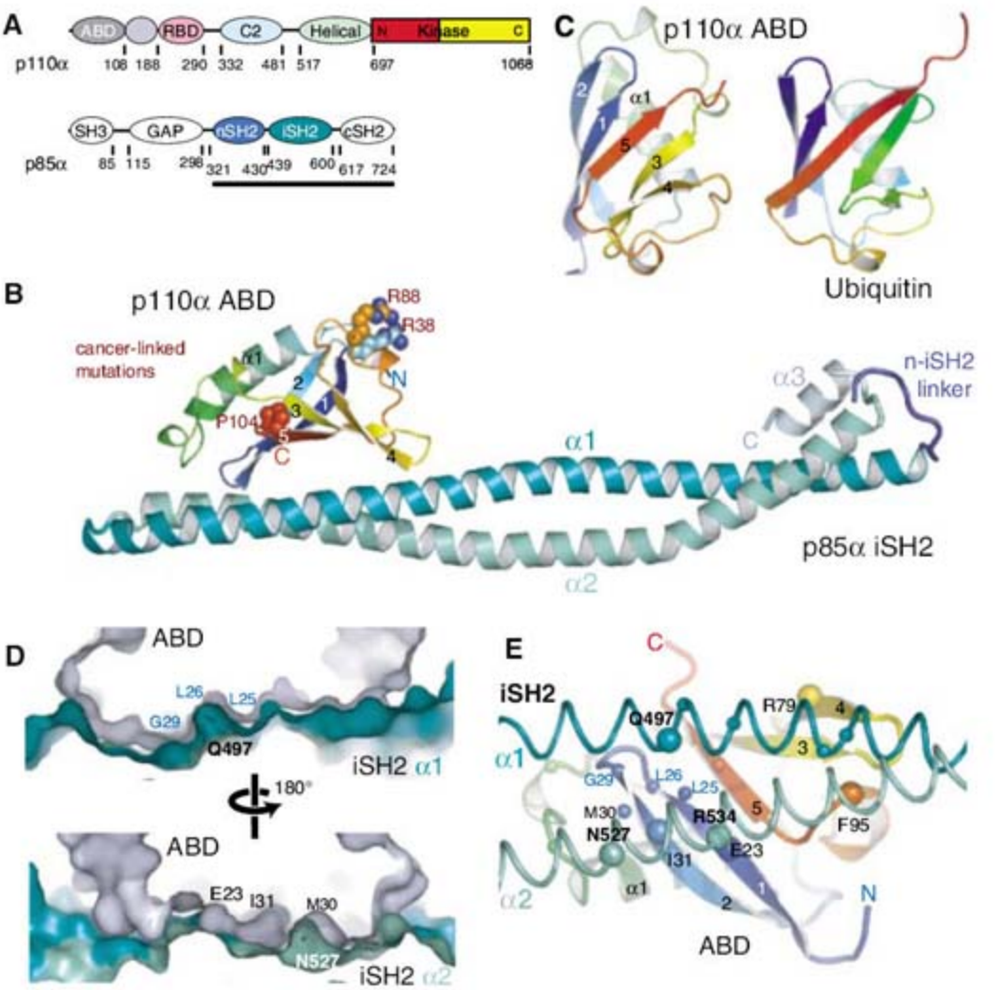

Fig. 1. Structure of a class IA PI3K heterodimerization core. (**A**) Domain organization of PI3K catalytic (classes IA and IB) and regulatory (class IA only) subunits. N and C, N- and C-terminal lobes of the kinase domain, respectively; GAP, Rho-GAP domain. (**B**) Ribbon representation of ABD/iSH2 heterodimer. The three ABD residues identified as somatic mutations in colon cancers (shown in spheres) are not in the ABD/iSH2 interface. (**C**) The ABD has a ubiquitin-like fold. (**D**) A cross-section through the ABD/iSH2 interface showing the surface complementarity. (**E**) Underside view of the heterodimer interface showing residues that contribute substantially to the binding. Cα atoms of residues forming prominent interactions with the iSH2 (contributing more than nine interatomic contacts, interatomic distance < 3.8 Å) are shown as large spheres. Smaller spheres represent residues involved in less extensive interactions (four to six interatomic contacts).

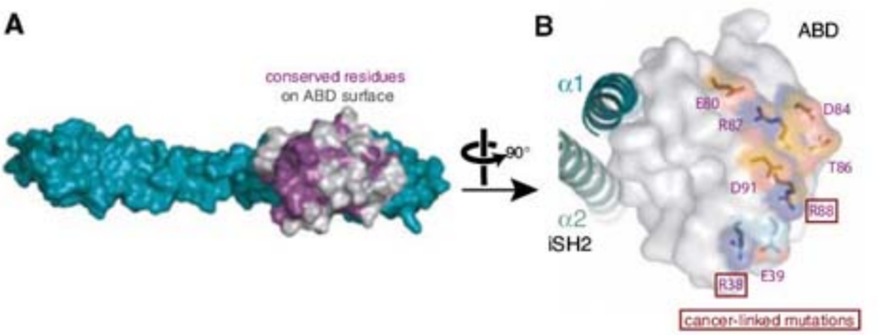

Fig. 2. A model of the minimal p110/p85 complex, showing the locations of rare cancer-specific mutations in the ABD. (**A**) Two ABD residues that are mutated in colon cancers map to a conserved, non–iSH2-binding surface patch (purple). (**B**) A view of the ABD/iSH2 complex rotated 90° around a vertical axis, showing conserved residues on the ABD surface and cancer-specific mutation sites (boxed).

helical domain, we speculated that there might be an inhibitory interaction between the nSH2 and the wild-type helical domain involving a charge-charge interaction between an acidic patch on the helical domain and a basic residue on the surface of the nSH2 domain. We singly mutated each of the lysine or arginine residues on the surface of the nSH2 domain into glutamate. Among these mutants, only the p85ni-R340E and p85ni-K379E mutants did not inhibit the wild-type p110α (Fig. 3B). The loss of inhibition for R340E and K379E suggests that these residues are involved in an inhibitory contact with the catalytic subunit. Consistent with this, the p85ni-K379E mutant inhibits the p110α-E545K oncogenic mutant, whereas the wild-type p85ni does not, suggesting that the charge reversal has reestablished the critical inhibitory interaction (Fig. 3C).

The p85 residues Arg^{340} and Lys^{379} are part of the phosphopeptide-binding surface on the nSH2 domain. Both are in direct contact with bound phosphopeptide in crystal structures of two nSH2/phosphotyrosine-peptide complexes (*31*), suggesting that the phosphopeptide activates the enzyme by competing with the inhibitory contact. A tandem Tyr-X-X-Met phosphopeptide from the Tyr^{608}/Tyr^{628} region of insulin receptor substrate 1 (IRS-1) roughly doubled the activation of the wild-type p110α/p85ni heterodimer but did not activate the p110α-E545K/p85ni complex (Fig. 3D). Figure 4 suggests how binding of the nSH2 domain to the p110α helical domain and to the phosphopeptide would be mutually exclusive. Currently, it is not clear how the nSH2 inhibits the wild-type enzyme. The helical domain interacts with the catalytic domain across a broad surface. The contact of the nSH2 domain with the helical domain might trigger a conformational change in the catalytic domain to affect the activity allosterically, or it may influence the orientation of the catalytic domain on the substrate-containing membrane.

The ABD/iSH2 crystal structure completes the architectural account of the whole p110 catalytic subunit and shows that oncogenic mutations in the ABD are not in the interface with the p85 regulatory subunit. Our results also suggest an unexpected function for the helical domain. A rationally designed nSH2 mutant counteracts the gain-of-function oncogenic p110α-E545K mutation, supporting the proposal that the p85 inhibition of p110α occurs through a charge-charge interaction between the helical domain and the p85ni. The crystallographic structures combined with the mutational analyses have enabled us to propose a rough partial model for the p110/p85 complex (*25*), but ongoing studies by nuclear magnetic resonance, electron paramagnetic resonance, and crystallography will be required to refine any such model.

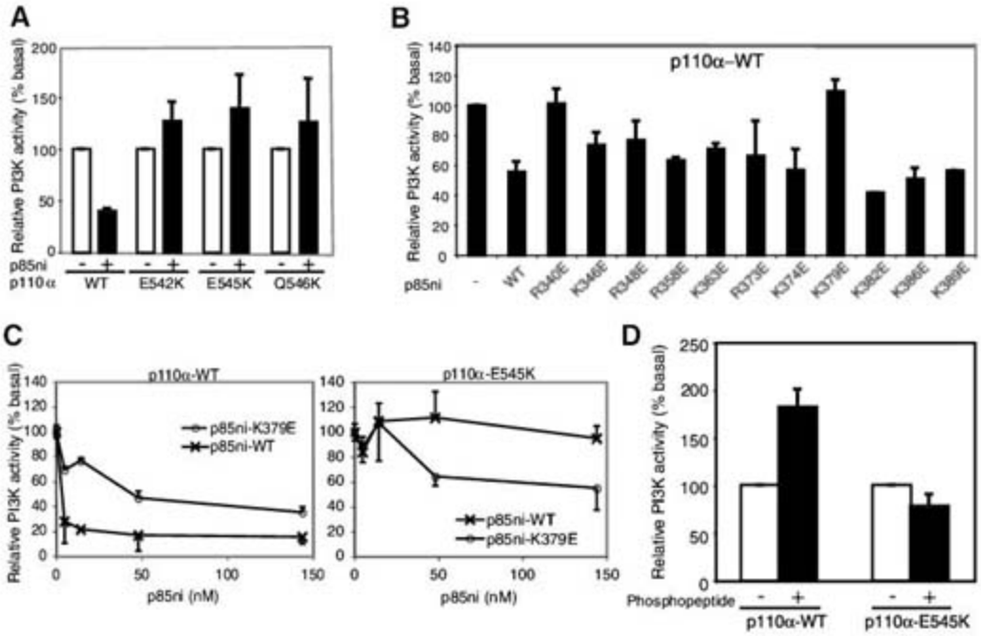

Fig. 3. Helical domain oncogenic mutants of p110α eliminate an autoinhibitory contact with the p85 nSH2 domain. (**A**) PI3K activity of the three p110α helical domain mutants was not inhibited by the p85ni fragment. Equal amounts of protein were assayed and the catalytic subunits had similar specific activities (fig. S3) (*25*). WT, wild type. (**B**) Charge-reversal mutagenesis screening of basic surface residues in the nSH2. (**C**) Simultaneous charge-reversal in p110α and p85ni restored inhibition, suggesting direct interaction between the p110α helical domain and the p85α nSH2 domain. A titration series was carried out for both the wild-type (left) and E545K mutant (right) p110 subunits to ascertain that the inhibition was at saturating levels of p85ni. (**D**) Binding of IRS-1 phosphotyrosine peptide activates wild-type p110α/p85ni but not p110-E545K/p85ni (*25*). [(A) to (D)] Lipid kinase assays were performed with Myc-p110α produced in transfected human embryonic kidney 293 cells (A) or baculovirus-infected Sf9 cells [(B) to (D)], incubated with or without excess p85ni [expressed in *Escherichia coli* (*25*)]. Basal activity refers to p110α activity in the absence of p85ni. Results are means from three to four experiments [(A) and (B)] or are representative of two experiments, each carried out in triplicate [(C) and (D)].

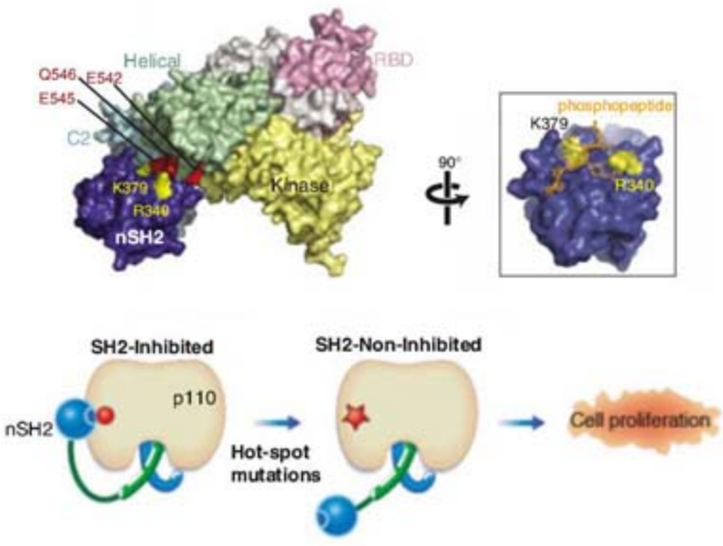

Fig. 4. A model showing the inhibitory contact between the nSH2 domain and the helical domain of p110α near the site of the helical domain hotspot mutations. [The p110α catalytic core was modeled on the p110γ catalytic core (*24*).] Arg^{340} and Lys^{379} are part of a highly conserved phosphopeptide-binding surface on nSH2. Binding of nSH2 to the p110α helical domain and to phosphopeptide are mutually exclusive (boxed image).

References and Notes

1. L. C. Cantley, *Science* **296**, 1655 (2002).
2. B. Vanhaesebroeck *et al.*, *Annu. Rev. Biochem.* **70**, 535 (2001).
3. M. P. Wymann, M. Zvelebil, M. Laffargue, *Trends Pharmacol. Sci.* **24**, 366 (2003).
4. J. Luo, B. D. Manning, L. C. Cantley, *Cancer Cell* **4**, 257 (2003).
5. L. H. Saal *et al.*, *Cancer Res.* **65**, 2554 (2005).
6. R. Wetzker, C. Rommel, *Curr. Pharm. Des.* **10**, 1915 (2004).
7. M. P. Wymann, R. Marone, *Curr. Opin. Cell Biol.* **17**, 141 (2005).
8. P. Workman, *Biochem. Soc. Trans.* **32**, 393 (2004).
9. B. Geering, P. R. Cutillas, G. Nock, S. I. Gharbi, B. Vanhaesebroeck, *Proc. Natl. Acad. Sci. U.S.A.* **104**, 7809 (2007).
10. J. Yu *et al.*, *Mol. Cell. Biol.* **18**, 1379 (1998).
11. K. Okkenhaug, B. Vanhaesebroeck, *Sci. STKE* **2001**, pe1 (2001).
12. C. Jimenez, C. Hernandez, B. Pimentel, A. C. Carrera, *J. Biol. Chem.* **277**, 41556 (2002).

13. C. L. Carpenter *et al.*, *J. Biol. Chem.* **268**, 9478 (1993).
14. R. Dhand *et al.*, *EMBO J.* **13**, 511 (1994).
15. J. Yu, C. Wjasow, J. M. Backer, *J. Biol. Chem.* **273**, 30199 (1998).
16. Y. Samuels *et al.*, *Science* **304**, 554 (2004).
17. A. G. Bader, S. Kang, L. Zhao, P. K. Vogt, *Nat. Rev. Cancer* **5**, 921 (2005).
18. S. Kang, A. G. Bader, P. K. Vogt, *Proc. Natl. Acad. Sci. U.S.A.* **102**, 802 (2005).
19. T. Ikenoue *et al.*, *Cancer Res.* **65**, 4562 (2005).
20. S. J. Isakoff *et al.*, *Cancer Res.* **65**, 10992 (2005).
21. M. Gymnopoulos, M. A. Elsliger, P. K. Vogt, *Proc. Natl. Acad. Sci. U.S.A.* **104**, 5569 (2007).
22. L. Stephens, R. Williams, P. Hawkins, *Curr. Opin. Pharmacol.* **5**, 357 (2005).
23. L. Pirola *et al.*, *J. Biol. Chem.* **276**, 21544 (2001).
24. E. H. Walker, O. Perisic, C. Ried, L. Stephens, R. L. Williams, *Nature* **402**, 313 (1999).
25. Materials and methods are available as supporting material on *Science* Online.
26. Z. Fu, E. Aronoff-Spencer, J. M. Backer, G. J. Gerfen, *Proc. Natl. Acad. Sci. U.S.A.* **100**, 3275 (2003).
27. W. Elis, E. Lessmann, M. Oelgeschlager, M. Huber, *Biol. Chem.* **387**, 1567 (2006).
28. Single-letter abbreviations for the amino acid residues are as follows: A, Ala; C, Cys; D, Asp; E, Glu; F, Phe; G, Gly; H, His; I, Ile; K, Lys; L, Leu; M, Met; N, Asn; P, Pro; Q, Gln; R, Arg; S, Ser; T, Thr; V, Val; W, Trp; and Y, Tyr.
29. M. Landau *et al.*, *Nucleic Acids Res.* **33**, W299 (2005).
30. S. C. Shekar *et al.*, *J. Biol. Chem.* **280**, 27850 (2005).
31. R. T. Nolte, M. J. Eck, J. Schlessinger, S. E. Shoelson, S. C. Harrison, *Nat. Struct. Biol.* **3**, 364 (1996).
32. We thank M. Waterfield and B. Vanhaesebroeck for the p110α plasmid, A. McCarthy for help at European Synchrotron Radiation Facility beamline ID14-4, and M. Girvin and G. Gerfen for helpful discussions. The work was supported by AstraZeneca (R.L.W.), Medical Research Council (R.L.W.), and NIH GM55692 (J.M.B.).

Supporting Online Material

www.sciencemag.org/cgi/content/full/317/5835/239/DC1
Materials and Methods
Figs. S1 to S5
Table S1
References

21 September 2006; accepted 31 May 2007
10.1126/science.1135394

Postreplicative Formation of Cohesion Is Required for Repair and Induced by a Single DNA Break

Lena Ström,[1] Charlotte Karlsson,[1] Hanna Betts Lindroos,[1] Sara Wedahl,[1] Yuki Katou,[2] Katsuhiko Shirahige,[2] Camilla Sjögren[1]*

Sister-chromatid cohesion, established during replication by the protein complex cohesin, is essential for both chromosome segregation and double-strand break (DSB) repair. Normally, cohesion formation is strictly limited to the S phase of the cell cycle, but DSBs can trigger cohesion also after DNA replication has been completed. The function of this damage-induced cohesion remains unknown. In this investigation, we show that damage-induced cohesion is essential for repair in postreplicative cells in yeast. Furthermore, it is established genome-wide after induction of a single DSB, and it is controlled by the DNA damage response and cohesin-regulating factors. We thus define a cohesion establishment pathway that is independent of DNA duplication and acts together with cohesion formed during replication in sister chromatid–based DSB repair.

The tethering of sister chromatids by the cohesin complex, so called sister-chromatid cohesion, is essential for chromosome segregation (*1*). Cohesin consists of Smc1, Smc3, Mcd1 (also called Scc1), and Scc3 and is loaded onto chromosomes before replication by Scc2 and Scc4 (*2*). The establishment of cohesion requires Eco1 (also called Ctf7) and occurs in the S phase of the unchallenged cell cycle (*3*–*8*). Cohesion then persists until anaphase, when it is resolved by proteolytic cleavage of Mcd1, which is triggered by the degradation of Pds1 (*9*–*11*). In addition to its central role in chromosome segregation, replication-established cohesion is needed for double-strand break (DSB) repair in postreplicative cells (*12*). Cohesin also has to be recruited to the site of damage for efficient repair (*13*, *14*), and de novo cohesion is established in G_2/M cells exposed to ionizing irradiation (*13*). This raises the possibility that chromatid-based DSB repair requires both cohesion formed during replication and postreplicative damage-induced cohesion. It also challenges present concepts that cohesion establishment is tightly connected to chromosome duplication. Therefore, we investigated how damage-induced cohesion is regulated and resolved its function in DSB repair and chromosome segregation.

Central to our investigations are experimental systems in which damage-induced cohesion can be distinguished from cohesion formed during replication (fig. S1, A to C). In one of these systems, *smc1-259* temperature-sensitive cells are first arrested in G_2/M at permissive temperature. Thereafter, temperature-resistant, damage-induced cohesion is generated by the expression of wild-type (WT) *SMC1* and treatment with γ-irradiation (Fig. 1, A and B, and fig. S1A) (*13*). We first ascertained that our results were not influenced by the absence of a mitotic spindle in nocodazole-arrested cells (Fig. 1, A and B). Thereafter, we investigated the function of central DNA damage-response proteins in damage-induced cohesion. Mre11 is one of the first proteins that localizes at a DSB (*15*) and is essential for the recruitment of cohesin to the damage (*14*, *16*). Accordingly, damage-induced cohesion was compromised in *mre11Δ* cells (Fig. 1C) (*17*). Other regulators of the DNA damage response that influence cohesin's break localization are the Tel1 and Mec1 kinases, which phosphorylate histone 2A (H2A) (in humans, H2AX) (*14*, *18*). Phosphorylated H2A (γ-H2A) marks the DSB and is required for DSB recruitment of cohesin (*14*). Correspondingly, the formation of damage-induced cohesion was defective in cells lacking Tel1 or Mec1 or in cells expressing nonphosphorylatable H2A (Fig. 1, D to F). However, in the absence of Tel1 or Mec1, substantial amounts of γ-H2A and cohesin still accumulate at a DSB because of the overlapping function of the other kinase (*14*, *18*). This indicates that Tel1 and/or Mec1 could influence cohesion in a way other than through γ-H2A–dependent recruitment of cohesin. The two kinases also activate Rad9, which in turn transmits the signal to downstream events in the DNA damage response (*19*–*21*). Damage-induced cohesion was, however, unaffected in *rad9Δ* cells (Fig. 1G), showing that if Mec1 and/or Tel1 affect damage-induced cohesion independently of cohesin recruitment, this pathway does not include the activation of Rad9.

To determine whether replication induced by the repair process influences cohesion, we investigated damage-induced cohesion in *rad52Δ* cells. Rad52 facilitates the direct interaction between the DNA flanking a DSB and an undamaged homologous template, which is essential for eliciting DNA synthesis at the break (*22*, *23*). Therefore, the unperturbed formation of cohesion in *rad52Δ* cells (Fig. 1F) shows that, in contrast to the establishment process in unchallenged cells, damage-induced cohesion is independent of ongoing DNA duplication (*17*).

We observed chromatid separation in a limited region of chromosome V (chr. V) that experiences roughly one DSB per cell at the irradiation dose applied (*13*). Because cohesin is recruited to only 50 to 100 kb around the DSB (*13*, *14*), the γ-ray–induced cohesion suggests a more general activation of cohesin (Fig. 1, A and B). To investigate whether a single genomic DSB triggers cohesion, we used an uncleavable

[1]Department of Cell and Molecular Biology, Karolinska Institute, 171 77 Stockholm, Sweden. [2]Gene Research Centre, Tokyo Institute of Technology, 4259 Nagatsuta, Midori-ku, 226-8501 Yokohama, Japan.

*To whom correspondence should be addressed. E-mail: camilla.sjogren@ki.se

variant of Mcd1 (Mcd1^{UNCL}) that blocks chromatid separation at anaphase when it is present in cohesion-forming complexes (*10*, *24*) (fig. S1C). When Mcd1^{UNCL} was expressed alone in G_2/M-arrested cells, chr. V separated normally during a release from the arrest. In contrast, chr. V separation did not occur when Mcd1^{UNCL} expression was combined with the induction of a homothallic switching (HO)–endonuclease that creates a DSB at the *MAT* locus on chr. III (Fig. 2, A to C). This inhibition was not due to a cell-cycle delay caused by the break, because Pds1 levels declined concomitantly in both cell populations (Fig. 2B), and HO expression alone left chromatid separation unperturbed (Fig. 2, D and E). Moreover, HO overexpression did not generate DSBs at unspecific sites in the genome, because the chromatids separated normally after the induction of HO and Mcd1^{UNCL} in *MATΔ* cells (Fig. 2, D and E). As a control of Mcd1^{UNCL} function, its chromosomal localization after expression in G_2/M was determined and shown to be identical to normally expressed Mcd1 (fig. S2) (*8*). This finding establishes that a break on chr. III triggers the formation of cohesion on chr. V, demonstrating that a single DSB reactivates cohesion in a genome-wide manner.

We next investigated how genome-wide cohesion is regulated using G_2/M-arrested temperature-sensitive *smc1-259* cells in which WT *SMC1* and a DSB on chr. III was induced before an upshift in temperature (fig. S1B). This experiment showed that "global" cohesion depends on Mec1 and partly on Tel1 and γ-H2A, but not on Rad9 (Fig. 3, A and B, and fig. S3A). In cells lacking γ-H2A, no cohesin is recruited to damaged chromosomes, but cohesion is only partly defective when compared with *mec1Δ* cells (*14*). This observation indicates that Mec1 is required for more than cohesin localization and could be a key factor in the transmission of a signal from damaged to undamaged chromosomes. If so, this transmission is achieved in a Rad9-independent manner. The partial requirement

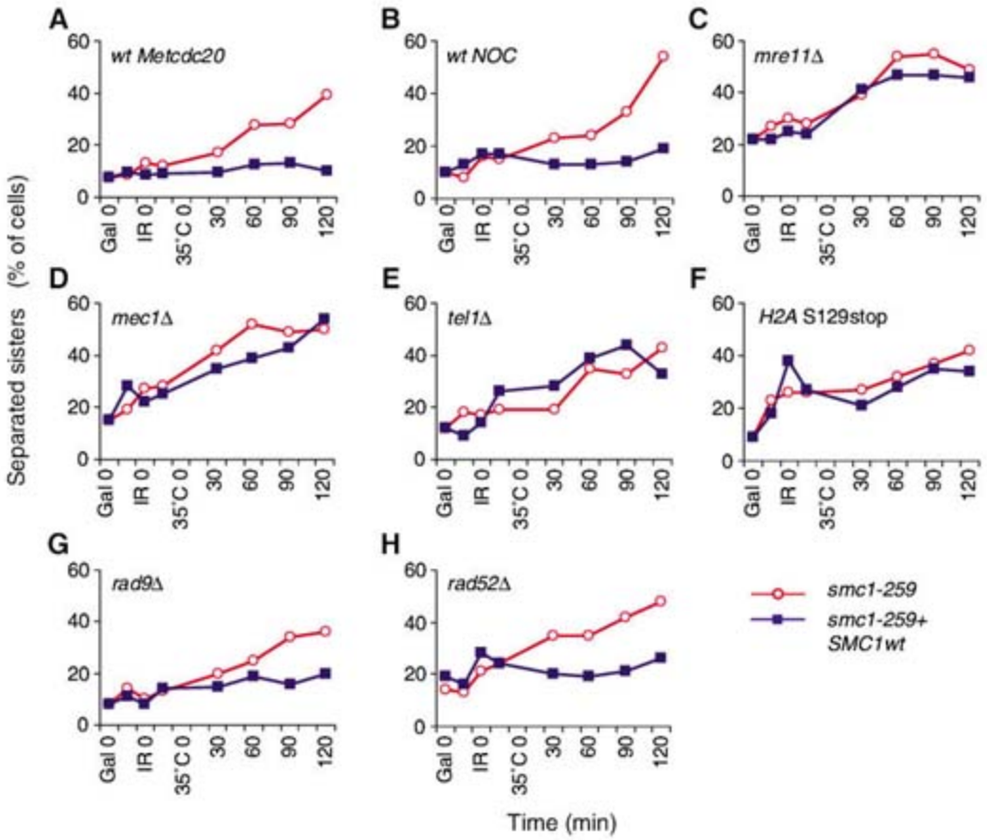

Fig. 1. Mre11, Mec1, Tel1, and γH2A, but not Rad9 and Rad52, are required for γ-ray–induced cohesion. (**A** to **H**) Chromatid separation at *URA3* on chr. V in G_2/M-arrested cells after γ-irradiation and destruction of S phase–established cohesion, as described in fig. S1A. (A) Chromatid separation in Cdc20-depleted G_2/M-arrested *smc1-259*, *GAL:SMC1-13MYC*, *MET:CDC20* cells (CB496). (B to H) Chromatid separation in nocodazole G_2/M-arrested (B) *smc1-259*, *GAL:SMC1-13MYC* cells (CB469), combined with (C) *mre11Δ* (CB478), (D) *mec1Δ* (CB784), (E) *tel1Δ* (CB693), (F) *hta1-S129stop*, *hta2-129stop* (CB742), (G) *rad9Δ* (CB696), or (H) *rad52Δ* (CB571). Gal, galactose addition; IR, irradiation.

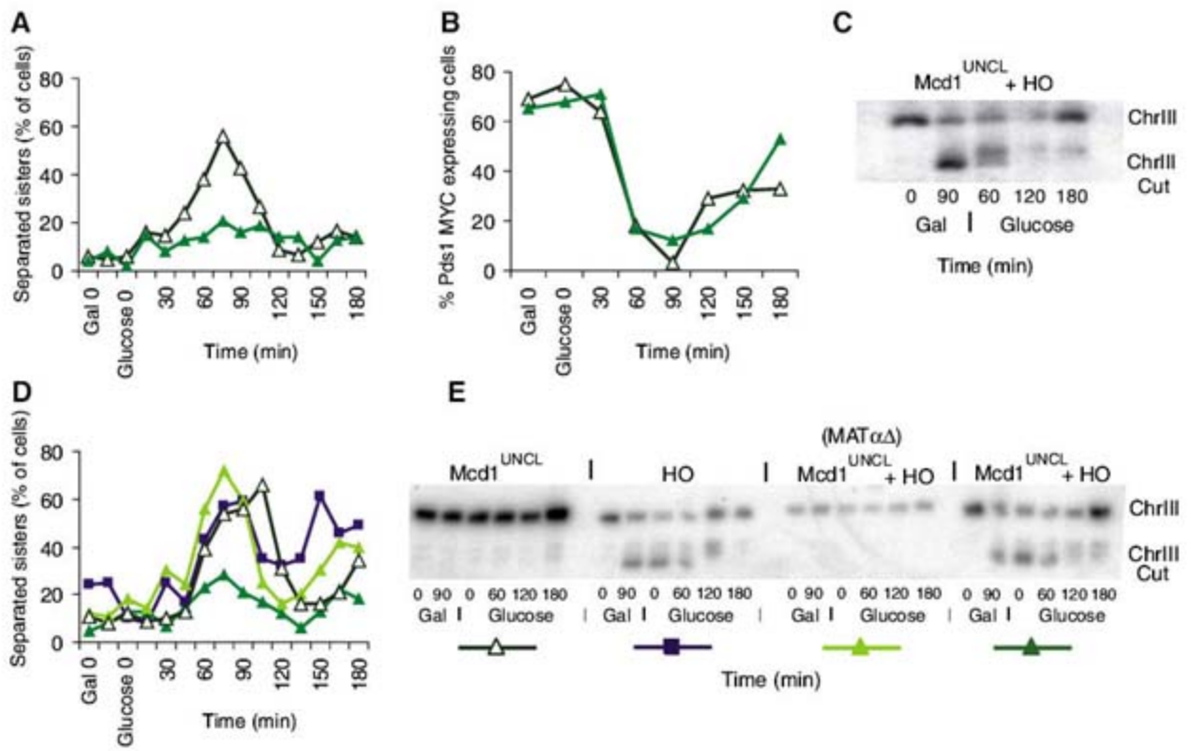

Fig. 2. A single DSB on chr. III leads to establishment of cohesion on chr. V. MCD1^{UNCL} was induced in G/M-arrested cells, with or without a concomitant DSB on chr. III. Cells were thereafter released into the next cell cycle under non-inducing conditions (fig. S1C). Chromatid separation at *URA3* on chr. V, the percentage of Pds1-positive cells, and chr. III breakage were determined. (**A**) Sister-chromatid separation in *GAL:MCD1*^{UNCL}, *PDS1-18MYC* cells without (CB699) or with *GAL:HO* (CB507). (**B**) Pds1-positive cells in (A). (**C**) Southern blot of chr. III isolated from cells examined in (A). (**D**) Sister-chromatid separation in *GAL:MCD1* (CB699), *GAL:MCD1 GAL:HO* (CB507), *GAL:HO* (CB524), or *MCD1*^{UNCL} *GAL:HO mat*Δ (CB586). (**E**) Analysis of chr. III in cells examined in (D).

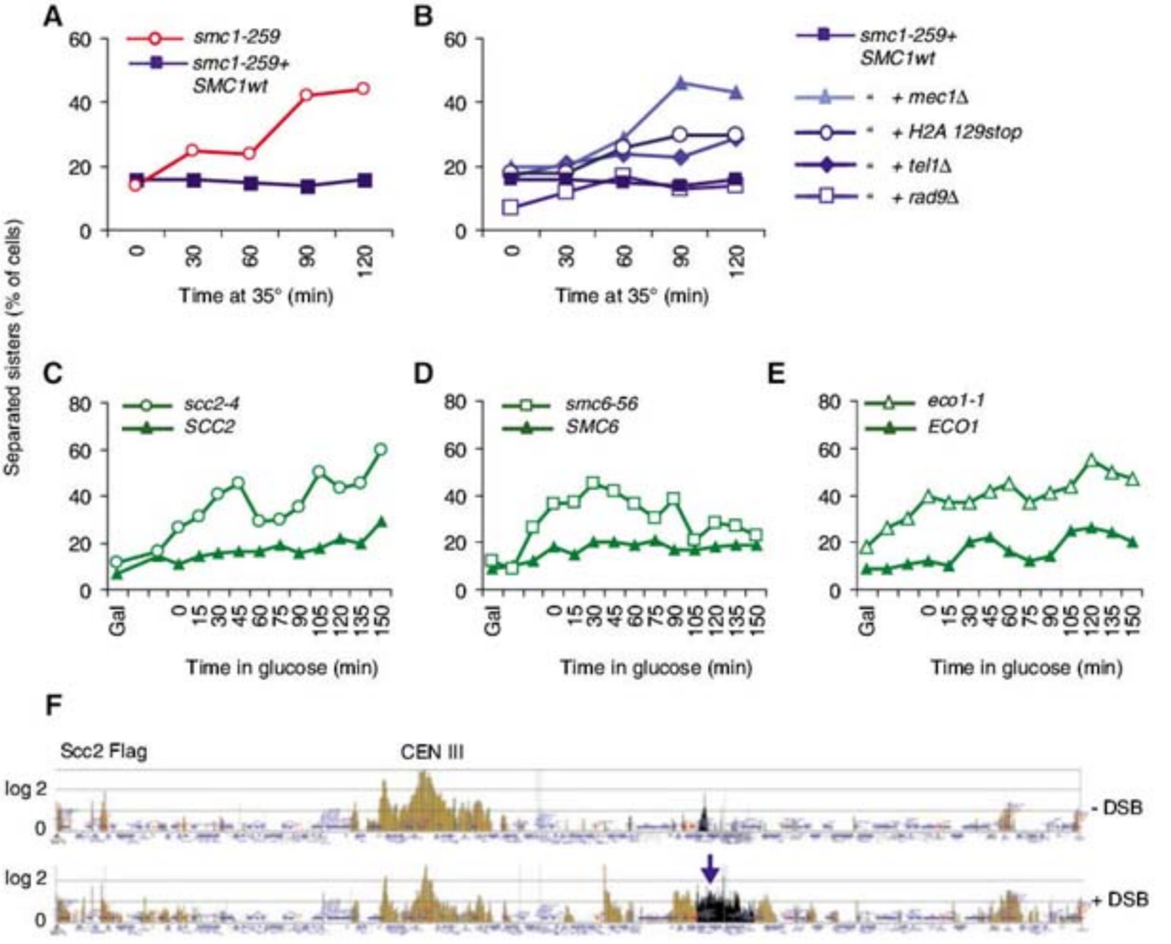

Fig. 3. Genome-wide cohesion depends both on the DNA damage response and on proteins regulating cohesin function. (**A** and **B**) Chr. V chromatid separation in G2/M-arrested cells after removal of S phase–established cohesion, in the absence or presence of a DSB on chr. III, as described in fig. S1B. (A) Chromatid separation in *smc1-259*, *GAL:HO* (CB583), and *smc1-259 GAL:SMC1-13MYC GAL:HO* (CB479). (B) Chromatid separation in *smc1-259*, *GAL:SMC1-13MYC*, *GAL:HO* cells (CB479), combined with *tel1*Δ (CB815), *mec1*Δ (CB753), *hta1-S129stop, hta2-129stop* (CB740), or *rad9*Δ (CB813). DSB formation on chr. III is shown in fig. S3A (**C** to **E**) Chromatid separation of chr. V in cells containing *GAL:MCD1*^{UNC1} and *GAL:HO*. The experiments were performed as in Fig. 2 and fig. S1C, with the exception that the temperature was up-shifted 30 min after the addition of galactose. (C) Wild type (CB507) and *scc2-4* (CB573), (D) wild type and *smc6-56* (CB537), and (E) wild type and *eco1-1* (CB732). (**F**) Chip-on-chip analysis of Scc2 localization on chr. III in the absence (–DSB) or presence (+DSB) of a DSB at the *MAT* locus. Arrow indicates a DSB. CENIII, chr. III centromere.

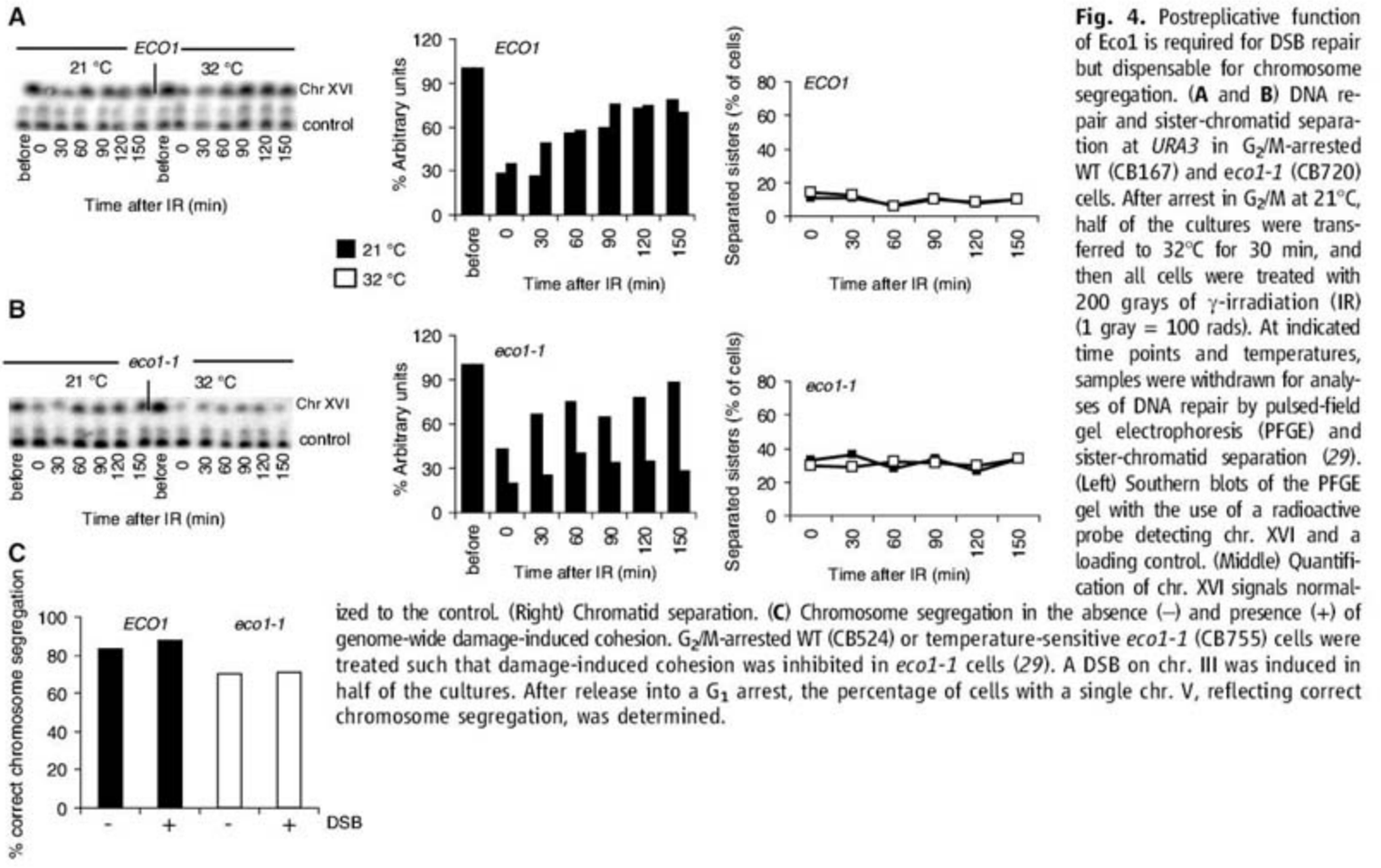

Fig. 4. Postreplicative function of Eco1 is required for DSB repair but dispensable for chromosome segregation. (**A** and **B**) DNA repair and sister-chromatid separation at *URA3* in G_2/M-arrested WT (CB167) and *eco1-1* (CB720) cells. After arrest in G_2/M at 21°C, half of the cultures were transferred to 32°C for 30 min, and then all cells were treated with 200 grays of γ-irradiation (IR) (1 gray = 100 rads). At indicated time points and temperatures, samples were withdrawn for analyses of DNA repair by pulsed-field gel electrophoresis (PFGE) and sister-chromatid separation (*29*). (Left) Southern blots of the PFGE gel with the use of a radioactive probe detecting chr. XVI and a loading control. (Middle) Quantification of chr. XVI signals normalized to the control. (Right) Chromatid separation. (**C**) Chromosome segregation in the absence (–) and presence (+) of genome-wide damage-induced cohesion. G_2/M-arrested WT (CB524) or temperature-sensitive *eco1-1* (CB755) cells were treated such that damage-induced cohesion was inhibited in *eco1-1* cells (*29*). A DSB on chr. III was induced in half of the cultures. After release into a G_1 arrest, the percentage of cells with a single chr. V, reflecting correct chromosome segregation, was determined.

for Tel1 and γ-H2A in global cohesion could be due to a function in amplifying the signal emanating from the DSB (*25*). Such a function of γ-H2A is supported by our finding that it covers the entire chr. III after the prolonged break induction that we used in our experiments, but is absent on undamaged chromosomes (fig. S3B).

We also explored the role of cohesin-regulating proteins in genome-wide cohesion by scoring chr. V separation after the induction of Mcd1^{UNCL} and a DSB on chr. III in temperature-sensitive *scc2-4*, *smc6-56*, or *eco1-1* cells. These experiments showed that Scc2, Smc6, and Eco1 are required for global cohesion (Fig. 3, C to E, and fig. S3C).

The prerequisite of Scc2 reveals that genome-wide formation of cohesion requires the loading of cohesin to chromosomes. Loading in G_2/M occurs also in the absence of DNA damage, and the cohesins present on chromosomes in this cell-cycle phase are thus a mixture of cohesive and noncohesive complexes (*8*). Our findings indicate that a DSB triggers an alteration of cohesin or its effectors that activate the cohesive function of the normally unproductive complexes. We investigated whether this is reflected by a change in the localization of Scc2 on undamaged chromosomes, but found that HO expression only induced its accumulation at the DSB (Fig. 3F). This is true also for cohesin (*13*), showing that genome-wide cohesion is generated without positional changes of cohesin or its loader in undamaged regions of the genome.

The Smc6 protein is part of the cohesin-related Smc5/6 complex, which also is required for sister-chromatid repair, and regulates the localization of cohesin to DNA breaks in human cells (*26*, *27*). In yeast, however, the chromosomal association of Mcd1 was unaltered after the destruction of *smc6-56* function in G_2/M-arrested cells (fig. S3D). This suggests that the requirement of Smc6 for genome-wide cohesion reflects a more direct influence on cohesin function, which is in accordance with the similar chromosomal localization patterns of cohesin and the Smc5/6 complex (*28*).

The finding that Eco1 is required for genome-wide cohesion shows that it can act independently of chromosome replication. It also indicates that the damage response removes an inhibitory mechanism and/or reactivates Eco1, thereby allowing cohesion formation in postreplicative cells. Because the *eco1-1* mutation leaves the chromosomal association of cohesin unaffected (fig. S4) (*4*), we examined whether the establishment of damage-induced cohesion and not only chromosomal loading of cohesin is needed for repair (*12*, *29*). The results showed that Eco1, and consequently damage-induced cohesion, is required for postreplicative DSB repair (Fig. 4, A and B). In contrast, the absence of damage-induced cohesion did not interfere with segregation in the presence of functional replication-established cohesion (Fig. 4C). Thus, a possible explanation for genome-wide cohesion is that postreplicative repair requires cohesion at a DSB, and this is achieved by a global activation of the cohesion machinery, leading to de novo cohesion on all chromosomes.

Our investigation characterizes an additional pathway for cohesion establishment that is crucial for DSB repair in postreplicative cells. This pathway generates cohesion on undamaged chromosomes in response to a single DSB, suggesting that the break triggers a diffusible signaling event that activates cohesin and/or Eco1 via Mec1. Consequently, the establishment of cohesion is not limited to active replication forks and has to occur both before and after DSB formation to repair broken sister chromatids.

References and Notes

1. K. Nasmyth, C. H. Haering, *Annu. Rev. Biochem.* **74**, 595 (2005).
2. R. Ciosk *et al.*, *Mol. Cell* **5**, 243 (2000).
3. R. V. Skibbens, L. B. Corson, D. Koshland, P. Hieter, *Genes Dev.* **13**, 307 (1999).
4. A. Toth *et al.*, *Genes Dev.* **13**, 320 (1999).
5. F. Uhlmann, K. Nasmyth, *Curr. Biol.* **8**, 1095 (1998).
6. M. A. Kenna, R. V. Skibbens, *Mol. Cell. Biol.* **23**, 2999 (2003).
7. G. L. Moldovan, B. Pfander, S. Jentsch, *Mol. Cell* **23**, 723 (2006).
8. A. Lengronne *et al.*, *Mol. Cell* **23**, 787 (2006).
9. O. Cohen-Fix, D. Koshland, *Genes Dev.* **13**, 1950 (1999).
10. F. Uhlmann, F. Lottspeich, K. Nasmyth, *Nature* **400**, 37 (1999).
11. F. Uhlmann, D. Wernic, M. A. Poupart, E. V. Koonin, K. Nasmyth, *Cell* **103**, 375 (2000).
12. C. Sjögren, K. Nasmyth, *Curr. Biol.* **11**, 991 (2001).
13. L. Ström, H. B. Lindroos, K. Shirahige, C. Sjögren, *Mol. Cell* **16**, 1003 (2004).
14. E. Ünal *et al.*, *Mol. Cell* **16**, 991 (2004).
15. M. Lisby, J. H. Barlow, R. C. Burgess, R. Rothstein, *Cell* **118**, 699 (2004).
16. J. S. Kim, T. B. Krasieva, V. LaMorte, A. M. Taylor, K. Yokomori, *J. Biol. Chem.* **277**, 45149 (2002).
17. E. Ünal, J. M. Heidinger-Pauli, D. Koshland, *Science* **317**, 245 (2007).
18. R. Shroff *et al.*, *Curr. Biol.* **14**, 1703 (2004).
19. R. T. Blankley, D. Lydall, *J. Cell Sci.* **117**, 601 (2004).
20. Y. Sanchez *et al.*, *Science* **286**, 1166 (1999).
21. J. E. Vialard, C. S. Gilbert, C. M. Green, N. F. Lowndes, *EMBO J.* **17**, 5679 (1998).
22. P. Sung, *J. Biol. Chem.* **272**, 28194 (1997).
23. L. Krejci *et al.*, *J. Biol. Chem.* **277**, 40132 (2002).
24. L. Ström, C. Sjögren, *Cell Cycle* **4**, 536 (2005).
25. M. Stucki, S. P. Jackson, *DNA Repair (Amsterdam)* **5**, 534 (2006).
26. G. De Piccoli *et al.*, *Nat. Cell Biol.* **8**, 1032 (2006).
27. P. R. Potts, M. H. Porteus, H. Yu, *EMBO J.* **25**, 3377 (2006).
28. H. B. Lindroos *et al.*, *Mol. Cell* **22**, 755 (2006).
29. Supporting material is available on *Science* Online.

30. We thank K. Nasmyth, F. Uhlmann, N. Lowndes, M. Grenon, and J. Downs for providing yeast strains; A. Verreault for γH2a antibodies; C. Höög for support; and D. Koshland for communicating unpublished results. For financial support, please see the supporting online material.

Supporting Online Material

www.sciencemag.org/cgi/content/full/317/5835/242/DC1
Materials and Methods
SOM Text
Figs. S1 to S4
References

31 January 2007; accepted 31 May 2007
10.1126/science.1140649

DNA Double-Strand Breaks Trigger Genome-Wide Sister-Chromatid Cohesion Through Eco1 (Ctf7)

Elçin Ünal,[1,2] Jill M. Heidinger-Pauli,[1,2] Douglas Koshland[1]*

Faithful chromosome segregation and repair of DNA double-strand breaks (DSBs) require cohesin, the protein complex that mediates sister-chromatid cohesion. Cohesion between sister chromatids is thought to be generated only during ongoing DNA replication by an obligate coupling between cohesion establishment factors such as Eco1 (Ctf7) and the replisome. Using budding yeast, we challenge this model by showing that cohesion is generated by an Eco1-dependent but replication-independent mechanism in response to DSBs in G_2/M. Furthermore, our studies reveal that Eco1 has two functions: a cohesive activity and a conserved acetyltransferase activity, which triggers the generation of cohesion in response to the DSB and the DNA damage checkpoint. Finally, the DSB-induced cohesion is not limited to broken chromosomes but occurs also on unbroken chromosomes, suggesting that the DNA damage checkpoint through Eco1 provides genome-wide protection of chromosome integrity.

A fundamental property of the eukaryotic chromosomes is sister-chromatid cohesion. Cohesion plays a crucial role in chromosome segregation (*1*) as well as postreplicative repair of double-strand breaks (DSBs) (*2*) and is mediated by a large ring-shaped complex, cohesin, and its associated protein, Pds5 (*3*, *4*). In late G_1 of budding yeast, cohesin is loaded onto chromosomes by the Scc2/Scc4 complex (*5*). This loading occurs around centromeres and at cohesin-associated regions (CARs) along chromosome arms (*4*). During S

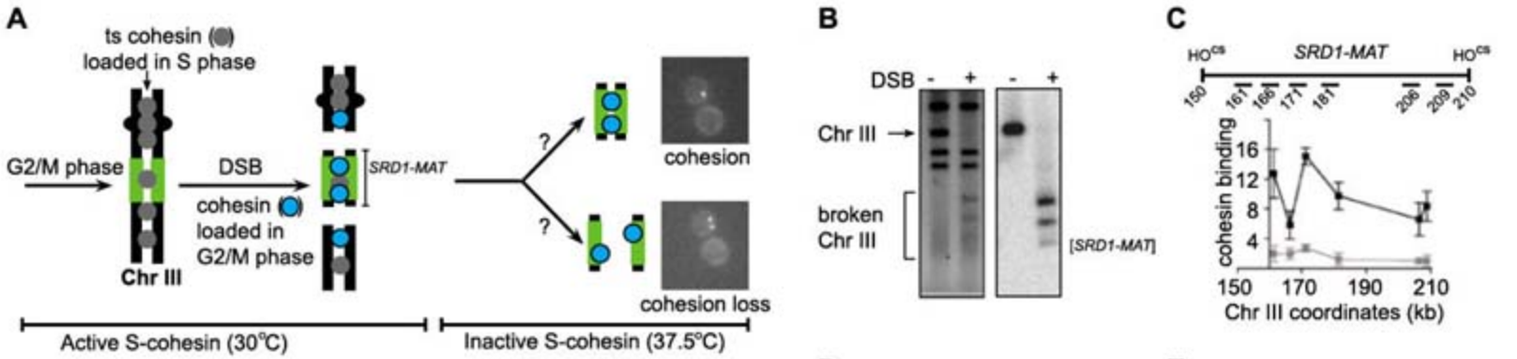

Fig. 1. DSB proximal cohesin generates sister-chromatid cohesion. (**A**) DSB-induced cohesion assay. See text and supporting online material (SOM) for details. (**B**) Chr. III cutting in EU3275 assayed by pulsed-field gel electrophoresis and Southern blotting. (**C**) Mcd1^{6HA} binding on *SRD1-MAT* fragment assayed by chromatin immunoprecipitation/real-time polymerase chain reaction. Gray squares: no DSB, black squares: DSB. Error bars indicate SD (n = 4). DSB-induced cohesion assay in (**D**) EU3275 and (**E**) EU3274 and EU3278. In (D) and (E) and subsequent figures, the genotype and location of the cohesion reporter are shown above each plot. Detailed information on strain genotypes are in table S1. a, active; i, inactive; ts, temperature-sensitive; HA, hemagglutinin. Error bars indicate SD (n = 3).

phase, Eco1 (also known as Ctf7) acts on the chromatin-bound cohesin complex to generate cohesion by an unknown mechanism (*6*, *7*).

The generation of cohesion is limited to S phase in undamaged cells (*8*–*10*). This limitation cannot be explained by regulating the association of cohesins with chromosomes because they continue to load onto chromosomes at CARs in G_2/M by an Scc2/Scc4-dependent mechanism (*8*). To explain this limitation, one model posits that cohesin can generate cohesion only by a replication-driven mechanism, facilitated by Eco1 (*8*) (herein called replication fork–driven cohesion model). The absence of a replication fork in G_2/M prevents cohesion generation. However, cohesion is generated in G_2/M upon irradiation (*9*) and was inferred to be mediated by cohesin loaded de novo around DSBs by a mechanism dependent on the DNA damage checkpoint (*9*, *11*, *12*). In the replication fork–driven cohesion model, a fork should be necessary for DSB-induced cohesion as well. Indeed, replication forks do occur at DSBs as part of the recombination-repair pathway.

To determine whether DNA replication is required for DSB-induced cohesion, we developed an assay to detect cohesion of specific regions on chromosomes in response to defined DSBs (Fig. 1A). This assay has three properties: First, formation of DSBs on the chromosomes is temporally and spatially controlled by placing the site-specific HO endonuclease under the control of an inducible promoter and by introducing two HO cleavage sites (HO-cs) on chromosome III (chr. III). One HO-cs is upstream of *SRD1* and the second site is 60 kb away at *MAT* locus. After 1 hour of HO induction, chr. III (>90%) is broken into three pieces: the 60-kb *SRD1-MAT* fragment and two larger fragments (Fig. 1B). Second, cohesion of specific sites in the genome is detected by a cohesion reporter consisting of a tandem array of Lac operators (LacO) that can be visualized by LacI–green fluorescent protein (LacI-GFP). A single GFP spot in the cell indicates cohesion between the broken chromatid pairs, whereas two GFP spots indicate cohesion loss (Fig. 1A, right panel). Third, de novo DSB-induced cohesion is distinguished from the cohesion established during S phase. S-phase cohesion is established by the use of a thermosensitive cohesin subunit, mcd1-1 (referred to as S-cohesin). In G_2/M, wild-type Mcd1 (also known as Scc1) is expressed concomitant with induction of DSBs, and subsequently S-cohesin is inactivated (Fig. 1, A and C).

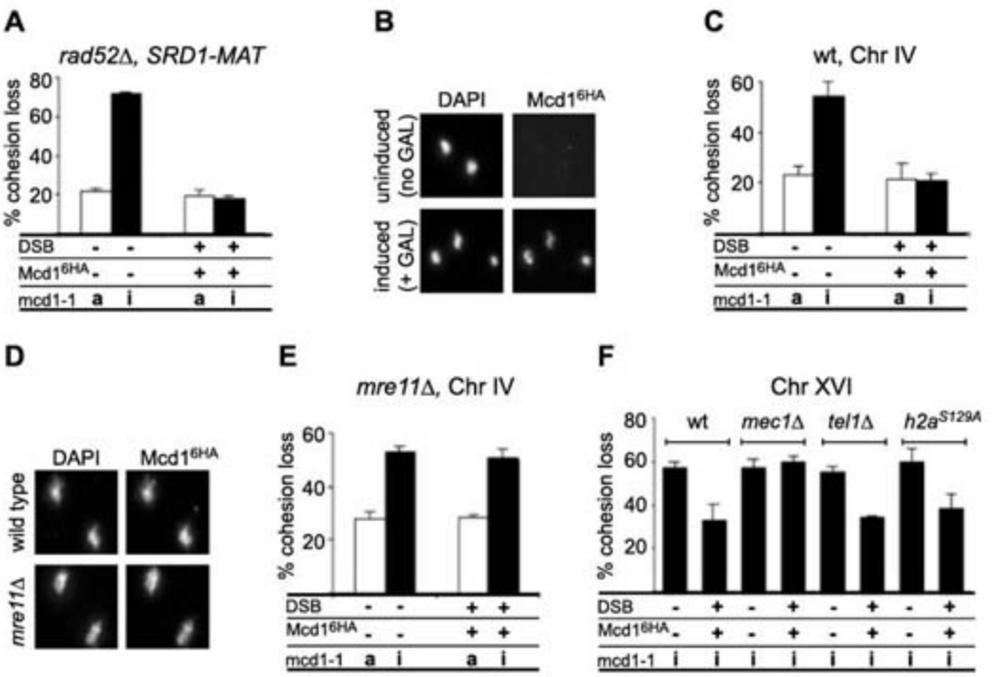

Fig. 2. DSB-induced cohesion is independent of DNA replication but is dependent on the DNA damage response pathway. DSB-induced cohesion assay in (**A**) EU3286, (**C**) EU3291, and (**E**) EU3321. Error bars indicate SD (n = 3). Chromosome binding of G_2/M-loaded cohesin in (**B**) EU3297, (**D**) EU3291, and EU3321. (**F**) DSB-induced cohesion assayed by fluorescence in situ hybridization in JH4112, JH4116, JH4115, and JH4117. See SOM for details.

[1]Carnegie Institution, Howard Hughes Medical Institute, Department of Embryology, 3520 San Martin Drive, Baltimore, MD 21218, USA. [2]Johns Hopkins University, Department of Biology, 3400 North Charles Street, Baltimore, MD 21218, USA.

*To whom correspondence should be addressed. E-mail: koshland@ciwemb.edu

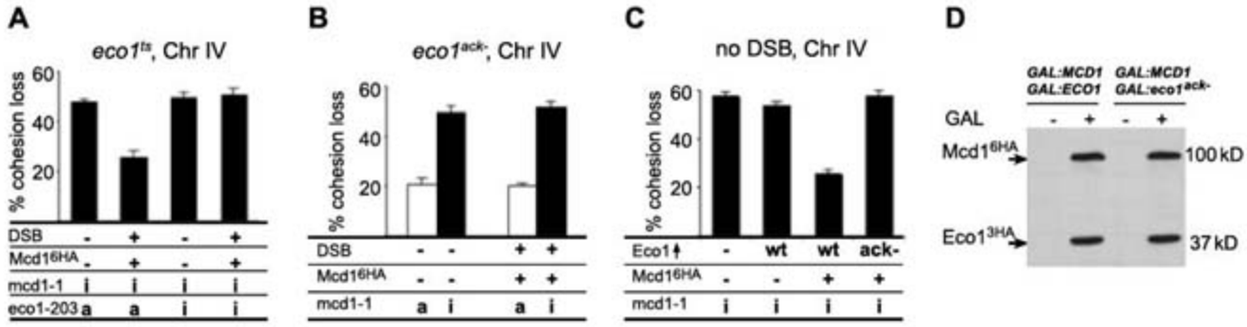

Fig. 3. Eco1 is necessary to generate cohesion in G_2/M and its acetyltransferase activity is required in response to DSBs. Cohesion assay in (**A**) EU3326, (**B**) EU3336, and (**C**) EU3307, EU3325, and EU3328. Arrow in (C) indicates overproduction. Error bars indicate SD (n = 3). (**D**) Immunoblot showing Mcd1^{6HA} and Eco1^{3HA} with or without galactose (GAL) induction in EU3307 and EU3328.

Using this assay, we asked whether cohesion can be generated in G_2/M in proximity of the DSB by following the cohesion of the *SRD1-MAT* region. Without DSBs, when S-cohesin is active (30°C, permissive temperature), ~20% of the chr. III sister chromatids are separated. As expected, upon inactivation of S-cohesin (37.5°C, nonpermissive temperature), >60% of chr. III sister chromatids separate (Fig. 1D). With DSBs, wild-type cohesin is loaded to the *SRD1-MAT* fragment (Fig. 1C), and this fragment retains cohesion upon the inactivation of S-cohesin (Fig. 1D). Both DSBs and wild-type cohesin are necessary, but neither is sufficient, to generate cohesion on the *SRD1-MAT* region in G_2/M (Fig. 1E). These results show that DSBs can induce cohesin-dependent cohesion in G_2/M, confirming that cohesion can be generated outside of S phase (*9*). In addition, these results show that as few as two DSBs are sufficient to induce cohesin-dependent cohesion in G_2/M.

The first prediction from the replication fork–driven cohesion model is that DSB-induced cohesion should require recombination-dependent replication. To test this prediction, we deleted *RAD52*. Rad52 is a prerequisite for recombination-dependent DNA replication (*13*). In *rad52*Δ cells, the extent of DSB-induced cohesion on *SRD1-MAT* fragment is indistinguishable from that of *RAD52* (Figs. 1D and 2A), indicating that recombination-dependent replication and/or DNA structures are dispensable for DSB-induced cohesion.

The second prediction from the replication fork–driven cohesion model is that DSB-induced cohesion should occur only around DSBs and not on unbroken chromosomes. To test cohesion on unbroken chromosomes, we moved the cohesion reporter to chr. IV or chr. I while keeping the HO-cs on chr. III. We found that the loss of cohesion on chr. IV and chr. I upon inactivation of S-phase cohesin is prevented by the induction of DSBs on chr. III (Fig. 2C and figs. S1 and S2, A and B). This generation of genome-wide cohesion cannot occur by a replication-dependent mechanism because there is no ongoing DNA replication on unbroken chromosomes in G_2/M.

How does a DSB in G_2/M induce sister-chromatid cohesion both proximal to the lesion and genome-wide? In G_2/M, in the absence of DSBs, cohesins load at CARs but cannot mediate cohesion (*8*–*10*). Upon DSBs, the DNA damage response pathway induces DSB-proximal cohesin loading (*11*). We posit that subsequently, cohesins loaded at CARs and DSBs becomes cohesive through the action of a critical factor that responds to cell cycle and DNA damage cues. In undamaged cells, this factor is active only during S phase. Hence, cohesins loaded at CARs in G_2/M cannot generate cohesion. However, in response to DSBs, this factor is reactivated by upstream components of the DNA damage response pathway to generate cohesion both proximal to the DSB and at CARs genome-wide.

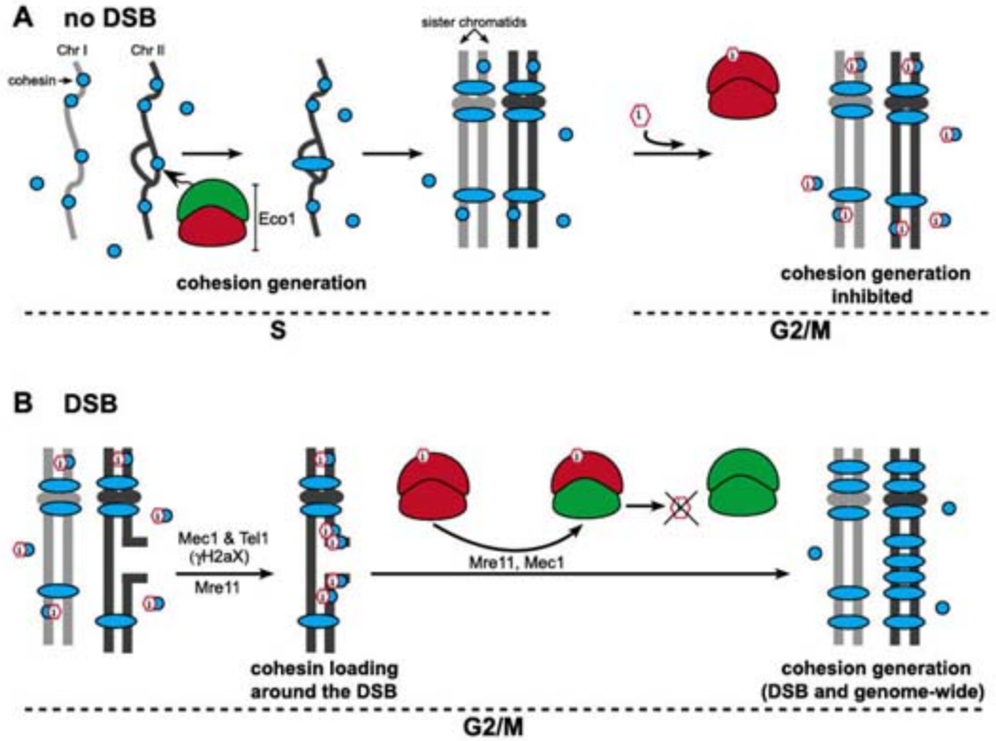

Fig. 4. (**A** and **B**) A model for cell-cycle and damage-induced regulation of sister-chromatid cohesion. Cohesin is represented in its noncohesive (circle) or cohesive (oval) state. (i) represents the inhibitor of cohesion generation in G_2/M. See text for details.

To identify the upstream components, we examined damage-induced cohesion in cells mutated for *MRE11*, *MEC1*/ATR (ataxia telangiectasia and Rad 3 related), *TEL1*/ATM (ataxia telangiectasia mutated), or *H2AX*. We were limited to analysis of genome-wide cohesion because only cohesin loading at CARs occurs independently of these factors (*11*) (Fig. 2D). In *mre11*Δ or *mec1*Δ cells, cohesion fails to form on chr. IV or on chr. XVI in response to DSBs on chr. III (Fig. 2, E and F). In contrast, neither Tel1 nor γ-H2AX is required for damage-induced cohesion (Fig. 2F and fig. S2C). Whereas all these factors are required for DSB-proximal cohesin loading, only Mre11 and Mec1 are also necessary for DSB-induced cohesion. Thus, the chromatin-bound cohesin complex is converted to a cohesive state by the DNA damage response pathway [also reported in (*14*)], presumably through a trans-acting factor.

A candidate for this trans-acting factor is Eco1 (Ctf7) because it is essential for cohesion establishment in S phase (*6*, *7*). To determine whether Eco1 is also necessary for DSB-induced cohesion, we first subjected G_2/M cells carrying both *eco1-203* and *mcd1-1* conditional alleles to a temperature shift (34°C), which inactivates only Eco1. After DSB induction, cells were subjected to a second, higher-temperature shift (37.5°C) to inactivate S-cohesin. We found that inactivation of Eco1 in G_2/M results in a failure to gen-

erate DSB-induced cohesion (Fig. 3A and fig. S3, A and B). In addition, impairment of Eco1 in G_2/M also compromises postreplicative repair, a process dependent on DSB-loaded cohesin (fig. S3C). Thus, Eco1 is necessary to generate sister-chromatid cohesion in G_2/M in response to DSBs as well as in S phase, suggesting that DSB-induced and S-phase cohesion occurs by a similar mechanism. Furthermore, these results suggest that Eco1 is the cohesion factor that is reactivated in response to DSBs.

One way of regulating Eco1 upon DSBs is through its C-terminal acetyltransferase (Ack) domain (*15*). Until now, the in vivo relevance of the Eco1 acetyltransferase domain has been elusive. It is dispensable for generating cohesion during S phase (*16*) (fig. S4A), suggesting that a distinct part of Eco1 is required for cohesion establishment. We asked whether the acetyltransferase activity of Eco1 is necessary for DSB-induced cohesion. We generated strains in which the sole copy of *ECO1* is replaced by *eco1*$^{R222G,\ K223G}$ (*eco1*$^{ack-}$) and monitored the cohesion of chr. III or chr. IV in response to DSBs. Similar to *eco1-203*, *eco1* $^{ack-}$ cells are compromised for DSB-induced cohesion (Fig. 3B and fig. S4, B to D) and for postreplicative repair in G_2/M (fig. S4E). These results show that Eco1 acetyltransferase activity is specifically required in G_2/M to generate DSB-induced cohesion. Furthermore, they suggest that Eco1 has at least two distinct biological functions: One function converts the chromatin-bound cohesin complex to a cohesive state, and the acetyltransferase function activates directly or indirectly its cohesive function during G_2/M.

Having established Eco1 as a critical factor for the generation of DSB-induced cohesion, we asked whether the failure to generate cohesion in undamaged G_2/M cells results from limiting Eco1 activity. To test this hypothesis, we overproduced Eco1 during G_2/M in the absence of HO-induced DSBs. Indeed, overproduction of Eco1 but not eco1^{ack-} bypasses the requirement for DSBs to generate cohesion in G_2/M (Fig. 3C). Both Eco1 and eco1^{ack-} are present at similar levels (Fig. 3D), and *eco1*$^{ack-}$ encodes a functional protein because it complements the *eco1-203* at nonpermissive temperature (fig. S4F). These results suggest that in G_2/M, Eco1 acetyltransferase activity is limiting in undamaged cells and, in response to DSBs, this activity is elevated through the DNA damage checkpoint.

Here we show that the generation of cohesion in G_2/M is Eco1 dependent but replication independent [also reported in (*14*)]. This contradicts the current model, which posits that cohesion generation can only occur in the context of DNA replication, and Eco1 (Ctf7) merely allows the replisome to slide through the cohesin ring in S phase (*8*). Rather, we suggest that Eco1 directly converts the chromatin-bound cohesin complex to its cohesive state. During S phase, Eco1 associates with replisome components (*7*, *17*), and this allows Eco1 to establish cohesion before the sister chromatids separate (*7*, *18*). We also show that the cohesive function of Eco1 requires its acetyltransferase domain in G_2/M but not in S phase. We suggest that the cohesive function of Eco1 is inactivated after S phase either by inhibiting Eco1 directly or its accessibility to cohesin (Fig. 4A). Upon DSBs, the DNA damage checkpoint initiates a signal that induces cohesin loading around the DSB and augments the acetyltransferase activity of Eco1 (Fig. 4B). Eco1 in turn acetylates itself, cohesin subunits, or Pds5 (*15*), and thus overcomes the G_2/M inhibition. Thus, like cohesion dissolution, cohesion establishment exhibits complex spatial and temporal regulation throughout the cell cycle, and Eco1 is the hub for this regulation.

The conservation of the Eco1 acetyltransferase domain suggests that it is critical for DSB-induced cohesion in all species. Defects in the DSB-induced cohesion pathway lead to genomic instability in humans (*19*). These defects have been attributed to improper repair of the broken chromosomes as a result of a failure to generate cohesion at the break site. The discovery that DNA damage response pathway activates cohesion on unbroken as well as broken chromosomes suggests that the role of this pathway extends beyond the repair of the break. Indeed, in G_2/M, absence of DSB-induced genome-wide cohesion increases loss of unbroken chromosomes about threefold (fig. S5), suggesting that enhanced cohesion during checkpoint delay prevents precocious sister-chromatid separation. Further studies of genome-wide cohesion may reveal additional functions such as the prevention of rearrangements through ectopic recombination.

References and Notes

1. D. E. Koshland, V. Guacci, *Curr. Opin. Cell Biol.* **12**, 297 (2000).
2. L. Ström, C. Sjögren, *Curr. Opin. Cell Biol.* (2007).
3. C. E. Huang, M. Milutinovich, D. Koshland, *Philos. Trans. R. Soc.* **360**, 537 (2005).
4. P. B. Meluh, A. V. Strunnikov, *Eur. J. Biochem.* **269**, 2300 (2002).
5. R. Ciosk *et al.*, *Mol. Cell* **5**, 243 (2000).
6. A. Toth *et al.*, *Genes Dev.* **13**, 320 (1999).
7. R. V. Skibbens, L. B. Corson, D. Koshland, P. Hieter, *Genes Dev.* **13**, 307 (1999).
8. A. Lengronne *et al.*, *Mol. Cell* **23**, 787 (2006).
9. L. Ström, H. B. Lindroos, K. Shirahige, C. Sjögren, *Mol. Cell* **16**, 1003 (2004).
10. C. H. Haering *et al.*, *Mol. Cell* **15**, 951 (2004).
11. E. Ünal *et al.*, *Mol. Cell* **16**, 991 (2004).
12. J. S. Kim, T. B. Krasieva, V. LaMorte, A. M. Taylor, K. Yokomori, *J. Biol. Chem.* **277**, 45149 (2002).
13. N. Sugawara, X. Wang, J. E. Haber, *Mol. Cell* **12**, 209 (2003).
14. L. Ström *et al.*, *Science* **317**, 242 (2007).
15. D. Ivanov *et al.*, *Curr. Biol.* **12**, 323 (2002).
16. A. Brands, R. V. Skibbens, *Curr. Biol.* **15**, R50 (2005).
17. G. L. Moldovan, B. Pfander, S. Jentsch, *Mol. Cell* **23**, 723 (2006).
18. M. Milutinovich, E. Ünal, C. Ward, R. V. Skibbens, D. Koshland, *PLoS Genet.* **3**, e12 (2007).
19. E. Watrin, J. M. Peters, *Exp. Cell Res.* **312**, 2687 (2006).

20. We thank C. Redon, M. Lichten, E. Cammon, and P. Cammon for technical support; C. Sjögren for communicating results before publication; C.-M. Fan, Y. Zhang, M. Hoang, V. Guacci for comments on the manuscript; and F. Uhlmann, J. Yanowitz, H.-G. Yu for discussions. D.K. is supported by the Howard Hughes Medical Institutes.

Supporting Online Material

www.sciencemag.org/cgi/content/full/317/5835/245/DC1
Methods
Figs. S1 to S4
Table S1
References

31 January 2007; accepted 25 May 2007
10.1126/science.1140637

Developmentally Regulated Activation of a SINE B2 Repeat as a Domain Boundary in Organogenesis

Victoria V. Lunyak,[1,2*] Gratien G. Prefontaine,[1]† Esperanza Núñez,[1]† Thorsten Cramer,[5]† Bong-Gun Ju,[1] Kenneth A. Ohgi,[1] Kasey Hutt,[1] Rosa Roy,[4] Angel García-Díaz,[4] Xiaoyan Zhu,[1] Yun Yung,[1] Lluís Montoliu,[4] Christopher K. Glass,[3] Michael G. Rosenfeld[1*]

The temporal and spatial regulation of gene expression in mammalian development is linked to the establishment of functional chromatin domains. Here, we report that tissue-specific transcription of a retrotransposon repeat in the murine growth hormone locus is required for gene activation. This repeat serves as a boundary to block the influence of repressive chromatin modifications. The repeat element is able to generate short, overlapping Pol II– and Pol III–driven transcripts, both of which are necessary and sufficient to enable a restructuring of the regulated locus into nuclear compartments. These data suggest that transcription of interspersed repetitive sequences may represent a developmental strategy for the establishment of functionally distinct domains within the mammalian genome to control gene activation.

The *growth hormone* (*GH*) gene provides a well-studied transcription unit that is highly suited for defining how specific chromatin modifications (*1*–*6*) might be responsible for the spatial and temporal order of lineage specification events in the developing pituitary gland. The human *GH* locus is represented by a cluster of five *GH*-related genes that are regulated by a Pit-1–

dependent locus control region (LCR) (*7*–*10*). The murine *GH* genomic locus is found on mouse chromosome 11 and encompasses five genes (Fig. 1A). In contrast to the human locus, the mouse locus does not contain tandem duplications of the *GH* gene, and there is no known murine LCR.

The *GH* gene is initially silenced at early stages of murine pituitary gland development but activated at embryonic stage 17.5 (e17.5) by the POU-homeodomain factor, Pit-1, in GH-producing cells (somatotropes) (fig. S1A). It remains actively repressed, or silenced, in the other pituitary cell types. Analysis of histone modifications was used to assess the chromatin state of the *GH* locus during development. Chromatin immunoprecipitation (ChIP) analysis (*5*, *11*–*16*) revealed high levels of triK9 methylation of histone H3, indicating a condensed heterochromatic state of the *GH* gene promoter, at e12.5, with a gradual decline to low levels by e14.5 and complete disappearance by e17.5 or in adult pituitary (Fig. 1B). Conversely, low levels of dimethylation of K9H3 on *GH* were observed at e12.5, but increased by e13.5 to e14.5, declined at 17.5, and disappeared in the adult gland. Based on complete loss of the condensed heterochromatin marks, we suggest that these chromatin events occurred and were sustained in all lineages. In *dw/dw* mice, containing an inactivating point mutation in the Pit-1 POU domain factor, the *GH* promoter lacked triMe K9H3 but contained elevated diMe K9H3, which suggests that these events occur in a Pit-1–independent manner (Fig. 1B). Two-step ChIP was performed using αPit and either αPol II or αNCoR immunoglobulin G (IgG). Together, the analysis of transcriptionally active or repressed Pit-1 bearing chromatin suggests that partitioning of these histone modifications occurs uniformly in the pituitary cell population in early pituitary development.

Fluorescence in situ hybridization (FISH) analysis was used to localize the *GH* gene within interphase nuclei at different stages of pituitary embryonic development (Fig. 1C) (*12*, *16*). Both alleles of the *GH* gene localized to 4′,6′-diamidino-2-phenylindole (DAPI)–stained heterochromatin in virtually all of the clearly stained (>90%) e12.5 nuclei (Fig. 1C and fig. S1B). In contrast, at e14.5, of the total population of clearly stained nuclei (102 out of 109 nuclei), the *GH* gene had relocated to euchromatic territories outside the DAPI regions (Fig. 1C and fig. S1B). This is temporally coincident with the observed exchange of branched triMe K9H3 or diMe K9H3 methylation marks on the *GH* promoter (Fig. 1B). ChIP analysis (*17*) across a 30-kb genomic interval revealed a specific region within the *GH* locus (between primer pairs 4 and 6) at which the exchange of branched triMe K9H3 or diMe K9H3 occurs temporally between e12.5 and e14.5 in pituitary development (Fig. 1, D and E, and fig. S1, C and D).

Because the region of diMe K9H3 and triMe K9H3 transition is located −14 to −10 kb upstream of the *GH* transcriptional start site (Fig. 1, A, D, and E), we considered that a putative boundary element(s) might exist within the *GH* locus to establish these regulatory domains. We used an assay to locate DNA sequences that might possess putative insulator properties by assessing the enhancer-blocking activity of each DNA sequence. We placed the experimental boundary element between a known enhancer and a reference promoter driving a reporter gene (*18*). This strategy has been used for a number of known insulators (*19*–*21*). The enhancer-blocking assay (EBA) was carried out with linearized constructs in transiently transfected HEK 293 cells (Fig. 2A). As controls, a 1.2-kb DNA fragment containing the 5′HS4 insulator of the chicken β-*globin* locus (*22*), and the FII/FIII core elements of this 5′HS4 boundary [wild-type (F8) and mutant (F6) forms] (*18*, *21*) were used. Each element (Fig. 1A) was cloned between the cytomegalovirus (CMV) enhancer and minimal CMV promoter (*Xho*I site), or at the 5′ end of the CMV enhancer (*Pst*I site), with enhancer-blocking occurring only when the experimental element is located between the enhancer and the promoter (Fig. 2A) (*18*, *19*).

The maximal (by a factor of 54.7) reduction in activity was observed in the case of the CD region or any construct that included the CD element, and this region coincided with the region of the transition between developmentally regulated diMe K4H3 and the branched triMe K9H3 (Fig. 1F), conceptually consistent with the description of boundary activity. Further examination of the CD region revealed the presence of a short interspersed nuclear element (SINE) B2 retrotransposon repeat (Figs. 1A and 2B), derived from the tRNA gene, consisting of a 190-bp consensus sequence, including an RNA polymerase III promoter with its two conserved regulatory elements, A-box and B-box (*23*, *24*). Recently, it was reported that SINE B2 expression can be driven in opposite strands by highly conserved Pol III or Pol II promoters (*25*, *26*).

Assessment of the presence of the Pol II– and Pol III–generated transcripts from the *GH* SINE B2 reporter construct was performed using strand-specific RT-PCR analysis with sequence-specific primers used for extension to generate single-stranded DNA for PCR amplification on

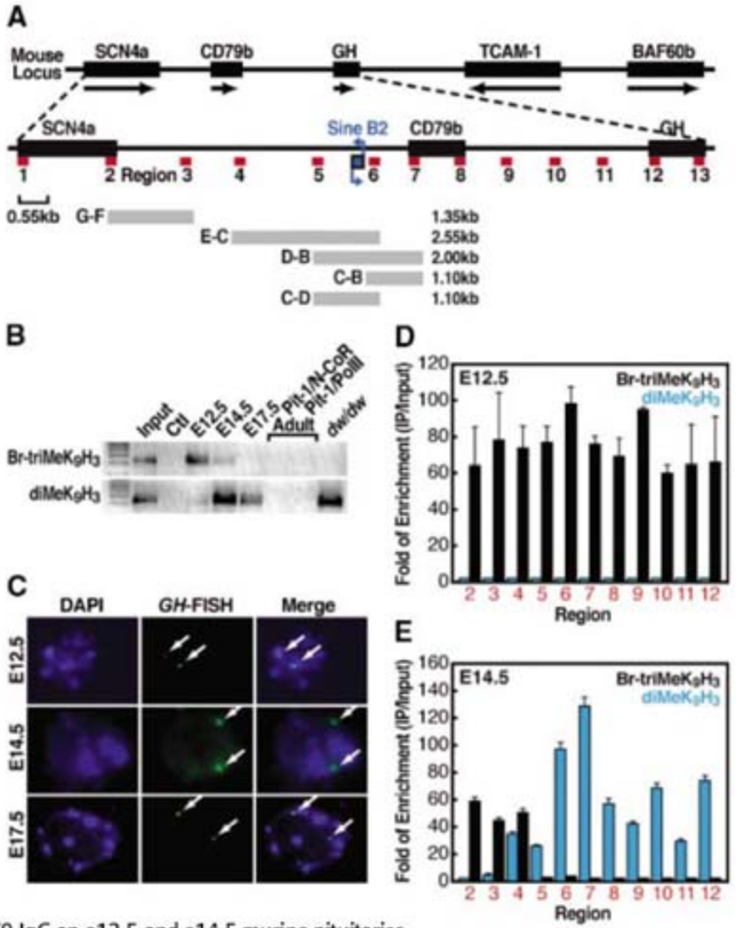

Fig. 1. Developmental repositioning of the *GH* locus. (**A**) Schematic diagram of *GH* genomic locus murine chromosome 11, showing the five transcription units in the locus. Arrows indicate the direction of each transcription unit. Red bars represent PCR amplification regions in ChIP experiments. The regions later examined for function are labeled in letters (e.g., G-F). (**B**) ChIP analysis of isolated pituitary using antibodies specific for branched trimethyl K9H3 (Br-triMeK9H3), and diMeK9H3. Multistep ChIPs with αPit-1 then αN-CoR, or αPit-1 then αPol II for initial selection of Pit-1 lineage cells. (**C**) Immuno-FISH analysis of e12.5, e14.5, and e17.5 nuclei from murine pituitaries using a *GH* probe. (**D** and **E**) Conventional ChIP analysis across the *GH* locus using α-Br-triMe H3-K9 or α-diMe H3-K9 IgG on e12.5 and e14.5 murine pituitaries. PCR primers diagrammed in (A).

[1]Howard Hughes Medical Institute, School of Medicine, University of California, San Diego, 9500 Gilman Drive, Room 345, La Jolla, CA 92093–0648, USA. [2]Department of Medicine, Division of Endocrinology, University of California, San Diego, La Jolla, CA 92093, USA. [3]Department of Cellular and Molecular Medicine, Department and School of Medicine, University of California, San Diego, La Jolla, CA 92093, USA. [4]Department of Molecular and Cellular Biology, Centro Nacional de Biotecnología (CNB-CSIC), Campus de Cantoblanco, C/Darwin 3, 28049 Madrid, Spain. [5]Department of Hepatology and Gastroenterology, Charité Universitätsmedizin Berlin, Campus Virchow-Klinikum, Augustenburger Platz 1, 13353 Berlin, Germany.

*To whom correspondence should be addressed. E-mail: mrosenfeld@ucsd.edu (M.G.R.); vlunyak@uscd.edu (V.V.L.)
†These authors contributed equally to this work.

RNA samples recovered from transfected HeLa cells (Fig. 2B). SINE B2 was efficiently transcribed (Fig. 2B) from both Pol II and Pol III promoters independent of its insertion site with respect to upstream (PstI) or downstream (XhoI) (Fig. 2B) of the enhancer, and deletion of the SINE B2 repeat (ΔSine B2 CD) abolished the enhancer-blocking activity (Fig. 2C).

To confirm a functional role for this putative boundary element in vivo, a 220-kb bacterial artificial chromosome (BAC) encompassing a centrally located *mGH* gene was modified to replace the *GH* coding sequence with a red fluorescent protein (RFP) dimer coding sequence (fig. S3, A and B). This transgene was clearly expressed in three transgenic founder mice generated, recapitulating the physiological temporal and spatial pattern of GH locus expression (*5*) (Fig. 2D). Deletion of the 160-bp region encompassing the *mGH* SINE B2 repeat in this BAC caused either complete loss of RFP expression (two transgenic founder mice) or loss of RFP expression in all but a few residual cells (one transgenic founder mouse) carrying this BAC transgene (Fig. 2D). Therefore, the SINE B2 transcription unit can be suggested to be required for developmentally regulated *GH* gene activation in vivo. However, this assay does not establish that this reflects its boundary function in vivo.

RT-PCR analysis of RNA recovered from developing pituitary at embryonic day e14.5 reveals that both Pol II and Pol III transcripts were present in vivo (Fig. 3, A to E) (*26*). Pol III transcripts originating in the SINE B2 repeat were detected in the pool of the pituitary-specific RNA at all the times during embryonic development, including e12.5 (Fig. 3, D and E), but the transcript generated from the Pol II promoter (*26*) initially appeared only at e13.5 to 14.5, because it was not present in the pooled e9.5 to e12.5 sample (Fig. 3C) but was present in the pooled e12.5 to e15.5 sample (Fig. 3C) in the pituitary gland (Fig. 3, B and C), correlating both with the timing and establishment of differential domains of chromatin modifications within the *GH* locus and nuclear repositioning detected by FISH (Fig. 1, C and E).

We next inserted the SINE B2 from the *GH* locus into a 1.2-kb coding sequence from the *Adam11* transcription unit that alone exhibited no activity in the enhancer-blocking assay. We evaluated deletion and substitution constructs in the enhancer-blocking assay (Fig. 4A) and found that insertion of SINE B2 transcription unit containing the minimal defined Pol II promoter (*26*) in *Adam11* constructs resulted in clear enhancer-blocking activity (ctl+SINE B2) (Fig. 4A). However, insertion of a shorter version of the SINE B2 in which the Pol II promoter was deleted in the same position within *Adam11* no longer exerted the enhancer-blocking activity. Substitution of nucleotide sequences representing the intragenic promoters for Poll III–mediated transcription (*23*) diminished enhancer-blocking activity of element CD (Fig. 4A). These results revealed that a bidirectional Pol III/Pol II-driven

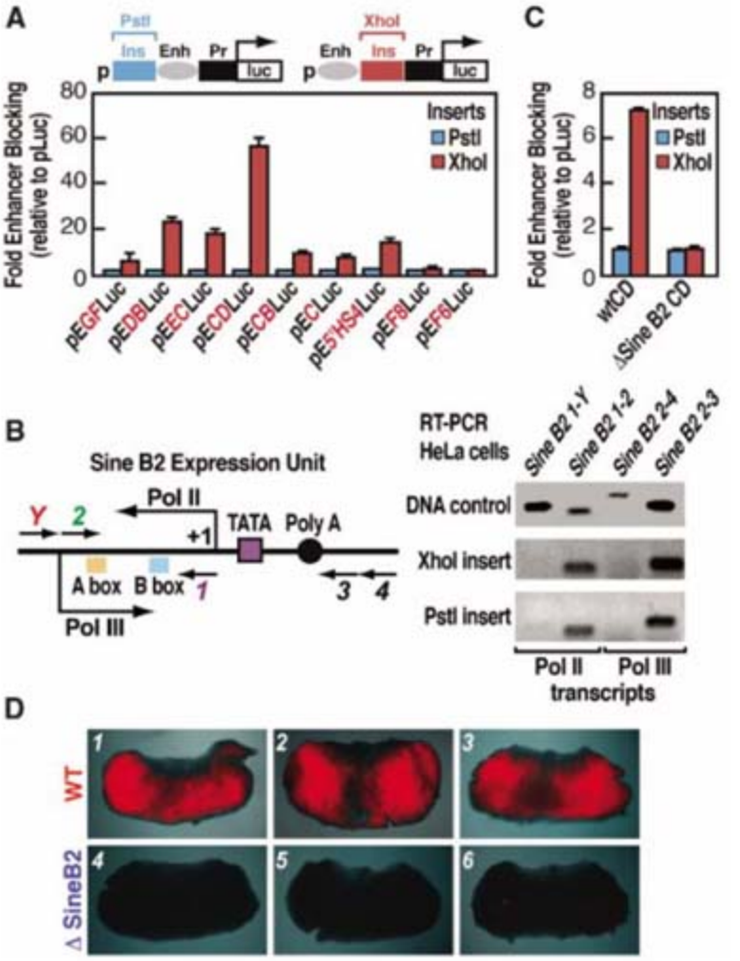

Fig. 2. Identification of a SINE B2 repeat in the *GH* boundary region. (**A**) Enhancer-blocking assay performed using the pE Luc (CMVEmPLuc) vector in human embryonic kidney (HEK) 293 cells, placing the tested element either upstream (*PstI*) or downstream (*XhoI*) of the enhancer (map of the construct is given in fig. S2C). (**B**) Schematic diagram of the *GH* SINE B2 expression unit showing position of primers used for reverse transcriptase reaction (Y or 2 for Pol II and 3 or 4 for Pol III transcription, respectively) and PCR (Y, 2, 1, 3, 4). Assessment of Pol II and Pol III–generated transcripts from the reporter construct using RT-PCR analysis with primers indicated above. Designations of +1 and TATA indicate the transcription start site and TATA box, respectively. [Poly A refers to a stretch of A residues in the sequence (fig. S2A)]. (**C**) Effect of deletion of the SINE B2 element on function of the CD *GH* element in the enhancer-blocking assay. All data are ±SEM. (**D**) RFP expression in transgenic founder mice with wild-type *mGH*/RFP BAC (founders 1,2,3) or with deletion of the SINE B2 element (founders 4,5,6).

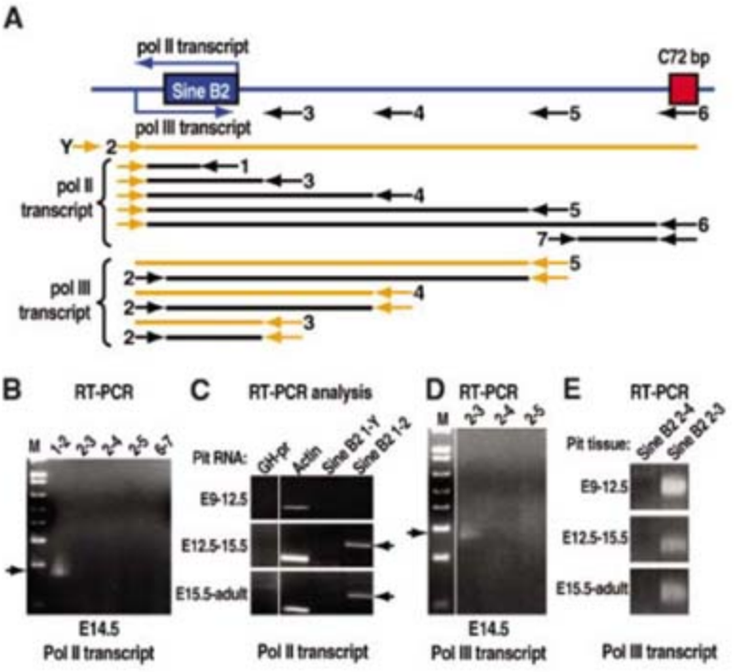

Fig. 3. In vivo expression of the *GH* SINE B2 transcripts during pituitary development. (**A**) Schematic diagram of primers used for reverse transcription, PCR, and primer extension analysis of the SINE B2 transcription units. Primers used for reverse transcription and ssDNA are shown in yellow, their PCR partnering primers and expecting PCR fragments are shown in black. (C72 bp = a 72-bp sequence conserved in human and mouse). (**B** and **C**) Identification of Pol II transcript by RT-PCR at e14.5, but not detected on e12.5, with actin-specific primers used as a positive control (see Actin lane). GH promoter–specific primers used as a negative control. (**D**) Demonstration of the Pol III transcript on e14.5 by RT-PCR using primers shown. (**E**) Ontogeny of expression of the Pol III transcripts, showing expression throughout pituitary development. The same RNA samples were used for RT-PCR as in (B) to (D).

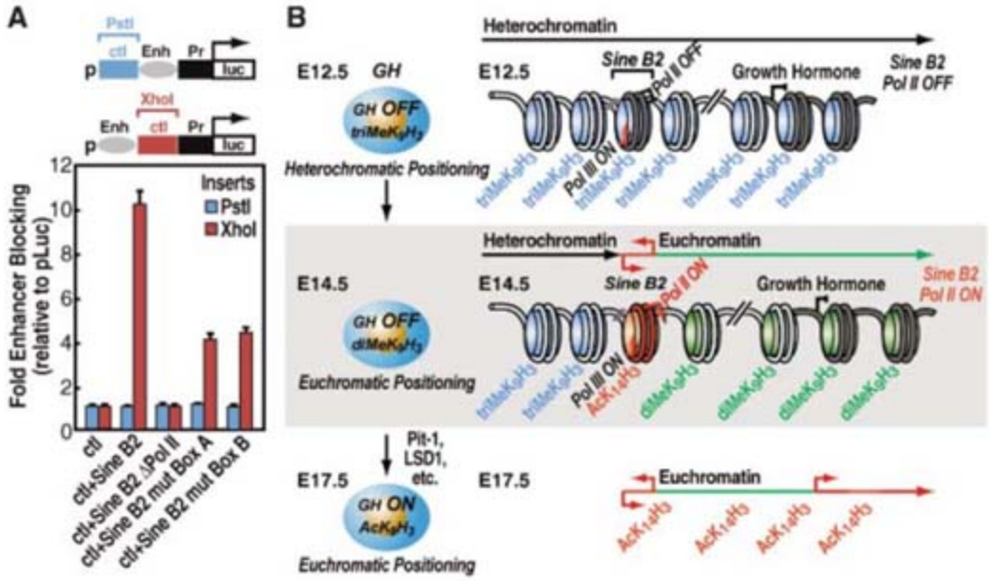

Fig. 4. Determinants of enhancer-blocking function of the *GH* SINE B2 transcription unit. (**A**) The enhancer-blocking assay was performed by inserting a minimal amount of SINE B2 transcription unit into 1.2 kb of *Adam 11* coding region in the pE Luc vector. Mutations included removal of the Pol II promoter (Δ Pol II), mutation of Box A (mut Box A) or mutation of Box B (mut Box B). (**B**) Model of regulation of a *GH* boundary control element based on developmentally regulated expression of the Pol II transcription unit of the *GH* SINE B2 transcription unit, correlated with chromosomal repositioning. AcK14H3 is acetylated K14 on histone H3.

transcription of the *GH* SINE B2 repeat was both necessary and sufficient to establish boundary activity, independently of the surrounding sequences. Ongoing transcription of the SINE B2 repeat was required to mediate enhancer-blocking activity, rather than generation of SINE B2 transcripts themselves in *trans* (fig. S4).

Together these data suggest that bidirectional, noncoding transcription from the murine *GH* SINE B2 transcription unit has the ability to contribute to establishing a putative boundary element by imposing a local perturbation in chromatin structure resulting in repositioning of the *GH* locus from a heterochromatic region to a more permissive euchromatic environment (Fig. 4B). Indeed, results obtained in fission yeast demonstrate a very similar organization of the boundary elements encompassing inverted repeats (*27*) and development changes in expression of SINE B2 reported for different systems (*28*), consistent with widespread use of SINE B2 elements in mammalian development. Our findings further support the notion that transcribed insulators/boundary elements may function as a dynamic infrastructure adapted to the transcriptional and/or developmental state of the cell, providing the required plasticity to respond to the developmental and environmental cues.

References and Notes

1. T. Cremer, C. Cremer, *Nat. Rev. Genet.* **2**, 292 (2001).
2. S. Rea *et al.*, *Nature* **406**, 593 (2000).
3. S. M. Gasser, *Science* **296**, 1412 (2002).
4. M. Capelson, V. G. Corces, *Biol. Cell* **96**, 617 (2004).
5. K. M. Scully *et al.*, *Science* **290**, 1127 (2000).
6. M. Treier *et al.*, *Genes Dev.* **12**, 1691 (1998).
7. B. M. Shewchuk, N. E. Cooke, S. A. Liebhaber, *Nucleic Acids Res.* **29**, 3356 (2001).
8. I. M. Bennani-Baiti *et al.*, *Proc. Natl. Acad. Sci. U.S.A.* **95**, 10655 (1998).
9. I. M. Bennani-Baiti, N. E. Cooke, S. A. Liebhaber, *Genomics* **48**, 258 (1998).
10. B. K. Jones, B. R. Monks, S. A. Liebhaber, N. E. Cooke, *Mol. Cell. Biol.* **15**, 7010 (1995).
11. C. Maison *et al.*, *Nat. Genet.* **30**, 329 (2002).
12. J. C. Rice *et al.*, *Mol. Cell* **12**, 1591 (2003).
13. A. H. Peters *et al.*, *Cell* **107**, 323 (2001).
14. E. J. Richards, S. C. Elgin, *Cell* **108**, 489 (2002).
15. V. L. Biron, K. J. McManus, N. Hu, M. J. Hendzel, D. A. Underhill, *Dev. Biol.* **276**, 337 (2004).
16. J. C. Rice, C. D. Allis, *Nature* **414**, 258 (2001).
17. Materials and methods are available as supporting material on *Science* Online.
18. F. Recillas-Targa, A. C. Bell, G. Felsenfeld, *Proc. Natl. Acad. Sci. U.S.A.* **96**, 14354 (1999).
19. T. J. Antes, S. J. Namciu, R. E. Fournier, B. Levy-Wilson, *Biochemistry* **40**, 6731 (2001).
20. P. Giraldo *et al.*, *Nucleic Acids Res.* **31**, 6290 (2003).
21. V. Valadez-Graham, S. V. Razin, F. Recillas-Targa, *Nucleic Acids Res.* **32**, 1354 (2004).
22. J. H. Chung, A. C. Bell, G. Felsenfeld, *Proc. Natl. Acad. Sci. U.S.A.* **94**, 575 (1997).
23. G. Ciliberto, G. Raugei, F. Costanzo, L. Dente, R. Cortese, *Cell* **32**, 725 (1983).
24. C. A. Espinoza, T. A. Allen, A. R. Hieb, J. F. Kugel, J. A. Goodrich, *Nat. Struct. Mol. Biol.* **11**, 822 (2004).
25. T. A. Allen, S. Von Kaenel, J. A. Goodrich, J. F. Kugel, *Nat. Struct. Mol. Biol.* **11**, 816 (2004).
26. O. Ferrigno *et al.*, *Nat. Genet.* **28**, 77 (2001).
27. K. Noma, H. P. Cam, R. J. Maraia, S. I. Grewal, *Cell* **125**, 859 (2006).
28. R. Bachvarova, *Dev. Biol.* **130**, 513 (1988).

29. We thank C. Nelson, C. Isidro, and S. Kanai for their assistance; T. Jenuwein, S. Watanabe, and F. Recillas-Targa for reagents; and William McGinnis for discussions and advice. We also thank J. Hightower and M. Fisher for assistance in figure and manuscript preparation; and M. Gonzalez (Santa Cruz Biotechnology) for advice on reagents. M.G.R. is an investigator with the Howard Hughes Medical Institute. These studies are supported by NIH grants to M.G.R. and C.K.G. and by a Medical Education and Research Foundation award to V.V.L.

Supporting Online Material

www.sciencemag.org/cgi/content/full/317/5835/248/DC1
Materials and Methods
Figs. S1 to S4
Tables S1 and S2

5 February 2007; accepted 13 June 2007
10.1126/science.1140871

Combinatorial ShcA Docking Interactions Support Diversity in Tissue Morphogenesis

W. Rod Hardy,[1,2] Lingying Li,[3] Zhi Wang,[3] Jiri Sedy,[4] James Fawcett,[1] Eric Frank,[3] Jan Kucera,[5,6]* Tony Pawson[1,2]*

Changes in protein-protein interactions may allow polypeptides to perform unexpected regulatory functions. Mammalian ShcA docking proteins have amino-terminal phosphotyrosine (pTyr) binding (PTB) and carboxyl-terminal Src homology 2 (SH2) domains, which recognize specific pTyr sites on activated receptors, and a central region with two phosphorylated tyrosine-X-asparagine (pYXN) motifs (where X represents any amino acid) that each bind the growth factor receptor–bound protein 2 (Grb2) adaptor. Phylogenetic analysis indicates that ShcA may signal through both pYXN-dependent and -independent pathways. We show that, in mice, cardiomyocyte-expressed ShcA directs mid-gestational heart development by a PTB-dependent mechanism that does not require the pYXN motifs. In contrast, the pYXN motifs are required with PTB and SH2 domains in the same ShcA molecule for the formation of muscle spindles, skeletal muscle sensory organs that regulate motor behavior. Thus, combinatorial differences in ShcA docking interactions may yield multiple signaling mechanisms to support diversity in tissue morphogenesis.

Docking proteins with multiple interaction domains and motifs act downstream of receptor tyrosine kinases (RTKs) and other cell-surface receptors (*1*, *2*). Although discrete protein-protein interactions are known to exert specific biological effects in RTK signaling (*3*, *4*), there is little information as to the combinatorial effects of these docking interactions in vivo. We have used the 46- and 52-kD protein products of the mouse *ShcA* gene (*5*)

(p46^{ShcA} and p52^{ShcA}, collectively ShcA) as a model to investigate this issue.

The PTB and SH2 domains of ShcA bind phosphorylated motifs with the consensus sequences Φ-X-Asn-Pro-X-pTyr (Φ-X-N-P-X-pY) and pTyr-Φ-X-Ile/Leu (pY-Φ-X-I/L) (*6*), respectively (where Φ represents any large hydrophobic amino acid), on various cell-surface receptors (*7*). The collagen homologous 1 (CH1) region contains two YXN motifs (Y^{239}Y^{240}N and Y^{313}VN of mouse p52^{ShcA}) (*7*). Upon phosphorylation, these motifs can each bind the SH2 domain of the adaptor Grb2, which recruits activators of the Ras and phosphatidylinositol 3-kinase signaling pathways through its SH3 domains (*7–10*). Although Shc proteins in metazoans are defined by their PTB-CH1-SH2 structure, the pYXN motifs are absent in some invertebrates (fig. S1), and additional CH1 pTyr motifs are present in certain vertebrate family members (*11*) (fig. S2). This suggests that ShcA and its homologs have alternative pYXN-dependent and -independent signaling functions, which are variably used in evolution (*12*).

Mutant mice selectively missing a third ShcA isoform, p66^{ShcA}, are long-lived (*13*), whereas mutants lacking all three ShcA proteins die around E11.5 (embryonic day 11.5) with cardiovascular defects (*14*). To explore the biological roles of the various pTyr-dependent interactions of ShcA, we generated mice with targeted *ShcA* knock-in (KI) alleles expressing either wild-type (WT) ShcA proteins with a single Flag (1×Flag) epitope tag (*ShcA$^{KI\text{-}WT}$* allele) or ShcA-1×Flag variants with substitutions that (i) disrupt pTyr binding by the PTB domain [*ShcA$^{\delta PTB}$* allele, Arg^{175}→Gln^{175}

[1]Samuel Lunenfeld Research Institute, Mount Sinai Hospital, 600 University Avenue, Toronto, Ontario M5G 1X5, Canada. [2]Department of Molecular and Medical Genetics, 4388 Medical Sciences Building, 1 King's College Circle, University of Toronto, Ontario M5S 1A8, Canada. [3]Department of Physiology, Tufts University School of Medicine, Boston, MA 02111, USA. [4]Institute of Anatomy, Charles University, First Faculty of Medicine, Prague 12000, Czech Republic. [5]Department of Neurology, Boston University School of Medicine, Boston, MA 02118, USA. [6]Veterans Administration Medical Center, Boston, MA 02130, USA.

*To whom correspondence should be addressed. E-mail: pawson@mshri.on.ca (T.P.); jfkucera@bu.edu (J.K.)

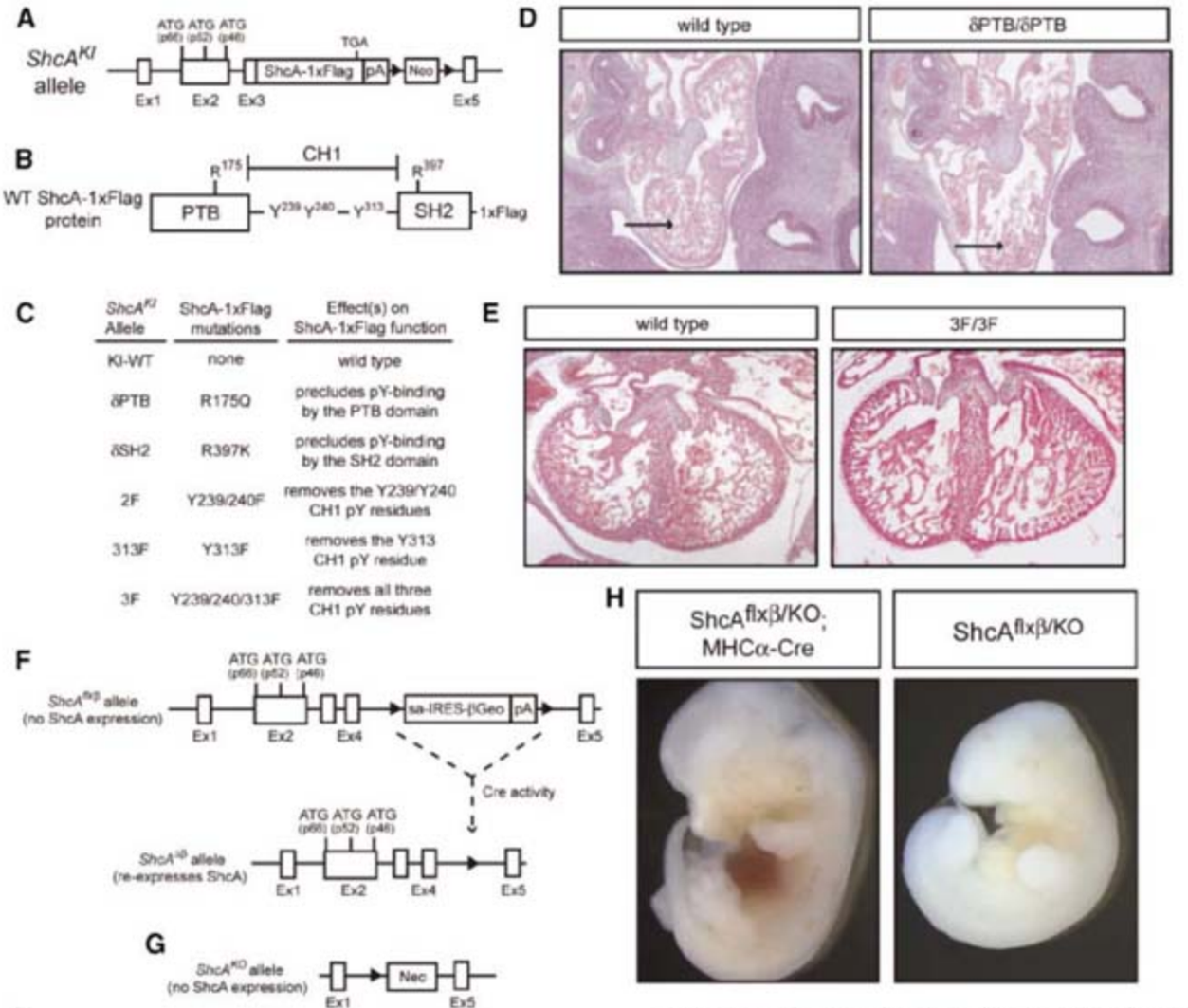

Fig. 1. Cardiomyocyte-expressed ShcA supports mid-gestational viability and heart formation by a PTB-dependent mechanism not requiring the CH1 pTyr residues. (**A**) Common structure of targeted *ShcA^{KI}* alleles generated by gene targeting in embryonic stem cells. Exons are indicated by boxes, introns by horizontal lines, and LoxP sites by arrowheads. ATG and TGA are start and stop codons, respectively. pA, polyA; Neo, neomycin resistance gene. (**B**) The WT ShcA-1×Flag protein product of the *ShcA$^{KI\text{-}WT}$* allele. Mutated amino acids are indicated. (**C**) Summary of *ShcA^{KI}* alleles introduced into mice. Amino acid changes and their effects on ShcA-1×Flag function are indicated. (**D**) Hematoxylin and eosin (H&E)–stained transverse sections showing that the formation of cardiac trabeculae (arrows) is severely impaired in E11.5 *ShcA$^{\delta PTB/\delta PTB}$* hearts. (**E**) H&E-stained transverse sections revealing the similar extent of trabeculation in E13.5 *ShcA$^{3F/3F}$* and WT hearts. (**F**) Depiction of the protein-null *ShcA$^{flx\beta}$* allele and its Cre-mediated conversion into the ShcA-expressing *ShcA$^{\Delta\beta}$* allele. sa-IRES-βgeo, splice acceptor–internal ribosomal entry site–β-galactasidase/neomycin fusion gene. (**G**) Structure of the irreversibly protein-null *ShcA^{KO}* allele. (**H**) Phenotypic rescue of lethality in an E12.5 *ShcA$^{flx\beta/KO}$; MHCα-Cre* embryo, as compared with a dead and necrotic *ShcA$^{flx\beta/KO}$* littermate. (**I**) H&E-stained transverse sections showing the comparable extent of trabeculation in E12.5 *ShcA$^{flx\beta/KO}$; MHCα-Cre* and WT hearts.

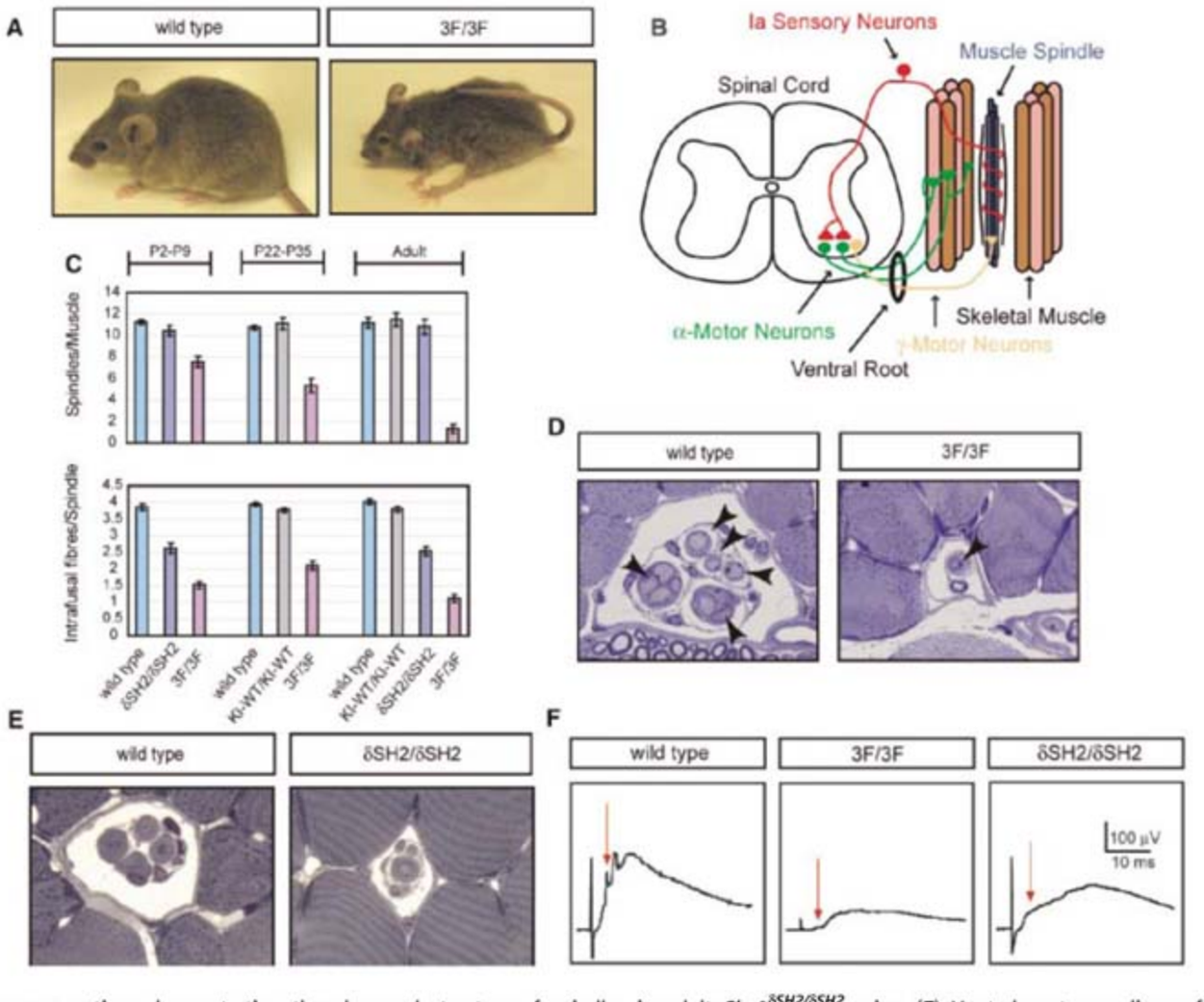

Fig. 2. Motor behavior and stretch reflex development are disrupted in viable *ShcA*$^{3F/3F}$ and *ShcA*$^{\delta SH2/\delta SH2}$ mice. (**A**) Adult WT and *ShcA*$^{3F/3F}$ mice. Note the inability of the *ShcA*$^{3F/3F}$ mutant to maintain normal limb position. (**B**) Diagram depicting the monosynaptic stretch reflex circuit. (**C**) Histograms representing the numbers of muscle spindles per muscle and numbers of intrafusal fibers per muscle spindle in *ShcA*$^{+/+}$, *ShcA*$^{KI\text{-}WT/KI\text{-}WT}$, *ShcA*$^{3F/3F}$, and *ShcA*$^{\delta SH2/\delta SH2}$ mice. Error bars indicate SEM; numbers and statistics are presented in table S1. (**D**) Toluidine-stained transverse sections through the equatorial regions of muscle spindles in adult WT and *ShcA*$^{3F/3F}$ mice. Note the structural differences between the stereotypical WT spindle with its multiple intrafusal fibers (arrowheads) and the atrophied *ShcA*$^{3F/3F}$ spindle with its single intrafusal fiber. (**E**) Toluidine-stained transverse sections demonstrating the abnormal structure of spindles in adult *ShcA*$^{\delta SH2/\delta SH2}$ mice. (**F**) Ventral root recordings of synaptic input to motor neurons evoked by electrical stimulation of DRG neurons in *ShcA*$^{+/+}$, *ShcA*$^{3F/3F}$, and *ShcA*$^{\delta SH2/\delta SH2}$ mice. Red arrows indicate short-latency EPSPs induced by group Ia sensory neurons.

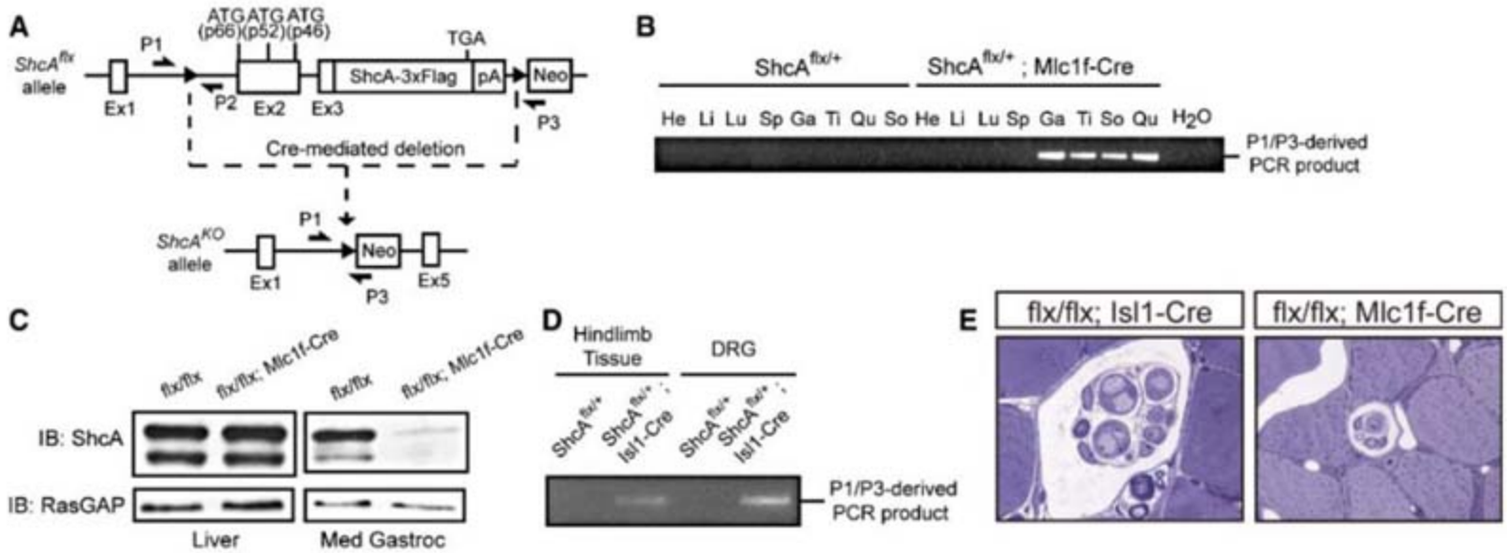

Fig. 3. Cre-mediated ablation of ShcA specifically from skeletal muscles disrupts motor behavior and spindle formation. (**A**) The *ShcA*^{flx} allele. P1/P2 and P1/P3 primer combinations were used to identify unrecombined (active) *ShcA*^{flx} alleles and Cre-recombined (inactive) *ShcA*^{KO} alleles, respectively. (**B**) PCR analysis showing that ShcA-3×Flag coding sequences are deleted from skeletal muscles but not other tissues in adult *Mlc1f-Cre* carriers. He, heart; Li, liver; Lu, lung; Sp, spleen. Skeletal muscles are also indicated: Ga, medial gastrocnemius; Ti, tibialis; Qu, quadricep; So, soleus. (**C**) Immunoblot (IB) analysis showing that ShcA-3×Flag is specifically ablated from the skeletal muscles in adult *ShcA*$^{flx/flx}$; *Mlc1f-Cre* mice. Med Gastroc, medial gastrocnemius muscle; RasGAP, guanosine triphosphatase activating protein of Ras. (**D**) PCR evidence of Cre activity in the DRGs of *ShcA*$^{flx/+}$; *Isl1-Cre* mice. (**E**) Toluidine-stained transverse sections demonstrating the disrupted structure of spindles in *ShcA*$^{flx/flx}$; *Mlc1f-Cre* mutants, as compared with the WT appearance of those in *ShcA*$^{flx/flx}$; *Isl1-Cre* mice, between P22 and P35.

(R175Q) substitution] or by the SH2 domain ($ShcA^{\delta SH2}$, R397K mutation) or (ii) alter the CH1 pTyr sites to phenylalanine, either separately ($ShcA^{2F}$ allele, Y239/240F substitutions; $ShcA^{313F}$ allele, Y313F substitution) or in combination ($ShcA^{3F}$ allele, Y239/240/313F substitutions) (Fig. 1, A to C, and fig. S3). Mutant embryos expressed similar levels of ShcA-1×Flag proteins that were slightly reduced as compared with endogenous ShcA in WT ($ShcA^{+/+}$) littermates (fig. S4). Heterozygotes all appeared normal and were fertile.

From intercrosses, $ShcA^{KI\text{-}WT/KI\text{-}WT}$ mutants were recovered at the expected Mendelian frequency of ~25% (24.6%; 58 $ShcA^{KI\text{-}WT/KI\text{-}WT}$ mice out of 236 mice in the total progeny), as were $ShcA^{2F/2F}$ mice (24.4%; 60 out of 245). In contrast, the numbers of $ShcA^{\delta SH2/\delta SH2}$, $ShcA^{3F/3F}$, and $ShcA^{313F/313F}$ mutant animals were reduced, representing 7.9% (30 out of 380), 12.2% (57 out of 466), and 17.5% (44 out of 251) of viable progeny, respectively ($P < 0.05$, chi-square test). No viable $ShcA^{\delta PTB/\delta PTB}$ mice were identified (0 out of 155). Whereas viable $ShcA^{KI\text{-}WT/KI\text{-}WT}$, $ShcA^{2F/2F}$, and $ShcA^{313F/313F}$ mice appeared normal, $ShcA^{3F/3F}$ and $ShcA^{\delta SH2/\delta SH2}$ mutants exhibited defects in limb coordination (movies S1 to S6). Thus, the PTB and SH2 domains and CH1 pTyr sites of ShcA are variably required for embryonic development and postnatal motor control.

Many E11.5 $ShcA^{\delta PTB/\delta PTB}$ embryos were dead (13 out of 27), while live mutants exhibited enlarged and irregularly beating hearts with poorly developed cardiac trabeculae (Fig. 1D). By E12.5, no live $ShcA^{\delta PTB/\delta PTB}$ embryos were present (0 out of 19). In contrast, between E12.5 and E13.5, virtually all $ShcA^{3F/3F}$ mutants were alive (27 out of 29), with regularly beating hearts in which cardiac trabeculae appeared grossly normal (Fig. 1E). As expected, ShcA-1×Flag proteins in $ShcA^{3F/3F}$ mouse embryo fibroblasts (MEFs) were not tyrosine-phosphorylated and selectively failed to coimmunoprecipitate with Grb2, in response to an activated ErbB2 RTK; conversely, ShcA-1×Flag proteins from $ShcA^{\delta PTB/\delta PTB}$ MEFs selectively failed to associate with an NPXpY phosphopeptide (fig. S5). These results indicate that ShcA regulates mid-gestational heart development by a PTB-dependent mechanism, whereas phosphorylation of the YXN motifs is not essential at this stage.

To test whether ShcA is intrinsically required in the heart, we produced mice with a protein-null *ShcA* allele ($ShcA^{flx\beta}$) that can be reactivated to express ShcA by Cre recombinase (Cre)–mediated DNA recombination (Fig. 1F and fig. S6). We then generated $ShcA^{flx\beta/KO}$; *MHCα-Cre* mice (KO, knock out; MHCα, myosin heavy chain α), in which the *MHCα-Cre* transgene selectively expresses Cre in cardiomyocytes beginning before E9 (*15*) and the $ShcA^{KO}$ allele is irreversibly protein-null (Fig. 1G and fig. S6). Polymerase chain reaction (PCR) analysis revealed Cre-mediated reactivation of the $ShcA^{flx\beta}$ allele in the hearts, but not in the heads, of *MHCα-Cre* carriers (fig. S6). Between E12.5 and E13.5, 21 out of 21 $ShcA^{flx\beta/KO}$ mutants were dead, whereas 8 out of 19 $ShcA^{flx\beta/KO}$; *MHCα-Cre* embryos were alive with regularly beating hearts and grossly normal cardiac trabeculae (Fig. 1, H and I). Thus, PTB-dependent ShcA signaling is required in cardiomyocytes for mid-gestational heart development.

All viable $ShcA^{3F/3F}$ mice were severely uncoordinated (Fig. 2A and movie S5). Mice with disruptions in signaling by tyrosine kinase C (TrkC) or ErbB2, two RTKs known to bind ShcA (*16*, *17*), display similar motor defects, whose physiological cause is abnormal stretch reflex development (*18*–*20*). The monosynaptic stretch reflex circuit detects alterations in skeletal muscle length and induces compensatory muscle contraction and relaxation (*21*). It has three major components: group Ia sensory neurons located in the dorsal root ganglia (DRG), α–motor neurons in the ventral spinal cord, and skeletal muscle sensory organs known as muscle spindles (Fig. 2B). Spindles differentiate from type I myotubes that are innervated by group Ia sensory neurons during embryogenesis (*21*). In newborn mice, skeletal muscles have their full complements of spindles, which reach structural maturity around the second postnatal week (*22*). Between postnatal days 2 and 9 (P2 and P9), between P22 and P35, and in adults (older than P56), spindle numbers in the soleus and medial gastrocnemius muscles of $ShcA^{3F/3F}$ mutants were, respectively, 70, 50, and 11.5% of those in age-matched controls (Fig. 2C and table S1). Properly developed spindles contain stereotypical numbers of intrafusal fibers (*22*). Between P2 and P9, between P22 and P35, and in adults, the numbers of intrafusal fibers in $ShcA^{3F/3F}$ spindles were, respectively, 38.5, 53.8, and 27.5% of those in controls (Fig. 2, C and D, and table S1). In contrast, extrafusal muscle fibers in adult $ShcA^{3F/3F}$ mice had WT morphologies and normal distributions of type I and type II myofibers, indicating that neuromuscular function was not overtly disrupted (fig. S7). Supporting this view, the ventral motor roots of adult $ShcA^{3F/3F}$ mice contained normal numbers of large-diameter (>3.5 μm) α–motor axons, which contact extrafusal fibers, whereas the numbers of small-diameter (≤3.5 μm) γ–motor axons, which contact muscle spindles, were only 20% of those of controls ($ShcA^{3F/3F}$, 53.3 ± 10.6 SEM, $n = 3$ mice; controls, 346.6 ± 6.7 SEM, $n = 3$ mice; $P < 0.001$) (fig. S7). The numbers and structures of spindles in adult $ShcA^{KI\text{-}WT/KI\text{-}WT}$ animals were similar to those in WT controls (Fig. 2C and table S1). Thus, muscle spindles develop abnormally and are lost with age in uncoordinated $ShcA^{3F/3F}$ mice.

The ataxic behavior of $ShcA^{\delta SH2/\delta SH2}$ mice was less severe than that of $ShcA^{3F/3F}$ mutants (movie S6). Between P2 and P9, and in adults, total spindle numbers in $ShcA^{\delta SH2/\delta SH2}$ animals were equivalent to those of controls (Fig. 2C and table S1), but their spindles appeared structurally abnormal, with intrafusal fiber numbers that were 66.7 and 62.5% of those in controls, respectively (Fig. 2, C and E, and table S1). Thus, spindle morphogenesis, but not spindle production, is disrupted in $ShcA^{\delta SH2/\delta SH2}$ mutants. The pYXN motifs and SH2 domain are therefore both required for proper spindle formation.

Abnormal spindle formation could result from defects intrinsic to group Ia sensory neurons (*23*). Labeling of DRG neurons with fluorescent dextran or DiI (1,1'-dioctadecyl-3,3,3',3'-tetramethylindocarbocyanine perchlorate) revealed axons of group Ia sensory neurons reaching their target regions in the ventral horn of the spinal cord in $ShcA^{3F/3F}$ and $ShcA^{\delta SH2/\delta SH2}$ mice (fig. S8). To test the functionality of these neurons, we stimulated DRG neurons electrically and recorded EPSPs (excitatory postsynaptic potentials) evoked in ventral root motor axons (*24*). The amplitudes of short-latency EPSPs (2 to 3 ms), which result from the monosynaptic input of group Ia sensory neurons, were smaller in $ShcA^{3F/3F}$ ($n = 9$ mice) and $ShcA^{\delta SH2/\delta SH2}$ ($n = 2$ mice) mutants as compared with those in WT mice ($n = 9$) (Fig. 2F). In the case of $ShcA^{3F/3F}$ animals, the amplitude was less than 20% of that in controls ($n = 9$ mice for both groups; $P < 0.001$, Student's t test). Thus, the synaptic conductivity of group Ia sensory neurons is impaired in ataxic $ShcA^{3F/3F}$ and $ShcA^{\delta SH2/\delta SH2}$ mutants.

The development of spindles and group Ia sensory neurons is mutually dependent (*23*, *24*), and ShcA is expressed in both skeletal muscles and DRG neurons (*25*, *26*). To investigate where ShcA acts in the stretch reflex circuit, we generated mice with a targeted *ShcA* allele ($ShcA^{flx}$) encoding WT ShcA isoforms with a triple Flag (3×Flag) tag, which could be inactivated by Cre (Fig. 3A and fig. S9). For this purpose, we used the *Mlc1f-Cre* allele, which is expressed in developing skeletal muscles starting before the onset of spindle formation (*27*), or the *Isl1-Cre* allele that expresses Cre in embryonic motor and sensory neurons, including group Ia sensory neurons (*28*). $ShcA^{flx/flx}$ mice were viable and appeared normal. All $ShcA^{flx/flx}$; *Mlc1f-Cre* animals exhibited $ShcA^{3F/3F}$-like motor coordination defects, whereas $ShcA^{flx/flx}$; *Isl1-Cre* and $ShcA^{flx/KO}$; *Isl1-Cre* mutants appeared normal (movies S7 and S8). PCR analysis revealed Cre-mediated deletion of ShcA-3×Flag coding sequences specifically in skeletal muscles of *Mlc1f-Cre* carriers (Fig. 3B), and immunoblotting showed that ShcA-3×Flag was specifically ablated from skeletal muscles (Fig. 3C). Cre-mediated excision of ShcA-3×Flag coding sequences was detected in DRG and hindlimb tissues of *Isl1-Cre* carriers (Fig. 3D), where this allele is known to be active in sensory neurons and mesenchymal cells, respectively (*29*). Between P22 and P35, spindle numbers in $ShcA^{flx/flx}$; *Mlc1f-Cre* animals were 50% of those of controls (table S2). $ShcA^{flx/flx}$; *Mlc1f-Cre* spindles were morphologically abnormal (Fig. 3E), with intrafusal fiber numbers that were 59%

of those of controls (table S2). By contrast, spindles in *ShcA*$^{flx/flx}$; *Isl1-Cre* mice were present in proper numbers and appeared structurally normal (Fig. 3E and table S2). Thus, ShcA is required in developing skeletal muscles and/or spindles for proper motor behavior and spindle formation, and the defective synaptic conductivity of group Ia sensory neurons in *ShcA*$^{3F/3F}$ and *ShcA*$^{\delta SH2/\delta SH2}$ mutants is likely a non–cell-autonomous effect.

The preceding data did not discount the possibility that the spindle phenotypes of germline *ShcA*$^{3F/3F}$ and *ShcA*$^{\delta SH2/\delta SH2}$ mutants resulted from the effects of these alleles in a combination of spindle, muscle, and nonmuscle cell types. Furthermore, the role of the ShcA PTB domain in spindle formation could not be analyzed in *ShcA*$^{\delta PTB/\delta PTB}$ mutants because of their embryonic lethality. To address these issues, we generated *ShcA*$^{\delta PTB/flx}$; *Mlc1f-Cre* mutants, *ShcA*$^{3F/flx}$; *Mlc1f-Cre* mutants, and *ShcA*$^{\delta SH2/flx}$; *Mlc1f-Cre* mutants, anticipating that the Cre-mediated inactivation of the *ShcA*^{flx} allele would selectively restrict the effects of the *ShcA*$^{\delta PTB}$, *ShcA*^{3F}, and *ShcA*$^{\delta SH2}$ alleles to developing skeletal muscles and spindles (Fig. 4A). *ShcA*$^{\delta PTB/flx}$; *Mlc1f-Cre* mice, *ShcA*$^{3F/flx}$; *Mlc1f-Cre* mice, and *ShcA*$^{\delta SH2/flx}$; *Mlc1f-Cre* mice were fully viable, with the former two mutants exhibiting *ShcA*$^{3F/3F}$-like motor abnormalities and the latter mutant displaying *ShcA*$^{\delta SH2/\delta SH2}$-like motor defects (movies S9 to S11). Between P22 and P35, the spindle and intrafusal fiber numbers in *ShcA*$^{\delta PTB/flx}$; *Mlc1f-Cre* and *ShcA*$^{3F/flx}$; *Mlc1f-Cre* mutants were reduced, whereas only intrafusal fiber numbers were decreased in *ShcA*$^{\delta SH2/flx}$; *Mlc1f-Cre* mice

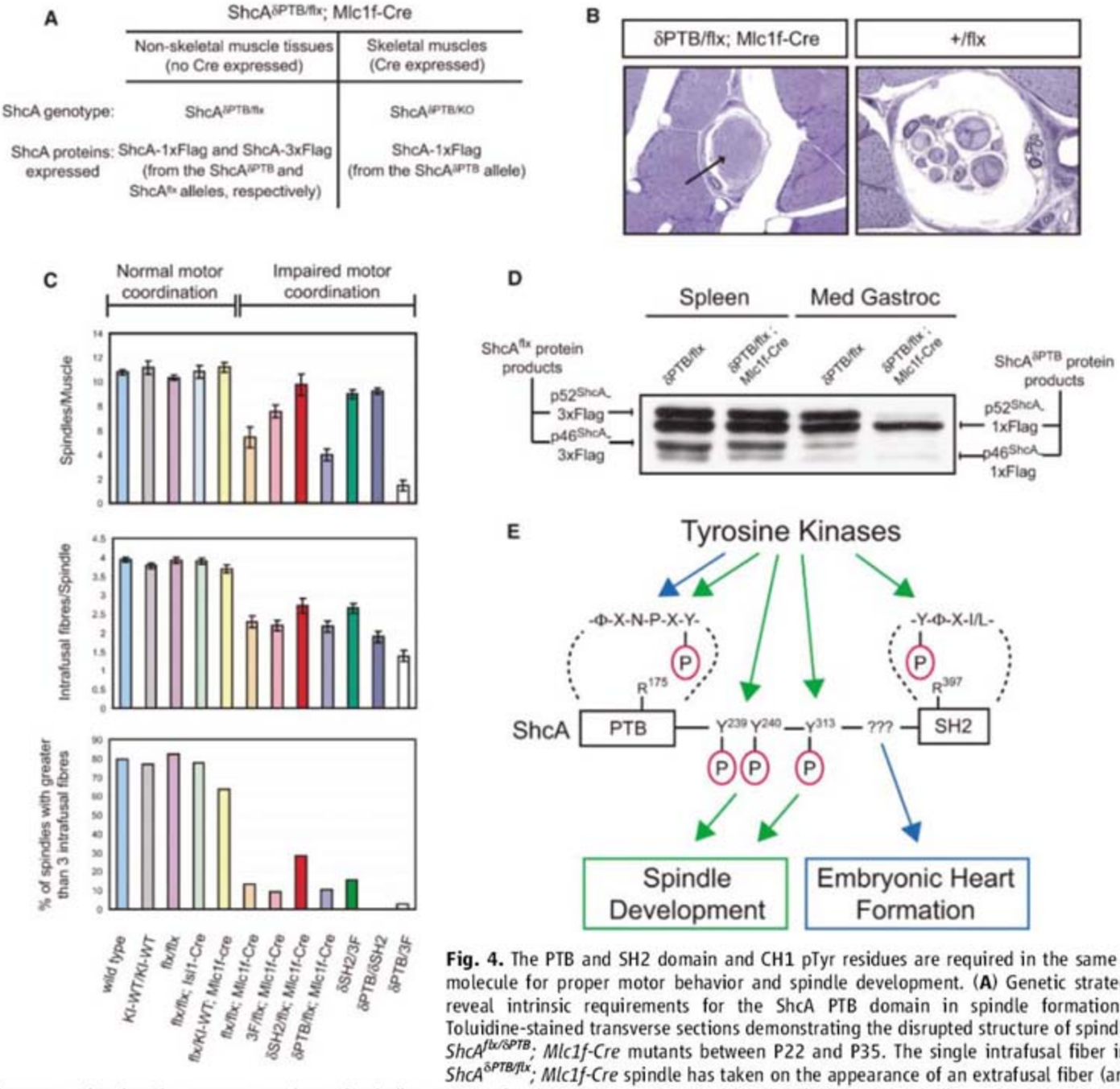

Fig. 4. The PTB and SH2 domain and CH1 pTyr residues are required in the same ShcA molecule for proper motor behavior and spindle development. (**A**) Genetic strategy to reveal intrinsic requirements for the ShcA PTB domain in spindle formation. (**B**) Toluidine-stained transverse sections demonstrating the disrupted structure of spindles in *ShcA*$^{flx/\delta PTB}$; *Mlc1f-Cre* mutants between P22 and P35. The single intrafusal fiber in the *ShcA*$^{\delta PTB/flx}$; *Mlc1f-Cre* spindle has taken on the appearance of an extrafusal fiber (arrow). (**C**) Histograms showing the average numbers of spindles per muscle, the average numbers of intrafusal fibers per spindle, and percentages of the average numbers of spindles with greater than three intrafusal fibers in muscle-restricted and transheterozygous *ShcA* mutants between P22 and P35. Mutants are grouped by whether they exhibit normal or impaired motor behavior. Error bars indicate SEM; numbers and statistics are presented in table S2. (**D**) Immunoblot analysis demonstrating that ShcA-1×Flag protein from the *ShcA*$^{\delta PTB}$ allele is selectively expressed in the skeletal muscles of *ShcA*$^{\delta PTB/flx}$; *Mlc1f-Cre* mice. (**E**) Diagram depicting combinatorial differences in the roles of the PTB and SH2 domains and CH1 pTyr residues of ShcA downstream of protein tyrosine kinases in spindle morphogenesis (green arrows and box) and embryonic heart formation (blue arrows and box). ???, presumptive CH1 pTyr–independent ShcA function.

(Fig. 4, B and C, and table S2). Immunoblot analysis confirmed that the slower-migrating ShcA-3×Flag proteins of the $ShcA^{flx}$ allele were selectively eliminated from the skeletal muscles of $ShcA^{\delta PTB/flx}$; *Mlc1f-Cre* mutants (Fig. 4D). Thus, the pTyr-binding functions of the ShcA PTB and SH2 domains, and phosphorylation of the YXN sites, are all required in skeletal muscles and/or spindles for proper motor coordination and spindle development.

To test whether the ShcA PTB domain, SH2 domain, and YXN phosphorylation sites act independently or in combination in spindle development, we tested for genetic complementation in animals with two different mutant alleles of ShcA. Transheterozygous $ShcA^{3F/\delta SH2}$, $ShcA^{\delta PTB/\delta SH2}$, and $ShcA^{3F/\delta PTB}$ mutants displayed motor defects of increasing severity. Between P22 to P35, spindle numbers in $ShcA^{\delta PTB/3F}$, $ShcA^{\delta PTB/\delta SH2}$, and $ShcA^{3F/\delta SH2}$ mutants were 13, 83.3, and 86.6%, respectively, of those in controls (Fig. 4C and table S2). Spindles in $ShcA^{3F/\delta PTB}$, $ShcA^{\delta PTB/\delta SH2}$, and $ShcA^{3F/\delta SH2}$ animals were structurally abnormal, with intrafusal fiber numbers that were 35.9, 66.6, and 48.7% of those in controls, respectively (Fig. 4C and table S2). This lack of complementation indicates that the PTB domain, SH2 domain, and phosphorylated YXN motifs are likely required in the same ShcA molecule (i.e., in cis) for proper spindle development and motor coordination.

Our findings imply that by combining the modular functions of a limited set of domains and motifs in alternate ways, ShcA is able to provide multiple signaling mechanisms to support diversity in tissue morphogenesis (Fig. 4E). This likely extends to other Shc family members and unrelated docking proteins with modular functions (*1*, *11*). The ShcA PTB domain is required in both spindle and midgestational heart formation, whereas the CH1 YXN motifs are only essential in the former case. This result indicates an important role for ShcA signaling in mammalian development that is independent of direct pYXN-mediated Grb2 binding. Genetic data from *Drosophila* suggest that this scheme is conserved in evolution, because the ShcA ortholog, DSHC, requires the PTB domain for signaling by the DER and Torso RTKs but can mediate RTK-dependent Ras activation in cells devoid of the Grb2 ortholog, DRK (*30*). By contrast, the pYXN motifs are required in cis with the PTB and SH2 domains for ShcA to elicit proper spindle formation, suggesting that pYXN-mediated ShcA-Grb2 interactions may be critical in this process. Based on the presence of both YXN motifs in some invertebrate Shc proteins (fig. S1), we speculate that this functional combination of ShcA domains and motifs, possibly acting in a signaling pathway downstream from ErbB RTKs (*19*, *20*, *23*), was coopted in evolution toward the development of muscle spindles as a novel tissue in vertebrates (*31*, *32*).

References and Notes

1. T. Pawson, P. Nash, *Science* **300**, 445 (2003).
2. J. Schlessinger, M. A. Lemmon, *Sci. STKE* **2003**, re12 (2003).
3. F. Maina *et al.*, *Cell* **87**, 531 (1996).
4. R. A. Klinghoffer, T. G. Hamilton, R. Hoch, P. Soriano, *Dev. Cell* **2**, 103 (2002).
5. G. Pelicci *et al.*, *Cell* **70**, 93 (1992).
6. Single-letter abbreviations for the amino acid residues are as follows: A, Ala; C, Cys; D, Asp; E, Glu; F, Phe; G, Gly; H, His; I, Ile; K, Lys; L, Leu; M, Met; N, Asn; P, Pro; Q, Gln; R, Arg; S, Ser; T, Thr; V, Val; W, Trp; and Y, Tyr.
7. K. S. Ravichandran, *Oncogene* **20**, 6322 (2001).
8. S. E. Egan *et al.*, *Nature* **363**, 45 (1993).
9. M. Rozakis-Adcock, R. Fernley, J. Wade, T. Pawson, D. Bowtell, *Nature* **363**, 83 (1993).
10. H. Gu *et al.*, *Mol. Cell. Biol.* **20**, 7109 (2000).
11. T. Nakamura *et al.*, *Oncogene* **21**, 22 (2002).
12. L. Luzi, S. Confalonieri, P. P. Di Fiore, P. G. Pelicci, *Curr. Opin. Genet. Dev.* **10**, 668 (2000).
13. E. Migliaccio *et al.*, *Nature* **402**, 309 (1999).
14. K. M. Lai, T. Pawson, *Genes Dev.* **14**, 1132 (2000).
15. R. Agah *et al.*, *J. Clin. Invest.* **100**, 169 (1997).
16. W. M. Kavanaugh, C. W. Turck, L. T. Williams, *Science* **268**, 1177 (1995).
17. A. Postigo *et al.*, *Genes Dev.* **16**, 633 (2002).
18. R. Klein *et al.*, *Nature* **368**, 249 (1994).
19. E. R. Andrechek *et al.*, *Mol. Cell. Biol.* **22**, 4714 (2002).
20. M. Leu *et al.*, *Development* **130**, 2291 (2003).
21. H. H. Chen, S. Hippenmeyer, S. Arber, E. Frank, *Curr. Opin. Neurobiol.* **13**, 96 (2003).
22. W. G. Tourtellotte, C. Keller-Peck, J. Milbrandt, J. Kucera, *Dev. Biol.* **232**, 388 (2001).
23. S. Hippenmeyer *et al.*, *Neuron* **36**, 1035 (2002).
24. H. H. Chen, W. G. Tourtellotte, E. Frank, *J. Neurosci.* **22**, 3512 (2002).
25. N. Altiok, S. Altiok, J. P. Changeux, *EMBO J.* **16**, 717 (1997).
26. P. Ganju, J. P. O'Bryan, C. Der, J. Winter, I. F. James, *Eur. J. Neurosci.* **10**, 1995 (1998).
27. G. W. Bothe, J. A. Haspel, C. L. Smith, H. H. Wiener, S. J. Burden, *Genesis* **26**, 165 (2000).
28. T. D. Patel *et al.*, *Neuron* **38**, 403 (2003).
29. L. Yang *et al.*, *Development* **133**, 1575 (2006).
30. S. Luschnig, J. Krauss, K. Bohmann, I. Desjeux, C. Nusslein-Volhard, *Mol. Cell* **5**, 231 (2000).
31. J. R. True, S. B. Carroll, *Annu. Rev. Cell Dev. Biol.* **18**, 53 (2002).
32. N. Maeda, S. Miyoshi, H. Toh, *Nature* **302**, 61 (1983).

33. W.R.H. and T.P. thank all lab and institute staff involved in this study for expert technical support, W. Muller and G. Hannon for providing plasmids, and J. Henderson for initial help. W.R.H. thanks L. MacNeil for her encouragement and insights. This work was supported by grants from the National Cancer Institute of Canada (NCIC), including a Terry Fox Program Project Grant, and from the Canadian Institutes for Health Research (CIHR). J.K. received funding from the Veterans Administration and NIH. E.F. received funding from the NIH. W.R.H was supported by a Terry Fox Ph.D. studentship from the NCIC. T.P. is a Distinguished Scientist of the CIHR.

Supporting Online Material

www.sciencemag.org/cgi/content/full/317/5835/251/DC1
Materials and Methods
Figs. S1 to S9
Tables S1 and S2
References
Movies S1 to S11

18 January 2007; accepted 7 June 2007
10.1126/science.1140114

Reciprocal T_H17 and Regulatory T Cell Differentiation Mediated by Retinoic Acid

Daniel Mucida, Yunji Park, Gisen Kim, Olga Turovskaya, Iain Scott, Mitchell Kronenberg, Hilde Cheroutre*

The cytokine transforming growth factor–β (TGF-β) converts naïve T cells into regulatory T (Treg) cells that prevent autoimmunity. However, in the presence of interleukin-6 (IL-6), TGF-β has also been found to promote the differentiation of naïve T lymphocytes into proinflammatory IL-17 cytokine-producing T helper 17 (T_H17) cells, which promote autoimmunity and inflammation. This raises the question of how TGF-β can generate such distinct outcomes. We identified the vitamin A metabolite retinoic acid as a key regulator of TGF-β–dependent immune responses, capable of inhibiting the IL-6–driven induction of proinflammatory T_H17 cells and promoting anti-inflammatory Treg cell differentiation. These findings indicate that a common metabolite can regulate the balance between pro- and anti-inflammatory immunity.

Helper T cells perform critical functions in the immune system through the production of distinct cytokine profiles. In addition to T helper-1 (T_H1) and T_H2 cells, a third subset of polarized effector T cells characterized by the production of interleukin-17 (IL-17) and other cytokines (and now called T_H17 cells) is associated with the pathogenesis of several autoimmune conditions (*1*). Transforming growth factor (TGF)–β is a suppressor of T_H1 and T_H2 cell differentiation and drives the conversion of T cells to those with a regulatory phenotype [so called regulatory T (Treg) cells]. In contrast to the suppression of T_H1 and T_H2 cells, in vitro activation of naïve T cells by dendritic cells (DCs) and TGF-β, together with proinflammatory cytokines including IL-6, leads to the differentiation of T_H17 cells (*2*–*4*). These observations indicate that the priming of T cells

La Jolla Institute for Allergy and Immunology, 9420 Athena Circle, La Jolla, CA 92037, USA.

*To whom correspondence should be addressed. E-mail: hilde@liai.org

by DCs in the presence of TGF-β might lead to opposing immune consequences.

Previous studies have indicated that mucosal DCs are immune suppressive (*5*), leading us to compare the ability of gut-associated DCs and peripheral DCs in driving T_H17 cell differentiation. Mesenteric lymph node (MLN) and spleen DCs were thus used to stimulate ovalbumin (OVA) peptide (OVAp)–specific, OT-II T cell receptor (TCR) transgenic CD4 T cells (Fig. 1A) or α-CD3–stimulated polyclonal CD4 T cells (fig. S1A) (*6*). In the presence of IL-6 and TGF-β, MLN DCs displayed a reduced capacity to induce T_H17 cell differentiation, as compared with their splenic counterparts. Mucosal DCs have been shown to imprint primed T cells with gut tropism, and the molecular mechanism for this has been attributed to DC-derived retinoic acid (RA) (*7*). To investigate if the reduced capacity of MLN DCs to drive T_H17 cell differentiation might also be controlled by RA, we included the RA receptor (RAR) antagonist LE135 (*8*) during the in vitro activation of T cells under conditions that promote T_H17 cell differentiation. In these experiments, the relative inefficiency of MLN DCs to mediate T_H17 cell differentiation was reversed such that they primed T cells at levels similar to those of spleen DCs. In comparison, the addition of all-trans RA to the cultures inhibited the T_H17 cell differentiation by spleen DCs (Fig. 1, A and B; fig. S1A; and SOM text 1). In addition to $CD4^+$ T_H17 cells, we observed that wild-type (Fig. 1C) or OT-I TCR^+ (fig. S1C) cytotoxic $CD8^+$T lymphocytes activated in the presence of TGF-β and IL-6 also generated IL-17^+T cells and that RA was again able to inhibit this process. This finding indicated that T cells can become IL-17^+cells, regardless of their effector phenotype, and that RA specifically suppresses IL-17 expression. T_H17 cells can also be generated in the absence of DCs if additional cytokines, such as IL-1 and TNF-α, are included in the culture conditions. Under such antigen-presenting cell (APC)–free conditions, RA also inhibited the generation of IL-17^+ T cells, demonstrating that RA targets T cells directly (fig. S1D).

RORγt is an orphan nuclear receptor that has been implicated in the gene transcription of T_H17 cells (*9*). To test whether RA controls RORγt, we activated CD4 T cells under T_H17 culture conditions, with or without RA. In the presence of inflammatory cytokines, TGF-β induced high levels of RORγt, whereas added RA greatly reduced its expression (Fig. 1D).

To investigate the apparent suppressive effect of RA on T_H17 cell development in vivo, mice were orally infected with *Listeria monocytogenes* (Lm) and treated with RA or an RAR inhibitor (LE540) (*8*). A measurable reduction of T_H17 mucosal T cells was seen in the animals that received RA, whereas RAR inhibitor–treated mice showed no apparent difference as compared to the controls (Fig. 1E). Collectively, these experiments suggest that RA acts to oppose T_H17 cell development in vitro and in vivo, and that this appears to operate directly on T cells via the reduction of RORγt.

The inefficiency of MLN DCs in promoting T_H17 cell differentiation and the reciprocal TGF-β–dependent conversion to either T_H17 or Treg cells led us to investigate whether mucosal DCs might drive enhanced TGF-β–dependent Treg cell differentiation (fig. S2, A and B, and SOM text 1). Because TGF-β–dependent Treg cells can be identified by expression of the forkhead/winged-helix transcription factor (Foxp3) (*10*–*13*), we tested for Foxp3 induction in OT-II CD4 cells cultured with spleen or MLN DCs in the presence of TGF-β and OVAp. In contrast to T_H17 cell differentiation that was seen with splenic DCs, MLN DCs were able to induce higher frequencies

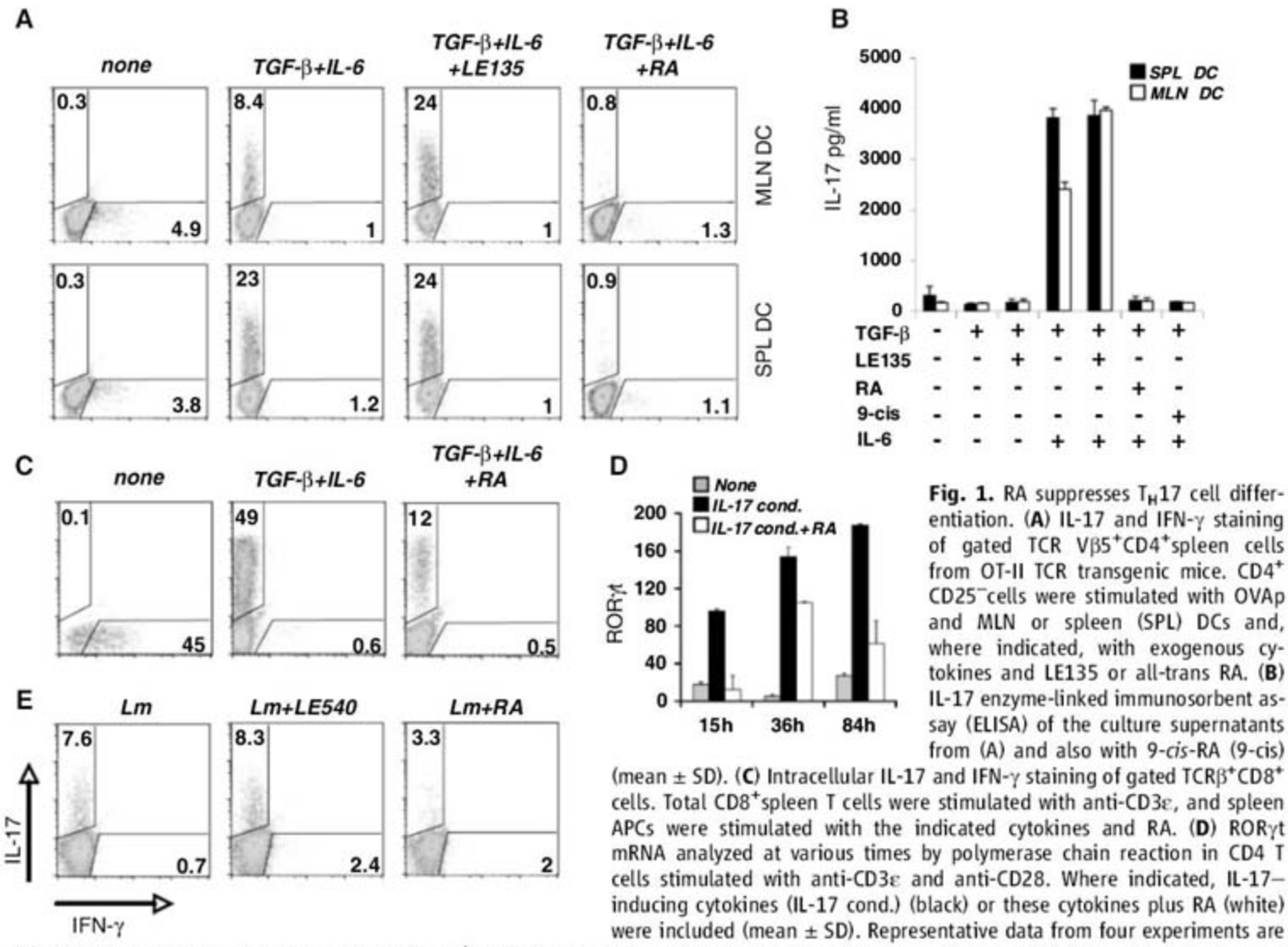

Fig. 1. RA suppresses T_H17 cell differentiation. (**A**) IL-17 and IFN-γ staining of gated TCR $V\beta5^+CD4^+$spleen cells from OT-II TCR transgenic mice. $CD4^+$ $CD25^-$cells were stimulated with OVAp and MLN or spleen (SPL) DCs and, where indicated, with exogenous cytokines and LE135 or all-trans RA. (**B**) IL-17 enzyme-linked immunosorbent assay (ELISA) of the culture supernatants from (A) and also with 9-*cis*-RA (9-cis) (mean ± SD). (**C**) Intracellular IL-17 and IFN-γ staining of gated $TCR\beta^+CD8^+$ cells. Total $CD8^+$spleen T cells were stimulated with anti-CD3ε, and spleen APCs were stimulated with the indicated cytokines and RA. (**D**) RORγt mRNA analyzed at various times by polymerase chain reaction in CD4 T cells stimulated with anti-CD3ε and anti-CD28. Where indicated, IL-17–inducing cytokines (IL-17 cond.) (black) or these cytokines plus RA (white) were included (mean ± SD). Representative data from four experiments are shown. (**E**) Intracellular IL-17 and IFN-γ staining of $CD4^+$T cells from small intestine lamina propria 5 days after oral infection with Lm. Data are representative of three to four mice per group.

of Foxp3$^+$cells (Fig. 2A). In the presence of an RAR inhibitor, TGF-β–dependent Foxp3 induction by MLN DCs was reduced, but it was enhanced by the addition of RA (Fig. 2A). In addition, RA promoted the expression of cytotoxic T lymphocyte antigen 4 (CTLA-4), a cell-surface receptor typically expressed by Treg cells, on most TGF-β–generated Foxp3$^+$cells (Fig. 2B and SOM text 2). The synergistic effect of RA on TGF-β–dependent Foxp3$^+$T cell differentiation was also apparent with CD8$^+$T cells (Fig. 2C), suggesting that the RA-mediated increase of Foxp3$^+$T cell differentiation might not be limited to CD25$^+$CD4$^+$Treg cells (fig. S2, C and D, and SOM text 3). Overall, these data indicate that RA controls the reciprocal differentiation of TGF-β–dependent Treg and T_H17 cells.

Mucosal DC-derived RA also mediates the induction of gut homing receptors, including the integrin $\alpha_4\beta_7$ and CCR9, specific for homing to the small intestine (*7*), whereas TGF-β has been found to promote the induction of CD103, the α_E subunit of the $\alpha_E\beta_7$ integrin (*14*). We therefore tested whether TGF-β and RA might synergize to induce these receptors. Consistent with synergy, RA greatly enhanced TGF-β–mediated CD103 expression. In contrast, TGF-β partially antagonized RA-induced CCR9 (Fig. 2D). These results show that the combination of RA and TGF-β results in CCR9$^+$ Treg cells with likely tropism for the small intestine and CCR9$^-$ Foxp3$^+$cells with potentially different homing capacities.

To further test the influence of RA in vivo, we treated Lm-infected mice with RA or an RAR inhibitor. Although RA alone did not measurably enhance the differentiation of Foxp3$^+$Treg cells in vivo, the inhibition of RAR significantly reduced the number of mucosal Foxp3$^+$Treg cells in Lm-challenged mice (Fig. 2E). No effect of RA or RAR on spleen Foxp3$^+$CD4 cells was observed (fig. S3C). The finding that RA combined with TGF-β, but not alone, can drive differentiation of Foxp3$^+$T cells in vitro (Fig. 2A) suggests that TGF-β might be a limiting factor in the lack of Treg cell differentiation induced by exogenous RA in vivo (fig. S3D and SOM text 4).

To examine whether in vitro–generated Foxp3$^+$CD4 T cells could function to suppress effector T cells in vivo, we performed cotransfer experiments using naïve CD45RB^{hi}CD4 T cells that induce colitis in immune-deficient mice (*15*), in combination with CD4 T cells that were previously cultured under different conditions. Mice that received CD4 T cells activated without cytokine conditioning, combined with naïve CD45RB^{hi}CD4 cells, developed severe colitis (Fig. 3). In contrast, mice that were cotransferred with CD4 T cells activated in the presence of TGF-β were partially protected from disease, and mice cotransferred with naïve T cells and CD4 T cells activated in vitro in the presence of both TGF-β and RA showed no apparent signs of disease (Fig. 3). Furthermore, fewer mucosal

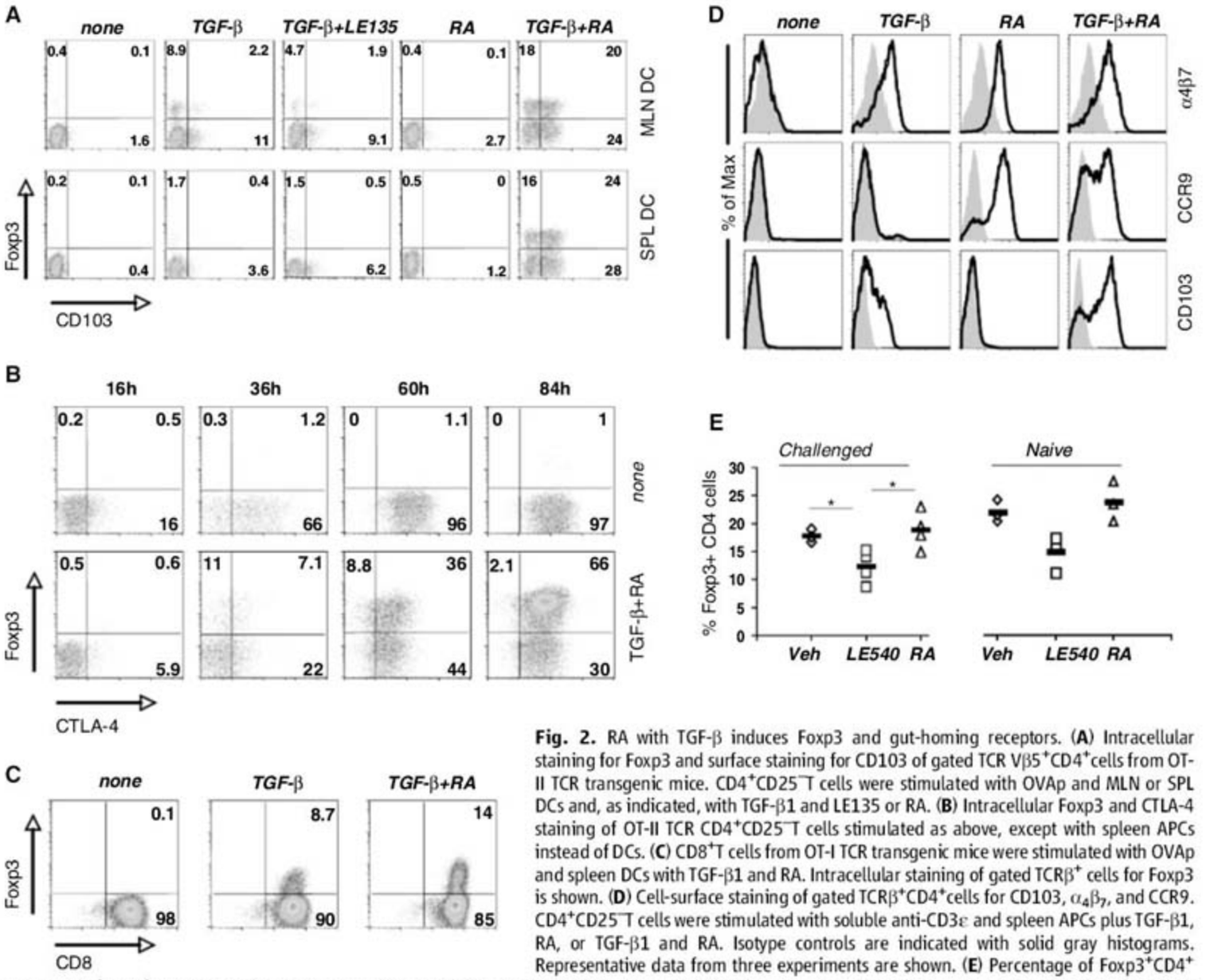

Fig. 2. RA with TGF-β induces Foxp3 and gut-homing receptors. (**A**) Intracellular staining for Foxp3 and surface staining for CD103 of gated TCR Vβ5$^+$CD4$^+$cells from OT-II TCR transgenic mice. CD4$^+$CD25$^-$T cells were stimulated with OVAp and MLN or SPL DCs and, as indicated, with TGF-β1 and LE135 or RA. (**B**) Intracellular Foxp3 and CTLA-4 staining of OT-II TCR CD4$^+$CD25$^-$T cells stimulated as above, except with spleen APCs instead of DCs. (**C**) CD8$^+$T cells from OT-I TCR transgenic mice were stimulated with OVAp and spleen DCs with TGF-β1 and RA. Intracellular staining of gated TCRβ$^+$ cells for Foxp3 is shown. (**D**) Cell-surface staining of gated TCRβ$^+$CD4$^+$cells for CD103, $\alpha_4\beta_7$, and CCR9. CD4$^+$CD25$^-$T cells were stimulated with soluble anti-CD3ε and spleen APCs plus TGF-β1, RA, or TGF-β1 and RA. Isotype controls are indicated with solid gray histograms. Representative data from three experiments are shown. (**E**) Percentage of Foxp3$^+$CD4$^+$ cells in CD4$^+$TCRβ$^+$lymphocytes from the small intestine lamina propria 5 days after oral infection with Lm (left) or in naïve controls (right). Veh, vehicle. Asterisks indicate $P < 0.05$ (Student's *t* test). Horizontal bars indicate averages of the mice that are represented individually.

CD4 T cells isolated from these animals produced IL-17 and interferon-γ (IFN-γ) (fig. S4). These results suggest that Foxp3$^+$T cells generated in vitro with RA and TGF-β have a measurable regulatory capacity and are able to control inflammation upon transfer in vivo. In addition, whereas Treg cells generated in vitro by TGF-β alone lost Foxp3 expression upon restimulation, most of the RA+TGF-β–differentiated Foxp3$^+$T cells remained Foxp3$^+$ after restimulation, indicating that RA drives the differentiation of a stable Treg cell lineage (Fig. 3D). Conversely, RA and TGF-β also suppressed committed T_H17 cells in secondary cultures, whereas TGF-β alone did not (Fig. 3E). The experiments thus far suggest that RA might directly counteract the activity of IL-6, and to test this hypothesis, we analyzed TGF-β–dependent T cell differentiation in the presence of RA, together with IL-6. CD4 (Fig. 4A) or CD8 (Fig. 4B) T cells cultured with RA under conditions that otherwise promote TGF-β–dependent T_H17 cell differentiation converted to Foxp3$^+$cells with a decrease in T_H17 cell differentiation. The antagonistic effect of RA on IL-6 was dose dependent (fig. S5A), suggesting that under physiological conditions, the RA-driven TGF-β–dependent Treg cell differentiation might override the IL-6–promoted TGF-β–dependent T_H17 cell generation.

IL-2 is required for the production of TGF-β–dependent Foxp3$^+$Treg cells (*16*), and it was recently shown that exogenously added IL-2 also suppresses T_H17 cell differentiation (*17*). To investigate whether RA-mediated regulation of T cell polarization required IL-2 signaling, we examined RA-mediated effects on T cell differentiation in vitro in the absence of IL-2, using IL-2–specific antibodies (anti–IL-2) or IL-2$^{-/-}$ T cells. In these experiments, the enhanced effect of RA in driving differentiation of Foxp3$^+$cells and the inhibitory effect of RA on TGF-β–dependent T_H17 cell differentiation were primarily dependent on IL-2 (Fig. 4, C to E, and fig. S5, B and C). RA-mediated regulation did not require exogenously added IL-2, although when added together, RA and exogenous IL-2 synergized to drive the reciprocal regulation of TGF-β–dependent T cell differentiation (Fig. 4). However, RA- and exogenous IL-2–controlled differentiation appeared distinct, in that RA-mediated TGF-β–dependent Foxp3 differentiation generated mostly CD103$^+$Treg cells, whereas most of the IL-2–driven Foxp3$^+$Treg cells were CD103$^-$ (Fig. 4C). Conversely, the mechanism of RA and IL-2 used to suppress T_H17 cells also appeared to have some distinctions, because RA measurably decreased IL-17 cytokine secretion, whereas exogenous IL-2 did not (Fig. 4E). Collectively, these experiments show that although both exogenous IL-2 and RA require initial IL-2 signaling for their regulatory function, the cooperation with TGF-β and the further downstream mechanisms they activate might be very different (SOM text 5).

The reciprocal activity of RA in inhibiting TGF-β–dependent T_H17 cell generation while promoting Foxp3$^+$Treg cell differentiation might provide a self-correcting mechanism for TGF-β to regulate both pro- and anti-inflammatory immunity. This regulatory capacity has particular relevance for the intestine, where efficient immune protection has to coincide with maintaining the mucosal-barrier integrity.

Vitamin A deficiency causes immune dysfunction and increased mortality (*18*). Our results show that RA-mediated effects might be important in vivo. The immune pathology characteristic of subphysiological levels of RA might in part be attributed to an imbalanced TGF-β function favoring proinflammatory T_H17 cells at the expense of anti-inflammatory Treg cells. These insights may stimulate new approaches for the treatment of immune disorders in which the imbalance mediated by TGF-β might be an important contributor to immune pathophysiology.

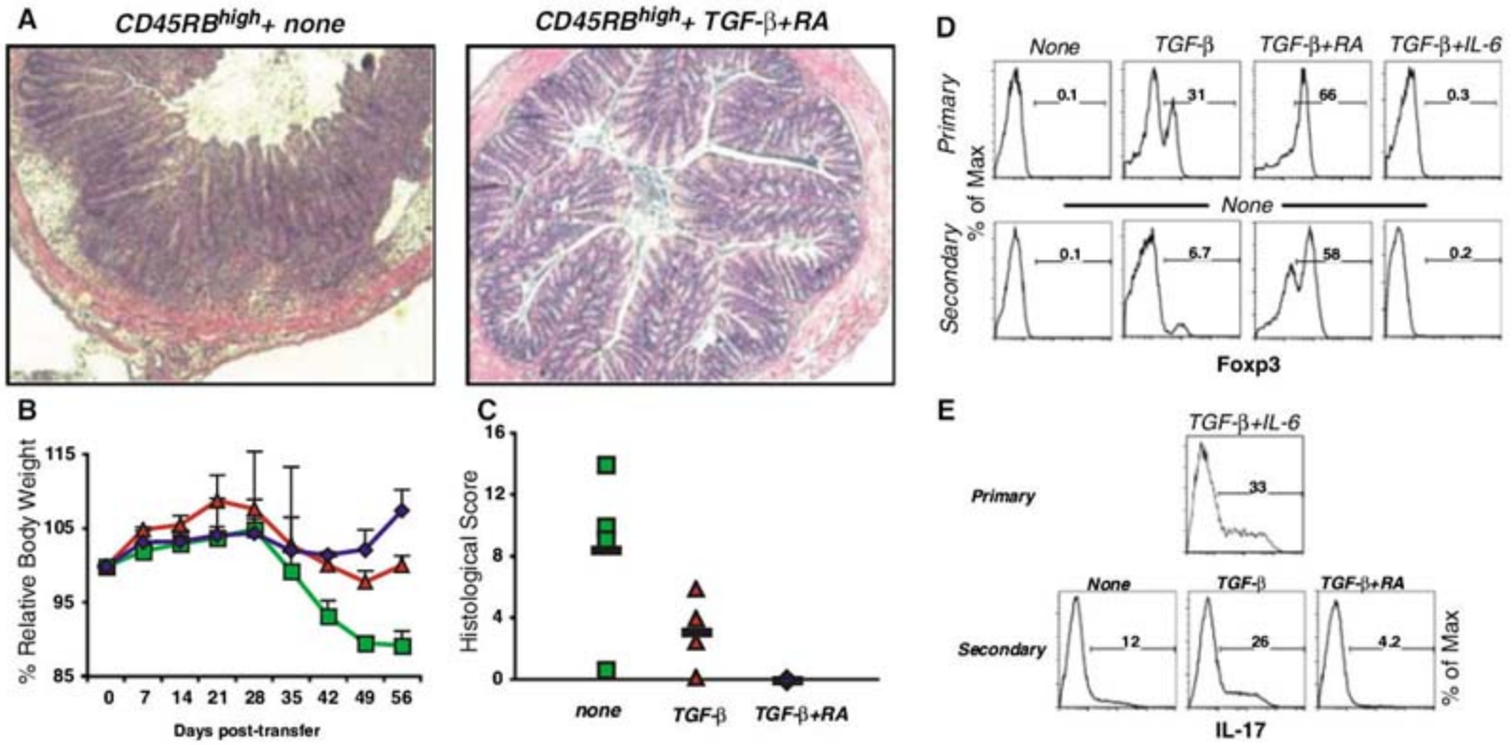

Fig. 3. TGF-β plus RA in vitro–differentiated Treg cells regulate in vivo. (**A**) Hematoxylin and eosin staining of the distal colon of mice deficient in recombination activating gene 1 (RAG-1$^{-/-}$) 6 to 7 weeks after cotransfer of 5×10^5 CD4$^+$CD45RB^{hi} cells with 2.5×10^5 CD4$^+$T cells stimulated in vitro with anti-CD3ε alone (none) or with TGF-β1 and RA. Original magnification, 40×. Representative data from four mice in each group are shown. (**B**) Body weight of RAG-1$^{-/-}$ mice after transfer of 5×10^5 CD4$^+$CD45RB^{hi}cells with 2.5×10^5 anti–CD3ε-stimulated CD4$^+$T cells with no additions (squares), TGF-β 1 (triangles), or TGF-β1 and RA (diamonds). The mean ± SD weight of four animals per group is shown; data are representative of three experiments. (**C**) Histological scores of the groups described in (B). Horizontal bars indicate averages of the mice that are represented individually. (**D**) Foxp3 intracellular staining of naïve TCRβ$^+$CD4$^+$ cells that were initially stimulated with soluble anti-CD3ε and spleen APCs with the indicated cytokines. The cells were rested for 2 days with IL-2 and then restimulated in the absence of exogenous cytokines before analysis. (**E**) Intracellular staining for IL-17 of naïve CD4$^+$T cells that were initially stimulated and rested as described in (D), but in the presence of TGF-β and IL-6, and then restimulated in the indicated conditions. The percentage of IL-17$^+$cells in the gated TCRβ$^+$CD4$^+$cells is depicted. Representative data from three experiments are shown.

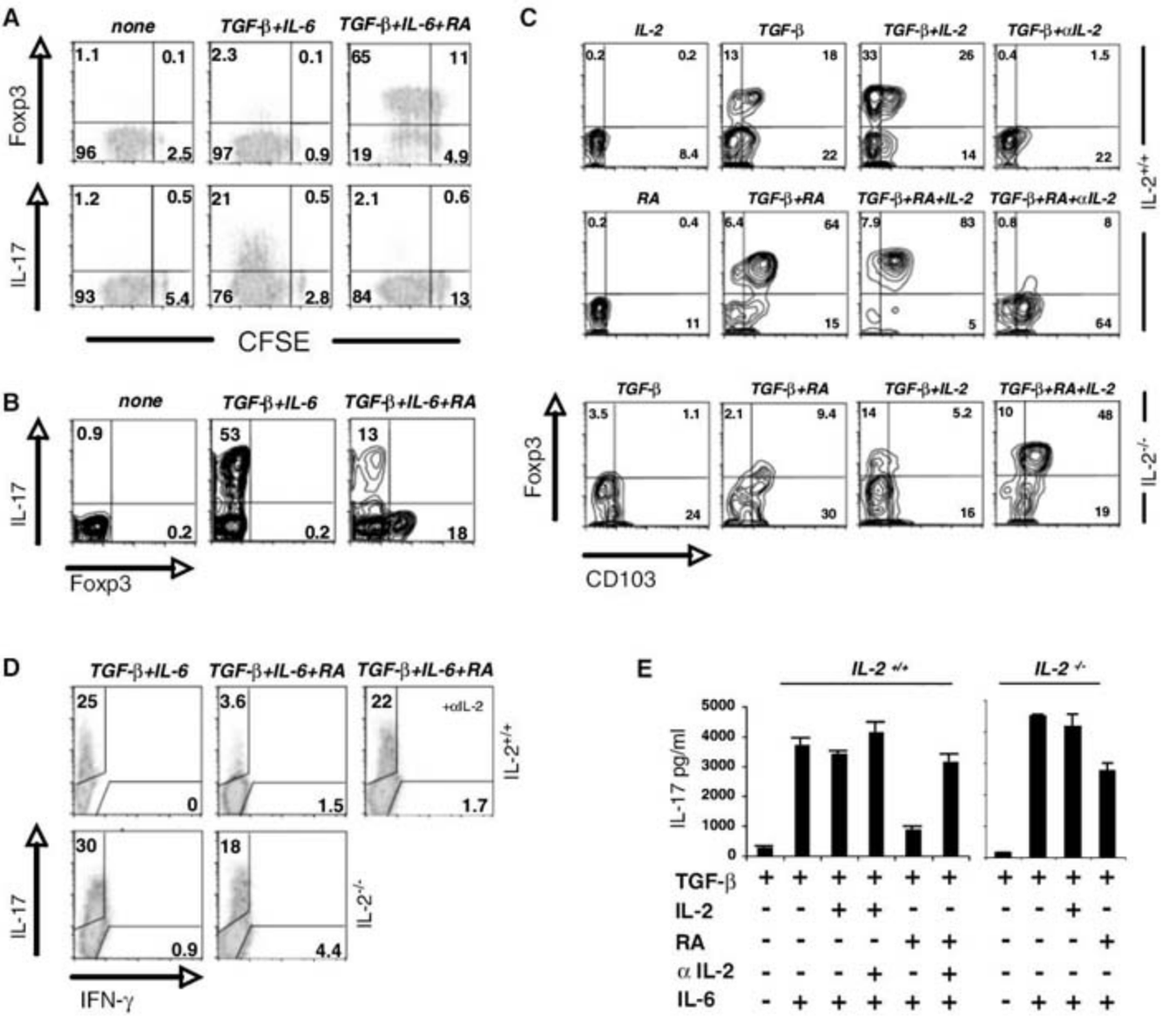

Fig. 4. Reciprocal TGF-β–dependent T cell differentiation by IL-6 and RA. (**A**) Naïve CD4$^+$T cells labeled with carboxyfluorescein diacetate succinimidyl ester (CFSE) were stimulated with anti-CD3ε, spleen APCs, the indicated cytokines, and RA. TNF-α, IL-1-β, TGF-β, and IL-6 were used to drive IL-17 differentiation. Intracellular staining of gated TCRβ$^+$CD4$^+$cells for Foxp3 and IL-17 is depicted. (**B**) Intracellular staining for Foxp3 and IL-17 of CD8$^+$T cells stimulated with soluble anti-CD3ε and spleen APCs under the indicated conditions. (**C** and **D**) Intracellular staining for Foxp3 and surface staining for CD103 (C) or intracellular staining of IL-17 and IFN-γ (D) of naïve CD4$^+$T cells from B7.1/2$^{-/-}$ IL-2$^{+/+}$ or B7.1/2$^{-/-}$ IL-2$^{-/-}$ mice. Cells were stimulated with soluble anti-CD3ε, spleen APCs and the indicated cytokines, and RA and/or a blocking antibody to IL-2 (20 μg/ml). The staining was performed on gated TCRβ$^+$CD4$^+$ cells. (**E**) ELISA of IL-17 in the supernatant of the cultures in (C) and (D) (mean ± SD). Representative data of two experiments are shown.

References and Notes

1. J. Furuzawa-Carballeda, M. I. Vargas-Rojas, A. R. Cabral, *Autoimmun. Rev.* **6**, 169 (2007).
2. M. Veldhoen, R. J. Hocking, C. J. Atkins, R. M. Locksley, B. Stockinger, *Immunity* **24**, 179 (2006).
3. E. Bettelli *et al.*, *Nature* **441**, 235 (2006).
4. P. R. Mangan *et al.*, *Nature* **441**, 231 (2006).
5. A. Iwasaki, *Annu. Rev. Immunol.* **25**, 381 (2007).
6. Materials and methods are available as supporting material on *Science* Online.
7. M. Iwata *et al.*, *Immunity* **21**, 527 (2004).
8. Y. Li, Y. Hashimoto, A. Agadir, H. Kagechika, X. Zhang, *J. Biol. Chem.* **274**, 15360 (1999).
9. I. Ivanov *et al.*, *Cell* **126**, 1121 (2006).
10. J. D. Fontenot, M. A. Gavin, A. Y. Rudensky, *Nat. Immunol.* **4**, 330 (2003).
11. S. Hori, T. Nomura, S. Sakaguchi, *Science* **299**, 1057 (2003).
12. R. Khattri, T. Cox, S. A. Yasayko, F. Ramsdell, *Nat. Immunol.* **4**, 337 (2003).
13. D. Mucida *et al.*, *J. Clin. Invest.* **115**, 1923 (2005).
14. G. A. Hadley, S. T. Bartlett, C. S. Via, E. A. Rostapshova, S. Moainie, *J. Immunol.* **159**, 3748 (1997).
15. A. Izcue, J. L. Coombes, F. Powrie, *Immunol. Rev.* **212**, 256 (2006).
16. T. S. Davidson, R. J. DiPaolo, J. Andersson, E. M. Shevach, *J. Immunol.* **178**, 4022 (2007).
17. A. Laurence *et al.*, *Immunity* **26**, 371 (2007).
18. A. Sommer, *J. Infect. Dis.* **167**, 1003 (1993).

19. We thank M. Steinberg, Y. Kinjo, and E. Tupin for helpful discussions; X. Zhang for providing the LE135 inhibitor; Y. Wang-Zhu for providing C57BL/6 mice; C. Lena for help in intraepithelial lymphocyte preparations; S. Feau and Y. Huang for help with Listeria infection; and M. Cheroutre for her contribution. This work was supported by NIH grant RO1 AI050265-06 and The Crohn's and Colitis Foundation of America fellowship (Y.P.).

Supporting Online Material

www.sciencemag.org/cgi/content/full/1145697/DC1

Materials and Methods
SOM Text
Figs. S1 to S5
References

22 February 2007; accepted 6 June 2007
Published online 14 June 2007;
10.1126/science.1145697
Include this information when citing this paper.

Ultra-Bright X-Ray Source

The Microstar Ultra is a bright x-ray source for structural biology that is comparable in brightness to many second-generation synchrotron beams. Featuring advanced electron optics and the patent-pending Hypercool anode cooling design, the Microstar Ultra produces x-ray intensities of 8×10^{10} x-rays/mm^2/sec, higher than any conventional rotating anode generator. This increase in performance is beneficial for all aspects of in-house crystallographic research, from high-throughput crystal screening to structural determination. It makes the instrument suitable for analyzing even the smallest crystals. The unit is compact and low maintenance, and offers an affordable path for existing Microstar generators to be upgraded to the Ultra.

Bruker AXS For information 978-663-3660 www.bruker-axs.com

Glyco Protein Staining

Glyco-Stain allows for the staining of glyco-protein bands that may not be visible if stained with ordinary Coomassie dye or silver staining methods. Using a modified silver enhancement, it achieves a nanogram level of sensitivity, with more than a two-fold increase in glycoprotein and proteoglycan detection. Glyco-Stain detects both glycosylated and non-glycosylated proteins.

Genotech/G-Biosciences For information 314-991-6034 www.GBiosciences.com

LabSafe GEL Blue

A sensitive Coomassie dye-based protein stain that is also environmentally safe can detect as little as 4 ng bovine serum albumin without any need for destaining. The ready-to-use format produces rapid protein band visualization on gels following electrophoresis. After a brief wash step, LabSafe GEL Blue is added directly to the protein gel.

Genotech/G-Biosciences For information 314-991-6034 www.GBiosciences.com

Antigen Unmasking Solution

The High pH Antigen Unmasking Solution is a TRIS-based formula that is highly effective at revealing antigens in formalin-fixed, paraffin-embedded tissue sections when used in combination with a high temperature treatment procedure. The solution is supplied as a concentrated stock, sufficient to prepare 25 liters of working solution.

Vector Laboratories For information 650-697-3600 www.vectorlabs.com

Flow Cytometry Cell Isolation

New DynaBeads FlowComp cell isolation technology is a tool compatible with flow cytometry that is designed to isolate cells and avoid the negative cellular effects caused by foreign immunogenic substances. Cells are isolated with a simple tube-based magnetic separation that leaves the isolated cells bead-free, allowing downstream use in any cell-based application. FlowComp products are built on the inert Dynabeads technology, so no harmful substances such as iron oxides or dextran, which remain following other isolation techniques, are left to negatively influence results. The first products featuring this new technology allow mouse and human T cell isolation.

Invitrogen For information 800-955-6288 www.invitrogen.com

Multiplexed PCR-Based Assays

QIAplex polymerase chain reaction (PCR) multiplex technology allows sensitive detection of multiple molecular targets in one test. Until now, samples that could contain multiple pathogens such as viruses, bacteria, and other disease markers have had to be analyzed with assays that typically test for one to three molecular targets. QIAplex-based multiplexing has great advantages compared with single-target assays, since one or more targets can be detected in one test from one sample. This permits sensitive and simultaneous analyses of multiple nucleic acid targets. The newly launched research-use QIAplex panels—ResPlex I Panel, ResPlex II Panel, and StaphPlex Panel—allow parallel detection of more than 10 bacterial and viral targets in a single reaction. The ResPlex I and ResPlex II panels detect respiratory bacterial and viral nucleic acids. The StaphPlex Panel allows identification of methicillin-resistant Staphylococcus aureus for research applications.

Qiagen For information 800-426-8157 www.qiagen.com

Imaging Agent Antibody Conjugates

Kodak X-Sight Imaging Agent Antibody Conjugates for in vitro imaging applications join an existing line of organic fluorescent nanoparticles for in vivo applications. The conjugates are suitable for protein immunoblotting applications, which use gel electrophoresis to separate proteins from a sample of cell or tissue based on molecular weight and size. Once the proteins are separated, a primary antibody targets the specific protein of interest. These conjugates attach to the primary antibody and illuminate when excited by the appropriate wavelength of fluorescent light, thus allowing researchers to visualize and quantify the protein under investigation. The superior brightness these conjugates offer means higher levels of sensitivity and detection of smaller amounts of proteins can be achieved. Designed to be biocompatible and nontoxic, they provide a bright and robust platform for translating molecular imaging experiments from in vitro to in vivo applications.

Eastman Kodak For information 877-747-4357 www.kodak.com/go/molecular

Blood Pressure Monitoring

The Non-Invasive Blood Pressure Monitoring System (NIPB) provides an easy and reliable technique for measuring systemic blood pressure and cardiovascular parameters in rodents without invasive catheterization. The NIPB calculates systolic, diastolic, and mean blood pressure in real time with complete reliability. The transducers and cuffs can be exchanged to accommodate up to 12 animals of varying sizes up to 500 g. Researchers can customize their NIBP systems with heaters, scanners, and specialized software.

Stoelting For information 630-860-9700 www.stoeltingco.com/physio

Newly offered instrumentation, apparatus, and laboratory materials of interest to researchers in all disciplines in academic, industrial, and government organizations are featured in this space. Emphasis is given to purpose, chief characteristics, and availability of products and materials. Endorsement by *Science* or AAAS of any products or materials mentioned is not implied. Additional information may be obtained from the manufacturer or supplier.

Science Careers
From the journal Science AAAS

Classified Advertising

From life on Mars
to life sciences

For full advertising details, go to
www.sciencecareers.org and click on
For Advertisers, or call one of our representatives.

United States & Canada

E-mail: advertise@sciencecareers.org
Fax: 202-289-6742

IAN KING Recruitment Sales Manager
Phone: 202-326-6528

NICHOLAS HINTIBIDZE
West Academic
Phone: 202-326-6533

DARYL ANDERSON
Midwest/Canada Academic
Phone: 202-326-6543

ALLISON MILLAR
Industry/Northeast Academic
Phone: 202-326-6572

TINA BURKS
Southeast Academic
Phone: 202-326-6577

Europe & International

E-mail: ads@science-int.co.uk
Fax: +44 (0) 1223 326532

TRACY HOLMES Sales Manager
Phone: +44 (0) 1223 326525

MARIUM HUDDA
Phone: +44 (0) 1223 326517

ALEX PALMER
Phone: +44 (0) 1223 326527

LOUISE MOORE
Phone: +44 (0) 1223 326528

Japan

JASON HANNAFORD
Phone: +81 (0) 52-757-5360
E-mail: jhannaford@sciencemag.jp
Fax: +81 (0) 52-757-5361

To subscribe to *Science*:
In U.S./Canada call 202-326-6417 or 1-800-731-4939
In the rest of the world call +44 (0) 1223-326-515

Science makes every effort to screen its ads for offensive and/or discriminatory language in accordance with U.S. and non-U.S. law. Since we are an international journal, you may see ads from non-U.S. countries that request applications from specific demographic groups. Since U.S. law does not apply to other countries we try to accommodate recruiting practices of other countries. However, we encourage our readers to alert us to any ads that they feel are discriminatory or offensive.

POSITIONS OPEN

EVOLUTIONARY DEVELOPMENTAL BIOLOGIST
Bryn Mawr College

The Department of Biology invites applications for a tenure-track position in evolutionary developmental biology at the rank of **ASSISTANT PROFESSOR,** beginning August 2008. We seek as a colleague someone who will thrive in an environment that combines teaching and research. The successful candidate is expected to teach at all levels of the curriculum and establish an externally funded research program that provides rigorous collaborative research projects for undergraduates. Individuals who study animal and/or plant development model systems with a strong evolutionary context are encouraged to apply. A Doctorate and at least one year of postdoctoral experience are required.

Please send a letter of application, curriculum vitae, a description of research plans that addresses the role of undergraduates in your research, and a statement of teaching philosophy that includes areas of teaching interests, and arrange for three letters of recommendation to be sent by September 21, 2007, to: **Chair, Biology Search, Department of Biology, Bryn Mawr College, 101 N. Merion Avenue, Bryn Mawr, PA 19010-2899.** (No electronic submissions, please.)

Located in suburban Philadelphia, Bryn Mawr College is a highly selective liberal arts college for women who share an intense intellectual commitment, a self-directed and purposeful vision of their lives, and a desire to make meaningful contributions to the world. Bryn Mawr comprises an undergraduate college with 1,200 students, as well as coeducational graduate schools in some humanities, sciences, and social work. The College supports faculty excellence in both teaching and research, and participates in consortial programs with the University of Pennsylvania, and Haverford and Swarthmore Colleges. *Bryn Mawr College is an Equal Opportunity, Affirmative Action Employer. Minority candidates and women are especially encouraged to apply.*

FACULTY POSITION in PHARMACOLOGY
Department of Pharmaceutical Sciences
Midwestern University
College of Pharmacy-Glendale

The Department of Pharmaceutical Sciences invites applications for a 12-month, tenure-track position at the rank of **ASSISTANT/ASSOCIATE PROFESSOR.** The Department of Pharmaceutical Sciences encompasses the disciplines of physiology, pathophysiology, pharmaceutics, pharmacokinetics, medicinal chemistry, and pharmacology. Applicants should possess a Ph.D. degree in pharmacology or in a related discipline. Candidates with postdoctoral experience or an active research program will be given preference. A professional degree in pharmacy is desirable but not required. The successful candidate must demonstrate a commitment to quality teaching and scholarship, be highly motivated and a team player, and have a constructive and cooperative approach to faculty and institutional affairs. This faculty member will teach didactic courses offered by the Department of Pharmaceutical Sciences and team teach in integrated courses with the Department of Pharmacy Practice. Engagement of students in research and the establishment of an active research program are expected.

The position is available immediately. Application review will continue until the position is filled. Applicants should submit a personal statement describing his/her teaching philosophy and research interest/experience, curriculum vitae, and names, addresses, telephone numbers, and e-mail addresses of at least three references. Midwestern University College of Pharmacy-Glendale is located on a picturesque 140 acre campus in the greater Phoenix area. Applicants should send information to: **Craig Johnston, Ph.D., Chair, Department of Pharmaceutical Sciences, College of Pharmacy-Glendale, Midwestern University, 19555 N. 59th Avenue, Glendale, AZ 85308, telephone: 623-572-3575, e-mail:cjohns@midwestern.edu.** *Midwestern University is an Equal Opportunity Employer.*

POSITIONS OPEN

USDA ARS Agricultural Research Service
www.ars.usda.gov

The U.S. Department of Agriculture, Agricultural Research Service (ARS), Crops Pathology and Genetics Research Unit, Davis, California, invites applications for a **RESEARCH BIOINFORMATICIST/COMPUTATIONAL BIOLOGIST/MOLECULAR GENETICIST/PLANT PATHOLOGIST**, GS-12/13/14 ($66,993.00 to $122,379.00 per annum). The USDA-ARS, Crops Pathology and Genetics Research Unit, located in Davis, California, is seeking a permanent, full-time scientist to conduct genomics-based research on *Phytophthora ramorum*, the causal agent of Sudden Oak Death. The successful candidate will develop an independent, innovative research program that focuses on understanding the genetic, biochemical, and molecular mechanisms of *P. ramorum* pathogenesis with the goal of developing effective disease control strategies. Research areas include, but are not limited to, computational analyses of the sequenced genomes of *Phytophthora spp.* and characterization of plant host infection and colonization by *P. ramorum* through global gene expression studies and/or proteomics approaches. The incumbent will participate in collaborative efforts with ARS and University researchers involved in the Sudden Oak Death Research Program. Salary will be competitive and commensurate with experience. For details and application directions, see **website: http://www.usajobs.com.** Announcement number ARS-X7W-0251. For additional information contact **Dr. Kluepfel** at **telephone: 530-752-1137** or **e-mail: dakluepfel@ucdavis.edu.**

U.S. citizenship is required. The USDA is an Equal Opportunity Provider and Employer.

HEAD, DEPARTMENT of BOTANY
Oklahoma State University

The Department of Botany **(website: http://botany.okstate.edu)** at Oklahoma State University (OSU) invites applications for the position of Professor and Department Head. We seek a dynamic and visionary leader who will have an extramurally supported, nationally recognized research program, administrative skills, a commitment to supporting innovative teaching, and a vision for curricular enhancement and reform at the graduate and undergraduate levels. Applicants should have qualifications appropriate for a tenured appointment at the rank of Professor. The preferred starting date is July 1, 2008.

OSU is a land-grant institution with 23,000 students located in north central Oklahoma, 70 miles from Oklahoma City and Tulsa. Applicants should submit by e-mail to the **Search Chair (Dr. Joe Bidwell, Zoology, e-mail: joe.bidwell@okstate.edu)** a single PDF file containing: a cover letter, statements of research, teaching, and administrative philosophies and accomplishments, curriculum vitae, and contact information of four professional references. Informal inquiries to **Dean Peter Sherwood** of the College of Arts and Sciences are welcome **(telephone: 405-744-5663; e-mail: peter.sherwood@okstate.edu).** Review of applications will begin September 15, 2007, and will continue until the position is filled. *OSU encourages applications from qualified women, minorities, and persons with disabilities.*

FACULTY POSITIONS
EVOLUTIONARY BIOLOGIST
PHYSIOLOGIST-PROTEOMICS BIOLOGIST

Two tenure-track positions in the Department of Biological Sciences at California State University, Long Beach, starting fall 2008; **ASSISTANT PROFESSOR** preferred, **ASSOCIATE PROFESSOR** considered. See **websites: http://www.csulb.edu/depts/biology** or **http://www.csulb.edu/divisions/aa/personnel/jobs/cnsm** for application details and additional information. Application review begins on September 10, 2007. *CSULB is an Equal Opportunity Employer committed to excellence through diversity, and takes pride in its multicultural environment.*

Pfizer

Working for a healthier world™

Biotherapeutics Research

When do large molecules become giant scientific breakthroughs?

Imagine what you can achieve at a biotech start-up with unrivaled global resources. Imagine translating leading research into life-saving biotherapeutics. Imagine a biotech company atmosphere within one of the world's largest pharmaceutical organizations.

At Pfizer Biotherapeutics Research, we want to leave a lasting legacy to the world. We're building on our current successes and capabilities, with the goal of developing the most compelling story of biotherapeutic scientific discoveries - and through this a compelling portfolio of biological therapies.

Representing a new aligned focus on biotherapeutics for the world's largest healthcare research organization, Pfizer Biotherapeutics Research has brought to market a wide-range of ground-breaking medicines including Fragmin, Genotropin, Macugen, Somavert and our first-in-class inhaled insulin product Exubera. And, now, with a blossoming late stage pipeline, we are focusing on further developing our research programs to deliver innovative and compelling biotherapeutics scientific research and discoveries.

Our accomplishments to date make us the eighth-largest biotech in the world with an anticipated $1.5 billion in sales. But there is much more work to be done, and we are investing in science in order to grow our biotherapeutics research to 20 percent of the overall Pfizer portfolio, leading to the launch of one biotherapeutic product every year by 2016. In doing so we hope to deliver exciting scientific discoveries that will forever change the treatment of disease.

But we can't do it alone. Our achievements are the direct result of our multidisciplinary teams working together to accomplish boundary-breaking results. That's why we're seeking you, world-renowned scientists, researchers and doctors, to help us - working in tandem we'll bring these exciting new therapies to patients and improve the health and well-being of people everywhere.

Your talent can change the world at Pfizer Biotherapeutics Research, a biotherapeutics company unlike any other.

To learn more about our people, our products, and our plans for the future, visit www.pfizerbiotherapeutics.com

We're proud to be an equal opportunity employer and welcome applications from people with different experiences, backgrounds and ethnic origins.

Positions @ NIH

THE NATIONAL INSTITUTES OF HEALTH

OFFICE OF PORTFOLIO ANALYSIS AND STRATEGIC INITATIVES
DIRECTOR, DIVISION OF STRATEGIC COORDINATION

The Office of the Director, National Institutes of Health (NIH) in Bethesda, Maryland, is seeking a Director of the Division of Strategic Coordination (DSC) within the Office of Portfolio Analysis and Strategic Initiatives (OPASI). If you are an exceptional candidate with an M.D. and/or Ph.D., we encourage your application.

The OPASI's primary objective is to develop: a transparent process of planning and priority-setting characterized by a defined scope of review with broad input from the scientific community and the public; valid and reliable information resources and tools, including uniform disease coding and accurate, current and comprehensive information on burden of disease; an institutionalized process of regularly scheduled evaluations based on current best practices; the ability to weigh scientific opportunity against public health urgency; a method of assessing outcomes to enhance accountability; and a system for identifying areas of scientific and health improvement opportunities and supporting regular trans-NIH scientific planning and initiatives.

As the DSC Director, you will be responsible for integrating information and developing recommendations to inform the priority-setting and decision-making processes of the NIH in formulating NIH-wide strategic initiatives. These initiatives will address exceptional scientific opportunities and emerging public health needs (akin to the Roadmap, Obesity, and Neuroscience Blueprint initiatives). You will also be responsible for providing the NIH Director with the information needed to allocate resources effectively for trans-NIH efforts.

Salary is commensurate with experience and includes a full benefits package. A detailed vacancy announcement with the mandatory qualifications and application procedures can be obtained on **USAJOBS at www.usajobs.gov (announcement number OD-07-172844-T42) and the NIH Web Site at http://www.jobs.nih.gov**. Questions on the application procedures may be addressed to **Brian Harper on 301-594-5332**. Applications must be received by midnight eastern standard time on **August 10, 2007.**

OFFICE OF PORTFOLIO ANALYSIS AND STRATEGIC INITATIVES
DIRECTOR, DIVISION OF EVALUATION AND SYSTEMIC ASSESSMENTS

The Office of the Director, National Institutes of Health (NIH) in Bethesda, Maryland, is seeking a Director of the Division of Evaluation and Systemic Assessments (DESA) within the Office of Portfolio Analysis and Strategic Initiatives (OPASI). If you are an exceptional candidate with an M.D. and/or Ph.D. and the vision and ability to integrate evaluation systems and programs across multiple disciplines and organizations, we encourage your application.

The OPASI's primary objective is to develop: a transparent process of planning and priority-setting characterized by a defined scope of review with broad input from the scientific community and the public; valid and reliable information resources and tools, including uniform disease coding and accurate, current and comprehensive information on burden of disease; an institutionalized process of regularly scheduled evaluations based on current best practices; the ability to weigh scientific opportunity against public health urgency; a method of assessing outcomes to enhance accountability; and a system for identifying areas of scientific and health improvement opportunities and supporting regular trans-NIH scientific planning and initiatives.

As the DESA Director, you will be responsible for planning, conducting, supporting, and coordinating, specific program evaluations and projects of NIH Institutes and Centers such as the Roadmap, Obesity, and Neuroscience Blueprint initiatives. In addition, you will serve as the liaison for conducting governmentally required assessments according to the Government Performance and Results Act (GPRA) and OMB Program Assessment Rating Tool (PART). You will also serve as a member of the OPASI Steering Committee involved in oversight of institution-wide planning and analysis.

Salary is commensurate with experience and includes a full benefits package. A detailed vacancy announcement with the mandatory qualifications and application procedures can be obtained on **USAJOBS at www.usajobs.gov (announcement number OD-07-172847-T42) and the NIH Web Site at http://www.jobs.nih.gov**. Questions on the application procedures may be addressed to **Brian Harper on 301-594-5332**. Applications must be received by midnight eastern standard time on **August 10, 2007**.

WWW.NIH.GOV

OFFICE OF PORTFOLIO ANALYSIS AND STRATEGIC INITATIVES
DIRECTOR, DIVISION OF RESOURCE DEVELOPMENT AND ANALYSIS

The Office of the Director, National Institutes of Health (NIH) in Bethesda, Maryland, is seeking a Director of the Division of Resource Development and Analysis (DRDA) within the Office of Portfolio Analysis and Strategic Initiatives (OPASI). If you are an exceptional candidate with an M.D. and/or Ph.D., we encourage your application.

The OPASI's primary objective is to develop: a transparent process of planning and priority-setting characterized by a defined scope of review with broad input from the scientific community and the public; valid and reliable information resources and tools, including uniform disease coding and accurate, current and comprehensive information on burden of disease; an institutionalized process of regularly scheduled evaluations based on current best practices; the ability to weigh scientific opportunity against public health urgency; a method of assessing outcomes to enhance accountability; and a system for identifying areas of scientific and health improvement opportunities and supporting regular trans-NIH scientific planning and initiatives.

As the DRDA Director, you will be responsible for employing resources (databases, analytic tools, and methodologies) and developing specifications for new resources, when needed, in order to conduct assessments based on NIH-owned and other databases in support of portfolio analyses and priority setting in scientific areas of interest across NIH.

Salary is commensurate with experience and includes a full benefits package. A detailed vacancy announcement with the mandatory qualifications and application procedures can be obtained on **USAJOBS at www..usajobs.gov (OD-07-172841-T42) and the NIH Web Site at http://www.jobs.nih.gov**. Questions on the application procedures may be addressed to **Brian Harper on 301-594-5332**. Applications must be received by midnight eastern standard time on **August 10, 2007**.

NIDDK

Program Director in Gestational Diabetes and Obesity Research
Health Scientist Administrator, GS-14

The Division of Diabetes, Endocrinology and Metabolic Diseases (DDEMD), National Institute of Diabetes and Digestive and Kidney Diseases (NIDDK), National Institutes of Health (NIH) is expanding its programs in obesity and diabetes research. An opportunity exists for a clinical scientist to join a dedicated and dynamic group of health scientist administrators to help guide NIH funding of research in diabetes and obesity.

A clinically-oriented scientist with expertise in the areas of obesity and gestational diabetes is sought for this new position. This individual will be responsible for managing and developing a program of research grants in the human physiology of gestational diabetes, imprinting and obesity. A person with an interest in fostering basic and clinical partnerships is desirable.

This position involves close interaction with leading researchers, scientific administration of grants and contracts, program planning and development, and the opportunity to organize and attend scientific meetings. The successful candidate will have independent research experience, with a track record of publications in areas of biomedical science relevant to the objectives of the program, excellent interpersonal and written communications skills, the ability to identify research priorities and opportunities, and the ability to track and analyze the success of initiatives and programs. In carrying out these responsibilities, the Program Director will interact with national leaders in diabetes, endocrine, obstetric, and obesity research. Many DDEMD research activities are conducted through partnerships between the NIDDK and other components of NIH and DHHS, as well as voluntary organizations. The Program Director will play a leadership role in fostering these partnerships.

This position is subject to a background investigation. Applicants must be U.S. citizens, resident aliens, or nonresident aliens with an employment-authorized visa, and have an advanced degree (M.D., Ph.D. or equivalent) along with relevant independent clinical and/or basic research. The position is located in Bethesda, Maryland. Salary and benefits will be commensurate with the experience of the applicant.

Position requirements and detailed application procedures are provided on Vacancy Announcement Numbers: **NIDDK-07-193870-DE, and NIDDK-07-193871-MP**, which can be obtained by accessing **WWW.USAJOBS.GOV**. All applications must be received by **07/31/2007**. For additional information contact Karen Page at **(301) 496-4232**.

Postdoctoral Position

The Biomolecular Structure Section (BSS) of the Macromolecular Crystallography Laboratory, National Cancer Institute at Frederick is inviting applications for a postdoctoral position. The appointment will be two years initially and renewable up to a total of 3-5 years on the basis of performance and mutual agreement. Qualified applicants should have experience in macromolecular crystallography and skills in either insect cell protein expression or structure-based drug design. Successful candidate will participate in the structure/activity studies of RNA-processing proteins or structure-based development of anticancer and antimicrobial agents. Additional information about research activities in the BSS can be found at: **http://mcl1.ncifcrf.gov/ji.html**. We provide excellent work environment, state-of-the-art facilities and regular access to synchrotron light source; we offer competitive salary and comprehensive health insurance. DHHS and NIH are Equal Opportunity Employers. Please send CV, research summary, and contact information of three references to **Dr. Xinhua Ji at: jix@ncifcrf.gov**.

INFLAMMATION AND CANCER
TENURE TRACK POSITION
LABORATORY OF HUMAN CARCINOGENESIS

The Laboratory of Human Carcinogenesis (LHC), Center for Cancer Research, National Cancer Institute, has a long tradition of excellence in the investigation of the molecular carcinogenesis and epidemiology of human cancer. The Laboratory now invites applications for a tenure track position to study the role of chronic inflammation in human cancer. The applicant should have previous postdoctoral experience; a substantive record of publications in quality, peer-reviewed journals; and the potential to develop an independent research program that utilizes basic research discoveries and their translation to investigate the role of chronic inflammation in the molecular pathogenesis and progression of human cancer. Previous translational studies of cancer-prone chronic inflammatory diseases in animal models and humans and/or molecular epidemiological studies are recommended.

This position is available for a Ph.D. or M.D. with a salary commensurate with education and experience. The position is available to U.S. citizens and foreign nationals. A one or two-page statement of research interests and goals should be submitted in addition to three letters of recommendation and a curriculum vitae to:

Ms. Shirley Swindell, Laboratory Program Specialist, LHC, CCR, NCI, Building 37, Room 3060C, Bethesda, MD 20892-4258, Phone: 301-496-2048, Fax: 301-496-0497, email: swindels@mail.nih.gov.

Applications must be postmarked by **October 1, 2007**.

Department of Health and Human Services
National Institutes of Health
National Center for Research Resources

The Division for Clinical Research Resources (DCRR) of the National Center for Research Resources (NCRR), a major component of the National Institutes of Health (NIH) extramural research programs, is seeking applicants for Medical Officer and Health Scientist Administrator positions. Medical Officers and Health Scientist Administrators have broad responsibilities in the planning, evaluation and scientific management of a portfolio of grants, cooperative agreements and other program activities. DCRR provides funding to biomedical research institutions to establish and maintain specialized research facilities that enable clinical, basic and translational research. DCRR supports resources including, among others: Clinical and Translational Science Awards (CTSA), General Clinical Research Centers (GCRC), Center for Genotyping and Analysis and pre- and post-doctoral research training and career development programs.

Applicants for this position must have a doctoral degree (M.D., Ph.D., D.D.S. or equivalent) and appropriate experience in health-related science fields. Applicants who also possess additional knowledge, training or degrees in clinical and translational research and a strong interest in moving forward our clinical research efforts are highly desirable. Experience in administering scientific grant programs is an asset but not required. U.S. citizenship is required. The position is at the GS-14 level and includes a full benefits package. DCRR offices are located in Bethesda, MD.

Candidates can view the detailed vacancy announcements, along with mandatory qualifications and application procedures on the NIH website at: **http://www.usajobs.gov (announcement numbers NCRR-07-200010 and NCRR-07-200020)**. Questions on announcement procedures may be addressed to **Ms. Carrie Williams at williaca@od.nih.gov** or by calling **301-594-2234**.

Department of Health and Human Services
National Institutes of Health
National Center for Research Resources

The Division of Comparative Medicine (DCM) within the National Center for Research Resources, a major research component of the National Institutes of Health (NIH) and the Department of Health and Human Services in Bethesda, MD, is seeking applicants for a Health Scientist Administrator (HSA) position. Working closely with the research community, the HSA has broad responsibilities in the planning, evaluation, and scientific management of the extramural research programs sponsored by DCM. These programs provide support for sophisticated mammalian and non-mammalian resources and repositories of genetically-modified animals, both vertebrate and invertebrate. Through grants, cooperative agreements, and contracts, DCM programs support activities associated with the national primate research centers, primate breeding and resource-related projects, national repositories for induced mutant rodents and other species, development of mammalian and non-mammalian model resources, and a variety of other highly specialized research projects. The DCM programs also support pre- and post-doctoral research training and career development for veterinarians. Applicants for this position must have a DVM (or equivalent) and a PhD or MS degree is desirable. Appropriate experience in health or health-related science research is required. Salary is commensurate with experience and full benefit packages (including retirement, health, life, long term care insurance, Thrift Savings Plan participation, etc.) are available.

Candidates can view the detailed vacancy announcement, along with mandatory qualifications and application procedures on the NIH website at: **http://www.usajobs.gov (announcement number NCRR-07-197098)**. Questions on announcement procedures may be addressed to **Ms. Carrie Williams at williaca@od.nih.gov** or by calling **301-594-2234**.

WWW.NIH.GOV

National Institutes of Health
Request for Information NOT-OD-07-074
NIH System to Support Biomedical and Behavioral Research and Peer Review
Release Date: July 9, 2007
Response Date: August 17, 2007, 5:00 p.m. EST

The National Institutes of Health (NIH) has issued Request for Information (RFI) NOT-OD-07-074 to solicit comments from reviewers, applicants, and members of the public on the NIH's two-tiered system of peer review and its system for support of biomedical and behavioral research. NIH has formed a Working Group of the Advisory Committee to the NIH Director **http://www.nih.gov/about/director/acd/index.htm** to look at these issues. The Working Group is interested in your opinion of how NIH can best support the needs of an increasingly complex scientific enterprise given the growing numbers of grant applications and the challenges these and other factors bring to the peer review process. The complete RFI is online at the following website: **http://grants.nih.gov/grants/guide/notice-files/NOT-OD-07-074.html**.

Responses will be accepted online at **http://grants.nih.gov/grants/guide/rfi_files/rfi_peer_review_add.htm** and through the following e-mail address, **PeerReviewRFI@mail.nih.gov**. Note that the form will limit the length of each response to the number of characters identified. The closing time for comments is 5:00 p.m. EST on August 17, 2007. This RFI is for planning purposes only and should not be construed as a solicitation for applications or an obligation on the part of the Government. Collected information will be analyzed and may appear in reports; there is no guarantee of confidentiality. A summary of results will be available to the public on the NIH Peer Review website: http://enhancing-peer-review.nih.gov. Inquiries concerning this Notice may be directed to **PeerReviewRFI@mail.nih.gov** or **Office of the Director, NIH, Attn: Peer Review RFI, 1 Center Drive, Bethesda, MD 20892-0189**.

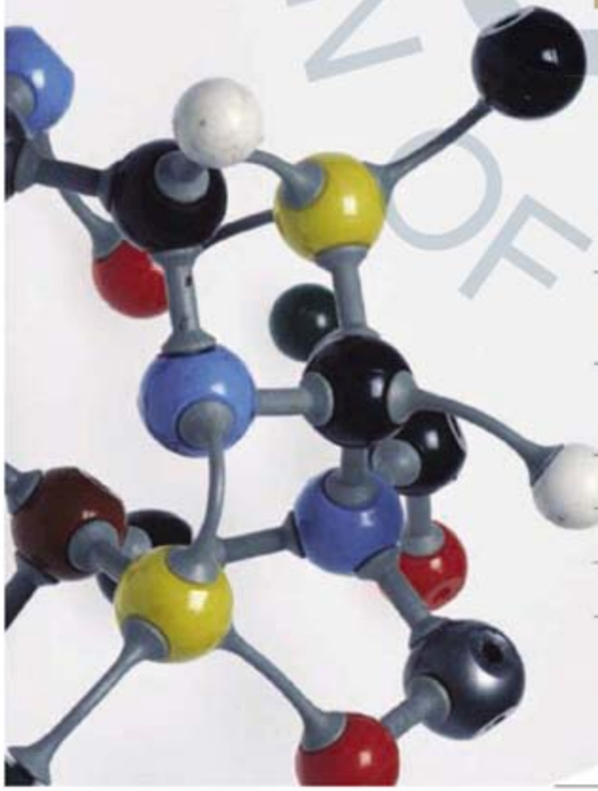

Postdoctoral Research Training at NIH

Launch a career to improve human health

Work in one of 1250 of the most innovative and well-equipped biomedical research laboratories in the world

Explore new options in interdisciplinary and bench-to-bedside research

Develop the professional skills essential for success

Earn an excellent stipend and benefits

Click on www.training.nih.gov

Office of Intramural Training and Education

Our work is someone's hope.

Join us.

MERCK

MERCK

Sirna Therapeutics, Inc., a wholly-owned subsidiary of Merck & Co., Inc., is leading the industry in developing a new class of drugs based on RNAi—drugs that we believe will significantly improve human health. With our unmatched chemistry and biology expertise, seasoned leadership and broad therapeutic pipeline, Sirna is demonstrating that short interfering RNA (siRNA) can be chemically optimized and efficiently delivered to create therapeutically relevant compounds with drug-like properties and clinical effect.

San Francisco, CA

MOL000206 - Senior Director, RNA Therapeutics

Reporting to the CSO and VP Sirna Therapeutics, the successful candidate will be responsible for establishing and guiding research programs focused on the optimization of siRNA therapies in order to establish Merck-Sirna as a global center of excellence and world leader in RNAi technology. As the senior scientific leader within the Merck-Sirna RNA Therapeutic initiative with headquarters located on the Mission Bay Campus of UCSF in San Francisco, CA, you will be responsible for enhancing an understanding of RNA chemical modifications on siRNA activity and safety, microRNA as a target and a therapeutic, combination siRNA therapies and in vivo analysis of on- and off-target siRNA effects.

Requirements include a Ph.D. with managerial experience and an established international research reputation in nucleic acid structure/function. Greater than ten years of post-Ph.D. work in industry or as an independent investigator preferred. Must be an accomplished scientist, recognized by peers as a leader in your field.

SCI003232 - Director, In Vivo Biology
MOL000190 - Sr. Methods Developer
MOL000187 - Research Molecular Biologist
MOL000188 - Research Chemist
MOL000189 - Associate Program Coordinator
MOL000192 - Automation Associate
MOL000196 - Sr. Systems Analyst
MOL000197 - LIMS Analyst/LIMS Programmer
MOL000204 - Sr. Research Scientist/Data Analyst
MOL000205 - Research Scientist, Bioinformatics

West Point, PA

Researchers here will play a critical role in the discovery and development of RNA-based therapeutics. In this collaborative and multidisciplinary environment, scientists will work to leverage their expertise culminating in the design and development of oligonucleotide therapeutics and safe and effective delivery vehicles, in support of multiple therapeutic areas at Merck.

BIO001506 - Sr. Research Biologist, Nucleic Acid Delivery
BIO001507 - Biologist, Microscopy Cell Based Assay Support
BIO001508 - Biologist, siRNA Biology & Pharmacology
BIO001497 - Medicinal Chemist, RNA Therapeutics Group - RNAi Technology
BIO001499 - Analytical Chemist, RNA Therapeutics Group - RNAi Technology

www.merck.com/careers

Merck is an equal opportunity employer, M/F/D/V - proudly embracing diversity in all of its manifestations.
Copyright © 2007 Merck & Co., Inc., Whitehouse Station, NJ, USA, All Rights Reserved.

MAYO CLINIC

Director, Microarray Core Facility

Rochester, Minnesota

The Advanced Genomics Technology Center (AGTC) of the Mayo Clinic College of Medicine (www.mayo.edu) seeks a Director of the Microarray Shared Resource (MSR). Applicants should have extensive research experience in the design and interpretation of RNA expression profiling studies using microarray technologies (Affymetrix, Illumina, custom spotted arrays) and RT-PCR. In addition to managing the operation and future growth of the MSR, the successful candidate will have the opportunity to develop an extramurally funded state-of-the-art research program in an area relevant to the prediction, prevention, diagnosis, and/or treatment of human diseases. The Mayo Clinic AGTC provides coordinated high-throughput, high-quality genomic resources, including sample accessioning and processing, genotyping, expression profiling, cytogenetics, and DNA synthesis and sequencing for all Mayo investigators.

To learn more about Mayo Clinic or Rochester, MN, please visit **www.mayoclinic.org**.

Send curriculum vitae, contact information for 3 references, and statement of research interests to:

Dr. Eric Wieben
Mayo Clinic
200 First Street SW
Rochester, MN 55905
Email: wieben.eric@mayo.edu

Mayo Foundation is an affimative action and equal opportunity employer and educator. Post offer/pre-employment drug screening is required.

THE UNIVERSITY OF IOWA

Chair
Department of Biology

The College of Liberal Arts and Sciences seeks a Chair for the Department of Biology at the rank of Professor. The candidate should be an internationally recognized scientist with an outstanding research program. We welcome applicants from any area of the biological sciences, while particularly encouraging candidates who would enhance one or more of our existing strengths in cell and developmental biology, evolution, genetics, and neurobiology.

The Department has embarked on an aggressive program of growth that includes ongoing faculty recruitment, the recent modernization of the biology complex, and the addition of a new building. It is active in interdisciplinary programs, with strong ties to the other colleges involved in biomedical research. The Biology faculty is well funded by both federal and private sources. The successful candidate will bring vision, energy, and a demonstrated commitment to diversity to shape the future of the Department through hiring and mentoring of new faculty, with an aim to further improve the Department's strong national reputation for research and teaching. More about the department may be viewed at **www.biology.uiowa.edu**.

The Applicant should submit a curriculum vitae, a statement of research interests and administrative philosophy, and the names and addresses of at least three references to: **Dean Joseph Kearney, College of Liberal Arts and Sciences, 240 Schaeffer Hall, The University of Iowa, Iowa City, IA 52242-1409**. Applications accepted by mail or electronically to **biology-chairsearch@uiowa.edu**.

The University of Iowa is an Affirmative Action/Equal Opportunity Employer. Minority candidates and women are encouraged to apply.

U.S. Department of Energy
Associate Director
Office of Science for
Biological and Environmental Research
Announcement # SES-SC-HQ-014 (kd)

The U.S. Department of Energy's (DOE's) Office of Science is seeking qualified candidates to lead its Biological and Environmental Research (BER) Program. With an annual budget of more than $500 million, the BER Program is the nation's leading program devoted to applications of biology to bio-energy production and use and to environmental remediation. The BER Program supports major research programs in genomics, proteomics, systems biology, and environmental remediation. The Program is also one of the nation's leading contributors to understanding the effects of greenhouse gas emissions, aerosols, and atmospheric particulates on global climate change.

The Director of Biological and Environmental Research is responsible for all strategic program planning in the BER Program; budget formulation and execution; management of the BER office including a federal workforce of more than 30 technical and administrative staff; program integration with other Office of Science activities and with the DOE technology offices; and interagency integration. The position is within the ranks of the U.S. government's Senior Executive Service (SES); members of the SES serve in key positions just below the top Presidential appointees. For more information on the program please go to **http://www.sc.doe.gov/ober/**.

For further information about this position and the instructions on how to apply and submit an application, please go to the following website: **http://jobsearch.usajobs.opm.gov/getjob.asp?JobID=58520806&AVSDM=2007%2D06%2D06+13%3A44%3A02&Logo=0&q=SES-SC-HQ-014+(kd)&FedEmp=N&sort=rv&vw=d&brd=3876&ss=0&FedPub=Y&SUBMIT1.x=47&SUBMIT1.y=18**. To be considered for this position you must apply online. It is important that you follow the instructions as stated on the announcement **SES-SC-HQ-014 (kd)** located at the website above.

University of Louisville, Stem Cell Institute at James Graham Brown Cancer Center

The newly created Stem Cell Institute at James Graham Brown Cancer Center at the University of Louisville (**www.bcc.louisville.edu**) plans an expansion of research in the biology of normal and malignant stem cells, with an emphasis on tissue/organ regeneration and molecular mechanisms that govern trafficking, engraftment and expansion of normal stem cells and metastasis of malignant stem cells. Positions are available at open rank of Full Professor, Associate Professors and Assistant Professors (tenure track). Applicants must have M.D. Ph.D., or Ph.D. with postdoctoral research experience, a strong track record of publications, history of successful funding, and will be expected to establish an independently funded research program. We are looking for candidates in the areas of (i) stem cell biology, (ii) isolating, purification and expansion of human hematopoietic and non-hematopoietic cells, (iii) molecular aspects of stem cell renewal/differentiation, (iv) developmental embryology and (v) animal in vivo models. The successful faculty candidates will be provided with laboratory space and generous start-up packages. The JGB Cancer Center houses excellent shared facilities for molecular and cellular biology, including flow cytometry and cell sorting, DNA sequencing, structural biology including molecular modeling, NMR, biophysics, crystallography, genomics and proteomics and facilities for transgenic mice. Please send curriculum vitae, with a bibliography, a synopsis of research interests, and the names and telephone/facsimile/e-mail of at least three references to:

Donald Miller MD, PhD
Director, James Graham Brown Cancer Center
University of Louisville
529 South Jackson Street
Louisville, KY 40202
email: Donaldmi@ulh.org

Mariusz Z. Ratajczak MD, PhD
Stella and Henry Hoenig Endowed Chair
Professor of Medicine
Director of Stem Cell Institute at
James Graham Brown Cancer Center
University of Louisville
500 Floyd Street
Louisville, KY 40202
email: mzrata01@gwise.Louisville.edu

Head of Sequencing

The Wellcome Trust Sanger Institute is a world leader in genomic research and in the delivery of high-quality, large-scale resources of lasting value to the global research community. During the coming years, we aim to make a major contribution to the understanding of genomes and genome variation in health and disease, similar in impact to our role in genome sequencing. Sequencing will continue as the central underpinning technology of the Institute in support of the scientific projects comprising the 2006-11 Strategic Plan and we aim to fully exploit the potential of new technologies and the scientific opportunities opened up by them.

We are seeking a senior scientist to provide strong leadership and direction for the Sanger's sequencing activities as the Institute moves to the new technologies. Working across multiple platforms, the post holder will play an important co-ordination role and will be responsible for further developing a scientific and informatics infrastructure that can respond flexibly to the requirements of the Institute's scientific programmes. With a background in genetic/genomic science including broad knowledge of sequencing and its technologies, applicants should have significant resource management experience and expertise coupled with a successful track record leading and motivating teams in a complex, changing environment. Strategic thinking and the ability to influence and persuade at board level are also key to success in the role.

The appointment may be at faculty or senior staff scientist level depending on background and experience. For further information and informal discussion, contact Mike Stratton **mrs@sanger.ac.uk**

Applicants should send curriculum vitae, complete list of publications and details of three referees accompanied by:

- a summary of scientific achievements (approx 1-2 pages);
- a summary of leadership experience and accomplishments to date together with an indication of the vision you will bring to the management of Sequencing (approx 1-2 pages).

Please email to seqsearch@sanger.ac.uk or post to
Sancha Martin, Search Committee,
The Wellcome Trust Sanger Institute,
Wellcome Trust Genome Campus,
Hinxton, Cambridge,
CB10 1SA, UK

Application deadline: 26 July 2007
www.sanger.ac.uk

Working towards equality through diversity

wellcome trust sanger institute

Genome Research Limited is a Registered Charity No.1021457

Want to search more job postings?

www.sciencecareers.org

Search thousands of job postings —updated daily— all for free.

Science Careers
From the journal *Science* AAAS

University of Maryland, College Park
Chair, Department of Cell Biology and Molecular Genetics

We seek a distinguished senior scientist with a vigorous research program and the broad vision, experience, and energy to lead a period of major growth and expansion of the Department of Cell Biology and Molecular Genetics (CBMG). The expansion will include the recruitment of new senior and junior faculty and the establishment of new facilities as part of an ambitious campus drive for enhancement in the life sciences. CBMG is a vibrant, interactive and cohesive department, with research strengths in microbiology, immunology, plant biology, molecular genetics, genomics, cell and developmental biology and virology. The CBMG faculty includes prominent scientists in their respective fields with outstanding records in research, teaching and service. The research programs of the future chair and new faculty appointees will be located in spacious new laboratory facilities in the recently opened Bioscience Research Building. The successful applicant will also share a leadership role in the development of one or more of the ongoing CBMG and College of Chemical and Life Sciences initiatives in comparative and functional genomics, signal transduction, gene expression, plant biology, and host-pathogen interactions. For more information about the department, the college, and the university, visit our web site at **www.cbmg.umd.edu**.

Applicants should apply electronically by emailing an application letter with the following attachments in PDF format: (1) curriculum vitae, (2) statement of research interests, (3) statement of academic vision and administrative experience, and (4) names and addresses of at least four references to **CLFS-CBMG_Chair@umd.edu**. Review of credentials is ongoing and will continue until the position is filled.

The University of Maryland, College Park is the flagship campus of the University System of Maryland and one of the most rapidly advancing public research universities in the country. Close proximity to Washington, Baltimore, and the Maryland Biotechnology Corridor facilitates interactions with an extraordinary range of major research institutions, including the NIH, FDA, Smithsonian Institution, and USDA.

The University of Maryland is an Equal Opportunity Affirmative Action Employer. Minorities and women are encouraged to apply.

UNIVERSITY OF MARYLAND

PARACELSUS
MEDIZINISCHE PRIVATUNIVERSITÄT

A Position for an

Endowed Professorship

by Land Salzburg

in Molecular Regenerative Medicine

is open at the Paracelsus Medical University (Salzburg/Austria).

The applicant should have exceptional international scientific qualifications and be an expert in the methodologies of molecular regenerative medicine (e.g. functional proteomics, signal transduction, angionesis, 3D cell cultures, stem cells).

The professorship is for immediate occupancy, initially set for five years. Continuation of this position after this time period is planned. In addition to the usual documents provided (curriculum vitae, scientific career history, publication list), we request a presentation of previous research programs, as well as of acquired third-party fundings and grants.

The Paracelsus Medical University strives in raising the percentage of female employees and therefore invites qualified women interested in this position to apply. When the qualifications are identical, preference will be given to female applicants.

For terms of employment and details of the professorship please see http://www.pmu.ac.at/789.htm

A cover letter of application should be sent by **August 25, 2007** via Email only to the following address: claudia.melchart@pmu.ac.at
The online submission of all supporting documents must be completed by August 28, 2007 as outlined in the letter of confirmation you will receive from the university in response to your letter of interest (Email).

www.pmu.ac.at

Human Molecular Embryology

The Division of Human Molecular Embryology at the Department of Pediatrics, Medical College of Wisconsin, is seeking applications for a faculty position at the Assistant Professor level from talented professionals who study mechanisms of embryonic development and disease. Investigators with interest in ocular or cardiac development are particularly encouraged to apply. An attractive start-up package will be provided to facilitate program development. Candidates should have a Ph.D. and/or M.D. degrees, proven excellence and productivity in research and demonstrate strong potential to attract and maintain external funding. Candidates with current K or R00 level funding are preferred. Please submit an application letter, curriculum vitae, research plan, and the names of three individuals to be contacted as references to:

Elena V. Semina, Ph.D.
Medical College of Wisconsin
Department of Pediatrics
Translational and Biomedical Research Center, CRI C3420
8701 Watertown Plank Road
P.O. Box 26509
Milwaukee, WI 53226
E-mail: esemina@mcw.edu

Children's Hospital and Health System™
MEDICAL COLLEGE OF WISCONSIN
Children's Specialty Group™

EOE/AA M/F/D/V

Washington University in St. Louis
SCHOOL OF MEDICINE

The **Department of Biochemistry and Molecular Biophysics** at Washington University School of Medicine is looking for outstanding junior or senior faculty who use **NMR spectroscopy** as their primary tool for studying functional dynamics of biological macromolecules. NMR studies would be augmented with biochemical and biophysical investigations. Areas of special interest include the study of disorder-to-order transitions of natively unfolded proteins, allosteric regulation in enzymes, and dynamics in protein-protein and protein-nucleic acid complexes. The successful candidate will join an interactive group of faculty who apply NMR, computational, and theoretical methods to understand the role of macromolecular dynamics in self-assembly and function. For more information on the Department, please refer to **http://biochem.wustl.edu** and **http://www.ccb.wustl.edu**. Applicants must have a Ph.D. or equivalent degree, postdoctoral experience, and have demonstrated excellent research qualifications.

Applications are due **September 1, 2007** for Fall, 2007 interviews. Applicants should provide a CV, summary of research interests, and names of at least three faculty as references. Materials should be sent via email to **nmrsearch@biochem.wustl.edu**, or by post to:

Professor Kathleen B. Hall
NMR Search Committee Chair
Department of Biochemistry and Molecular Biophysics
Box 8231
Washington University School of Medicine
660 S. Euclid Ave.
Saint Louis, MO 63110

Washington University is an Equal Opportunity Employer.

GRANTS

THINK MITOCHONDRIA

UMDF Research Grant Program

♦ REQUEST FOR PROPOSALS ♦

UNITED MITOCHONDRIAL DISEASE FOUNDATION®
HOPE. ENERGY. LIFE.

The United Mitochondrial Disease Foundation (UMDF) is seeking new, innovative research to continue its mission to find cures and better treatments for mitochondrial illnesses.

Proposals will be considered in basic science and clinical areas and must fall under at least one of the following categories:

- Seed money for new researchers
- Post-doctoral fellowship
- New area of research for experienced investigators

Letter Of Intent (LOI) Application and additional information about the grant process is available on the UMDF web site at www.umdf.org or by contacting the UMDF office.

UMDF must receive LOI by September 14, 2007. Incomplete LOIs or those received past the deadline will not be considered. FAX transmittal is not acceptable.

Contact Information: UMDF Research Grant Program
8085 Saltsburg Rd, Suite 201, Pittsburgh, PA 15239 USA
Tel: (412) 793-8077 • Fax: (412) 793-6477 • Email: jean@umdf.org

IEO
Istituto Europeo di Oncologia

IFOM

IFOM – IEO CAMPUS
MILAN, ITALY
www.ifom-ieo-campus.it
HEAD OF TECHNOLOGY TRANSFER/INDUSTRIAL LIAISONS OFFICE

The IFOM–IEO CAMPUS was created by the joint efforts of two major private Cancer research Institutions in Italy, the FIRC Institute of Molecular Oncology (IFOM) and the European Institute of Oncology (IEO) that have expanded and integrated their research activities into a common campus. The IFOM-IEO Campus is also home to the PhD program of the European School of Molecular Medicine (**www.semm.it**). It presently comprises 35 independent Research Groups that utilize a number of Central services, including Animal Facilities (mouse, zebrafish, and C.elegans), Imaging, Protein and Antibody Production, DNA and Tissue Microarrays, DNA Sequencing, Proteomics and Bioinformatics. In addition, the IEO Hospital is a dedicated cancer hospital engaged in patient care, therapy and clinical research including clinical trials.

We are looking for an experienced individual to head our Technology Transfer/ industrial liaisons office (TTO), starting approximately January 1st 2008. The successful candidate will be responsible for creating a system of "invention reports" within the Institutions, filing of patent applications, promote the commercialization and licensing of such inventions, as well as monitoring and supervising new or already existing license agreements or research contracts with commercial entities. In addition the TTO will be responsible for stipulating and regulating the financial agreements related to the execution of clinical drug trials at the IEO hospital and interface with the IRB and conflict of interest committees of the institutions.

Candidates should have experience in interacting with the pharmaceutical and biotechnology industry and with regulatory agencies, as well as leadership and organizational skills.

The official language of the institution is English but some knowledge of Italian may be desirable. A competitive salary/resources package is available.

Applications should be sent by e-mail to **search-TTO@ifom-ieo-campus.it** and should include: CV, statement of Achievements and Interests (Max 2 pages), names and e-mail addresses of 3-4 referees. Deadline for applications is **30th of October 2007**.

CHICAGO
SIGNAL TRANSDUCTION IN BREAST CANCER RESEARCH POSITION

Rush University, a prominent university medical center in Chicago, invites applications for a **Tenure-Track Faculty** Position to establish the Rush Breast Cancer Research Laboratory. The candidate should have specific research interest, experience and publications in translational research in signal transduction cancer, preferably in breast cancer. The candidate must hold a Ph.D. or M.D./Ph.D. degree and preference will be given to candidates with external funding, established research programs, and training in signaling in breast cancer. Academic rank and salary are commensurate with training and experience. Appointments are possible in the Division of Oncology, the Department of Medicine and the Department of Biochemistry. Excellent startup funds are available.

The Comprehensive Breast Cancer Center at Rush offers a multidisciplinary approach to patients with breast cancer. Here, patients are seen by a team, consisting of surgeons, medical oncologists, radiation oncologists, psychologists and nurses. Approximately 500 new breast cancer patients are seen annually. **Dr. Melody A. Cobleigh**, a medical oncologist and Director of the Breast Cancer Center, oversees the Comprehensive Breast Cancer team, which provides patients with a full range of the latest and most innovative treatment options. The Center is part of **Rush University Medical Center**, which is an academic medical center with an 830-bed hospital serving adults and children and has national rankings in **more specialty areas than any other hospital in Illinois** (*U.S. News & World Report's* 2006 "America's Best Hospitals"). Rush is also a thriving center for basic and clinical research, with more than $70 million in NIH programs in fiscal year 2006 and a recent state-of-the-art Robert H. Cohn and Terri Cohn Research Building.

Send CV and 3 references to:

Dr. Melody A. Cobleigh
Melody_Cobleigh@rush.edu

RUSH UNIVERSITY MEDICAL CENTER

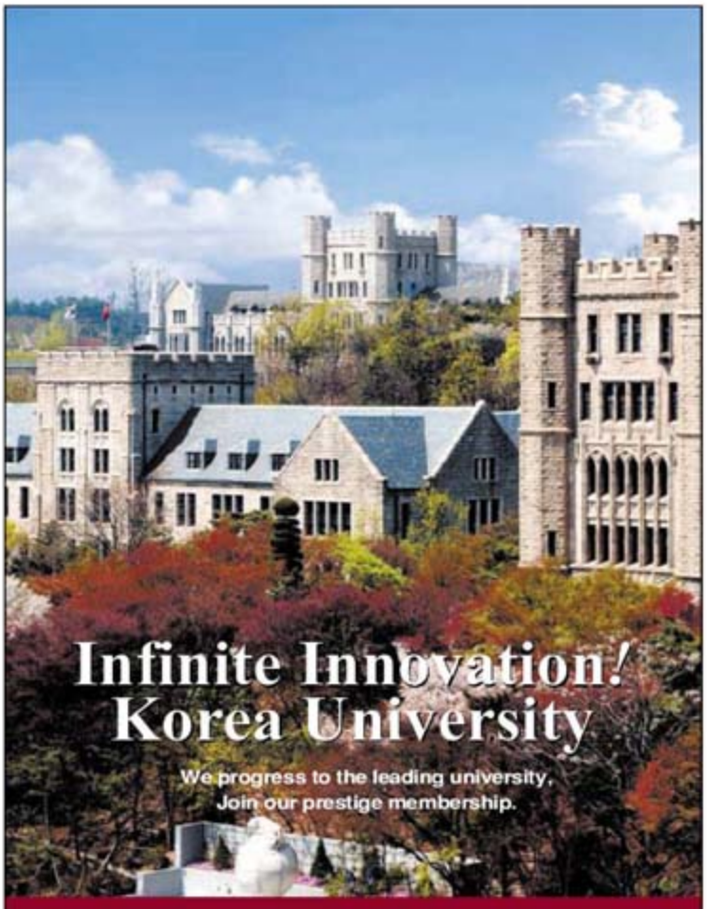

Professor Positions

Korea University invites applicants for tenure and non-tenure track positions to begin in March 2008. Responsibilities for tenure-track, for example, include teaching two courses per semester (in English), conducting/publishing research, and assuming various administrative duties to support academic functions. Applicants must possess near-native/native fluency in English and have a Ph. D. in hand. Applicants must also have experience in teaching at a college level, a strong commitment to excellence in scholarship, and dedication to undergraduate and graduate teaching in their research area. Visit our homepage at **www.korea.ac.kr/~faculty** to submit application on-line and upload the research plan in file.

Enquires : Phone : +82-2-3290-1071~3
Fax : +82-2-929-9164
Email : faculty@korea.ac.kr.

Application deadline : July 27, 2007.

Korea University is an Equal Opportunity/Affirmative Employer and is committed to a diverse faculty, staff, and student body. Korea University, which celebrated its centennial in 2005, is one of the most prestigious universities in Korea, serving more than 30,000 students. Furthermore, Korea University ranked 66th on the Social Science field and 89th on Cultural Science field rounding up to the 184th place overall in the Top 200 Universities selected by The Times in 2005. Last year the rank rose up to the 150th place. Korea University is a dynamic and innovative doctoral/research-intensive academic institution recognized for higher quality of undergraduate education and a range of focused graduate programs and research. For more information about Korea University, visit our home page at **www.korea.edu.**

KOREA UNIVERSITY

PROFESSOR AND FOUNDING CHAIR

Department of Systems and Computational Biology

The **Albert Einstein College of Medicine** invites applications and nominations for the position of **Professor and Founding Chair** of the Department of Systems and Computational Biology. The major goal of the new department will be to advance our understanding of living systems by developing theoretical, computational and experimental approaches to reveal the properties and functions of the component parts and the higher level behavior of complex biological systems. It will have the infrastructure, authority, responsibility and accountability for integrating and coordinating research and education. The new Chair will oversee the development of a full educational and research program that will nurture medical and graduate students, post-doctoral fellows and faculty who are expected to have international impact and add to the overall mission of the College. Einstein boasts a strong research faculty covering a broad area of experimental biology offering outstanding opportunities for the development of collaborative interactions with members of the new department. The opening in late 2007 of the 200,000 square foot Center for Genetic and Translational Medicine at Einstein offers the potential of locating computational, systems and experimental scientists in physical proximity, a prime opportunity to foster interdisciplinary communication and collaboration.

Einstein offers an extremely interactive environment with numerous, well-equipped core facilities subsidized by the College (http://www.aecom.yu.edu/home/shared.asp). There are currently 750 medical students, 325 graduate students and 360 post-doctoral fellows in training. We seek an outstanding scientist with broad experience and vision for appointment as full professor with tenure. Interested applicants should send a letter of interest and C.V. in electronic format to: **Dr. E. Richard Stanley, Chair, Systems and Computational Biology Search Committee, Albert Einstein College of Medicine, Jack and Pearl Resnick Campus, 1300 Morris Park Avenue, 312 Belfer, Bronx, New York, 10461. Tel: (718) 430-2344, E-mail: rstanley@aecom.yu.edu.**

We particularly welcome applicants who will add diversity to our academic leadership and faculty. Equal Opportunity Employer.

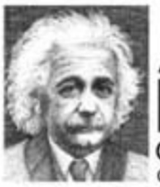

ALBERT EINSTEIN COLLEGE OF MEDICINE OF YESHIVA UNIVERSITY

IUPUI

INDIANA UNIVERSITY-PURDUE UNIVERSITY INDIANAPOLIS

DEAN
School of Science

IUPUI (Indiana University-Purdue University Indianapolis) seeks an outstanding leader with the vision, scientific standing, and administrative abilities to direct its School of Science. IUPUI is Indiana's urban research campus, offering undergraduate and graduate education, professional degrees in medicine, dentistry, nursing, law, business and social work. IUPUI serves over 29,000 U.S. and international students, leads Indiana's research campuses in annual external research funding, and is recognized nationally for its contributions in the area of civic engagement. Located adjacent to the state's capitol, IUPUI is helping to lead Indiana's public and private economic development initiatives such as those in life and information sciences. The School of Science, which awards degrees from both Purdue and Indiana Universities, consists of the departments of Biology, Chemistry and Chemical Biology, Computer and Information Science, Earth Sciences, Mathematical Sciences, Physics, and Psychology. School Faculty actively collaborate with other campus units, especially the schools of Medicine and Engineering. The School has 160 faculty members (120 tenure-track and 40 lecturers), over 1,300 undergraduate majors, and over 350 graduate students (250 Master's and 100 Ph.D.). A description of special programs and research centers can be found at **http://www.science.iupui.edu/science/deansearch/**. The web site also carries information on the accomplishments and status of the School.

A primary objective of the School is to raise its profile in research, external funding, and graduate education. The successful candidate for this position will have (a) demonstrated success and leadership in teaching, scientific research, and academic administration, (b) the ability to set goals for the School and pursue them by generating and allocating resources effectively, hiring faculty, and working with campus colleagues and administrators, and (c) the ability to build constructive relationships with the community including leaders in private industry and government. Candidates must have the academic qualifications and achievements consistent with an appointment as a tenured, full professor.

The target date for receipt of applications is **September 15, 2007**, but the search will remain open until the position is filled. Applications must include a letter of intent, curriculum vitae, and the names, addresses (including e-mail) and telephone numbers of six references, who will be contacted with the candidate's approval. All communications will be treated confidentially. *Nominators and candidates are urged to submit materials by e-mail utilizing attachments.* Materials should be submitted to: **Associate Dean Greg Lindsey, Chair, SOS Dean Search Committee, c/o Ms. Tamekia Anderson, School of Science IUPUI, 402 North Blackford St., Indianapolis, IN 46202, tlander1@iupui.edu.**

IUPUI is an EEOAA Employer.
Women and underrepresented minorities are particularly encouraged to apply.

POSITIONS OPEN

UNIVERSITY OF SOUTH CAROLINA

POSTDOCTORAL POSITION
HIV Molecular Biology and Neuro-AIDS (Pathogenesis)

A Postdoctoral position in HIV molecular biology is available immediately. A Ph.D., M.D./Ph.D., or doctoral degree in infectious disease, molecular biology, virology, or related field is required. The research involves HIV infection, molecular biology, signal transduction in neuro-glial cells and peripheral blood mononuclear cells. Knowledge in gene cloning, gene expression, and virology is essential. Please submit your curriculum vitae with research goals and names of three references with their addresses to: **Ashok Chauhan, Ph.D.; Department of Pathology, Microbiology and Immunology, University of South Carolina School of Medicine, Columbia, SC 29208** or **e-mail: achauhan@gw.med.sc.edu.** *USC Columbia is an Equal Opportunity Affirmative Action Employer and encourages applications from women and minorities.*

FACULTY POSITIONS
University of Vermont
Vermont Center for Immunology and Infectious Diseases

The Vermont Center for Immunology and Infectious Diseases is undergoing significant expansion and is seeking outstanding tenure-track faculty at the **ASSISTANT, ASSOCIATE, and FULL PROFESSOR** levels to contribute to the Center's research and teaching programs. Those appointed at the level of Assistant Professor may be eligible for research funding from a recently awarded NIH Center of Biomedical Research Excellence (COBRE) Award. We are seeking both Ph.D. and M.D. scientists with innovative research programs in the areas of microbial/viral pathogenesis or immune response to infectious agents. Extensive opportunities for collaborative research exist both within and outside the Center in cell, molecular, and structural biology. Primary appointments will be in either the Department of Medicine (Immunobiology or Infectious Disease) or the Department of Microbiology and Molecular Genetics. Details about the Departments, the University, and the Burlington area may be accessed at **websites: http://www.med.uvm.edu/medicine/immunobiology/; http://med.uvm.edu/medicine/id/;** and **http://www.uvm.edu/microbiology/mmg.** Curriculum vitae, a summary of research interests, and three letters of reference should be sent electronically (if possible) to: **Search Committee Chair, c/o Pamela Carter (e-mail: pamela.carter@uvm.edu), Vermont Center for Immunology and Infectious Diseases, College of Medicine, University of Vermont, D305 Given, 89 Beaumont Avenue, Burlington, VT 05405** or apply online at **website: https://www.uvmjobs.com.** Review of applications will begin July 25, 2007, and continue until suitable candidates are identified. *The University of Vermont is an Equal Opportunity, Affirmative Action Employer. Women and minorities are encouraged to apply.*

POSTDOCTORAL FELLOWSHIPS

The Michigan Society of Fellows, with the support from the Andrew W. Mellon Foundation, is pleased to invite applications for postdoctoral fellowship programs for recent Ph.D.s in the humanities, arts, sciences, and professions. Three-year positions at the University of Michigan are open to recent Ph.D.s who wish to pursue research opportunities while teaching at a major research university. Annual stipend will be $50,000. Application postal deadline: October 1, 2007. Information and applications are available online at **website: http:// www.rackham.umich.edu/Faculty/sof.html,** or by writing: **Society of Fellows, 3572 Rackham Building, University of Michigan, 915 E. Washington Street, Ann Arbor, MI 48109-1070. E-mail: society.of.fellows@umich.edu.** No e-mail applications accepted.

From primates
to proteomics

For careers in science,
turn to *Science*

www.ScienceCareers.org

- Search Jobs
- Career Advice
- Job Alerts
- Resume/CV Database
- Career Forum
- Graduate Programs

All of these features are FREE to job seekers.

Science Careers
From the journal *Science* AAAS

U.S. Department of Energy
Office of Science
Deputy for Programs
Announcement #*SES-SC-HQ-013 (kd)*

The U.S. Department of Energy's (DOE) Office of Science is seeking highly qualified candidates with outstanding scientific achievements to fill the Deputy for Programs position. The Office of Science is the single largest supporter of basic research in the physical sciences in the United States, with a 2007 budget of $3.8 billion. It oversees the Nation's research programs in high-energy and nuclear physics, basic and fusion energy sciences, and biological, environmental and computational sciences. The Office of Science is the Federal Government's largest single funder of materials and chemical sciences, and it supports unique and vital parts of U.S. research in climate change, geophysics, genomics, life sciences, and science education. The Office of Science also manages 10 world-class laboratories and oversees the construction and operation of some of the Nation's most advanced R&D user facilities, located at national laboratories and universities. These include particle and nuclear physics accelerators, synchrotron light sources, nanoscale science research centers, neutron scattering facilities, bio-energy research centers, supercomputers and high-speed computer networks. More information on the Office of Science can be found at **http://science.doe.gov**.

The Deputy for Programs provides scientific and management oversight of the six program offices by ensuring program activities are strategically conceived and executed; formulating and defending the Office of Science budget request; establishing policies, plans, and procedures related to the management of the program offices; ensuring the research portfolio is integrated across the program offices with other DOE program offices and other Federal agencies; and representing the organization and make commitments for the Department in discussions and meetings with high-level government and private sector officials. The position is within the ranks of the U.S. government's Senior Executive Service (SES); members of the SES serve in key positions just below the top Presidential appointees.

To apply for this position, please see the announcement and application instructions at **http://jobsearch.usajobs.opm.gov/ses.asp** under the vacancy announcement of **#SES-SC-HQ-013 (kd)**. Qualified candidates are asked to submit their online applications by **August 29, 2007**.

CHAMPALIMAUD FOUNDATION NEUROSCIENCE PROGRAMME AT THE INSTITUTO GULBENKIAN DE CIÊNCIA

Innovative, risk-taking research in Neuroscience:
Call for Group Leaders

The Champalimaud Foundation (CF) is seeking 2 Group Leaders in the area of systems neuroscience with special interest in the relationship between neural circuits and behavior. Applicants that use genetic, electrophysiological, optical and/or theoretical methods, preferably in rodent model systems, are sought.

Successful applicants will join an international group of 3 other laboratories in founding the Champalimaud Program in Neuroscience at the Instituto Gulbenkian de Ciência, in Portugal. The Program has a broad aim of understanding the relationship between brain function and behavior through an integrative, organism-centered approach, thereby contributing to the CF's mission of improving human health. The Program will include up to 8 groups and will in addition host an international neuroscience Ph.D. program, as well as series of international workshops and conferences.

The Instituto Gulbenkian de Ciência is a rich international scientific environment with some 30 research groups on life sciences, including evolutionary biology and genetics, cell and developmental biology, inflammation and immunology, computational and theoretical biology.

Applications for group leaders at the equivalent of Assistant or Associate Professor are sought, but applications at all levels will be considered, notably, newly graduated young investigators (Fellows). Applicants should have completed a Ph.D. and postdoctoral training (except Fellows) in neuroscience or a related field. Applications from scientists with a medical education are encouraged.

Initial appointments will be for a period of 6 years, with renewal or extension based on a 3-4 year review. To encourage innovative, risk-taking research, the Foundation is prepared to provide support for both startup and running costs to the groups in the Program. Investigators are also encouraged to obtain competitive external grants, in which case the Foundation will constitute a personal fund at the discretion of the investigator.

Applicants should submit a cover letter, C.V., statement of research interests and request three letters of reference to be sent to Maria Matoso Caetano de Carvalho at **mmatoso@igc.gulbenkian.pt**. Applications will be reviewed beginning 31 August 2007. Further information on the Program can be found at **www.fchampalimaud.org/cf/neuroscience** and **www.igc.gulbenkian.pt**

Centre for Molecular Medicine and Therapeutics
THE UNIVERSITY OF BRITISH COLUMBIA

The Faculty of Medicine and Centre for Molecular Medicine and Therapeutics at the Univeristy of British Columbia in Vancouver seeks applications for the following:

Professor/British Columbia Leadership Chair in Genetic Medicine

This prestigious appointment provides a unique opportunity for an internationally recognized individual to perform research in an outstanding environment, positioning the province as a leader in genetic medicine. The successful applicant will conduct innovative research generating new knowledge relevant to genetic contributions to illness, molecular determinants and mechanisms of disease and/or development of novel therapeutic approaches and technologies to improve treatment for disease. He/she should also demonstrate teaching excellence.

Assistant Professor/Canada Research Chair – Tier II

This tenure-track appointment provides significant start-up resources for an outstanding new researcher who has the potential to be a leader in his/her field. The successful candidate must demonstrate teaching excellence potential. His/her research will interface with scientific programs within the Centre directly addressing issues of medical relevance.

We are especially interested in applicants working in: • Genetic variation and susceptibility to disease • Statistical genetics • Bioinformatics • Pharmacogenomics • Experimental therapeutics • Mechanisms of genetic disease • Gene Therapy

Located on the Children's and Women's Health Centre of BC site, the CMMT is one of the main programs of the Child and Family Research Institute (**www.cfri.ca**). For more detailed information regarding the positions and the CMMT, please visit **http://www.cmmt.ubc.ca**.

Applicants should ideally hold an M.D. and/or Ph.D. degree or equivalent and a record of recognized accomplishment in areas relevant to **Human Biology and Disease**. Salary and rank will be commensurate with qualifications and experience. These are full-time tenured or tenure-track appointments. The CRC is subject to final budgetary approval.

Anticipated start date is **July 1, 2008**. Application closing date is **August 13, 2007**. Please send CV, names of three references, a teaching dossier and a brief statement of research interests to: **Hilary Stoddart, Manager of Human Resources, hstoddart@cmmt.ubc.ca, CMMT, 950 West 28th Avenue, Vancouver, BC V5Z 4H4**.

UBC and its affiliates hire on the basis of merit and are committed to employment equity. We encourage all qualified applicants to apply. These positions are open to individuals of any nationality; offers will be made in accordance with the CRC program and LEEF.

Do what you love.

Love what you do.

www.sciencecareers.org

Science Careers
From the journal *Science* AAAS

What's your next career move?

- Job Postings
- Job Alerts
- Resume/CV Database
- Career Advice from Next Wave
- Career Forum

Get help from the experts.

ScienceCareers.org
We know science AAAS
www.sciencecareers.org

POSITIONS OPEN

PROFESSOR and CHAIR
Department of Physiology
Southern Illinois University School of Medicine

Southern Illinois University School of Medicine invites applications for the position of Professor and Chair of the Department of Physiology. The successful candidate will be responsible for the continued development of the Department and will guide its research and education missions. Qualified candidates must have a Ph.D. and/or M.D. (or equivalent) degree, outstanding academic experience, research productivity with publication in nationally or internationally referred journals and professional service activities. Candidates must also have proven ability to secure and sustain extramural funding as well as excellent interpersonal and leadership skills.

The Department of Physiology is located on the campus of Southern Illinois University Carbondale, a large, public, comprehensive research-intensive university situated in a pleasant community surrounded by the Shawnee National Forest and located two hours southeast of St. Louis. This is a vibrant, growing Department with 12-month, state-funded faculty positions. Current research strengths include cancer biology, endocrinology, neurobiology, and reproduction. Opportunities for collaboration exist with the Simmons Cooper Cancer Institute, the Center for Integrated Research in Cognitive and Neural Sciences, as well as other basic and clinical science departments within the University. The Department is responsible for various educational programs including an integrative medical curriculum and both graduate and undergraduate physiology degree programs.

For more information about the Department, please visit our **website: http://www.siumed.edu/physiology/.**

Applicants should submit a cover letter highlighting their interests and qualifications, their curriculum vitae, and the contact information for five or more persons qualified and willing to discuss the applicant's abilities to fill this position. Applications may be submitted electronically in PDF or RTF format to: **Professor Ronald A. Browning (e-mail: rbrowning@siumed.edu), Physiology Search Committee Chair, Department of Physiology, School of Medicine, Mail Code 6523, Southern Illinois University Carbondale, 1135 Lincoln Drive, Carbondale, IL 62901.**

Applications will be reviewed beginning September 1, 2007, and will continue until the position is filled. Effective date of employment is August 15, 2008, but is negotiable. *Before any offer of employment is made the University will conduct a pre-employment background investigation, which includes a criminal background check.*

SIUC is an Affirmative Action/Equal Opportunity Employer that strives to enhance its ability to develop a diverse faculty and staff and to increase its potential to serve a diverse student population. All applications are welcomed and encouraged and will receive consideration.

POSTDOCTORAL POSITION studying the role of the innate immune system in cardiovascular disease is available. Projects involving diabetes, oxidative stress and stem cells are underway. A Ph.D. in cardiovascular physiology/pharmacology, biochemistry, or cellular/molecular biology is required. Please send letter of interest, names of three references, and curriculum vitae to:

Professor Gregory L. Stahl, Ph.D.
Center for Experimental
Therapeutics and Reperfusion Injury
Brigham and Women's Hospital
Harvard Medical School, 75 Francis Street
Boston, MA 02115
E-mail: gstahl@zeus.bwh.harvard.edu

POSTDOCTORAL FELLOW/RESEARCH ASSISTANT PROFESSOR position is available in the translational neuroscience program for studies in Alzheimer's, Parkinson's disease, and amyotrophic lateral sclerosis. Interested candidates should send curriculum vitae to: **Isabela Diaconescu, Program Manager, Department of Psychiatry, the Mount Sinai School of Medicine, New York City, e-mail: isabela.diaconescu@mssm.edu.**

AWARDS

LAGRANGE PRIZE – FONDAZIONE CRT
On Complex Systems
Notice of Competition - Year 2007

Fondazione CRT ***(Cassa di Risparmio di Torino Foundation)***, a private non profit body founded in 1991 that operates mainly in the North-Western Italian region, intends to establish with the scientific coordination of **ISI Foundation** the **Lagrange Prize – Fondazione CRT**, dedicated to scientific research in the field of complex systems.

AIM AND CRITERIA
The **Lagrange Prize – Fondazione CRT** aims at promoting research activities on complex systems. Both theoretical and experimental research activities are taken into account. In particular, the prize will be awarded to such scientific research which, having generated a large impact on the international scientific community, has enabled the accomplishment of exceptional results in the science field of complex systems and its applications in the decade prior to the publishing of this notice of competition.

THE PRIZE
The **Lagrange Prize – Fondazione CRT** is assigned every year to two researchers. The prizes, each one endowed with the amount of **€ 75,000** (seventy-five thousand euros), are assigned to individual researchers whom will be proclaimed as winners within **December 2007** by the Scientific Commission. The prize-awarding ceremony will take place in Turin by **April 2008**.

SUBMISSION OF CANDIDACIES
Each candidacy can be submitted by at least one **guarantor**, who will have to attach a dossier motivating the specific candidacy completing it with minimum 5 - maximum 10 supporting letters from a matching number of sponsors of the candidacy itself. Guarantors or sponsors of the candidature can be considered: directors and researchers of national and international research centres; professors of national and international university institutes; partners and members of Scientific Academies.
Self-candidatures will not be accepted.

CANDIDATURE DOSSIER
The guarantor of the candidacy is required to submit the related candidature dossier drawn up in English and including the following:
1) Candidacy proposal of the guarantor.
2) A written text presenting the research made by the candidate, the importance of results achieved and an analysis of the scientific impact (theoretical or experimental) brought about by the candidate's work.
3) Candidate *curriculum vitae*.
4) List of scientific publications related to the candidate's research activities. The whole dossier has to be submitted via email to **segreteria@isi.it**. The files related to the candidacy documents will have to be in pdf or word format.
5) 5-10 letters supporting the candidacy.
The prize regulation is available on the website **www.progettolagrange.it**.

SELECTION OF CANDIDATURES
The Scientific Commission will communicate the choice of the two winners within **December 2007**.

DEADLINE FOR CANDIDACY SUBMISSION
The candidacy dossier related to the year 2007 and including all documents as per art. 4, has to be received by ISI Foundation within **October 30th, 2007**.

The complete notice of the competition is available upon request addressed to the Prize Organizing Secretary (segreteria@isi.it) and can be retrieved in electronic format by accessing the website www.progettolagrange.it.

MEETINGS

Hepatic Inflammation and Immunity 2008
Institute for Human Infections and Immunity
The University of Texas Medical Branch
Children's Research Institute
Ohio State University
January 25–27, 2008
Galveston, Texas

Organizers: I.N. Crispe, C. Walker, C. O'Farrelly, and S.M. Lemon *in conjunction with the Joint Hepatitis Panels and Immunology Board of the U.S. Japan Cooperative Medical Sciences Program*

This interdisciplinary meeting will examine unique aspects of the intrahepatic immune system and its role in health and disease in 7 sessions over 2.5 days:
Opening Session (I. Arias)

I. *Tolerance, Immunity, and Antigen Presentation in the Liver* (P. Bertolino, K. Lang, P. Knolle, A. Thomson, F. Winau, N. Crispe)
II. *Regulation and Subversion of Innate and Adaptive Intrahepatic Immunity* (B. Beutler, S. Akira, T. Fujita, T. Saito, M. Gale, S. Lemon)
III. *Regulation of Adaptive Cellular Immunity in the Liver* (A. Grakoui, R. Ahmed, K. Sugamura, P. Klenerman, F. Chisari)
IV. *Mechanisms of Liver Injury* (D. Brenner, S. Friedman, A.M. Diehl, G. Cheng, K. Koike, C. Morishima)
V. *Natural Lymphocytes, Immunity, and Immunopathology* (C. O'Farrelly, M. Maini, B. Gao, J. Reimann)
VI. *Natural Lymphocytes, Dendritic Cells and the Interface of Innate and Adaptive Immunity* (M. Kronenberg, H. Kiyono, L. Lanier,T. Kanto, A. Bendelac)
VII. *Autoimmunity and the Liver* (D. Vergani, A. Rao, M. Manns, K. Inaba, J. Gorham, E. Gershwin, T. Sasazuki)

A poster session is planned. For further information and registration details, see **http://www.utmb.edu/chr/hii2008** or contact: **M. Susman, Center for Hepatitis Research, IHII, The University of Texas Medical Branch, Galveston, TX 77555-1019; TEL: 409-772-2319; FAX: 409-772-2495; email msusman@utmb.edu.**

Skirball Institute of Biomolecular Medicine

SCHOOL OF MEDICINE
NEW YORK UNIVERSITY

Faculty Positions

The Skirball Institute and the Kimmel Center of Biology and Medicine at New York University School of Medicine invite applicants for tenure-track positions at the assistant, associate or full professor level. We seek applicants with an exceptional record of achievement to join our existing programs in Molecular Neurobiology, Developmental Genetics, Structural Biology and Molecular Pathogenesis. These programs are interdisciplinary and reflect strengths at NYU's School of Medicine and College of Arts and Sciences. Special priority will be given to applicants with broad interests working at the cutting edge of mammalian genetics, stem cell research, neurobiology or molecular cell biology.

NYU School of Medicine offers excellent resources to support new faculty, including generous start-up packages and core facilities for cell sorting, imaging, proteomics, mouse molecular genetics, genomics and structural biology.

Successful candidates are expected to initiate and maintain vigorous independent research programs that will enrich and be enriched by the highly collaborative environment at the Skirball Institute and throughout the NYU research community.

This is an electronic application process. No mail applications will be accepted. Create your application packet by formatting it as a single PDF document. Use the following page order: (1) Cover Letter - **indicating Program preference**, (2) Curriculum Vitae, (3) Research Statement.
Email application packet to
skirballsearch@saturn.med.nyu.edu.

Three letters of reference should be sent independently to: **skirballsearch@saturn.med.nyu.edu**

New York University School of Medicine was founded in 1841 and is an equal opportunity affirmative action employer. Women and minority candidates are encouraged to apply.

http://saturn.med.nyu.edu

POSITIONS OPEN

POSTDOCTORAL SCIENTISTS
Mechanisms of HIV-1 Entry Antagonism and Design of Entry Inhibitors

Postdoctoral positions are available immediately to investigate structure-based antagonism of HIV-1 envelope function in cell entry using peptide chemistry and molecular biology approaches. We investigate HIV-1 envelope protein interactions with its host cell receptors and seek to identify inhibitors of the envelope protein. We use a multidisciplinary strategy that includes miniprotein scaffolds, peptidomimetics, mutagenic modification of protein targets and surface plasmon resonance (Biacore), and other interaction analysis methods to support inhibitor design and mechanism-of-action studies.

For peptide chemistry/peptidomimetics: We seek candidates with a strong organic chemistry expertise and an ability to apply this expertise in the area of peptides and peptidomimetics.

For molecular biology: We seek candidates with strong molecular biology skills and experience in applying these to investigate protein structure-function relationships at both biochemical and biophysical levels.

Resumes and names/contact for three references to:

Irwin Chaiken, Ph.D.
Professor, Department of Biochemistry and Molecular Biology
Drexel University College of Medicine
11102 New College Building, MS#497
245 N. 15th Street
Philadelphia, PA 19102
Telephone: 215-762-4197
Fax: 215-762-4452
E-mail: ichaiken@drexelmed.edu

ENDOWED CHAIR
for Biomedical Research in the University of Louisville Department of Pediatrics

The Department of Pediatrics at the University of Louisville invites applications to fill an Endowed Chair in a tenure-track academic position. The Department of Pediatrics has a well-funded and expanding faculty dedicated to pediatric care, research, and education. This position offers an outstanding opportunity for development of an independent research program in a multidisciplinary research environment. The Department provides wide opportunities for collaborative research including NIH-funded basic and clinical programs in pediatric pharmacology, diabetes, and sleep. The successful candidate will be jointly appointed in the Department of Pharmacology and Toxicology or other basic science departments to facilitate training of graduate students. The position will be expected to maintain an independently funded research program and foster new collaborations with the faculty. Applicants must have a strong publication record. Applicants for **ASSOCIATE or FULL PROFESSOR** are anticipated to have a nationally recognized and currently funded research program. Candidates with an M.D. and/or Ph.D. will be considered. Applications will be reviewed until the position is filled. Please submit curriculum vitae, contact information for three references, and a cover letter including a statement of research interests to:

Paul N. Epstein, Ph.D.
Chair of the Search Committee
E-mail: paul.epstein@louisville.edu

POSTDOCTORAL/RESEARCH SCIENTIST position for an individual with a Ph.D. in chemistry/biochemistry available at the University of Michigan to study the mechanism of action of microsomal cytochrome P450 using biophysical and biochemical techniques including rapid chemical quench electron paramagnetic resonance, stopped-flow-spectrophotometry, and rapid freeze quench under anaerobic conditions. Knowledge of the structure and function of heme- and flavoproteins, as well as enzyme kinetics is desirable. Salary commensurate with experience. Send resume and names of three references to **Dr. L. Waskell** at **e-mail: waskell@umich.edu.**

POSITIONS OPEN

POSTDOCTORAL RESEARCH ASSOCIATE

The Department of Physiology at the Kirksville College of Osteopathic Medicine has a vacancy for a one-year Postdoctoral Research Associate to examine the therapeutic efficacy of two new compounds in the treatment of Duchene and Becker muscular dystrophy. The research will primarily involve translational studies using the mdx mouse model for Duchene muscular dystrophy, and will include several measurements of pathology in treated mice along with biochemical studies examining the effects of the treatments on the disposition of the NFkappaB pathway in dystrophic skeletal muscle. The Research Associate will be responsible for performing conventional biochemical assays and will also be responsible for supervising the laboratory activities of various laboratory assistants, research technicians, and graduate students that are currently working on the project. Previous experience in muscular dystrophy research or musde biology is desired but not required. Candidates with Ph.D. in biological or related sciences will be considered. Send curriculum vitae, brief statement of research background, and names and addresses (city, e-mail, telephone number) of three references to:

C. George Carlson, Ph.D.
Department of Physiology
A.T. Still University Human Resources
800 W. Jefferson
Kirksville, MO 63501
E-mail: hr@atsu.edu
Telephone: 660-626-2790
Fax: 660-626-2085

A.T. Still University of Health Sciences does not discriminate on the basis of race, color, religion, national origin, sex, sexual orientation, age, disability, or status as a Vietnam-era veteran in admission and access to, or treatment and employment in its programs and activities.

CLIMATE SCIENTIST
Environmental Studies Department

The Environmental Studies Department of Macalester College invites applications for a tenure-track Climate Scientist to begin fall 2008. Appointment will be at the **ASSISTANT, ASSOCIATE, or FULL PROFESSOR** rank. Specific areas of climate-related interest could include climate dynamics, biosphere-climate interaction (including agricultural systems), biogeochemical cycles, climatology, meteorology, oceanography, geochemistry, and geophysics, among others. The successful candidate is expected to build and maintain an active research program with students. Teaching duties include environmental science, courses in the area of specialty, including climate change, and rotating responsibility for the senior seminar course. Send letter of application, curriculum vitae, statement of teaching philosophy and research plans, and three letters of reference to: **Dr. Dan Hornbach, Chair, Department of Environmental Studies, Macalester College, 1600 Grand Avenue, St. Paul, MN 55105.** Applications received by October 15, 2007, will receive first consideration. More information is at **website: http://www.macalester.edu/provost/positions/index.html.** *Macalester College is an Equal Opportunity/Affirmative Action Employer and strongly encourages applications from women and minorities.*

POSTDOCTORAL POSITION available immediately in the Laboratory of **Dr. Julie Saba** to study how sphingolipid-mediated signaling pathways contribute to cancer development, progression, and responses to chemotherapy and radiotherapy (*Cell Cycle* **6**:522-7, 2007; *Proc. Nat. Acad. Sci.* **103**:17384-9, 2006 and **101**:17825-30, 2004). Experience with murine models of cancer, molecular biology, cell biology, tissue culture, and microscopic imaging technology are required. Candidates with a Ph.D. or M.D. *and with U.S. citizenship or permanent resident status* are strongly encouraged to apply. Please submit curriculum vitae, brief statement of research interests and goals, and the names of three references to: **Julie D. Saba, M.D., Ph.D.** at **e-mail: jsaba@chori.org.**

POSITIONS OPEN

POSTDOCTORATE in CELLULAR IMMUNOLOGY

NewLink Genetics Corporation is a biopharmaceutical company in Ames, Iowa, developing new therapeutic alternatives for cancer patients.

We seek an individual to perform the development of immunologic assays to conduct the immunomonitoring in patients. The individual should have a background in cellular immunology and be proficient in culturing human lymphocytes.

Applicants must possess knowledge in immunologic techniques and have hands-on experience in flow cytometry, tissue culture, and enzyme-linked immunosorbent assay. The candidate will work with a multidiscipline scientific team providing analytical expertise in support of this company's tumor immunology program. S/he will identify appropriate technique(s) and develop methods necessary for the characterization and quantification of the immune reactions induced by current experimental vaccines.

Ph.D./M.D. in immunology with a strong emphasis in cellular immunology strongly preferred.

Candidates must also have a current work authorization to work in the United States to be considered. Please submit curriculum vitae, letter of application, together with a list of three references and salary history to **e-mail: apply@linkp.com** or mailed to: **NewLink Genetics, 2901 South Loop Drive, Suite 3900, Ames, IA 50010** or **fax: 515-296-5557.**

We offer a diverse workforce with a competitive salary and benefit package.

Equal Opportunity Employer.

We deliver — customized job alerts.
ScienceCareers.org
We know science AAAS

MARKETPLACE

Widely Recognized Original & Guaranteed
KlenTaq1
8¢/u Truncated Taq DNA Polymerase Withstand 99°C
US Pat #5,436,149
Call: **Ab Peptides**
Fax: 314•968•8988
e-mail: abpeps@msn.com
1•800•383•3362
www.abpeps.com

EZBiolab www.ezbiolab.com
Custom Peptide 10mg 90%: $19.59/aa
AB Production $785 peptide included
Gene Synthesis $1.20/bp
siRNA 20 nmol PAGE purified: $285

Oligo Synthesis Columns
- Columns For All Synthesizers
- Standard and Specialty CPGs
- Bulk Column Pricing Available

BIOSEARCH TECHNOLOGIES
+1.800.GENOME.1
www.bticolumns.com

"Fascinating,"[1] "informative"[2] science *from* YALE

THE LAST HUMAN
A Guide to Twenty-Two Species of Extinct Humans
Created by G. J. Sawyer and Viktor Deak
Text by Esteban Sarmiento, G.J. Sawyer, and Richard Milner
With Contributions by Donald C. Johanson, Meave Leakey, and Ian Tattersall

"A magnificent matching of precisely researched science and inspired popularization. . . . **Fascinating.**"
—Adrian Barnett, *New Scientist* [1]
63 color +8 b/w illus. + 21 maps $45.00

MATTERS OF EXCHANGE
Commerce, Medicine, and Science in the Dutch Golden Age
Harold J. Cook

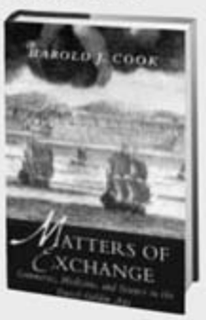

"Admirable. . . .
A book that will undoubtedly be fruitful, not least in stimulating fresh debate about the sources of the scientific revolution."
—Jonathan I. Israel, *Science* 60 illus. $35.00

THE ORIGINS OF THE FUTURE
Ten Questions for the Next Ten Years
John Gribbin

"This is the ultimate book on ultimate origins from strings, to quarks, to present day particles, galaxies, WIMPS, the solar system, life and the ultimate death, written by the premiere science expositor in John Gribbin."—Allan Sandage $27.50

QUANTUM PHYSICS AND THEOLOGY
An Unexpected Kinship
John Polkinghorne

"Polkinghorne explores the underlying truth-seeking connection between science and religion and executes this task with **a rare blend of precision and clarity.**"
—Nathan J. Hallanger $26.00

MARSHES
The Disappearing Edens
William Burt

"Burt has an enviable gift: the power, with prose and camera lens, to persuade a reader of *Marshes* that these 'disappearing Edens' are **among the most remarkable places on earth.** Believe him." —*House & Garden*
92 color illus. $35.00

BREATHING SPACE
How Allergies Shape Our Lives and Landscapes
Gregg Mitman

"A **critically important** analysis of the emergence of allergies as strikingly common and increasingly serious health maladies. . . . [Mitman] vividly shows how our bodies, our environment, and our health are indivisible."—Allan M. Brandt 48 illus. $30.00

SECOND NATURE
Brain Science and Human Knowledge
Gerald M. Edelman, M.D., Ph.D.

"For anyone who is interested in human consciousness, this is **required reading.**"
—Oliver Sacks $24.00

INTO THE BLACK
JPL and the American Space Program, 1976–2004
Peter J. Westwick

"Comprehensive, rich and revealing. . . . Westwick's impressively well-crafted history [is also a] probing institutional study."
—David H. DeVorkin, *American Scientist*
24 illus. $40.00

SAVING NATURE'S LEGACY
Origins of the Idea of Biological Diversity
Timothy J. Farnham

"In examining an idea that is now driving conservation worldwide, **Farnham gets the story right** in a way that no one else has. His book is richly detailed, yet catches the large themes beautifully."—Elliott Norse
$45.00

New in paper

CLIMATE CHANGE AND BIODIVERSITY
Edited by Thomas E. Lovejoy and Lee Hannah

"This book will be **a milestone** in the emerging discipline of climate change biology."—Edward O. Wilson
107 b/w + 11 color illus. $35.00 paperback

MANAGING THE ENVIRONMENT, MANAGING OURSELVES
A History of American Environmental Policy, Second Edition
Richard N. L. Andrews

A substantially revised new edition of this "readable . . . history of American environmental policy. . . . **Well-written, informative, and meaningful.**"
—Martha S. Salk, *Quarterly Review of Biology* [2]
34 illus. $40.00 paperback

IMPERIAL NATURE
The World Bank and Struggles for Social Justice in the Age of Globalization
Michael Goldman

"An excellent critique of the Bank's inner workings and external image-making."
—*Publishers Weekly*
Yale Agrarian Studies Series $22.00 paperback

WRITING FOR SCIENCE
Robert Goldbort

"Addresses writing across the entire enterprise of science. . . . Useful to students and faculty across a wide range of scientific disciplines."—Mary Arthur
$50.00 cloth; $20.00 paperback

IN THE COMPANY OF CROWS AND RAVENS
John M. Marzluff and Tony Angell
Illustrated by Tony Angell
Foreword by Paul Ehrlich
108 illus. $18.00 paperback

THE PLAUSIBILITY OF LIFE
Resolving Darwin's Dilemma
Marc W. Kirschner and John C. Gerhart
Illustrated by John Norton
40 illus. $18.00 paperback

THE RETREAT OF THE ELEPHANTS
An Environmental History of China
Mark Elvin
$22.00 paperback

YALE University Press
Available wherever books are sold • yalebooks.com

R&D Systems

Your Complete Source for Embryonic Stem Cell Research.

MARKER ANTIBODIES Antibodies & antibody panels for monitoring undifferentiated and lineage specific differentiation of ES cells

For expansion of undifferentiated ES cells & directed differentiation along specific lineages **GROWTH FACTORS & CYTOKINES**

EMBRYONIC STEM CELL KITS & PANELS Assess the differentiation status of ES cells at the RNA level

Oct-3/4 Detected by Flow Cytometry

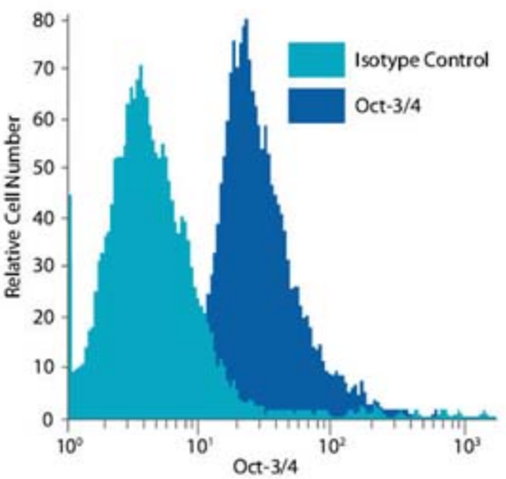

Oct-3/4 in human ES cells (BG01V) using PE-conjugated anti human/mouse Oct-3/4 antibody (Catalog # IC1759P).

Nanog Detected in Human ES Cells

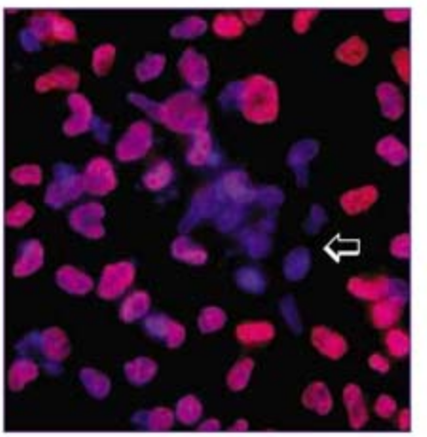

Nanog detected (BG01V) with anti-human Nanog (Catalog # AF1997) and NorthernLights™ 557 secondary antibody (Catalog # NL001; red). Cells were counterstained with DAPI (blue). Differentiated cells no longer express Nanog (arrow).

NEW! Tissue Culture Grade FGF basic

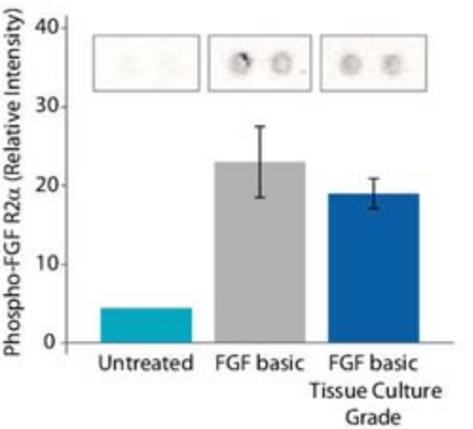

FGF basic (Catalog # 3718-FB) and cost-effective tissue culture grade FGF basic (Catalog # 4114-TC) stimulate FGF R2α phosphorylation in human ES cells as measured using the Proteome Profiler™ Phospho-RTK Array (Catalog # ARY001). Inset shows corresponding array dot blots.

For more information visit our website at **www.RnDSystems.com/go/StemCells**

Tools for Cell Biology Research™

Selection expanding weekly—visit www.RnDSystems.com to sign up for weekly new product updates.

USA & Canada **R&D Systems, Inc.** Tel: (800) 343-7475 info@RnDSystems.com

Europe **R&D Systems Europe, Ltd.** Tel: +44 (0)1235 529449 info@RnDSystems.co.uk

For research use only. Not for use in diagnostic procedures.

R&D SYSTEMS®